Geochemistry of Marine Bivalve Shells:

the potential for paleoenvironmental reconstruction

David Paul Gillikin

2005

Vrije Universiteit Brussel
Faculty of Science
Laboratory of Analytical and Environmental Chemistry

Geochemistry of Marine Bivalve Shells: the potential for paleoenvironmental reconstruction

David Paul Gillikin

Proefschrift voorgedragen tot het behalen van
de graad van Doctor in de Wetenschappen

Academic year 2004-2005

Advisor
Frank Dehairs
(VUB)

Co-advisors
Willy Baeyens
(VUB)
Eddy Keppens
(VUB)

Committee
Peter K. Swart
(RSMAS/MGG University of Miami)
Yves-Marie Paulet
(IUEM – UBO, Brest)
Philippe Claeys
(VUB)
Luc André
(Royal Museum for Central Africa)

to

Anouk and my mother

ACKNOWLEDGEMENTS

The work presented here would not have been achieved without the aid and support of others. I would like to thank my promoter Frank Dehairs for giving me the opportunity to pursue this Ph.D. Frank's enthusiasm, encouragement, constructive comments and help in the laboratory and field made this work possible and enjoyable. I also thank my co-promoters Willy Baeyens and Eddy Keppens for their constructive comments throughout this work. I would further like to express my gratitude to the Belgian Federal Science Policy Office, Brussels, Belgium, who funded this work and the CALMARS project (contract: EV/03/04B) and to the 'Onderzoeksraad' (OZR) of the VUB for their additional financial support to help present these results at international meetings.

During my Ph.D. research I greatly enjoyed working closely with the other members of the CALMARS project: Philippe Willenz (project coordinator) and Lorraine Berry (Royal Belgian Institute of Natural Sciences); Philippe Claeys and Fjo De Ridder (VUB); Luc André, Jacques Navez, Denis Langlet, Sophie Verheyden and Anne Lorrain (Royal Museum for Central Africa); Philippe Dubois and Herwig Ranner (Université Libre de Bruxelles); Ronny Blust and Valentine Mubiana Kayawe (University of Antwerp); and the M.Sc. students I guided: Hans Ulens, Dirk Steenmans, Li Meng and Ivy Meert.

I also thank all my colleagues at the VUB for their continued support, especially S. Bouillon, N. Savoye, M. Elskens, N. Brion, M. Leermakers, L. Dewaersegger, M. De Valck and P. De Geest.

Many of these chapters would not have been possible without the samples supplied by C.H. Peterson (University of North Carolina, Chapel Hill), who kindly provided the *Mercenaria mercenaria* shells collected in the early 1980's; L. Campbell (University of South Carolina) who kindly provided the Pliocene *M. mercenaria* shell; and K. Li and S. Mickelson of the King County Department of Natural Resources and Parks, Water and Land Resources Division, Marine Monitoring group (WA, USA) and J. Taylor (U. Washington) who supplied the *Saxidomus giganteus* shells and water data. W.C. Gillikin and L. Daniels both kindly assisted with sample collection in North Carolina and C. Setterstrom collected the Puget Sound water samples. After obtaining these samples, I was only able to analyze them because of the technical expertise of M. Korntheuer (ANCH), J.-P. Clement (ANCH), A. Van de Maele (GEOL), J. Nijs (GEOL) and L. Monin (MRAC). Moreover, superb reviews have been given for certain chapters by D.W. Lea, H.A. Stecher, D.L. Dettman, B.R. Schöne, R. Takesue, L. D. Labeyrie, C. Sheppard and other anonymous reviewers and helpful discussions were provided by J. Erez, D.J. Sinclair, I. Horn, E.L. Grossman, J. Bijma, B.K. Linsley and countless others.

In addition to the friends I made in Europe, I would like to thank all my friends back in the US for the much needed respite they provided in the form of good food, a place to stay and excellent company, namely F. Zito, S. Ryan, M. Manzo, S. Manzo, L.A. Ciccone, R. DeRuvo, J. Ryan, P. Ryan, A. Shedd, P. Eichler, S. Paik, R. Genser, R. Buckey and others; without that, I would never have made it to this point! Finally, I would like to thank the people who are closest to my heart: my mother and my four sisters and their families, for their love, support and encouragement during all these years; the Verheyden family for accepting me into their family and treating me like a son; and Anouk Verheyden, for being there for me, for your help in the field, your friendship, your patience, your understanding, your constructive comments on my manuscripts, your encouragement, your trust and your love, thank you so much.

David Paul Gillikin
Brussels, June 2005

TABLE OF CONTENTS

Geochemistry of marine bivalve shells:
the potential for paleoenvironmental reconstruction

ABSTRACT

Bivalve shells offer a great potential as environmental proxies, since they have a wide geographical range and are well represented in the fossil record since the Cretaceous. Nevertheless, they are much less studied than corals and foraminifera and are largely limited to isotopic studies. This is probably due to the fact that the literature has been contradictory regarding the faithfulness of elemental proxies in bivalves. The general aim of this dissertation is to increase our knowledge of proxies in bivalve carbonate. More specifically, $\delta^{18}O$, $\delta^{13}C$, Sr/Ca, Mg/Ca, U/Ca, Ba/Ca, and Pb/Ca were investigated in both aragonite and calcite bivalve shells and their potential as environmental proxies were evaluated.

The most well studied proxy of sea surface temperature (SST) in bivalve carbonate is $\delta^{18}O$, and it is well known that in addition to SST, the $\delta^{18}O$ of the water dictates the $\delta^{18}O$ value of the shell. This study clearly demonstrates that unknown $\delta^{18}O$ of the water can cause severe errors when calculating SST from estuarine bivalve shells; with the example presented here providing calculated SSTs 1.7 to 6.4 °C warmer than measured. Therefore, a salinity independent or salinity proxy would greatly benefit SST reconstructions. In estuaries, shell $\delta^{13}C$ has long been regarded as a potential salinity indicator. However, more recent works have demonstrated that the incorporation of light carbon from metabolic CO_2 interferes with the environmental signal. This study confirms that the amount of metabolic CO_2 increases in internal fluids with age, resulting in the strong ontogenic decrease in $\delta^{13}C$ values of bivalve shells. However, this is not always the case, with *Saxidomus giganteus* shells showing no discernable decrease over ~10 years growth. On the other hand, this study also demonstrates that the percent metabolic CO_2 (%M) incorporated into bivalve shells can be large - up to 35 % in some individuals of *Mercenaria mercenaria*. An attempt was made to remove this metabolic influence using the relationship between %M and shell biometrics; however the inter- and intra-site variability was too large. This was also the case for the relatively short-lived bivalve *Mytilus edulis*, where the %M varied between 0 and 10%. Within the studied estuary (Schelde) the shells were close to equilibrium, but at the seaward site, where wave action is stronger, the shells contained ~10 %M and the absolute $\delta^{13}C$ values were indistinguishable from specimens within the estuary, despite a salinity difference of 4. Therefore, interpreting $\delta^{13}C$ values in bivalve carbonate should be done with caution. In addition to $\delta^{13}C$, Ba/Ca ratios were investigated as a salinity proxy as well. In the calcite shells of *M. edulis* a strong linear relationship between shell 'background' Ba/Ca and water Ba/Ca was found in both the laboratory and field. Although each estuary will have different relationships between salinity and water Ba/Ca, shell Ba/Ca can be used as an indicator of salinity within one estuary. Similar patterns of relatively stable background levels interrupted with sharp episodic peaks were also found in the aragonite shells of *S. giganteus*, and appear nearly ubiquitous to all bivalves. However, there was an ontogenic decrease in *S. giganteus* background Ba/Ca ratios, illustrating that these proxies can be species specific. Previous hypotheses regarding the cause of the peaks include ingestion of Ba rich phytoplankton or barite. This study illustrates that there is no direct relationship between Chl a and Ba/Ca peaks in *S. giganteus* shells, but they still may be related to blooms of specific species of phytoplankton.

The ratios of Sr/Ca and Mg/Ca were investigated as salinity independent SST proxies. Ratios of Sr/Ca were found to be highly correlated to growth rate in *S. giganteus*, but not in *M. mercenaria*, contradictory to an earlier study on *M. mercenaria*. Although growth rates and temperature are often correlated, there was only a poor correlation between Sr/Ca and SST in *S. giganteus* (maximum R^2 = 0.27). Similarly, Mg/Ca and U/Ca ratios in *S. giganteus* were not correlated to SST, with U/Ca exhibiting a strong ontogenic trend.

Finally, the use of bivalve shells as recorders of pollution was also assessed. There was both large inter- and intra-specimen variability in Pb/Ca ratios of *M. mercenaria* shells, but when enough shells were averaged, the typical anthropogenic Pb profile from 1949 to 2003 was evident.

Overall, this study demonstrates the difficulties inherent to utilizing bivalve shells as recorders of their environment. It is clear that factors determining proxy incorporation are strongly species specific and that a mechanistic understanding is needed before we can progress further in this line of research. However, this study also illustrates that there is indeed environmental information that can be extracted from bivalve shells. Furthermore, the physiological influence on many of the studied proxies may prove to be useful as proxies of bivalve physiology, which in turn could provide information about bivalve paleo-ecology.

General Introduction

All of what we know about the history of the Earth's climate and environment is obtained from records stored in substrates formed during the period of interest. As early as ~540 B.C., Xenophanes of Colophan recognized that fossils were remnants of former life that lived on the sea floor. However, modern geology was 'born' in the late 1700's to early 1800's when early geologic theories were constructed (e.g., James Hutton [uniformitarianism, i.e., the past = the present] and Chalrles Lyell's book: Principles of Geology), which allowed past environmental information to be extracted from rocks. Armed with these theories, William Smith produced a geologic map in 1815 using the principle of faunal succession, and the geologic time scale was conceived.

In a more modern context, global climate change has become a major task and a multidisciplinary endeavor. As Lea (2003) wrote: "Temperature is the most primary representation of the state of the climate system, and the temperature of the oceans is critical because the oceans are the most important single component of the Earth's climate system." Considering the idea that the 'past is equal to the present,' and that the thermometer was only invented at the turn of the 17th century (Middleton, 1966), it should be clear why records of paleotemperature are important. In order to obtain this information, proxies are used, which are geochemical or physical signals recorded in different biological or geological deposits that reflect an environmental signal. However, many records are restricted in their distribution, and the importance of regional climate is becoming increasingly clear (IPCC, 2001). Moreover, many proxies used to extract information from these substrates are not fully understood. Each type of archive provides a valuable record, with unique strengths and weaknesses. For example, trees are of course only terrestrial, sediments often provide low resolution profiles and bioturbation may be a problem, scleractinian corals are mostly restricted to the tropics, and foraminifera are small organisms making detailed ontogenic studies difficult (although this has recently been achieved; Eggins et al., 2004). To circumvent any problem associated with one proxy, multi-proxy approaches are gaining popularity (see Kucera et al., 2005).

The chemical or isotopic composition of calcareous skeletons has long been recognized as records of past and present environmental conditions and thus allows reconstruction of the environmental history. Recent efforts have given a high priority to coral and foraminiferal research to produce indicators of specific aspects of climate that can be integrated with other high resolution paleoclimate data derived from tree rings, ice cores or sediments. Because the composition of biogenic carbonates is also clearly influenced by biological factors, the correct interpretation of these chemical archives requires a precise understanding of the processes controlling the incorporation of elements. Furthermore, to make the reconstruction of past environmental conditions as reliable as possible at a global scale implies that recorders from the widest taxonomic, geographical, and ecological ranges are used. Currently, such a large range is not available. Therefore, **it is the aim of this dissertation to increase our knowledge of proxy incorporation in bivalve shells.** Bivalves are beneficial in that they can provide high resolution seasonal records of environmental conditions and have a wide geographical distribution. Although environmental information can be stored in the physical shell structure of bivalves

(e.g., growth lines), this work focuses on shell geochemistry. This work forms part of the project '**CAL**careous **MAR**ine **S**keletons as recorders of global climate changes: **CALMARS**' (funded by the Belgian Federal Science Policy Office).

First a general *overview* of the subject is given in Chapter 1, where the main objective is put in context and different geochemical proxies are introduced.

Next, in Chapters 2 and 3 the *methods* used in this work are detailed along with *precision and accuracy*, which is important to understand the analytical limitations of this work.

In Chapter 4 the problems associated with using *oxygen isotopes* ($\delta^{18}O$) in an estuarine bivalve shell are discussed. $\delta^{18}O$ is one of the oldest and best studied geochemical proxy in biological carbonates. However, the problem of unknown source water $\delta^{18}O$ (which is related to salinity) complicates this proxy and thus the need for either a salinity proxy or a salinity independent proxy is needed.

The potential of using stable *carbon isotopes* ($\delta^{13}C$) as a salinity proxy (through the relationship between salinity and $\delta^{13}C$ of dissolved inorganic carbon) are discussed in the following two chapters: Chapters 5 and 6. More specifically, the problem of metabolic carbon incorporation in bivalve shells is addressed.

Chapter 7 marks the start of discussions on *elemental proxies*. In this Chapter, several elements which were measured in two aragonitic clams (*Saxidomus giganteus*) that grew at the same location and a third clam that grew in a different environment are compared and discussed.

Sr/Ca ratios in biogenic aragonites have been shown to be a robust proxy of *sea surface temperatures*, with no salinity effect. However, in Chapter 8 it is clearly illustrated that there are strong biological controls on Sr/Ca ratios in bivalve shells.

In Chapter 9 the use of aragonitic bivalve shells as *recorders of coastal pollution* is assessed. Data on *Pb/Ca* ratios in shells is compared with historical Pb discharges and records from other biogenic carbonates.

In Chapter 10 *Ba/Ca* ratios are investigated in a calcitic bivalve, *Mytilus edulis*. Here the path of Ba through the animal to the shell from both the water and food is investigated and shell Ba/Ca ratios are proposed as a relative salinity indicator.

Chapter 11 presents auxiliary data from the Ba experiment of Chapter 10. Here 10 elements are discussed in terms of their *path from the environment to the shell*. Additionally, *biological filtration or concentration* from the environment to the body fluids is discussed.

Finally, an effort is made to integrate the data presented in the different chapters and to view these conclusions in a broader perspective in Chapter 12.

Chapter 1

Bivalve shell geochemistry as an environmental proxy: An introduction

Foreword

The present chapter aims at providing the reader of this dissertation with enough background information to understand the basic concepts of using biogenic carbonates as environmental archives, with an emphasis on bivalve shells. Some of these concepts will further be elaborated in individual chapters. For those readers interested in more detailed and comprehensive reviews on this subject, I refer to Rhoads and Lutz (1980); Druffel (1997), Vander Putten (2000), Richardson (2001), Lea (2003), Zeebe and Wolf-Gladrow (2003), and Hoefs (2004), to name a few.

Publication of the author related to this chapter:

Gillikin, D. P., and A. Lorrain, *submitted.* Bivalves as proxies. In L. Chauvaud, Y.-M. Paulet, J.-M Guarini and J.-Y. Monnat (eds.) *The scallop, environmental archive.* Institut océanographique (Monaco) vol spécial. Océanis

1. INTRODUCTION

With future climate change at the forefront of environmental policy making (UN, 1997; IPCC, 2001), studies of past climatic changes and their environmental effects are important because they provide a way to understand the processes responsible for these changes. By using the past as the key to the future, we can better predict how the globe will respond to certain environmental perturbations. Information about past climatic conditions and changes can be obtained through proxies, which are geochemical or physical signals recorded in biological or geological structures that reflect an environmental signal. Properties of these biological or geological structures are, to some degree, dependent on the environment in which they were formed. As they accrete through time they can thus record a time-series of environmental information. For example, environmental information has been obtained from **tree rings** (e.g., Shvedov, 1892; Fritts et al., 1971; Schweingruber, 1988; Mann and Hughes, 2002; D'Arrigo et al., 2003; Cook et al., 2004; Verheyden et al., 2004, 2005a), **sclerosponges** (e.g., Druffel and Benavides, 1986; Lazareth et al., 2000; Swart et al., 2002a; Rosenheim et al., 2004, 2005), **speleothems** (e.g., Winograd, 1992; Verheyden et al., 2000; Finch et al., 2001), **corals** (e.g., Weber and Woodhead 1970; Weber, 1973; Emiliani et al., 1978; Fairbanks and Dodge, 1979; Swart et al., 1996a, 1996b, 1998, 1999, 2002b; Sinclair et al., 1998; Linsley et al., 2000; Swart and Grottoli, 2003), **mollusk shells** (e.g., Davenport, 1938; Clark, 1968; Jones et al., 1989; Vander Putten et al., 2000; Lazareth et al., 2003), **Foraminifera** (e.g., Emiliani, 1954; Lea, 1993; Nürnberg et al., 1996; Lea et al., 1999), **sediment cores** (e.g., Chow and Patterson, 1962; Degens, 1965; Clark, 1971; Hall, 1979; Chillrud et al., 2003; Kim et al., 2004) and **ice cores** (e.g., Murozumi et al., 1969; Johnsen et al., 1972; Dansgaard, 1981; Neftel et al., 1982; Hong et al., 1996; Petit et al., 1999).

For more than 50 years, bivalve shells have been known archives of past environmental conditions (Davenport, 1938; Epstein et al., 1953). As bivalves grow they sequentially deposit new layers of shell, and the chemical composition of these layers may reflect the environmental conditions at the time they formed. Indeed, environmental data have been extracted from both bivalve shell geochemistry (e.g., stable isotopes and elemental composition (see later references)) as well as from

external or internal growth marks (Davenport, 1938; Clark, 1968; Chauvaud et al., 1998; Lorrain et al., 2000; Schöne et al., 2002, 2004; Witbaard et al., 2003; Strom et al., 2004). Bivalves are beneficial in that they can provide high resolution seasonal records of environmental conditions and have a wide geographic distribution, whereas many other substrates, such as corals, are limited in their latitudinal extent. Although most bivalves typically live less than 10 years, some readily achieve 50 years (Peterson, 1986) and there have been reports of bivalves (*Arctica islandica*) living up to 225 years (Ropes, 1985), or even 374 years (Schöne et al., 2005, in press). In addition, bivalve shells are often found in archeological middens or as fossils, potentially allowing records of environmental conditions to be extended into the past. However, it is becoming increasingly clear that the animals' physiology significantly impacts the chemical proxies recorded in the shell (Klein et al., 1996a, b; Purton et al., 1999; Vander Putten et al., 2000; Lorrain et al., 2004a). Although bivalve shells can provide environmental information in other ways, this chapter will focus on the aim of this dissertation: bivalve shell geochemistry as an environmental proxy.

2. BIOMINERALIZATION

To understand how environmental information can be incorporated in the shell, at least a basic background in shell formation or biomineralization is necessary. Biomineralization in bivalves takes place in the extrapallial fluid (EPF), a thin film of liquid between the calcifying shell surface and the mantle epithelium (Fig. 1; Wheeler, 1992). The central EPF (or inner EPF) is where the inner shell layer is precipitated, whereas the outer and/ or middle shell layer is precipitated from the marginal EPF (or outer EPF). Typically the EPF is isolated from seawater and therefore may have different elemental and/ or isotopic concentrations than seawater.

Elements from the environment may reach the site of calcification via many possible routes. Typically, ions enter the hemolymph of marine mollusks primarily through the gills, although they may also enter via the gut or by direct uptake by the outer mantle epithelium (see Wilbur and Saleuddin, 1983 and references therein). Elements supplied by the hemolymph then move into the EPF through the epithelial mantle cells (Wilbur and Saleuddin, 1983).

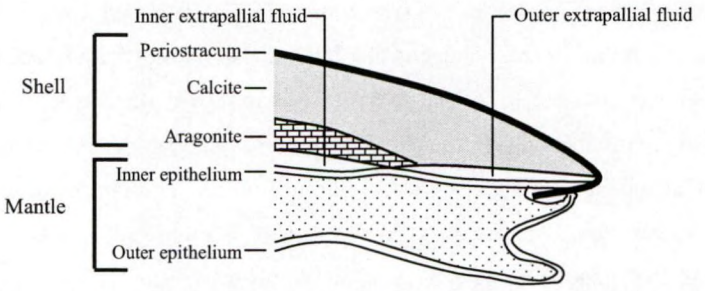

Figure 1. Illustration of a cross-section through a mussel shell with the different shell layers (aragonite and calcite), the mantle, and the sites of calcification (central or inner extrapallial fluid (EPF) and marginal or outer EPF) shown (figure modified from Vander Putten, 2000).

In order for elements to move through these membranes, they are facilitated by certain enzymes, although intercellular routes also exist. Two enzymes, which have been determined to be of great importance in calcification are Ca^{2+}-ATPase and carbonic anhydrase (CA). The enzyme Ca^{2+}-ATPase pumps Ca^{2+} to the EPF while removing $2H^+$, and CA catalyses the reaction $HCO_3^- + H^+ \leftrightarrow CO_2 + H_2O$, then CO_2 can easily diffuse through membranes (Crenshaw, 1980; Cohen and McConnaughey, 2003). Once inside the EPF, CO_2 reacts with H_2O to form $2H^+ + CO_3^{2-}$. The ion CO_3^{2-} then combines with Ca^{2+} to form $CaCO_3$ (while Ca^{2+}-ATPase removes the $2H^+$). Other organic molecules are also very important in biomineralization. For instance, soluble polyanionic proteins have been shown to determine which polymorph of carbonate (i.e., calcite or aragonite) is deposited (Falini et al., 1996).

It is currently believed that the carbonate is deposited in previously deposited organic matrix sheets, with a brick and mortar pattern (i.e., the carbonate being the 'bricks' and the organic matrix sheets being the mortar) (Watabe, 1965; Addadi and Weiner, 1997). However, this matrix mediated hypothesis has recently been moderated by Mount and co-workers (2004). Mount et al. (2004) found that in the oyster, *Crassostrea virginica*, seed crystals were directly formed in granulocytic hemocytes. Thus their alternative to the matrix-mediated hypothesis is that crystal nucleation is intracellular and that crystallogenic cells supply nascent crystals to the mineralization front, thereby at least augmenting matrix-mediated crystal-forming processes in this system. However, many aspects of biomineralization are still poorly understood. For example, although organic complexation can have serious effects on the availability of elements in the EPF, few researchers look into this aspect. Indeed Nair and

Robinson (1998) found that 85 % of Ca in the hemolymph of the clam *Mercenaria mercenaria* is bound to macromolecules. Furthermore, pathogens can cause a response that alters the organic parameters of the EPF (Allam et al., 2000) and membrane enzyme activity can be affected by toxic elements (see Vitale et al., 1999). In conclusion, although we can generalize about some aspects of biomineralization, it is highly complex and far from being completely understood.

3. STABLE ISOTOPES

3.1 Background

Isotopes are atoms of the same element (i.e., they have the same number of protons) having a different number of neutrons, resulting in a different atomic mass. As a result of different atomic masses, isotopes may react differently during chemical and physical reactions causing differences in the abundance of heavy and light isotopes between the source and end product. The process causing this difference is termed *fractionation* and is expressed as the *fractionation factor* (α), defined as:

$$\alpha = R_A / R_B \text{ (for A} \leftrightarrow \text{B)} \qquad (1)$$

where A and B are the source and end products, respectively, and R is the isotopic ratio (abundance of heavy isotope / abundance of light isotope). Two types of fractionation are possible, thermodynamic (or equilibrium) fractionation (according to equilibrium constants) and kinetic fractionation (see further). The fractionation factors are very small and are close to one; therefore the deviation of α from one, or the *discrimination* (ε), is used:

$$\varepsilon = (\alpha - 1) * 1000 = [(R_A - R_B) / R_B] * 1000 \text{ (in ‰)} \qquad (2)$$

For practical reasons, data are presented as δ values, which is the isotopic ratio of compound A (R_A) relative to the isotopic ratio of a well defined standard ($R_{standard}$):

$$\delta_A = ((R_A / R_{standard}) - 1) * 1000 \text{ (in ‰)} \qquad (3)$$

Oxygen isotopes in water and most mineral phases are usually expressed relative to Vienna Standard Mean Ocean Water (VSMOW), while stable carbon isotopes, and sometimes oxygen isotopes, in carbonates are expressed relative to the PeeDee Belemnite (now exhausted and referred to as the Vienna PDB or VPDB). Meanwhile, N, S and H isotopes and the non-traditional isotopes (e.g., B, Sr, Mg, Si, Pb, etc.) all also have their own standards (see Hoefs, 2004; Carignan et al., 2004 and references therein).

After simplification, ε and α can be estimated from:

$$\varepsilon = (\delta_A - \delta_B) / (1 + \delta_B / 1000) \approx \Delta = \delta_A - \delta_B \quad (\text{in } ‰) \qquad (4)$$

$$\alpha = (\delta_A + 1000) / (\delta_B + 1000) \quad (\text{in } ‰) \qquad (5)$$

Comprehensive discussions on isotope fundamentals can be found in Mook (2000), Zeebe and Wolf-Gladrow (2003), and Hoefs (2004).

3.2 Carbonate $\delta^{18}O$: A record of past temperatures

3.2.1 Paleotemperature equations

In 1947, Urey determined that the oxygen isotope fractionation between carbonates and water were temperature dependent. Consequently, Epstein et al. (1953) found that the oxygen isotopic signature recorded in mollusk shells ($\delta^{18}O_S$) not only reflects the temperature of crystallization, but also the oxygen isotopic signature of the water ($\delta^{18}O_w$) within which they formed. Furthermore, shell mineralogy is also important; bivalves are known to precipitate either of the two polymorphs of calcium carbonate, calcite or aragonite (or both), and calcite is depleted in ^{18}O by about 0.6 to 1.0 ‰ relative to aragonite (Tarutani et al., 1969; Böhm et al., 2000). Yet, a more coarse recent study on marine mollusks has suggested that there is no difference between the two polymorphs of $CaCO_3$ (Lécuyer et al., 2004). However, this seems unlikely because it is well known that the vibrational frequencies of the rhombohedral calcite and orthorhombic aragonite leads to different physical and chemical properties such

as density, solubility and elemental and isotopic fractionation factors (for review see Zeebe and Wolf-Gladrow, 2003; Hoefs, 2004).

Ever since Urey's discovery, scientists started to develop empirical paleotemperature equations, which were determined by sampling bivalves grown under different temperatures with known $\delta^{18}O_w$. The two most popular empirically derived paleotemperature equations for mollusks are the equation developed by Epstein et al. (1953) (modified by Anderson and Arthur (1983)) for calcitic bivalves:

$$T(°C) = 16 - 4.14 * (\delta^{18}O_S - \delta^{18}O_w) + 0.13 * (\delta^{18}O_S - \delta^{18}O_w)^2 \qquad (6)$$

and the equation developed by Grossman and Ku (1986) for aragonite mollusks:

$$T(°C) = 19.7 - 4.34*(\delta^{18}O_S - \delta^{18}O_w) \qquad (7)$$

where $\delta^{18}O_S$ is the $\delta^{18}O$ value of CO_2 (vs. VPDB) liberated from the reaction between carbonate and phosphoric acid at 25°C, and $\delta^{18}O_w$ is the $\delta^{18}O$ value of CO_2 (vs. VSMOW) equilibrated with water at 25°C. However, there are many other paleotemperature equations in the literature. Table 1 illustrates six different equations based on different types of aragonite, and three for calcite. From the 9.5 °C range in temperature for aragonite and 3.3 °C range for calcite calculated using constant arbitrary values ($\delta^{18}O_S$ = 1.0 ‰ and $\delta^{18}O_w$ = 0.06 ‰), it is clear that there is no general consensus of oxygen isotopic fractionation in biogenic carbonates. However, as stated in Zhou and Zheng (2003), the empirical equations derived for biogenic aragonite reflect 'steady-state equilibrium' (a dynamic equilibrium state different from thermodynamic equilibrium), whereas experimentally determined inorganic fractionation factors are near thermodynamic equilibrium (the minimum free energy for isotope exchange reactions). Nonetheless, some calcitic bivalves precipitate near thermodynamic equilibrium (Chauvaud et al., in press) and the empirical paleotemperature equations based on mollusks (see Table 1) have been used with much success.

Table 1. Temperature calculated using $\delta^{18}O_w$ = 0.6 ‰ and $\delta^{18}O_S$ = 1.0 ‰ and various paleotemperature equations (see Bemis et al., 1998 for a complete list of calcite equations).

Author	Equation	Result (°C)	mineralogy	substrate
Zhou & Zheng (2003)	$1000\ln\alpha = 20.44 * 1000/T(K) - 41.48$	9.5	aragonite	inorganic
‡McCrea (1950)	$1000\ln\alpha = 16.26 * 1000/T(K) - 26.01$	12.9	aragonite	inorganic
Patterson et al. (1993)	$1000\ln\alpha = 18.56 * 1000/T(K) - 33.49$	15.4	aragonite	otolith
Thorrold et al. (1997)	$1000\ln\alpha = 18.56 * 1000/T(K) - 32.54$	19.7	aragonite	otolith
§Böhm et al. (2000)	$1000\ln\alpha = 18.45 * 1000/T(K) - 32.54$	17.9	aragonite	sponge
*Grossman & Ku (1986)	$1000\ln\alpha = 18.07 * 1000/T(K) - 31.08$	18.7	aragonite	mollusk
Grossman & Ku (1986)	$t(°C) = 20.86 - 4.69 * (d^{18}Oc - d^{18}Ow)$	19.0	aragonite	mollusk
Kim & O'Neil (1997)	$1000\ln\alpha = 18.03 * 1000/T(K) - 32.42$	11.9	calcite	inorganic
†Epstein et al. (1953)	$t(°C) = 16 - 4.14 * (d^{18}Oc - d^{18}Ow) + 0.13 * (d^{18}Oc - d^{18}Ow)^2$	14.4	calcite	mollusk
Erez & Luz (1983)	$t(°C) = 16.998 - 4.52 * (d^{18}Oc - d^{18}Ow) + 0.028 * (d^{18}Oc - d^{18}Ow)^2$	15.2	calcite	foraminifera

‡ Recalculated by Zhou & Zheng (2003); § Böhm et al. (2000) added their sclerosponge data to the Grossman and Ku (1986) calibration; * Grossman & Ku (1986) reworked to the form of $1000\ln\alpha$ by Böhm et al. (2000); † Modified by Anderson and Arthur (1983).

3.2.2 Limitations of the paleotemperature equations

Many paleoclimatic studies (e.g., Purton and Brasier, 1997; Dutton et al., 2002; Holmden and Hudson, 2003) use these equations relying on the assumption that bivalves fractionate isotopes in equilibrium. However, without species-specific verification with recent specimens, this is a risky practice. As opposed to corals and brachiopods, bivalves do generally secrete their skeletons in equilibrium (Wefer and Berger, 1991; Chauvaud et al., in press), yet this might not always hold true. In addition, bivalve physiology also plays an important role in the stable isotope ratios recorded in the shells due to the effect of temperature and salinity on growth. Bivalves may be euryhaline (inhabit a wide salinity range) or stenohaline (inhabit a narrow salinity range) and may continue to grow in extreme temperatures or have minimum and or maximum temperature growth hiatuses, all of which will affect the isotopic signal recorded in the shell (e.g., Ivany et al., 2003). The effect of rapidly changing temperature and salinity (and thus $\delta^{18}O_w$) is especially important in coastal areas and even more so in estuaries.

3.2.2.1 Vital effects

Despite the fact that corals and bivalves both calcify rapidly from an internal fluid with varying pH, they show vastly different vital effects. Corals generally precipitate out of isotopic equilibrium, whereas bivalves precipitate in, or close to, equilibrium. The term "vital effect" has been applied to biogenic carbonates that are apparently not formed in isotopic equilibrium (Urey et al., 1951). Different explanations for the vital

effect have been proposed: *kinetic effects* and *carbonate ion effects*. *Kinetic effects* can cause depletions in ^{18}O relative to equilibrium when $CaCO_3$ precipitation is fast enough to allow precipitation of HCO_3^- and/ or CO_3^{2-} before equilibration with H_2O (McConnaughey, 1989a, b). As both C and O are on the same molecule, kinetic effects will act on both isotopes and cause a correlation between the two (Fig. 2B; McConnaughey, 1989a). *Carbonate ion effects* involve equilibrium between $CaCO_3$ and the individual inorganic carbon species (CO_2, H_2CO_3, HCO_3^-, and CO_3^{2-}) of the dissolved inorganic carbon (DIC). The relative abundance of the inorganic carbon species is a function of the pH, with more CO_2 at low pH and more CO_3^{2-} at high pH. McCrea (1950) first demonstrated that the $\delta^{18}O$ value of inorganically precipitated carbonates varied with pH. Usdowski and co-workers suggested that this was the result of equilibrium with the carbonate species, each of which has their own fractionation factor with water (Usdowski et al., 1991; Usdowski and Hoefs, 1993); with the $\delta^{18}O_{VSMOW}$ values at equilibrium with H_2O being 41.2 ‰ for CO_2 (Kim and O'Neil, 1997), 34.3 ‰ for HCO_3^- (Zeebe and Wolf-Gladrow, 2001), 18.4 ‰ for CO_3^{2-} (Usdowski et al., 1991), and -41.1 ‰ for OH^- (McCrea, 1950) (at 19 °C and 25 °C for CO_2) (Fig. 3) [note that $\delta^{18}O_{VPDB} = 0.97002 * \delta^{18}O_{VSMOW} - 29.98$]. Therefore, at low pH, carbonates are enriched in ^{18}O and are depleted in ^{18}O at high pH (Fig. 3). Similarly, pH also changes the $\delta^{13}C$ value of $CaCO_3$, with carbonic acid having the more positive $\delta^{13}C$ value and the carbonate ion having the more negative $\delta^{13}C$ value (see Zhang et al., 1995). These effects are thus equilibrium reactions between the DIC and $CaCO_3$, and no kinetic effects are involved. The carbonate model outlined above has been proposed for both foraminifera (Spero et al., 1997; Zeebe, 1999) and corals (Adkins et al., 2003).

Rollion-Bard et al. (2003) measured $\delta^{11}B$ in addition to $\delta^{18}O$ and $\delta^{13}C$ in their coral samples and used the $\delta^{11}B$ data as a proxy for pH at the site of calcification (see section 3.5). They found that $\delta^{18}O$ did in fact change with pH, but that the change in $\delta^{18}O$ was too large to be explained by the carbonate model, considering the range of pH indicated by the $\delta^{11}B$ data. They therefore hypothesized that this effect is the result of both i) the relative abundance of carbonate species (carbonate model) and ii) pH changing the amount of HCO_3^- formed from the reaction of CO_2 hydration ($CO_2 + H_2O \leftrightarrow HCO_3^- + H^+$) and hydroxylation ($CO_2 + OH^- \leftrightarrow HCO_3^-$), which each have their own equilibration times (Fig. 3), and thus result in different kinetic effects.

Hydroxylation takes considerably more time to reach equilibration then hydration (Johnson, 1982); therefore, more negative $\delta^{18}O$ is expected at higher pH with more HCO_3^- being formed by hydroxylation (i.e., more kinetic effects). Interestingly, Spero et al. (1997) discussed the pH of the external medium and both Adkins et al. (2003) and Rollion-Bard et al. (2003) discuss the pH at the internal calcification site. Nevertheless, McConnaughey suggests that these effects can still be explained by purely kinetic effects (McConnaughey, 2003; Cohen and McConnaughey, 2003).

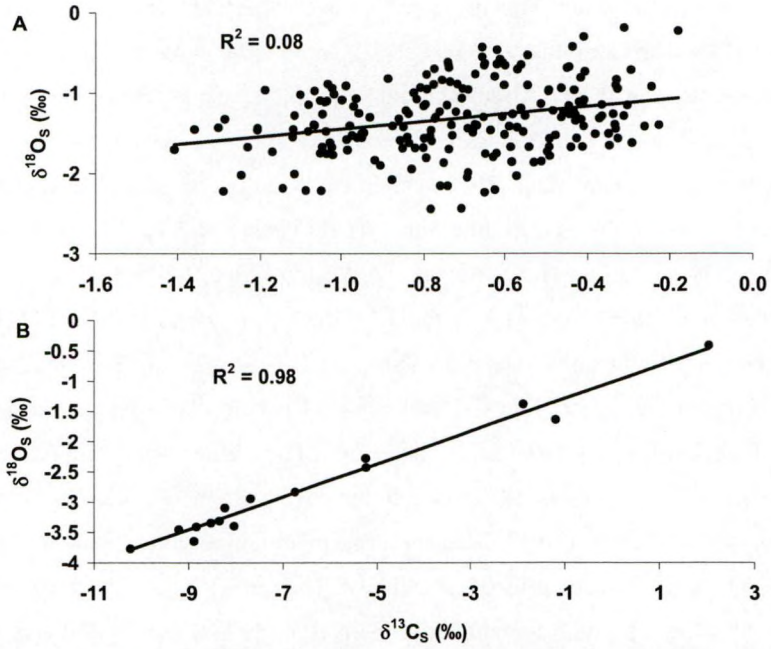

Figure 2. Regression between $\delta^{18}O_S$ and $\delta^{13}C_S$ for a *Saxidomus giganteus* shell (A) and a coral from the Galapagos Islands (B). *S. giganteus* data from Chapter 4 and coral data from McConnaughey (1989a).

The models mentioned above do not explain why bivalves apparently fractionate in isotopic equilibrium with seawater. The pH of bivalve EPF decreases during valve closure and slowly increases after the valves open; Crenshaw and Neff (1969) documented EPF pH changes of ~0.7 units. Changes in calcification rate should also change the pH of the EPF (Crenshaw, 1980). Zeebe (1999) writes that a pH increase of 0.2 to 0.3 results in a decrease in $\delta^{18}O$ of 0.22 to 0.33 ‰ in foraminiferal calcite. Considering a pH change of ~1 in bivalve EPF, we could expect temperature independent changes of nearly 1‰ in bivalve shell carbonate. However, a recent

study has shown that bivalves can precipitate their shells extremely close to oxygen isotopic equilibrium (Chauvaud et al., in press). Therefore, it does not seem that the carbonate ion model is applicable to bivalves being that bivalve EPF pH is most likely changing.

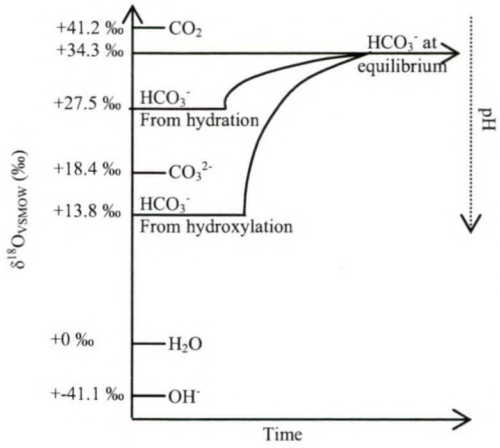

Figure 3. Theoretical evolution of the oxygen isotopic composition of HCO_3^- in solution versus time (at 19 °C and 25 °C for CO_2 and $\delta^{18}O_{H2O} = 0$ ‰). Dotted line illustrates the dominant carbonate species changes from CO_2 to HCO_3^- to CO_3^{2-} with increasing pH, and the HCO_3^- formed by hydroxylation. The HCO_3^- formed by hydroxylation and hydration only reach equilibration after some time as is shown. Figure modified from Rollion-Bard et al. (2003).

The kinetic model is also difficult to apply to bivalves. First, as explained above kinetic effects act on both carbon and oxygen isotopes and result in a significant relationship between both $\delta^{18}O_S$ and $\delta^{13}C_S$, which can be used as a diagnostic of the presence of kinetic effects (McConnaughey, 1989a, b). Figure 2 demonstrates the strong correlation between $\delta^{18}O_S$ and $\delta^{13}C_S$ in a coral with large kinetic effects and the lack of a relationship in a bivalve with little or no kinetic effects present. Second, a prerequisite of kinetic effects is fast calcification rates, and bivalves are known to calcify rapidly. In fact, bivalves often calcify faster than corals. For example, corals have less dense skeletons than bivalves, and can have extension rates ranging from 0.2 to 1 cm/year (e.g., Swart et al. 2005), whereas bivalves can have extension rates ranging from 0.2 to 2 cm/year (e.g., Chapter 8). So why is this kinetic effect not seen in bivalves? Perhaps, as suggested by Weiner and Dove (2003), it is because of the presence of carbonic anhydrase in the shell organic matrix (Miyamoto et al. 1996), which is known to catalyze CO_2 hydration and reduce the kinetic effect (see section 2 above). Another possibility is that the EPF is 'leaky' and a significant amount of H_2O equilibrated carbonate species are entering the EPF directly from seawater (cf. Hickson et al., 1999; Adkins et al., 2003). However, these hypotheses need to be

tested. A model that can account for the isotopic values found in both bivalve shells and corals is required.

3.2.2.2 Time-averaging effects

If environmental factors dominate proxy incorporation, then the signal recorded in the shell should be similar between specimens grown under the same conditions. The $\delta^{18}O_S$ of the aragonite clam *Mercenaria mercenaria*, is a good example of this. Elliot et al. (2003) found that two shells from the same site had very similar $\delta^{18}O_S$ profiles. Nevertheless, there were still important differences between the shells of up to ~0.5 ‰ in some portions of the profiles. They attributed this to the result of time averaging caused by differences in growth rate between shells. Time averaging occurs when shell growth slows and sample interval remains the same, resulting in the same sample size representing (and averaging) more time (see Goodwin et al., 2003, 2004). Time averaging will thus bring the amplitude of the $\delta^{18}O_S$ cycle closer to the mean.

3.2.2.3 The problem of $\delta^{18}O_W$

Coastal settings were important to early people, resulting in numerous shell middens spanning the late Quaternary (e.g., Hetherington and Reid, 2003). It would be beneficial to both archeologists and paleoclimatologists to have well calibrated proxies of temperature in these regions. However, the fact that coastal regions are highly dynamic in nature and the stable isotope ratios in carbonates are dependent on the isotope ratio of the water, which co-varies with salinity (Fig. 4), make these areas difficult for isotope geochemistry. In addition to the problem of variable salinity, variable or multiple source freshwater end-members will cause changes in the salinity-$\delta^{18}O_W$ relationship. This makes using salinity to determine $\delta^{18}O_W$ prone to errors. For example, Ingram et al. (1996) developed a salinity-$\delta^{18}O_W$ relationship for San Francisco Bay based on measurements taken along a salinity gradient over one year ($\delta^{18}O_W$ = Salinity * 0.32 (± 0.01) – 10.90 (± 0.23) (R^2 = 0.98, $p < 0.0001$, n = 64)). The prediction intervals on this relationship are rather large (~ 2 ‰ at a salinity of 27; see Chapter 4); thus using this relationship to determine $\delta^{18}O_W$ for studies involving $\delta^{18}O$ of carbonates is not suitable. Comparable errors were found on the slope and intercept for a salinity-$\delta^{18}O_W$ relationship from the Schelde estuary (see Fig. 4). Although this variability poses serious problems, this variability seems constant, as

an earlier study on the Schelde estuary (1996-1998) found the same relationship as is presented in Figure 4 ($\delta^{18}O_W$ = Salinity * 0.2 – 6.6; Van den Driessche, 2001).

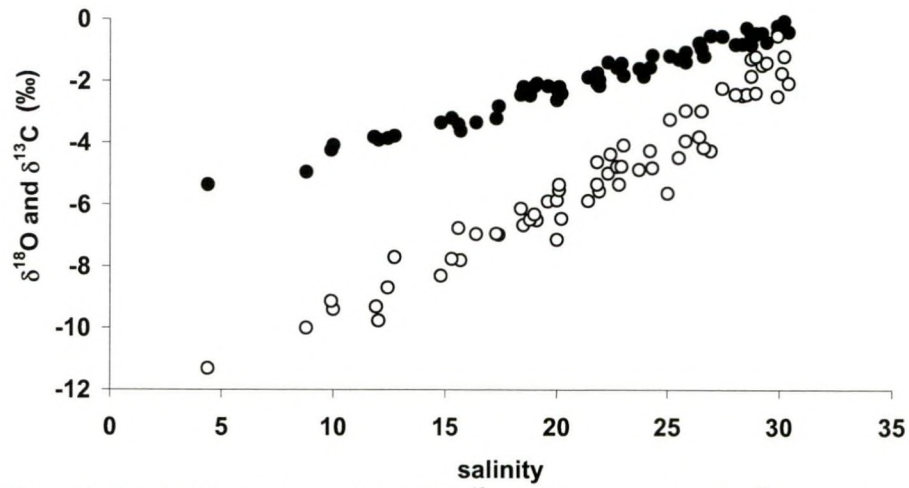

Figure 4. Relationship between salinity and $\delta^{18}O_W$ (filled symbols) and $\delta^{13}C_W$ (open symbols) in Schelde waters (see Chapter 10 for sampling locations) sampled at least monthly over a full year (data from Gillikin, unpublished). The simple linear regressions are $\delta^{18}O_W$ = Salinity * 0.20 (± 0.01) – 6.31 (± 0.20) (R^2 = 0.97, $p < 0.0001$, n = 63) and $\delta^{13}C_W$ = Salinity * 0.39 (± 0.03) – 13.71 (± 0.57) (R^2 = 0.94, $p < 0.0001$, n = 63).

Therefore, choosing species that are stenohaline can partially circumvent the problem of $\delta^{18}O_W$ (Chauvaud et al., in press). However, even the oxygen isotopic signature of open marine waters has changed through geologic time because of glacial – interglacial successions (Shackleton, 1967; Dansgaard and Tauber, 1969; Zachos et al., 1994), which complicates paleotemperature reconstruction even for stenohaline species. Moreover, due to the Raleigh distillation process, marine $\delta^{18}O_W$ is lighter at higher latitudes (see Fig. 5 and Broecker and Peng, 1982; Schmidt, 1998 and Bigg and Rohling, 2000; Benway and Mix, 2004), resulting in different salinity-$\delta^{18}O_W$ relationships at different latitudes (Fig. 5). Having a good estimation of the $\delta^{18}O_W$ is crucial when calculating temperature from $\delta^{18}O_S$, especially in estuarine conditions. For example, only a 0.25 ‰ change in $\delta^{18}O_W$ (or roughly about 1 PSU at mid-latitudes, Fig. 4) results in a calculated temperature difference of 1.1 °C (see section 3.2.1).

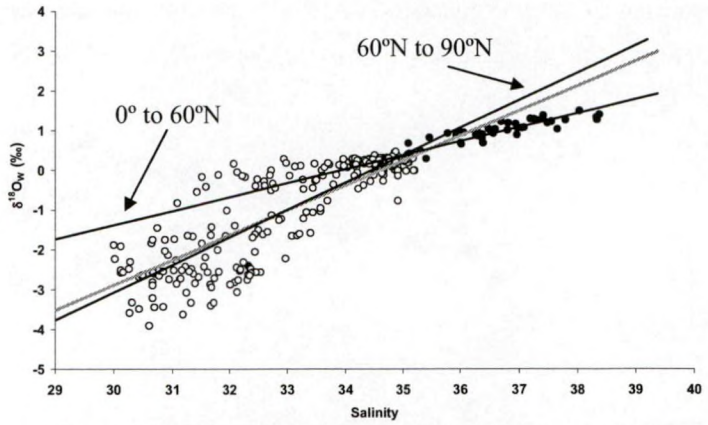

Figure 5. Oxygen isotope data from Atlantic waters plotted against salinity (longitude = 30°W to 10°E). The grey line is the regression of all data (slope = 0.63, R^2 = 0.80) and the other regression lines are for data from the equator to 60 °N (closed symbols; slope = 0.35, R^2 = 0.84) and from 60 °N to 90 °N (open symbols; slope = 0.69, R^2 = 0.78). Data from Schmidt et al. (1999).

A possibility of obtaining paleo- $\delta^{18}O_W$ could be to measure fluid inclusions in bivalve shells, if this fluid was in equilibrium with ambient water in which the bivalves grew. However, Lécuyer and O'Neil (1994) found that fluid inclusions in the shells of six bivalve species were not in oxygen isotope equilibrium with ambient water, but had higher $\delta^{18}O$ values (6 to 18 ‰ higher than the environmental water). They postulated that inclusion waters in shells represent remnants of metabolic fluids produced by the mantle. Thus, inclusion waters in shells probably cannot help solve the paleo- $\delta^{18}O_W$ problem.

3.2.3 Bivalve $\delta^{18}O_S$ as a proxy of past temperatures

With our current analytical capabilities, $\delta^{18}O_S$ can be measured with a precision of about 0.06 ‰ (1σ). This would infer a minimum temperature error of about 0.25 °C. However, given the uncertainties with time averaging, poorly constrained $\delta^{18}O_W$, and possible "vital effects", a more appropriate 'best minimum uncertainty' using bivalve shells is probably on the order of about 1 °C (e.g., Weidman et al., 1994), but large errors can be common when $\delta^{18}O_W$ is unknown (Fig. 6). However, as previously stated, stenohaline species will reduce the $\delta^{18}O_W$ error on SST calculations. Errors may be further reduced by choosing fast growing bivalve species (reduced time

averaging) that have been validated for the absence of vital effects (Chauvaud et al., in press).

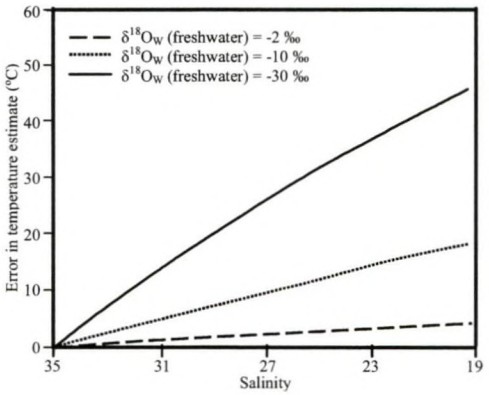

Figure 6. Error in seawater temperature estimate calculated using $\delta^{18}O_S$, assuming $\delta^{18}O_W$ = 0 ‰ and salinity = 35. Error in temperature estimate is a function of both the extent of mixing and the $\delta^{18}O_W$ of the fresh-water and seawater end members. Errors calculated using the calcite-water fractionation factor of Friedman and O'Neil (1977); figure from Klein et al., 1997.

Finally, to use the oxygen isotope paleothermometer, it must be certain that the shells have not undergone diagenetic alteration. Aragonite is metastable (at Earth surface conditions) and is more prone to recrystallization than calcite. However, two types of diagenesis can be distinguished: pre- and post-recrystallization. Pre- recrystallization changes generally affect elemental composition of the carbonate without altering the crystallography or isotopic composition (i.e., seasonal cyclicitity in $\delta^{18}O_S$ and $\delta^{13}C_S$ is preserved) (Walls et al., 1977; Rosenberg, 1980). However, cases where pre-recrystallization stable isotope changes have occurred are known, but the values were far from expected (Elorza and Garcia-Garmilla, 1996, 1998). This is usually diagnosed by high trace element contents of Mn, U, and Fe, accompanied by low Sr and Mg contents (Brand and Veizer, 1980; Kaufman et al., 1996), however, higher Sr in non-recrystallized, diagenically altered *M. mercenaria* shells was also found by Walls et al. (1977). The change in elemental composition can be a result of either ion mobility in the carbonate (Walls et al., 1977) or loss of the organic matrix (Labonne and Hillaire-Marcel, 2000). After recrystallization, aragonite is transformed to calcite and the seasonal cyclicitity in isotope profiles is generally lost and replaced with 'unreasonable' values (Labonne and Hillaire-Marcel, 2000).

Despite the difficulties with the $\delta^{18}O_S$ proxy, it can still be very informative. For example, previous workers have used oxygen isotope ratios in the carbonate of bivalve shells as both salinity (Ingram et al., 1996) and temperature proxies (Weidman et al., 1994; Surge et al., 2001). Moreover, anthropogenic and ecological studies have benefited from $\delta^{18}O_S$ studies. By analyzing shells collected by pre-historic people, the season they inhabited coastal regions can be determined by investigating the last seasonal cycle of $\delta^{18}O_S$ recorded in the shell before it was collected as food (Shackleton, 1973; Jones and Kennett, 1999; Mannino et al., 2003). Ecological data extracted from $\delta^{18}O_S$ data include temperature of growth shutdown, season of maximal growth and longevity (e.g., Buick and Ivany, 2004). However, it is clear that an independent paleothermometer or salinity proxy would be greatly beneficial.

3.3 Carbonate $\delta^{13}C$: Dissolved inorganic carbon or bivalve metabolism?

Early work suggested that skeletal carbon originates directly from dissolved inorganic carbon (DIC) in seawater (Mook and Vogel 1968; Killingley and Berger 1979; Arthur et al., 1983). Since the stable carbon isotopic composition of the DIC ($\delta^{13}C_{DIC}$) is related to salinity (Fig. 4), anthropogenic carbon inputs, productivity, and respiration, $\delta^{13}C_S$ was proposed as a proxy for these environmental variables.

According to the inorganic experiments of Romanek et al. (1992), the equilibration ^{13}C fractionation for aragonite relative to HCO_3^- ($\varepsilon_{carbonate\text{-}bicarbonate}$) is $+ 2.7 \pm 0.6$ ‰ and is $+ 1.0 \pm 0.2$ ‰ for calcite. Therefore, to calculate equilibrium values, the values above are simply added to the $\delta^{13}C$ value of DIC in seawater, which is mainly composed of HCO_3^-. However, more recently, Dillman and Ford (1982); Swart (1983), Tanaka et al. (1986), McConnaughey et al. (1997), Furla et al. (2000), Lorrain et al. (2004a), and others have proposed that the process of calcification utilizes carbon from two reservoirs, seawater DIC and metabolic DIC, with the latter composed of respiratory CO_2. The external source of carbon, seawater DIC, typically has a $\delta^{13}C$ value close to 1 ‰, whereas the internal carbon source, metabolically derived CO_2, has a highly depleted ^{13}C isotopic signature similar to the respiring tissues (about −10 to −25 ‰; Nier and Gulbransen, 1939; Craig, 1953; Fry, 2002;

Lorrain et al., 2002; Bouillon et al., 2004a). The incorporation of such carbon would result in lower $\delta^{13}C_S$ values, obscuring the signal derived from water $\delta^{13}C_{DIC}$. Tanaka et al. (1986) first suggested that up to 85% of the carbon in bivalve shells was metabolic in origin, but McConnaughey et al. (1997) have moderated this idea, suggesting that in aquatic invertebrates, less than 10 % of respired CO_2 is incorporated in the shell, resulting in only small decreases of shell $\delta^{13}C$ (< 2 ‰) with respect to equilibrium values.

Strong ontogenic decreases in $\delta^{13}C_S$ are evident in many bivalves (Kennedy et al., 2001; Elliot et al., 2003). Lorrain et al. (2004a) proposed a simple model where this ontogenic decrease is caused by an increase in the amount of respiratory CO_2 produced by the bivalve. This model is based on the relationship between metabolic rate and body size: as bivalves grow, their metabolism increases while shell growth slows. Therefore, more metabolic CO_2 will be available while the amount needed for shell growth is reduced, resulting in more metabolic carbon being incorporated into the shell. However, this is apparently species-specific. While in some species, strong ontogenic decreases in $\delta^{13}C_S$ have been noted (Krantz et al., 1987; Kennedy et al., 2001; Keller et al., 2002; Elliot et al., 2003; Lorrain et al., 2004a), in others there is no discernable decrease (Buick and Ivany, 2004; Gillikin et al., 2005a; Chapter 4).

Although metabolic carbon can complicate the $\delta^{13}C_S$ profile, $\delta^{13}C_S$ can still be a useful indicator of environmental conditions. It is known that $\delta^{13}C_{DIC}$ has large seasonal fluctuations due to respiration, photosynthesis, carbonate dissolution/ precipitation, etc. (Mook, 1971; Hellings et al., 2001; Bouillon et al., 2003). However, in well-flushed estuaries with short residence times, $\delta^{13}C_{DIC}$ may follow a simple linear relationship with salinity, especially in salinities above 25 (Fig. 4 and Mook, 1968, 1971; Surge et al., 2001; Fry, 2002). Furthermore, it is well known that freshwater input is depleted in ^{13}C (Mook, 1971). Therefore, a drop in salinity will undoubtedly cause a decrease in $\delta^{13}C_{DIC}$. The $\delta^{13}C_S$ profile obtained from a transplantation experiment clearly illustrates this (Fig. 7, see also Chapter 10). The shell in Figure 7 was transplanted from a marine to an estuarine site, resulting in the abrupt drop in $\delta^{13}C_S$ values.

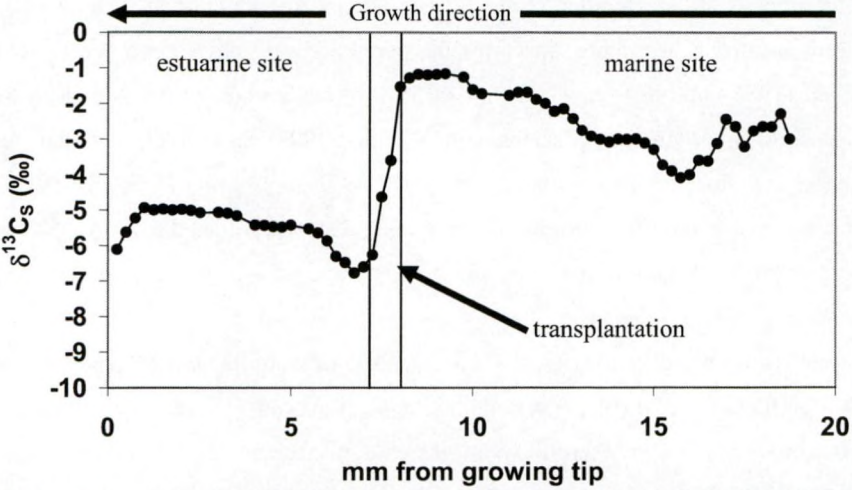

Figure 7. Carbon isotope signature recorded in a *Mytilus edulis* shell transplanted from a marine site (salinity ~ 35) to an estuarine site (salinity ~ 20). The change is probably more abrupt, but time averaging slightly smoothes the signal. Data from this study, see Chapter 10.

3.4 Organic matrix stable isotopes: An indicator of paleo-foodwebs

In addition to calcium carbonate, bivalve shells also contain up to 5 % organic matter (Marin and Luquet, 2004; Rueda and Smaal, 2004). The stable isotope composition of this organic matter has also been used to extract information about past environments. O'Donnell et al. (2003) measured $\delta^{13}C$, $\delta^{15}N$ and $\delta^{34}S$ in both the soft tissues and shell organic matter of modern and fossil *M. mercenaria*. They found that the difference ($\Delta_{tissue\text{-}shell}$) was minimal for $\delta^{13}C$ (0.1 ‰) and slightly larger for $\delta^{15}N$ (0.7 ‰) and $\delta^{34}S$ (1.8 ‰). Using these offsets ($\Delta_{tissue\text{-}shell}$), they were able to extract information about the diet of these bivalves from the Quaternary. Data regarding the $\delta^{13}C$ values of fossil bivalve respiration can also assist in understanding the influence of metabolic carbon and possibly help to decipher past $\delta^{13}C_{DIC}$. For example, if the $\delta^{13}C$ of metabolic CO_2 is known, and if the percent metabolic carbon incorporation is constant and known, then the $\delta^{13}C_{DIC}$ can be calculated. Furthermore, compound specific carbon isotopic analysis also can provide both dietary and environmental information (Cobabe and Pratt 1995; CoBabe and Ptak, 1999). However, more knowledge of species-specific metabolic carbon incorporation is needed. For example, Stott (2002) could not find a relationship between shell organic matter $\delta^{13}C$ and diet $\delta^{13}C$ in a

snail. Analysis of stable isotopes in shell organic matter is a promising field and has received some attention in studies on foraminifera (Stott, 1992; Shemesh et al., 1993; Maslin et al., 1996, 1997; Kump and Arthur, 1999), but remains relatively unstudied in bivalves.

3.5 Non-traditional stable isotopes: New potentials for environmental proxies

Since the arrival of multi collector - inductively coupled plasma mass spectrometry (MC-ICP-MS) technology, isotopes other than the traditional H, C, O, N and S have been receiving much attention. Strontium isotopes in bivalve shells have proven to be an excellent indicator of salinity and water source (Holmden and Hudson, 2003; Vonhof et al., 1998, 2003), with no vital effects occurring (Reinhardt et al., 1999). Boron isotopes have been recently shown to be an indicator of pH in foraminifera (Sanyal et al., 2001) and corals (Hönisch et al., 2004). This is due to the pH influence on the availability of isotopically light $B(OH)_4^-$ versus $B(OH)_3^-$ (Hemming and Hanson, 1992). However, Pagani, et al. (2005) showed the presence of vital effects, which complicate the use of this proxy in foraminifera. Calcium isotopes ($\delta^{44}Ca$) in inorganic aragonite and cultured planktonic foraminifera are positively correlated to temperature (Nägler et al., 2000; Gussone et al., 2003), however, a recent study has highlighted problems with this proxy in foraminifera from core-top sediments (Sime et al., 2005). Magnesium isotopes have been used to gain insight on the $\delta^{26}Mg$ ratio of past seawater. de Villiers et al. (2005) have shown that the $\delta^{26}Mg$ ratio of seawater allows important inferences about the relative contribution of different lithologies to the global continental weathering flux to be made, particularly carbonate versus silicate weathering. They also suggest that echinoderm skeletons can serve as archives of seawater $\delta^{26}Mg$, allowing the reconstruction of past weathering fluxes. However, this proxy also is species-specific. For example, Chang et al. (2004) report that $\delta^{26}Mg$ ratios in coral aragonite are similar to seawater indicating little biologic influence on Mg incorporation; but in opposition, there was a large difference between foraminiferal calcite and seawater, indicating a biological fractionation. Studies involving these isotopes (and others) are rather new and offer promising results for both understanding bivalve biomineralization and paleo-climate reconstruction.

4 TRACE ELEMENTS

4.1 Background

Trace elements in biogenic carbonates other than bivalves have been used as environmental proxies with much success (Beck et al., 1992; Lazareth et al., 2000; Rosenheim et al., 2004, 2005). Data on bivalves, however, have been somewhat contradictory and seem less promising, but more work is needed to confirm this.

Elements (Me) are typically reported as a ratio to calcium (i.e., Me/Ca). The partitioning between the water and shell is expressed as a non-thermodynamic partition coefficient (D_{Me}), which is defined as:

$$D_{Me} = (Me/Ca)_{carbonate} / (Me/Ca)_{water} \quad (8)$$

where Me/Ca are typically given as molar ratios (Henderson and Kraček, 1927). This uses the idea of "trace" (Me) and "carrier" (in this case Ca) components in the solid and solution. A major problem with the partition coefficient given above is that it does not take activity coefficients into account. Activity coefficients can seriously alter D_{Me} as calculated above (Morse and Bender, 1990). However, due to the difficulties in calculating activity coefficients (Morse and Bender, 1990), they are often not considered in studies using elements in carbonates as proxies. For example, Lea and Spero (1992, p. 2673) write "Because of the inherent difficultly in determining the true activity coefficients of ions in seawater, it is common practice to … [use] … a single distribution coefficient relating the ion ratios of the shell material to the total concentration ratios in seawater." There is some confusion about the definitions of partition coefficient and distribution coefficient. Morse and Bender (1990) suggested we do not use 'distribution coefficient' to "avoid confusion with a thermodynamic distribution constant, K_D"; but this does not unambiguously define partition coefficient and distribution coefficients in terms of activity coefficients. However, Mucci and Morse (1990) clearly state that the *partition coefficient* (D_{Me}) is non-thermodyanmic and does not include activity coefficients, while in opposition the thermodynamic *distribution coefficient* (K_D) must include activity coefficients. Yet,

there has still been some confusion about the use of these terms. Some papers use distribution coefficient (Shen et al., 1996; Stecher et al., 1996; Campana, 1999), while others use partition coefficient (Bath et al., 2000; Reuer et al., 2003; Zacherl et al., 2003; Freitas et al., 2005) and neither include activity coefficients. Considering that some papers dealing with inorganic precipitates do use activity coefficients (e.g., Dietzel et al., 2004), which are then used to compare with biogenic carbonates, makes it clear that some standardization is required. Therefore, in this text D_{Me} (eq. 8) is defined as a partition coefficient, according to Mucci and Morse (1990).

To understand if bivalve shells are partitioning elements in equilibrium with the water in which they grow, we typically look at data of inorganic precipitation experiments. However, as stated earlier, the shell is precipitated from the EPF and not directly from seawater. Thus to compare biogenic carbonates with inorganic precipitations, the EPF should ideally be used for $(Me/Ca)_{water}$, which has not often been done. It should also be stated here, in light of the discussion above, that the higher amount of organic molecules in the EPF (or calcifying space of any organism that calcifies from an internal fluid, e.g., corals, fish, sclerosponges, etc.) will undoubtedly change the activity coefficient as compared to the external water and alter the partition coefficient. Nevertheless, D_{Me} is discussed here in terms of external water (i.e., not EPF), because there are limited or no data available regarding shell – EPF partition coefficients and it provides a basic starting point. However, it should also be kept in mind that many bivalves live at the sediment-water interface, where the chemistry of the water can be different than the overlying water, in terms of both elemental composition (Thamdrup et al., 1994; RiveraDuarte and Flegal, 1997; Gueiros et al., 2003) and isotopic composition (McCorkle et al., 1985).

In addition to the partition coefficient, it is important to note that similar to stable isotopes, shell mineralogy will also influence the inorganic composition of the shell. The different polymorphs of $CaCO_3$ (e.g., calcite or aragonite) differ significantly in their chemical compositions due to the differences in the crystal structure of the polymorphs. Finally, diagenesis can more easily affect elemental contents than isotopes (see last paragraph of section 3.2.3), thus diagenesis must be assessed chemically before shells can be used. Nevertheless, several elements have shown their

potential as environmental proxies: Sr/Ca, Mg/Ca, Ba/Ca, Mn/Ca, B/Ca and Pb/Ca, which will be discussed below.

4.2 Trace element proxies

4.2.1 Sr/Ca and Mg/Ca: Temperature and salinity proxies?

Strontium and magnesium are probably the most well-studied elements in carbonates. Both Sr/Ca and Mg/Ca ratios have been proposed as salinity-independent temperature proxies in carbonates (Weber 1973; Beck et al., 1992; Nürnberg et al., 1996; Elderfield and Ganssen, 2000; Rosenheim et al., 2004) as these ratios in water usually only significantly differ from seawater at salinities less than 10 (Dodd and Crisp, 1982, Klein et al., 1996a, b). However, these proxies are probably strongly species-specific, and thus calibrations must be carried out for each new species studied (Skinner and Elderfield, 2005).

Mineralogy significantly affects Sr incorporation, with aragonite typically containing about seven times more Sr than calcite due to the differences in the crystal lattice structure and D_{Sr} being strongly precipitation rate dependent in calcite (Kinsman and Holland, 1969; Lorens, 1981; Tesoriero and Pankow, 1996). However, aragonitic bivalve shells seemingly do not contain much more Sr than calcite bivalve shells (e.g., Stecher et al., 1996 and Vander Putten et al., 2000), indicating biological regulation. Inorganic precipitation experiments have shown that D_{Sr} in aragonite is inversely related to temperature (Kinsman and Holland, 1969; Dietzel et al., 2004) and is independent of precipitation rate (Zhong and Mucci, 1989). In opposition to aragonite, experimental studies on inorganic calcite have shown that the Sr/Ca ratios of calcite are strongly dependent on precipitation rates (Lorens, 1981; Morse and Bender, 1990; Tesoriero and Pankow, 1996), while there is only minor temperature dependence for Sr incorporation (Katz et al., 1972). Indeed, such kinetic effects have been shown to control Sr/Ca variations in biogenic calcite such as coccoliths (Stoll and Schrag, 2000; Stoll et al., 2002a, b), planktonic foraminifera (Lea, 1999), and bivalves (Lorrain et al., subm. a). Nevertheless, a positive temperature influence on Sr incorporation has been observed in coccoliths (Stoll et al., 2002a, b) and foraminifera (Lea et al., 1999), although temperature and growth rate are highly correlated themselves (Lea et al., 1995). However, Lorrain et al. (subm. a) were able to illustrate that the total quantity

of carbonate precipitated for a given time by the scallop, *Pecten maximus*, was highly correlated with Sr/Ca ratios (R^2 = 0.74), thus illustrating strong kinetic effects. In addition to mineralogy, temperature and precipitation rates, water Sr/Ca ratios and shell Mg/Ca ratios have also been proposed as possible co-variables of Sr incorporation in biogenic and abiogenic calcite (Lorens and Bender, 1980; Mucci and Morse, 1983, Carpenter and Lohmann, 1992).

Inorganic aragonite studies have shown that the Mg/Ca ratio displays a negative dependence on temperature (Gaetani and Cohen, 2004). This is similar to what has been found in sclerosponges (Swart et al., 2002a; Rosenheim et al., in press), but is in contrast to the positive trend observed in coral skeletons (Watanabe et al., 2001) and aragonitic bivalve shells (Takesue and van Geen, 2004). The inverse is true for inorganic calcite where a positive trend is observed between Mg/Ca and temperature (Mucci, 1987), which is similar to bivalve shells (Klein et al., 1996a).

In conclusion, Sr/Ca in both aragonitic and calcitic bivalves is seemingly dominated by growth rate (Stecher et al., 1996; Klein et al., 1996b), despite the lack of precipitation rate effects in inorganic aragonite. Therefore, unlike corals, Sr/Ca in bivalves is not a direct paleotemperature proxy, however, may be linked to temperature through growth rate, which itself is often temperature controlled (Schöne et al., 2002, 2003a; Strom et al., 2004). Ratios of Mg/Ca in aragonitic bivalves have been shown to weakly correlate with temperature (Takesue and van Geen, 2004), however, other processes most likely are present and complicate the use of this proxy. Klein et al. (1996a) reported that Mg/Ca in the calcitic bivalve *Mytilus trossulus* is an excellent temperature proxy, which can provide temperature with an approximate error of ± 1.5 °C. However, Vander Putten et al. (2000) did not find a clear relationship between Mg/Ca and temperature in *Mytilus edulis*. Clearly more work is needed to determine if Mg/Ca ratios can be used as a temperature proxy in bivalves, however, it does not seem promising.

4.2.2 Ba/Ca & Mn/Ca: A proxy of productivity?

Inorganic studies have found that there is an even stronger negative relationship between D_{Ba} and temperature than between D_{Sr} and temperature in aragonite (Dietzel et al., 2004). To our knowledge, there have not been similar studies on the

temperature dependence of D_{Ba} in inorganic calcite. However, a precipitation rate effect was noted in calcite (Tesoriero and Pankow, 1996) as well as an influence of Mg^{2+} content of the calcite (Kitano et al., 1971). Nevertheless, the typical bivalve Ba/Ca profile in both aragonite and calcite bivalve shells does not indicate a temperature, precipitation rate or Mg^{2+} content effect (see Stecher et al., 1996 and Vander Putten et al., 2000).

Stecher et al. (1996) found sharp episodic Ba/Ca peaks in the aragonite shell of *Mercenaria mercenaria*. They postulated that these peaks were caused by sudden influxes of barite to the bottom waters caused by phytoplankton blooms. Later, Vander Putten et al. (2000) and Lazareth et al. (2003) also reported similar Ba/Ca profiles in calcitic bivalves. To date, no study has confirmed the link between Ba/Ca peaks in the shell and barium rich phytoplankton blooms. However, Torres et al. (2001) found a relationship between the Ba/Ca ratios in clam shells and water Ba/Ca ratios and Becker et al. (2005) found that juvenile mussel shells (< 2.5 mm) from bays had significantly higher Ba/Ca ratios than mussels from the open coast. This indicates that Ba/Ca ratios in bivalve shells may be a promising proxy of seawater Ba/Ca ratios. Although the relationship between Ba/Ca and salinity is estuary dependent (Coffey et al., 1997), Ba/Ca in estuarine bivalve shells may be used as a salinity indicator, akin to $\delta^{13}C_S$. Moreover, paleo-Ba/Ca river discharge to the ocean is valuable information for work involving the sedimentary barium record.

There has been limited work focusing on Mn/Ca ratios in bivalve shells. Both Vander Putten et al. (2000) and Lazareth et al. (2003) found that Mn/Ca profiles in calcite bivalve shells were similar to Ba/Ca profiles ($R^2 = 0.76$ from Lazareth et al., 2003). They postulate that this could be caused by an increase in Mn rich phytoplankton or an increase in dissolved Mn. They further propose that the Ba/Ca and Mn/Ca peaks may each be associated with the occurrence of specific types of phytoplankton. However, in inorganic calcite, D_{Mn} is heavily precipitation rate dependent, exhibiting a strong negative correlation (Lorens, 1981). Furthermore, in aragonitic corals, Mn/Ca ratios have been shown to have seasonal cycles that follows SST and not river discharge, with a possible biological overprint (Alibert et al., 2003) and has also been linked with upwelling (Delaney et al., 1993).

4.2.3 B/Ca as a salinity proxy

Furst et al. (1976) was the first to propose that the boron content of bivalve shells may be used to determine paleo-salinity and later Roopnarine et al. (1998) and Takesue et al. (2003) confirmed this. However, in both foraminifera and corals, a primary temperature control on B concentration was noted (Sinclair et al., 1998; Fallon et al., 1999; Wara et al., 2003), which could overprint the salinity effect and complicate interpretation.

4.2.4 Pb/Ca and other heavy metals as records of anthropogenic pollution

There has been much interest in using biogenic carbonates as recorders of anthropogenic pollution. Both corals and sclerosponges have been shown to accurately record dissolved lead concentrations (Shen and Boyle, 1987; Lazareth et al., 2000). In bivalve shells, lead has received much attention and seemingly reflects environmental Pb concentrations in both calcite (Bourgoin, 1990) and aragonite (Pitts and Wallace, 1994) shells. Other heavy metals in bivalve shells such as Cu, Zn and Cd have also been shown to be promising recorders of the environmental pollution (Richardson et al., 2001; Yap et al., 2003). Bivalve shells not only allow retrospective studies of pollution, but are easier to handle then soft tissues and have often reported to have less inter-shell variability (Bourgoin, 1990; Yap et al., 2003; Cravo et al., 2004).

5. CONCLUSIONS

Bivalve shell geochemistry, despite being studied for more than 50 years, is still not a straightforward link to paleo-environmental conditions. There are strong species-specific effects present for many proxies. Furthermore, biomineralization is an organic process, which is not fully understood. Many proxies remain un- or under-studied and new proxies still need to be explored when technology opens new avenues (e.g., MC-ICP-MS). Therefore, there is an urgent need to fill the gaps in bivalve shell geochemistry and biomineralization in order to deconvolve exogenous and endogenous effects.

Chapter 2

Materials and methods:
Procedures, equipment, precision and accuracy

Foreword

This section is meant to give more details to the material and methods outlined in the separate chapters. Each chapter has been written in the form of a scientific paper to be submitted to an international peer-reviewed journal, which limits the amount of information in each chapter's materials and methods.

Table of Contents

1 SAMPLE COLLECTION AND PREPARATION

1.1 Bivalves

1.1.1 Shells

Three species of bivalves are included in this study: the common blue mussel *Mytilus edulis* (L.), from the family Mytilidae, and two species from the Veneroidea family, the hard clam *Mercenaria mercenaria* (L.), and the butter clam *Saxidomus giganteus* (DeShayes, 1839) (Fig. 1). All bivalves used in this study were **collected** by hand aside from some of the specimens of *Mercenaria mercenaria* provided by C. H. Peterson (see Chapters 5, 8, and 9), which were collected using a mechanical harvesting method (see Peterson et al., 1983, 1987). After collection, the valves were pried apart and tissues were removed. Individual valves were then air dried and sectioned as outlined below.

Shells to be **sectioned** were glued to glass slides with quick setting epoxy and then placed in an oven at 60°C for 10 minutes to set the epoxy. Shells were then cut with a wet slow speed diamond saw at approximately 200-350 RPM. Purified water was used in the water well of the saw. Shells were sectioned along the axis of maximal growth to obtain the maximal time resolution (i.e., more shell per unit time = more samples per unit time and less time averaging). Shell sections were then rinsed with MilliQ water and air dried.

The shell sections were originally broken by hand to a desirable size (to fit in the laser ablation cell of the LA-ICP-MS, see section 2.4.3), but it was noticed that the laser responded differently near this break. The signal intensities of the ICP-MS would consistently lower near this break, which was hypothesized to be caused by micro-fractures in the shell slightly changing the structure. To avoid this, shell sections were cut with the saw to the desirable length (< 5 cm) and the 1 mm thickness of the saw blade was taken into account when assembling the geochemical profiles. Afterwards, sections were mounted on glass slides to facilitate sampling with the microdrill (Fig. 2).

For certain aspects of this study, bivalve shells were **marked with calcein** ($C_{30}H_{26}N_2O_{13}$), a fluorescent dye, in order to have a clear dateable mark in the shells (see Willenz and Hartman, 1985; Rowley and Mackinnon, 1995; Rosenheim et al., 2004). Initially, the method of Kaehler and McQuaid (1999) was attempted. Their method involves injecting calcein directly into the mantle cavity of the bivalve *in situ*. However, no trace of calcein was found in the shell using this method, so the method outlined in Rowley and Mackinnon (1995) was used. Briefly, living bivalves were placed in seawater containing 200 mg of calcein per liter for 12 to 24 hours. Afterwards, they were placed in clean seawater for a few hours to allow them to purge themselves of the dye before being placed back into their holding tanks. To visualize the calcein stain, shells were sectioned as described above.

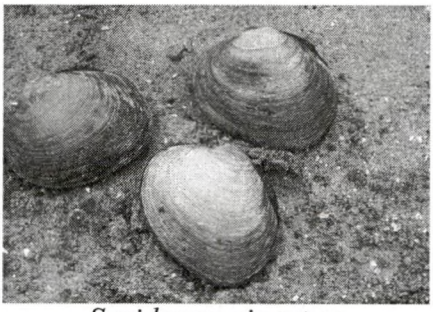

Saxidomus giganteus

Mercenaria mercenaria

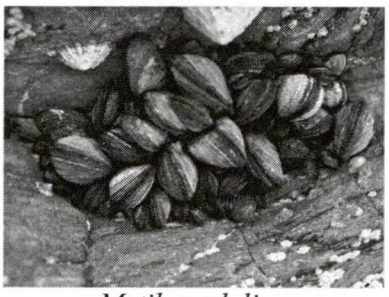

Mytilus edulis

Figure 1. The three bivalve species used in this study (note that only *M. edulis* is in natural position, the two clam species are infaunal – they burrow in the sediment). Approximate shell sizes can be seen in Fig. 4.

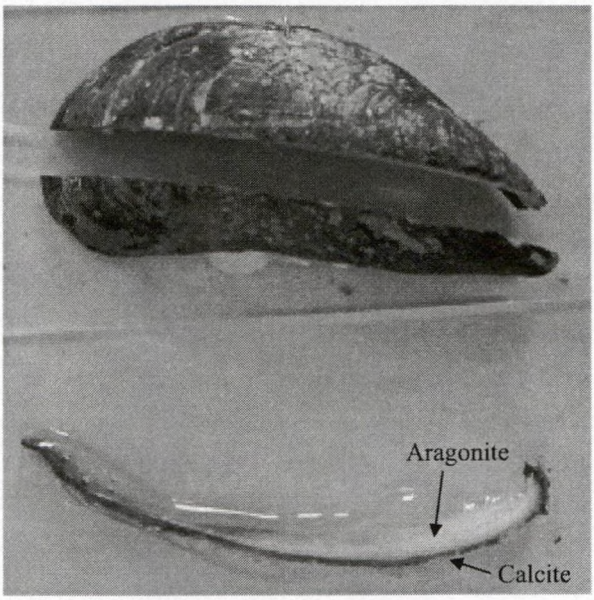

Figure 2. Sectioned *M. edulis* shell (top) and section mounted on glass slide (bottom). Notice the dark calcite layer and white aragonite layer on the section. The shell is ~ 5 cm in length.

1.1.2 Soft tissues

Soft tissues were removed from the valves using a scalpel. In some instances, separate tissues were dissected (e.g., mantle, gills, foot, muscle) whereas in other cases, the bulk tissue was used. After dissection, tissues were frozen to -20 °C and then freeze dried. For stable isotope analysis, dry tissues were homogenized using an agate mortar and pestle. Whole tissues were used for elemental analysis (e.g., Ba, Sr, Ca) and were not homogenized to reduce contamination.

Tissues designated for **stable isotope** analysis were prepared following Bouillon (2002). Briefly, one mg of homogenized tissue was subsampled and placed in a silver cup (5 x 12 mm). The sample was then decalcified by adding a few drops of dilute HCl *in situ*, after which the sample was dried for 24 hours at 60 °C and folded closed.

Tissues designated for **elemental analysis** were prepared following the protocol of Blust et al. (1988). Briefly, samples were transferred to clean Teflon containers

(bomb, or Savilex) and were weighed. Then 2 ml of bi-distilled HNO_3 was added and the containers were closed and allowed to digest overnight in a fume hood. The next day the samples were microwave digested in open vials, using the following power program: 4 minutes at 80 watts, 2 minutes at 160 watts, then 1 ml of H_2O_2 was added and samples were microwaved again for 2 minutes at 240 watts and finally for 3 minutes at 320 watts. The digested tissue samples were then analyzed with the High Resolution - Inductively Coupled Plasma - Mass Spectrometer (HR-ICP-MS; see section 2.4.2).

1.1.3 Hemolymph

After draining the mantle cavity fluid, hemolymph was drawn from the adductor muscle using a sterile syringe and needle after slightly prying the valves apart with a scalpel blade. Other studies have sampled hemolymph by inserting the needle through the umbone and into the adductor muscle (Fyhn and Costlow, 1975; Allam et al., 2000; Lorrain et al., 2004b, in prep), however, I found the method of prying the valves apart an easier method which avoided sampling other fluids with a higher degree of certainty. A strong vacuum and slow retrieval of hemolymph with no tissue mater indicated a successful hemolymph extraction (C. Paillard, Institut Universitaire Européen de la Mer, Plouzané, France, pers. comm.). Furthermore, this method was tested using a highly visible dye: calcein (see also section 1.1.1). After a few minutes in calcein, bivalves were sampled for hemolymph and the hemolymph was visually inspected for calcein. In all five individuals tested, no calcein was present in the hemolymph sample although it was clearly visible in the fluid remaining in the mantle cavity. This indicates that the hemolymph sampling procedure included only hemolymph.

Samples for **hemolymph $\delta^{13}C$** analysis were immediately transferred to He flushed and sealed headspace vials (6 ml, 22 x 38 mm, Supelco, ref. 27292) and one or two drops of supersaturated $HgCl_2$ solution (7 g $HgCl_2$ in 100 ml of MilliQ water) was added using a syringe and needle (see note about using copper sulfate instead of $HgCl_2$; section 1.2.1, page 36). Samples were stored at room temperature until analysis using the same procedure as for $\delta^{13}C_{DIC}$ (see section 2.2.4).

Samples for **elemental analyses** were transferred to Eppendorf micro-centrifuge tubes and were stored frozen until analysis. Procedural blanks were prepared by drawing MilliQ water into a new syringe and injecting it into an Eppendorf tube; blanks were treated in the exact same manner as samples. The day before analysis, samples were defrosted and 150 µl sample (if total sample volume was < 150 µl, then the maximum available was used) was pipetted into a clean Teflon bomb. The sample was digested by adding 150 µl HNO_3 (sub-boiling distillation) and 150 µl H_2O_2 (Merck suprapur) and allowing the reaction to take place in the sealed bomb at 60 °C for more than 12 hours (overnight). The bombs were then cooled at room temperature and 300 µl of 10 ppb In and Re was added as internal standards to control instrument fluctuations (1 ppb final concentration). The sample was further diluted by adding MilliQ until the final volume was 3 ml. Samples were then analyzed on the HR-ICP-MS (see section 2.4.2).

1.2 Water column

1.2.1 $\delta^{18}O$ of water

Water samples for $\delta^{18}O$ analysis were taken by filling 100 ml polyethylene containers and adding 60 µl of supersaturated $HgCl_2$ solution (7 g per 100 ml). Containers were capped tightly and wrapped with Parafilm to avoid evaporation and were stored at room temperature. Although $HgCl_2$ was used throughout this study, its use as a biocide is not recommended: $HgCl_2$ is highly toxic and difficult to dispose of properly. A better biocide is copper sulfate ($CuSO_4$), which is efficient at stopping biological activity and is far less toxic to humans (see Winslow et al., 2001). Although there have been some problems using this biocide in some groundwater samples, with a blue milky precipitate forming (Bassett et al., 2002), this seems an adequate alternative for most samples. Copper sulfate has been evaluated in waters with salinities ranging from 0 to 32 and at ~2.5 mg/ml, $CuSO_4$ outperformed $HgCl_2$ as a biocide (T. J. Boyd, US Naval Research Laboratory, Washington, DC, USA, posted to ISOGEOCHEM list, 31 March 2004). It is recommended that future studies assess using $CuSO_4$ in place of $HgCl_2$.

1.2.2 $\delta^{13}C$ of DIC

Water samples for determination of $\delta^{13}C$ of dissolved inorganic carbon (DIC) were sampled by gently over-filling headspace vials (25, 20, 10 or 6 ml) with seawater. Vials were rinsed with seawater three times before sampling. Sixty microliters of supersaturated $HgCl_2$ solution was added and the vials were capped and stored at room temperature until analysis. However, copper sulfate is recommended in place of $HgCl_2$ here as well (see section 1.2.1 above)

1.2.3 $\delta^{13}C$ of particulate organic matter

Particulate organic matter was sampled by filtering 250 to 500 ml of water through 47 mm diameter pre-combusted (12 hours at 450 °C) glass fiber filters (Whatman, GF-F). Filters were then processed following Lorrain et al. (2003). Briefly, filters were dried at 60 °C and stored in Millipore PetriSlides until analysis. Before analysis, filters (samples and blanks) were subsampled by punching out circular sections with a 14 mm diameter hand punch. These punch-outs were then decalcified by placing them in acid fumes (HCl) for several hours under partial vacuum (see Lorrain et al., 2003). After drying at 60 °C, filters were placed into tin cups which were folded closed.

1.2.4 Dissolved elements

Field samples for dissolved elements were usually transported back to the laboratory for filtration (except when syringe filters were used, see further). 250 to 500 ml of seawater was filtered through cellulose filters (Osmonics poretics, polycarbonate, 0.4 micron, 47 mm) using a dedicated filtration apparatus. The filtration apparatus was stored in 5 % HNO_3 between uses. Blanks were prepared by filtering MilliQ water through the same system and blank filter. A few ml of the filtered water sample was first used to rinse a 30 ml Nalgene polyethylene bottle after which 30 ml of sample was added to the bottle with 60 µl bi-distilled HNO_3. For certain applications where the particulate matter was not important, samples were filtered with syringe filters (Macherey-Nagel; Chromafil A45/25; cellulose mixed esters; 0.45 µm pore size, 25

mm diameter) and stored as detailed above. Procedural blanks were also taken when using this method by filtering MilliQ water.

1.2.5 Particulate elements

Particulate elements were sampled by using the preweighed cellulose filters discussed above (section 1.2.4). After filtered water samples were removed from the filtration apparatus, filters were rinsed with about 10 ml of MilliQ water, dried at 60 °C overnight and stored in Millipore PetriSlides until digestion. Digestion took place in clean Teflon bombs (cleaned with a blank digestion). 3 ml 'suprapur' HCl, 1 ml 'suprapur' HNO_3 and 2 ml Merck 'suprapur' HF were added to the filter in the bomb and the bomb was tightly capped and placed in the oven at 60 °C overnight. The next day, bombs were visually inspected for completion of digestion. On a few occasions, more acid was added due to incomplete digestion. Then bombs were cooled and opened and were evaporated to near dryness on a hot plate at 90 °C. The sample was then reconstituted with 750 µl suprapur HNO_3 and brought to a final volume of 15 ml with MilliQ water. Note that samples taken from laboratory experiments in aquaria did not include HF in the digestion due to the unlikelihood of particulate silica being present.

1.2.6 Phytoplankton pigments

In the field (i.e., within 15 to 30 minutes of sample collection), 200 to 500 ml of seawater was filtered through a Whatman GF-F filter, wrapped in aluminum foil and place in liquid nitrogen; three replicates were taken at each sampling. Upon return to the laboratory, samples were transferred to a –85 °C freezer until analysis. It has been previously determined that the samples are preserved like this for up to 1 year (E. Antajan, VUB, pers. comm.). Samples were either analyzed at the Vrije Universiteit Brussel (VUB) or at the Netherlands Institute for Ecology – Center for Estuarine and Marine Ecology (NIOO-CEME), Yerseke, The Netherlands. The samples (Schelde, November 2001 to March 2002) analyzed at the VUB were treated as outlined in Antajan et al. (2004). Briefly, the frozen filters were cut into small pieces and were sonicated in centrifuge tubes (on crushed ice), with 2 ml of 100 % cold acetone using

a Labsonic sonicator equipped with a 4 mm diameter probe inserted directly into the solvent (2 x 15 seconds). After sonication, samples were kept at 4 °C for 2 h before centrifugation for 3 minutes at about 700 g. Supernatants transferred to 1 ml vials and placed in the high performance liquid chromatograph (HPLC) autosampler (kept at 4 °C) prior to injection in the HPLC (for more details see Antajan, 2004; Antajan et al., 2004 and Antajan and Gasparini, 2004). Samples analyzed at NIOO (Schelde, April 2002 to November 2002) used a similar method as at the VUB, which is detailed in Barranguet et al. (1997). Briefly, the extraction differed in that 5 or 7 ml 90 % cold acetone was used (depending on the amount of material on the filter) and the sample was extracted in a "mill flask", containing a half centimeter of clean glass beads, which was shaken for 20 seconds in a shaker while being cooled with compressed CO_2. Afterwards the supernatant was centrifuged at 1500 rpm for 3 minutes. An in-house sediment standard was run every 10^{th} sample.

1.2.7 Temperature, salinity, pH and dissolved oxygen

Temperature was monitored at certain sites and during laboratory studies using temperature data loggers (± 0.1 °C; Onset Computer Corporation, StowAway TidbiT), usually set to record temperature every hour. Salinity (± 0.01), pH (± 0.05) and dissolved oxygen (± 0.1 mg/l) were measured either *in situ* or in a bucket (immediately after collection) with a WTW multiline P4 multimeter.

2 SAMPLE ANALYSIS

2.1 Calcein marks

Calcein marks were viewed on thick sections of shells (see section 1.1.1) under UV light on an optical microscope. The calcein stain was clearly visible on this surface (thin sections are not necessary, nor does the surface need to be polished). Figure 3 is an example of a calcein stain in both a thick (A) and thin section (B) of *Mytilus edulis*.

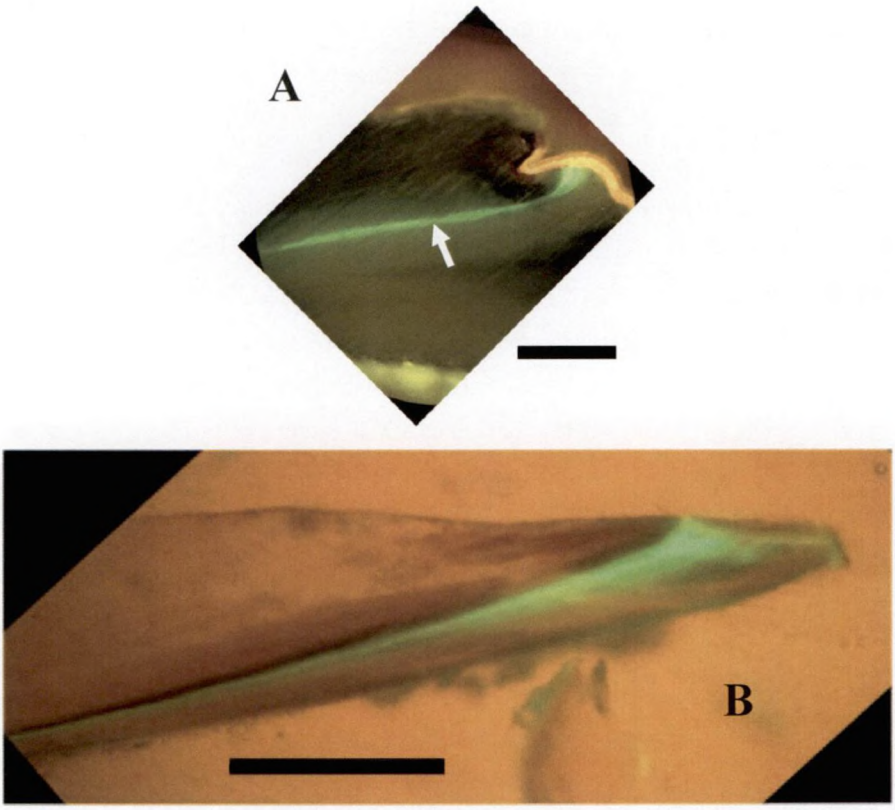

Figure 3. Example of calcein stains in *Mytilus edulis* on a thick section (A, arrow) and a thin section (B). Scale bars = 100 μm; growth is from left to right, outside of shell is to the top of pictures.

2.2 Stable isotopes

2.2.1 Shells

There is no agreement regarding **pre-treatment** of biogenic carbonates for stable isotope analysis. Some insist that **roasting** samples to remove organic impurities is a prerequisite for proper analysis (Keller et al., 2002), whereas others do not believe it to be important (Grossman and Ku, 1986). Vander Putten et al. (2000) tested the effect of roasting on *Mytilus edulis* calcite and found no difference. Similarly, McConnaughey (1989a) found no difference between roasted and non-roasted coral aragonite. In addition to this, roasting can potentially increase the chance of contamination and isotopic exchange. Therefore, in this work, no samples were roasted.

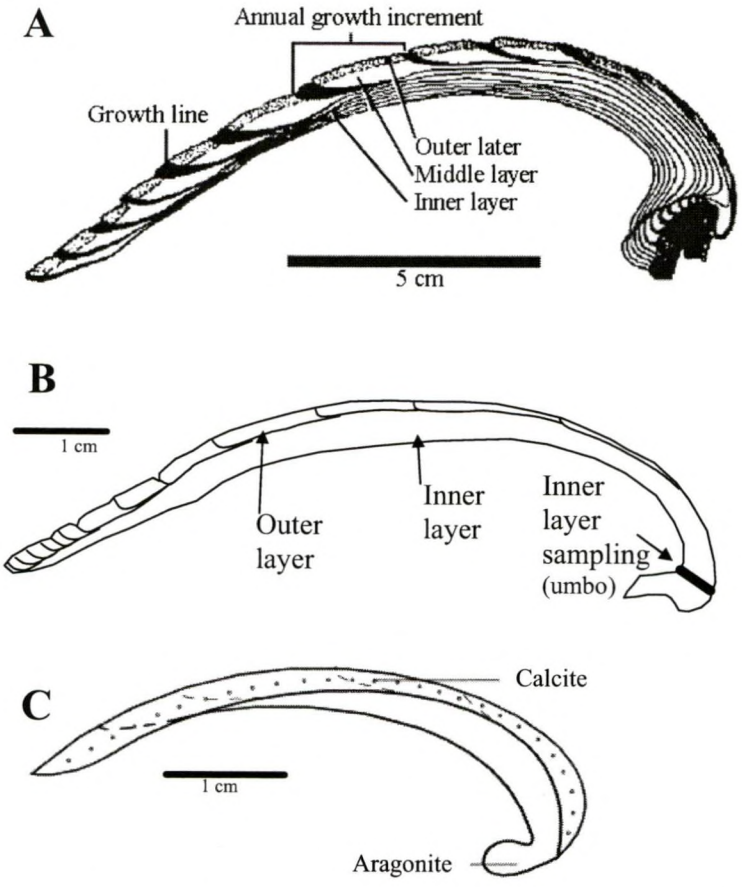

Figure 4. Shell cross sections of the three species used in this study and location of sampling. (A) The aragonite *M. mercenaria* was sampled in the middle layer, (B) the aragonite *S. giganteus* was sampled in the outer layer (and also umbo, see chapter 4), and (C) the outer calcite layer of *M. edulis* was sampled. A is from Quitmyer et al. (1997), B is from Gillikin et al. (2005a) and C is from Vander Putten et al. (2000).

Samples for $\delta^{13}C$ and $\delta^{18}O$ were drilled from the cross sections of shells (Fig. 4). Typically, the middle or outer layer was sampled, depending on the application and species (e.g., outer for *Saxidomus* and *Mytilus* and middle for *Mercenaria*, Fig. 4). Carbonate powders were drilled using a **Mercantek MicroMill**. Either lines or spots were used, again depending on application and species (see individual chapters), typically, a 300 μm bit was used. After drilling, samples were collected using scalpels and were placed in glass inserts and stored at 50 °C to be later analyzed using a ThermoFinnigan Kiel III (automated carbonate preparation device) coupled to a

ThermoFinnigan Delta^{plus}XL dual inlet IRMS. Samples were placed in the inserts instead of directly in the vials supplied with the Kiel III for two reasons. The first is that these vials are expensive (~ 20.00 € from ThermoFinnigan or 10.00 € from a local glass blower; inserts cost less than 0.10 € each). The second reason is that many more samples can be stored in the same oven when using the small inserts. Due to the large amount of inserts we have, and can keep in the oven, hundreds of samples can be drilled in advance while the Kiel III is running (the Kiel III can run about 40 samples every 24 hours). Running standards in both inserts and vials demonstrated that there was no effect of using the smaller inserts. It was verified that **storing small samples** in the oven for extended periods of time did not alter the isotopic composition of the sample by analyzing standards stored in inserts at 50 °C for four months, which did not give any indication of alteration when analyzed.

The **Kiel III** is simply an automated carbonate preparation device that works using the method originally outlined by McCrea in 1950. Briefly, carbonates are reacted with 100 % phosphoric acid at 70 °C for six minutes, and then are cryogenically purified using liquid nitrogen. The reaction of phosphoric acid with $CaCO_3$ produces solid calcium hydrogen phosphate, water, and carbon dioxide through the following chemical reaction:

$$CaCO_3 + H_3PO_4 \rightarrow CaHPO_4 + H_2O + CO_2 \qquad (1)$$

The sample gas volume is then, if necessary, reduced to a predefined pressure to assure that the IRMS is measuring between 1 and 5 volts. The sample magazine has two lines, each with 24 positions. The first position on both lines is left empty and is used to keep the system under vacuum during sample preparation. The second position is also left empty in our laboratory, although not necessary. This way acid is dropped in this second position before each sample. By leaving position 2 empty, it is assured that clean fresh acid is dropped on the first samples.

Standards are measured during every run at positions 3, 4, 9 and 16. The IRMS refills its standard gas at the beginning of the run (corresponding to position 3) and then again before position 9 and 16. This way, each refill of reference gas first has a standard run with it. The standard used for correction in our laboratory is MAR1,

produced by the University of Gent, Belgium. Its isotopic values can be found in Table 1. Position 4 is used to run NBS-19 to check for accuracy. Furthermore, NBS-18 is sporadically run, also to check for accuracy (see Table 1). Both NBS-19 and NBS-18 illustrate that our analyses are very precise and accurate (see table 2).

Table 1. Carbonate and water isotopic standards used in this study and accepted values.

Standard	$\delta^{18}O_{VSMOW}$ (‰)	$\delta^{13}C_{VPDB}$ (‰)	Source
§MAR1	-2.74	+1.84	Van den Driessche, 2001
NBS19*	-2.20	+1.95	Coplen, 1996
NBS18	-23.05 ± 0.19	-5.04 ± 0.06	NIST, 1992
VSMOW*	0.00	nd	Coplen, 1996
GISP	-24.78 ± 0.09	nd	NIST, 2003
SLAP*	-55.5	nd	Coplen, 1996
§TAP0409	-7.36	nd	Bouillon and Gillikin, unpubl.
§SW1	+0.15	nd	Bouillon and Gillikin, unpubl.
§Na_2CO_3 DIC std	nd	(-1.35 ± 0.18)	This study: injections‡
§Na_2CO_3 DIC std	nd	(-1.10 ± 0.07)	This study: Kiel III ‡

§ In-house standards; * By definition (Coplen, 1996); nd = not determined; ‡ See section 2.2.4.

Table 2. Long-term (Nov. 2003 – Oct. 2004) NBS-19 and NBS-18 data corrected using MAR1.

	NBS-19		NBS-18	
	$\delta^{13}C_{VPDB}$ (‰)	$\delta^{18}O_{VPDB}$ (‰)	$\delta^{13}C_{VPDB}$ (‰)	$\delta^{18}O_{VPDB}$ (‰)
Actual*	1.95	-2.20	-5.04	-23.05
Measured‡	1.93	-2.19	-5.03	-23.06
SD‡	0.039	0.085	0.068	0.111
N	292	292	22	22

*See also Table 1; ‡ Mean and standard deviation; N = number of standards run

As previously stated, when the sample is too large, **expansions** occur. When a gas is manipulated in this manner there is a risk of isotope fractionation. Therefore, the NBS-19 data were separated according to the number of expansions. Indeed, there is an effect of expansions on the $\delta^{18}O$ values (Fig. 5; ANOVA, $p < 0.01$), however, there was no significant difference between 0 and 1 expansions (p = n.s.). Only data with 2 expansions were significantly different from 0 expansions ($p < 0.01$). Although statistically significant, the deviation was within the analytical uncertainty of the method (deviation between 0 and 2 expansions = 0.02 ‰ for $\delta^{13}C$ and 0.07 ‰ for $\delta^{18}O$). Nonetheless, caution should be taken when utilizing data with 2 or more expansions. In this study, however, microdrill sampling facilitated obtaining similar sample sizes and therefore samples usually did not require expansion.

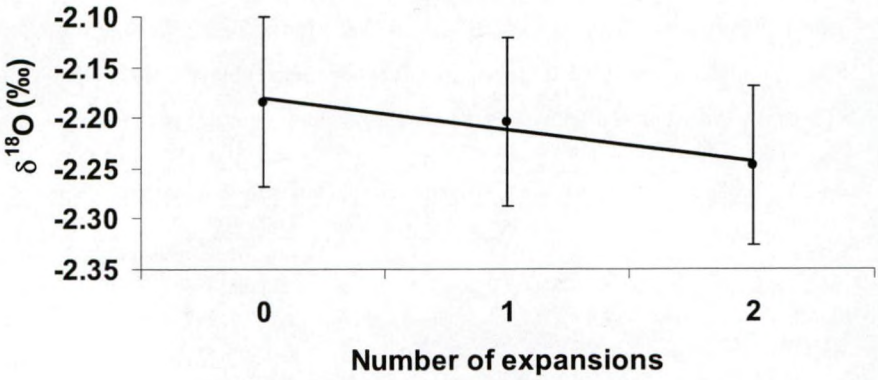

Figure 5. Effect of expansions in the Kiel III on $\delta^{18}O$ values of NBS-19 (0: n = 191, 1: n = 83, 2: n = 18, total: n = 292). There is an overall effect of expansions (ANOVA, $p < 0.01$), but only 0 and 2 expansions are significantly different from each other ($p < 0.01$).

2.2.2 Soft tissues

Samples were analyzed for $\delta^{13}C$ with an Element Analyzer (Flash 1112 Series EA ThermoFinnigan) coupled via a CONFLO III to an IRMS (Delta^{plus}XL, ThermoFinnigan). Sucrose was used as a standard (IAEA-CH-6, $\delta^{13}C = -10.4 \pm 0.1$ ‰). Results are reported using the conventional δ notation relative to the VPDB standard (see Chapter 1). The analytical precision of the method is on the order of 0.1 ‰. Using this same instrument and method, Verheyden et al. (2004) report a long term analytical precision of 0.08 ‰ on 214 analyses of the IAEA-CH-6 standard (1σ). Empty cups run as blanks gave a very small signal (< 10 mV; or < 1% of the sample signal) and therefore were not corrected for.

2.2.3 $\delta^{18}O$ of water

All water $\delta^{18}O$ was measured using the CO_2 equilibration technique of Epstein and Mayeda (1953). Two different procedures were followed. The samples from the Schelde estuary were primarily analyzed by equilibrating CO_2 with five ml of water in an agitated temperature controlled water bath at 25 °C for 48 hours. This is more than enough time to compensate for the **salt effect** on the kinetics of CO_2-H_2O isotopic exchange equilibrium, which has been determined to be three times longer in salt water as compared to freshwater (or at least 24 hours; Verma, 2004). After

equilibration, CO_2 was cryogenically purified and sealed in a quartz glass tube. These tubes were then cracked in either a Finnigan MAT Delta E dual inlet isotope ratio mass spectrometer (IRMS) or a ThermoFinnigan Delta^{plus}XL dual inlet IRMS. Precision was better than 0.2 ‰ using this method based on replicate samples, which is similar to what was reported in Van den Driessche (2001) and Verheyden (2001) using the same method and instrumentation. The second procedure for measuring $\delta^{18}O_W$ is modified from Prosser et al. (1991) and is both easier and faster than the first method. It is similar to the previously described method, except that equilibration and gas extraction is done directly in a headspace vial. 10 ml headspace vials are first flushed with He gas and are capped with a rubber septum and aluminum seal. Approximately 500 µl of sample water is injected into the vial, then 200 µl of pure CO_2 from a tank is injected using a gas tight syringe. The samples are then placed in a shaker for 2 hours and left to equilibrate for about 24 hours for freshwater and more than 48 hours for seawater at ambient laboratory temperature (± 23 °C). In addition to samples, two in-house well-calibrated (against VSMOW, GISP and SLAP) secondary standard water samples were similarly processed (a seawater (SW1) and tap water (TAP0409) standard; see Table 1). After equilibration, 1000 µl of CO_2 from the headspace is drawn into a gas tight syringe and is injected into the carrier gas stream after the combustion columns of a ThermoFinnigan Delta^{plus}XL continuous flow IRMS. Precision was better than 0.15 ‰ (1σ), determined by repeated analysis of the seawater standard and replicate sample analyses. This precision is similar or better than was obtained using the 'tube cracking' method (i.e., ≤ 0.2 ‰; see Van den Driessche, 2001; Verheyden, 2001).

2.2.4 $\delta^{13}C$ of DIC

A method slightly modified from Salata et al. (2000) was used for $\delta^{13}C_{DIC}$ analysis. For vials with water samples for $\delta^{13}C_{DIC}$ analysis that were filled to the top (see section 1.2.2; e.g., not hemolymph samples, see section 1.1.3), a headspace was created by inserting an empty, fully depressed, syringe and needle through the septum, then inserting a needle attached to a He bottle, until the required volume of water has been replaced (typically 5 ml for vials > 10 ml and 3 ml for vials < 10 ml). After the He syringe is removed, the pressure is equalized in the other syringe. Once the headspace is created (or for vials already with a headspace, e.g., hemolymph

samples), 99 % phosphoric acid was added (typically ~ 500 µl for vials > 10 ml and 250 µl for vials < 10 ml). Samples were shaken, and placed on their side or turned upside down so that there is no contact between headspace and septum to reduce the possibility of exchange with atmospheric CO_2. Samples were allowed to equilibrate for one day in a sample shaker. Salata et al. (2000) reported that the results are stable after 16 to 36 hours of **equilibration time**. A similar experiment was carried out here with 24 replicate tap water samples injected between 1 and 57 hours and found that samples were within ± 0.1 ‰ between 6 and 56 hours (Fig. 6). Nonetheless, samples were always allowed to equilibrate for 15 to 24 hours before injection. Furthermore, a small experiment involving different **vial sizes** was also tested with tap water samples. Replicate tap water samples were analyzed in two 25 ml, two 10 ml and three 2 ml vials (2 ml vials contained 0.5, 1 and 1.5 ml of sample). The standard deviation on these seven samples was 0.05 ‰ and no sample deviated more than 0.1 ‰ from the mean. This indicates that vial size is not an important factor, but it should be noted that Brussels tap water has high DIC concentrations and therefore produces a lot of CO_2 after acidification. Samples with less DIC (e.g., seawater and hemolymph) will produce less CO_2 and therefore may not contain enough CO_2 for injection. A method to circumvent this problem has been proposed by Capasso and Inguaggiato (1998) where MilliQ water is injected into the sample vial just before gas sampling thereby concentrating the CO_2. However, this method was not tested.

To correct for the partitioning of CO_2 between headspace and the water phase and to calculate the $\delta^{13}C$ of the total DIC, the equation of Miyajima et al. (1995) was used:

$$\delta^{13}C_{DIC} = \frac{V_{headspace} * \delta^{13}C_{measured} + (V_{bottle} - V_{headspace}) * \beta * (\delta^{13}C_{measured} + \varepsilon_g^a)}{V_{headspace} + (V_{bottle} - V_{headspace}) * \beta} \quad (2)$$

where $\beta = 0.872$ at 23 °C (Ostwald solubility coefficient); ε_g^a is calculated from ε = -373 / T(K) + 0.19 thus ε = -1.07 at 23 °C; V_{bottle} and $V_{headspace}$ = internal volume of sampling vial and headspace volume, respectively.

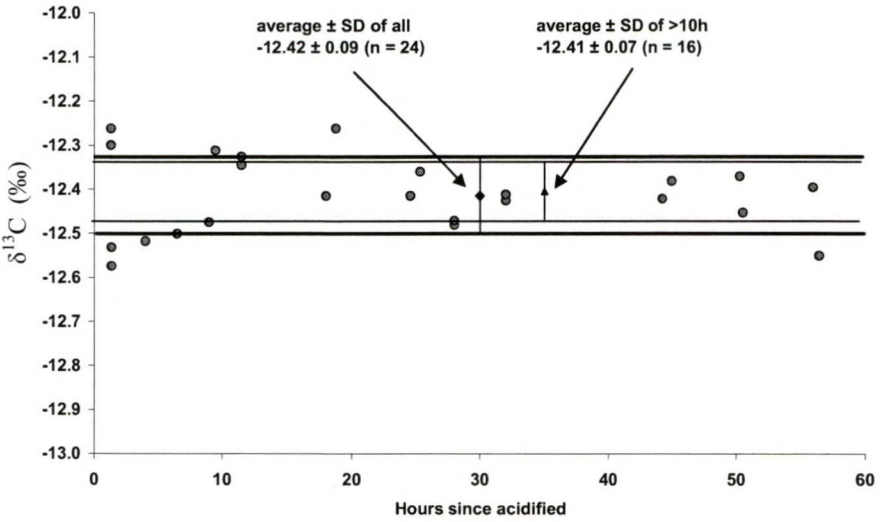

Figure 6. $\delta^{13}C_{DIC}$ of 24 replicate tap water samples all acidified at the same moment and injected in the IRMS over a 57 hour period.

These data were further corrected using calibrated CO_2 gas (from a tank), which is injected periodically throughout the analysis period. Typically, the standard deviation of this gas was less than 0.2 ‰ for the day. As there is no certified $\delta^{13}C_{DIC}$ standard, to check the day to day variability of this method, an in-house seawater standard (SW1) was produced. Furthermore, to test both the precision and accuracy of the method, a standard was produced using Na_2CO_3 dissolved in degassed seawater in which all DIC was removed (see Box 1 for the detailed recipe of this standard). The Na_2CO_3 powder was analyzed on the Kiel III vs. NBS-19 to obtain a '*true*' $\delta^{13}C$ value.

The 0.25 ‰ difference between the Na_2CO_3 solid measured in the Kiel III and the Na_2CO_3 dissolved in seawater (see Table 1) can be attributed to several factors. It may be caused by an incorrect acid fractionation factor calculated in the Kiel III, as this is based on calcium carbonate and the $\delta^{13}C_{DIC}$ standard is a sodium carbonate. Furthermore, the error might arise from exchange with atmosphere during preparation of the standard or minor errors in the calculations used to correct the data. Nevertheless, considering that these means are within 2σ of the analytical precision of the method (1σ = 0.2 ‰), the data can be considered indistinguishable using this method. In addition to this standard, the $\delta^{13}C$ of both a carbonate precipitated from

DIC and the original water DIC from which this solid was precipitated were measured. A simple linear regression illustrates that there is no difference between either method ($p < 0.00001$; Fig. 7). The data illustrate that the injection method is accurate.

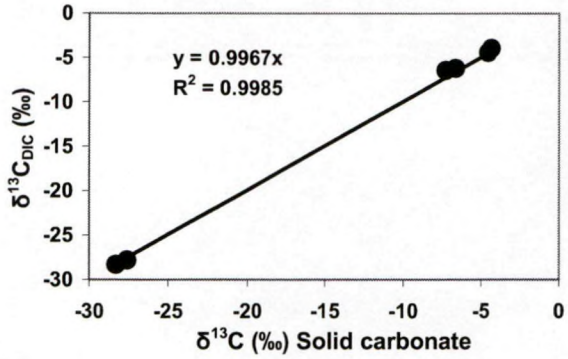

Figure 7. Simple linear regression between $\delta^{13}C_{DIC}$ and the $\delta^{13}C$ of the solid barium carbonate precipitated from the same waters.

2.2.5 $\delta^{13}C$ of POM

Particulate organic matter collected on filters (see section 1.2.3) was analyzed for $\delta^{13}C$ in the same manner as soft tissues (see section 2.2.2). However, due to the smaller sample size (and thus smaller ion beam intensity) and slightly higher blank (tin cup plus empty filter), blanks were subtracted from the samples. Blank subtraction was done using

$$\delta^{13}C_{corrected} = (\delta^{13}C_{measured} \times C_{measured} - \delta^{13}C_{blank} \times C_{blank}) / (C_{measured} - C_{blank}) \quad (3)$$

with C equal to the total amount of carbon.

2.3 Phytoplankton pigments

Phytoplankton pigments were analyzed using standard laboratory operating procedures for HPLC of the VUB and NIOO-CEME (see section 1.2.6). See Antajan (2004) for a detailed description of the HPLC. The reproducibility of the NIOO-CEME method was determined to be within 2.7 % (or 0.3 µg/l; 1σ) for chlorophyll a, based on seven sediment standards (chlorophyll a = 10.1 µg/l).

Box 1. Recipe for Na_2CO_3 $\delta^{13}C_{DIC}$ standard.

As there is no available $\delta^{13}C_{DIC}$ standard, the following outlines the procedure for producing a $\delta^{13}C_{DIC}$ standard that can be measured vs. NBS-19. It is recommended to take more Na_2CO_3 than needed and to homogenize it with a mortar and pestle. Then sub-sample this for solid analysis with a Kiel or off-line extraction before adding it to the seawater. This will assure a homogenous δ value for both methods.

Procedure:

1. Filter ~1.5 liter of seawater using at least a 0.45 µm porosity filter.
2. Transfer the filtered water into a 2 liter Erlenmeyer flask and place on a magnetic stirrer. Place a Teflon magnet in the flask and turn on the stirrer.
3. Add ~8ml of 1N HCl to lower the pH to 3.00.
4. Add 2ml $HgCl_2$ (or another suitable fixative, see section 1.2.2)
5. Cover the flask with parafilm and aerate water vigorously for 90 minutes using argon (this removes all dissolved CO_2; prevent exposure to atmosphere from this step on).
6. Add 0.5N NaOH until pH = 8.0 ± 0.1
7. Add Na_2CO_3 $\delta^{13}C_{DIC}$ standard powder (with 212 mg per liter)

   Note: pH will rise to about 9.2 after adding Na_2CO_3.

8. Adjust pH to slightly higher than 8.3 by slowly adding 1N HCl. Be careful; the pH will drop sharply after going below ~8.8. Wait about 15 minutes for pH to stabilize, and then adjust to 8.2 ± 0.05 (if you go below this, start over).
9. After correct pH is achieved, transfer standard to vials using a pipette and cap immediately (always avoid exposure to air)
10. Label vials with standard name and date made.

Original recipe by D. Andreasen (1993), modified by H. J. Spero (1995) and by F. J. C. Peeters (U. Amsterdam, 2003) –all are personal communications.

2.4 Elemental analysis

2.4.1 ICP-MS & ICP-OES

All **water samples** for dissolved Sr, Mg, Ba and Ca analysis were diluted with MilliQ water to assure a salt concentration less than 0.2 %. Strontium, Mg, and Ba were measured on a VG PlasmaQuad II+ inductively coupled plasma mass spectrometer (ICP-MS) using In as an internal standard. Calcium was measured with an IRIS Thermo Jarrell Ash Corp. ICP- optical emission spectrometer (ICP-OES) using Yt and Au as internal standards. An overview of these types of instruments and their limitations can be found in Brown and Milton (2005). Certified reference materials (CRM) were also run to check for precision and accuracy. The reproducibility of the NRCC-SLRS-3 riverine water standard (National Research Council of Canada) was < 4 % (percent relative standard deviation (%RSD)) for Sr, Mg, Ba and Ca and mean values were within 5 % of the recommended values for all elements (n = 8).

Barium and calcium analysis of the **particulate** phase were measured on the same machines using 1646a (NIST, estuarine sediment) and BCR414 (European Community, trace elements in phytoplankton) CRM. Although more elements were analyzed, they were not used in this study, so are not listed here. The results of these CRM are summarized in Table 3.

Table 3. Summary of particulate CRM data.

Standard	Element	%RSD	%RV	N
1646a	Ba	5.2	95.5	5
	Ca	4.8	97.8	5
BCR414	Ba	8.8	109.8	3
	Ca	9.3	87.5	3

%RV = % recommended value, N = number of replicates.

2.4.2 HR-ICP-MS

Carbonate powders for high resolution ICP-MS (HR-ICP-MS; ThermoFinnigan Element2) were dissolved in a 1 ml 5 % bi-distilled HNO_3 solution containing 1 $\mu g\ l^{-1}$ of In and Bi, which were used as internal standards. Multi-element calibration standards were prepared from certified single element stock solutions. The isotopes

^{111}Cd, ^{135}Ba, ^{208}Pb were analyzed in low resolution, and ^{11}B, ^{26}Mg, ^{43}Ca, ^{55}Mn, ^{59}Co, ^{65}Cu, ^{86}Sr were analyzed in medium resolution. Four reference materials were run MACS1, CCH1, and two in-house shell standards (S-gig and M-ed). The MACS1 is a pressed powder carbonate standard developed by S. Wilson of the USGS. The natural limestone standard, CCH1 was run to obtain accuracy for Mg/Ca and U/Ca (data from Govindaraju, 1994), for which there are no data for MACS1. The in-house standards, were produced from a *S. giganteus* shell (S-gig; approximately 25 mg of milled carbonate was dissolved in 50 ml of 5 % bi-distilled HNO_3, diluting this four times at the time of analysis provided similar concentrations to the samples) and a *M. edulis* shell (M-ed; approximately 12 mg of milled carbonate was dissolved in 25 ml of 5 % bi-distilled HNO_3). Elemental concentrations as provided by the Element2 software were directly converted to molar ratios (Me/Ca). Typical operating conditions can be found in Table 4.

Table 4. Typical HR-ICP-MS operating conditions.

Low resolution [m/Δm]	300
Medium resolution [m/Δm]	4000
High resolution [m/Δm]	10000
Runs	3
Passes	3
Wash time [s]	20
Take-up Time [s]	80
Deadtime [s]	25
Plasma Power [Watt]	1225
Peri. Pump Speed [rpm]	1.75
Cool Gas [l/min]	16.00
Aux Gas [l/min]	1.15
Sample Gas [l/min]	1.20
Spray Chamber	Cyclonic
Nebuliser	Concentric
Nebuliser flow rate [ml/min]	0.4
Sample and Skimer Cones	Ni

Settings varied in order to optimize the machine each day

Table 5. Detection limit, precision, and accuracy of HR-ICP-MS carbonate standards.

		Sr/Ca	Mg/Ca	Ba/Ca	Pb/Ca	Mn/Ca	U/Ca	Cd/Ca	Co/Ca	Cu/Ca	B/Ca
DL (3σ)	(ppt)	11.1	63	0.42	0.59	NM	0.007	0.069	1.33	6.12	NM
S-gig	Mean	1.99	1.09	3.76	0.36	4.00	0.02	0.03	1.20	1.19	8.35
N = 9	sd	0.05	0.03	0.15	0.04	0.27	0.00	0.01	0.09	0.15	1.30
	%RSD	2.6	3.0	3.9	9.8	6.8	13.5	20.9	7.5	12.3	15.5
M-ed	Mean	1.30	5.94	1.21	0.25	27.21	BDL	0.04	0.19	0.78	NM
N = 10	sd	0.05	0.24	0.08	0.03	3.12	BDL	0.06	0.02	0.09	NM
	%RSD	3.9	4.06	6.41	11.54	11.45		128.3	12.5	12.0	NM
MACS1	RV	0.255	*77.68**	84.76	59.56	218.86	*1.67**	106.2	210.81	195.55	NV
N = 18	Mean	0.258	*78.11**	88.27	61.72	207.52	*1.96**	91.57	201.14	229.31	118.18
	%RV	101.1	*100.5**	100.9	103.6	94.8	*116.9**	86.2	95.4	115.5	NV

DL = detection limit (in ppt or ng/kg, not ratios); S-gig is *S. giganteus* standard and M-ed is *M. edulis* standard. All data given as µmol/mol except for Sr/Ca and Mg/Ca which are given in mmol/mol; * = data from CCH1 standard; NV = no recommended value; NM = not measured; N = number of replicates, %RV = % recommended value, BDL = below detection limit.

The HR-ICP-MS reproducibility data over the entire sampling period, as determined from the in-house shell standards, is given in Table 5 along with accuracy data from MACS1. The reproducibility for the shell standards are given because they had a similar concentration to the samples, whereas the MACS1 did not. Note that accuracy data for Mg/Ca and U/Ca are from the CCH standard as these elements are not present in MACS1. The minor elemental data, Sr/Ca and Mg/Ca, are both precise (%RSD $\leq$ 3 %) and accurate (within 2 % RV). The trace element data are good as well (%RSD < 10 %, within ~ 5 % RV), aside from U/Ca, Cd/Ca, Cu/Ca and B/Ca. The poor results for U/Ca and Cu/Ca are undoubtedly due to the low concentrations. Reproducibility of B/Ca is most likely poor because of the low concentration (~ 10 µmol/g) and an unstable blank, possibly caused by the borosilicate nebulizer used in this study.

For **hemolymph** samples, In and Re were used as internal standards to control instrument fluctuations. Samples were diluted 20 times with MilliQ water to assure a salt concentration less than 0.2 %. Reproducibility of a large hemolymph sample taken from a clam (*Ruditapes decussatus*) from the Noyalo River, Brittany, France (salinity ~ 17) and digested 10 times is listed in Table 6.

The digested **tissue** samples were analyzed in the same manner as hemolymph. Reproducibility was established by analyzing the NIST 1566a oyster tissue; data are given in Table 7.

Table 6. Precision for HR-ICP-MS hemolymph samples (*per mol Ca, n = 10).

	Sr/Ca	Mg/Ca	Ba/Ca	Pb/Ca	Mn/Ca	U/Ca	Cd/Ca	Zn/Ca	B/Ca
Unit*	mmol	mol	µmol	µmol	µmol	µmol	µmol	mmol	mmol
Mean	10.37	4.17	66.15	2.59	151.38	4.27	0.44	20.67	10.32
sd	0.17	0.07	3.44	0.13	4.84	0.26	0.02	0.52	0.24
%RSD	1.6	1.6	5.2	5.2	3.2	6.1	5.0	2.5	2.3

Table 7. Precision and accuracy of NIST 1566a oyster tissue (data in µg/kg, n = 5).

	Cd	Ba	Pb	U	B	Mg	Ca	Mn	Cu	Zn	Sr
Mean	3.96	1.50	0.34	0.11	5.45	1294.3	2086.7	11.25	74.8	784.0	12.01
sd	0.05	0.14	0.01	0.00	0.16	30.5	45.5	0.36	0.6	7.45	0.25
%RSD	1.3	9.0	2.9	1.5	2.9	2.4	2.2	3.2	0.8	1.0	2.1
RV	4.15	1.77*	0.37	0.13	NC	1180	1960	12.3	66.3	830	11.1
%RV	95.4	84.9	91.5	85.7	NC	109.7	106.5	91.5	112.8	94.5	108.2

*no certified value, data taken from Buckel et al. (2004); NC = not certified. See previous tables for abbreviations.

2.4.3 LA-ICP-MS

The LA-ICP-MS system consists of a Fisons-VG frequency quadrupled Nd-YAG laser (λ = 266 nm) coupled to a Fisons-VG PlasmaQuad II+ mass spectrometer. An overview of LA-ICP-MS technology and limitations can be found in Günther and Hattendorf (2005). Details of LA-ICP-MS operating conditions can be found in Table 8. When applicable, the laser was shot (~50 µm spots) directly in the drill holes of either HR-ICP-MS or stable isotope sampling (Fig. 8), allowing direct alignment of the two elemental profiles, as well as alignment with $\delta^{18}O$ data (cf. Toland et al., 2000). Signal intensities of ^{11}B, ^{26}Mg, ^{43}Ca, ^{55}Mn, ^{59}Co, ^{65}Cu, ^{86}Sr, ^{111}Cd, ^{138}Ba, and ^{208}Pb were recorded. Gas blank intensities were recorded every 10th sample. Approximately after every 50th sample, two standards (NIST 610 and MACS1) were analyzed five to six times each.

Table 8. Typical LA-ICP-MS operating conditions.

Laser probe		ICP-MS	
Laser mode	Q-switched	Argon flow rate	1 min^{-1}
Laser power [mJ]	2	Carrier gas	0.90
Frequency [Hz]	10	Auxiliary gas	1.0
Preablation time [s]	10 - 15	Cooling gas	13.27
Spot size [μm]	50	Acquisition mode	Peak jumping
		Points per peak	3
		Dwell time [ms]	10.24
		Acquisition time [s]	15 - 20

The **raw counts per second (CPS) were manipulated off line** following Toland et al. (2000). The carrier gas (argon) was used to measure the blank signal. The drift on the blank, or the gas drift (GD) was calculated using the following equation:

$$GD = \frac{Ab}{Bb - Cb} \quad (4)$$

where A_b is the CPS of the first measured blank minus the CPS of the final blank, B_b the time decimal of the final blank, and C_b is the time decimal of the first blank, with the time decimal being a fraction representing a time of the day (i.e., 0 to 0.9999 for 0:00:00 [midnight] to 23:59:59). The gas drift corrected blank (eq. 4) was then subtracted from the analyte measurement using the following:

$$GBA = A - \{B + [GD * (A1 - B1)] \} \quad (5)$$

where GBA is the gas blanked analyte, A is the uncorrected CPS of the analyte, B is the CPS of the first blank, GD is the gas drift, A1 is the time decimal of the analyte measurement, and B1 is the time decimal of the first blank measurement. This procedure was carried out approximately every 10 measurements.

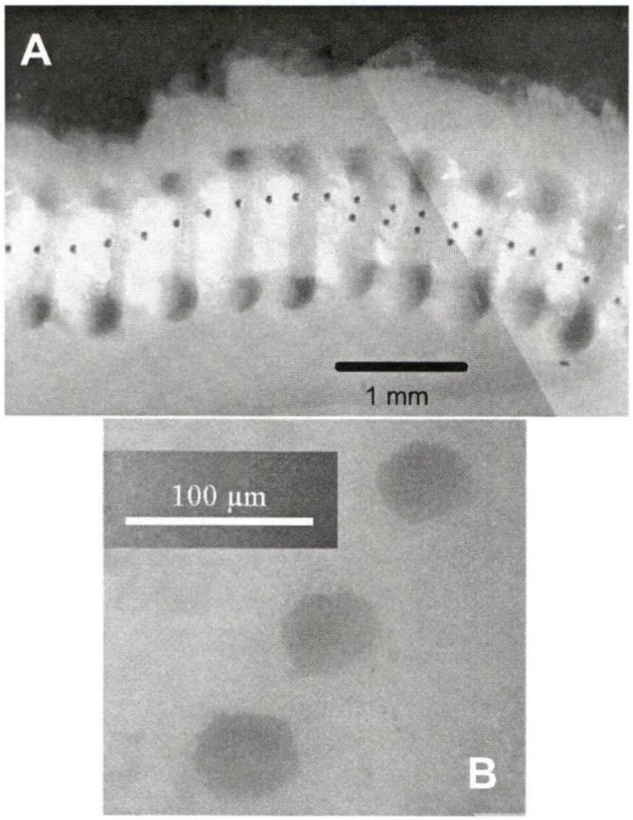

Figure 8. (A) Laser ablation holes in drill holes in a *S. giganteus* shell and (B) a close up of Laser ablation holes in the MACS1 standard.

Although multiple internal standards can reduce the uncertainty of the analysis (De Ridder et al., 2002), only ^{43}Ca was suitable for this study for two reasons, 1) Ca is the only homogenously distributed element, and 2) mass interferences in the ICP-MS on other isotopes of Ca. After blank subtractions, the ^{43}Ca signal was normalized to correct for machine instability (i.e., internal standard) and different concentrations of calcium between the glass NIST 610 and carbonate samples and standards. First the ^{43}Ca was normalized to the percent CaO in the analyte (i.e., in $CaCO_3$ = 56 % (assuming 100 % $CaCO_3$; cf. Vander Putten et al., 1999) and in NIST610 = 11.45 % (Pearce et al., 1997)). To correct for signal instability (in both the ICP-MS and laser energy) and matrix effects, the ^{43}Ca was subsequently normalized to the first measurement. The above procedure was facilitated by software written by M. Korntheuer (VUB - ANCH) in Perl.

Finally, the gas blanked CPS of each element measured (eq. 5) was divided by the normalized ^{43}Ca for each measurement. Using known concentrations for the NIST610 (from Pearce et al., 1997) and MACS1 (values from S. Wilson, USGS, unpublished data, 2004; also see Munksgaard et al., 2004) and the normalized CPS (nCPS), calibration lines (S) were constructed. The drift between two calibrations was corrected for in a similar manner to the gas blank drift described above, and concentrations were calculated as follows:

$$CD = (S2 - S1) / (TS2 - TS1) \quad (6)$$

where CD is the calibration drift, S1 and S2 are the calibration slopes of the current and next calibration series, and TS1 and TS2 are the corresponding time decimals of the first standard for each calibration series. This drift was then applied using:

$$\text{Drift corrected concentration} = nCPS / (S1 + (CD * (A1 - TS1)) \quad (7)$$

Molar ratios were calculated assuming 100 % $CaCO_3$ (cf. Vander Putten et al., 1999). To assess the accuracy of the method, the MACS1 (25 analyses spread over an operating day) was analyzed using the NIST610 as the calibration standard.

Reproducibility and accuracy for LA-ICP-MS are given in Table 9. Reproducibility is good for all ratios (< 8 %), aside from Mg/Ca, due to low Mg concentrations in MACS1 (0.06 mmol/mol in MACS1, compared with 1.09 mmol/mol in the shell). Accuracy is also good, with the data being within 8 % of the recommended value, aside from Pb/Ca, which was overestimated by nearly 50 %. This overestimation is apparently not a problem of an incorrect recommended value, as this study's HR-ICP-MS data and the LA-ICP-MS data of Munksgaard et al. (2004) are within 5 % of the recommended value. This discrepancy is probably due to fractionation, as Pb is known to be one of the most problematic elements in this regard (Fryer et al., 1995; Longerich et al., 1996). Munksgaard et al. (2004) used LA-ICP-MS systems with shorter wavelengths (λ = 193 and 213 nm) which produce smaller particles during ablation and reduces elemental fractionation in the plasma (Guillong and Gunther, 2002). However, Pb/Ca results from the LA-ICP-MS are reproducible, thus they are considered as qualitative at this point (see next chapter,

where using both the NIST610 and MACS1 standards in the calibration lead to near-quantitative results).

Table 9. Detection limit, precision, accuracy of LA-ICP-MS for various elemental ratios.

		Sr/Ca	Mg/Ca	Ba/Ca	Pb/Ca	Mn/Ca	U/Ca	B/Ca
DL (3σ)	(ppm)	1.20	3.24	0.04	0.01	1.26	0.01	0.25
MACS1	Mean	0.249	0.06	81.4	87.2	203.1	NP	229.7
	sd	0.005	0.02	3.13	5.95	9.91	NP	17.1
N = 25	%RSD	2.0	30.1	3.8	6.8	4.9	NP	7.5
	%RV	97.6	NV	96.0	146.5	92.9	NP	NV

All data given as µmol/mol except for Sr/Ca and Mg/Ca which are given in mmol/mol; DL = detection limit (in ppm or µg/g, not ratios); NV = no recommended value; NP = not present; N = number of replicates. See previous tables for other abbreviations.

Chapter 3

Validation of LA-ICP-MS results with micromilling and SN-HR-ICP-MS

Foreword

In this Chapter data collected from a *Saxidomus giganteus* shell using LA-ICP-MS is compared with data collected by micromilling samples and acid digesting them for analysis in a HR-ICP-MS. While there have been many reports of accuracy and precision of calibration pellets, only few studies have compared LA-ICP-MS data with data collected using more traditional methods (e.g., acid digested samples).

Abstract

Laser ablation – inductively coupled plasma - mass spectrometry (LA-ICP-MS) is an easy and rapid method for obtaining large quantities of high resolution multi-element data from solid substrates. However, the lack of matrix matched standards hinders the accuracy of this method. Therefore, LA-ICP-MS (λ = 266 nm) data are compared with data collected from the same shell using acid digested micromilled samples measured by solution nebulization – high resolution – ICP-MS (SN-HR-ICP-MS). High resolution element to calcium ratios collected using LA-ICP-MS were very similar to results from SN-HR-ICP-MS. Ratios of Sr/Ca were the most similar with no statistical difference between the two methods. Ratios of Pb/Ca, Ba/Ca and U/Ca were near-quantitative, and Mg/Ca was semi-qualitative using this LA-ICP-MS setup. Ratios of B/Ca, Mn/Ca, Co/Ca, Cu/Ca, and Cd/Ca were either below the detection limit or were not reproducible between the two methods. Despite the non-matrix matched standards used in the LA-ICP-MS calibration (NIST610 and USGS-MACS1), these data are both accurate and precise enough for the elements used in this study.

1. INTRODUCTION

In this dissertation, trace elemental concentrations were primarily measured by laser ablation – inductively coupled plasma - mass spectrometry (LA-ICP-MS). LA-ICP-MS has become a widespread tool for the elemental analysis of solid materials (see Russo et al., 2002 for a review) and is an excellent method to obtain high resolution profiles from bivalve shells (Stecher et al., 1996; Vander Putten et al., 2000; Lazareth et al., 2003; Takesue and van Geen, 2004). Laser Ablation ICP-MS is advantageous over other manual sampling techniques (e.g., micromilling) because there is a reduced chance of contamination and sample throughput is much higher. Typically, either multi-element glass or pressed carbonate standards are employed for LA-ICP-MS calibration (see previous references and Vander Putten et al., 1999). However, these calibration standards are not perfectly matrix matched and therefore may not be suitable standards to obtain quantitative data (Craig et al., 2000). Indeed, many studies report results from LA-ICP-MS qualitatively (Vander Putten et al., 1999, 2000; Lazareth et al., 2003; Becker et al., 2005).

In recent years, there have been many advances in our understanding of the fractionation processes involved with the LA-ICP-MS systems (see Günther and Hattendorf, 2005 for review). This in turn has lead to an increased use of newer lasers with shorter wavelength and improved ICP-MS systems. However, many laboratories are still using the older systems, and all previous studies are based on these older systems. Therefore, it is of interest to assess how precise and accurate these older systems are for the analytical substrate itself. To evaluate the use of non-matrix matched standards in 266 nm wavelength LA-ICP-MS, data obtained from LA-ICP-MS are compared with acid digested micromilled samples measured by solution nebulization – high resolution – ICP-MS (SN-HR-ICP-MS).

2. MATERIALS AND METHODS

2.1 Sample collection and preparation

A living *Saxidomus giganteus* was collected from Carkeek Park, Puget Sound, Washington, USA (shell B1, collected Sept. 2001). A section of the shell was cut with

a diamond saw along the axis of maximal growth, rinsed with deionised water, air-dried and mounted on a microscopic slide. The section was placed directly in the ablation cell of the LA-ICP-MS. For SN-HR-ICP-MS sampling, the shell section was mounted on a computer controlled Merchantek Micromill Sampler (a fixed drill and computer controlled micro positioning device), which allows precise sampling. A high resolution profile was obtained by milling a succession of grooves 600 μm in length, 200 μm depth and 300 μm width, using a 300 μm drill bit (325 μm deep spots were used near the umbo due to the thinning of the carbonate layer). Before each sampling, 300 μm of carbonate was milled and collected for stable isotope analysis, which also removed surface contamination. Samples were taken from the outer shell layer, avoiding the outermost part of the shell which is in contact with the water (see Chapters 2, 4, 7 and 8 for more details).

2.2 SN-HR-ICP-MS

Carbonate powders for solution nebulization high resolution ICP-MS (SN-HR-ICP-MS; Finnigan MAT Element2) were dissolved in a 1 ml 5 % bi-distilled HNO_3 solution containing 1 μg l^{-1} of In and Bi, which were used as internal standards. The isotopes ^{111}Cd, ^{135}Ba, and ^{208}Pb were analyzed in low resolution, and ^{11}B, ^{26}Mg, ^{43}Ca, ^{55}Mn, ^{59}Co, ^{65}Cu, and ^{86}Sr were analyzed in medium resolution. Three reference materials were run with the samples MACS1, CCH1, and an in-house shell standard, S-gig. The MACS1 is a pressed powder carbonate standard developed by S. Wilson of the USGS. To obtain accuracy for Mg/Ca and U/Ca, for which there are no data for MACS1, CCH1 was run as well (data from Govindaraju, 1994). The in-house S-GIG standard was produced from a *S. giganteus* shell (approximately 25 mg of milled carbonate was dissolved in 50 ml of 5 % bi-distilled HNO_3). Solution Nebulization HR-ICP-MS analyses were carried out over three analytical sessions spanning several months (Oct. 2003 to Mar. 2004). Elemental concentrations, as provided by the Element2 software, were directly converted to molar ratios (Me/Ca). See Chapter 2 for detection limits, accuracy and precision.

2.3 LA-ICP-MS

The LA-ICP-MS system consists of a Fisons-VG frequency quadrupled Nd-YAG laser (λ = 266 nm) coupled to a Fisons-VG PlasmaQuad II+ mass spectrometer.

Details of LA-ICP-MS operating conditions can be found in Chapter 2. The laser was shot (~50 μm spots) directly in the holes of the SN-HR-ICP-MS sampling (and stable isotope sampling holes; see section 2.1) allowing direct alignment of the two elemental profiles. Signal intensities of ^{11}B, ^{26}Mg, ^{43}Ca, ^{55}Mn, ^{59}Co, ^{65}Cu, ^{86}Sr, ^{111}Cd, ^{138}Ba, and ^{208}Pb were recorded. Gas blank intensities were recorded every 10^{th} sample. Approximately after every 50^{th} sample, two standards (NIST 610 and MACS1) were analyzed five to six times each, as well as in the beginning and at the end of every analytical session.

The raw counts per second (CPS) were manipulated off line following Toland et al. (2000). The carrier gas (argon) was used to measure the blank signal. After blank subtractions, the ^{43}Ca signal was normalized to correct for machine instability (i.e., internal standard) and different concentrations of calcium between the glass NIST 610 and carbonate samples and standards. To correct for signal instability (in both the ICP-MS and laser energy) and matrix effects, the ^{43}Ca was subsequently normalized to the first measurement. Finally, the gas blanked CPS of each element measured was divided by the normalized ^{43}Ca for each measurement. Using known concentrations for the NIST610 (from Pearce et al., 1997) and MACS1 (values from S. Wilson, USGS, unpublished data, 2004; also see Munksgaard et al., 2004) and the normalized CPS, calibration lines were constructed. The drift between two calibrations was corrected and concentrations were calculated. This procedure was carried out for each calibration-bracketed series. Molar ratios were calculated assuming 100 % $CaCO_3$ (cf. Vander Putten et al., 1999). A more detailed description of this procedure, as well as detection limits, accuracy and precision of standards can be found in Chapter 2.

2.4 Statistics

Regressions were calculated using bivariate least squares (BLS) statistics. Unlike ordinary least square regressions, the BLS considers errors on both the dependent and independent variables and is more appropriate for methods comparison (see Riu and Rius, 1996; Verheyden et al., 2005b). Significance tests for the slope and intercept of the regressions and correlation coefficients are based on the joint confidence interval. Errors of the regression coefficients are given as 95 % confidence intervals.

3. RESULTS AND DISCUSSION

3.1 Potential interfering elements

There are potential interferences of La^{138} and Ce^{138} on Ba^{138} when using the NIST610 and MACS-1 for calibration (I. Horn, University of Hannover, pers. comm., 2004). These elements are present in these calibration standards at similar concentrations to barium (Pearce et al., 1997; S. Wilson, pers. comm., 2002); however, the natural abundance of these particular isotopes are much lower than the natural abundance of barium (Table 1). Furthermore, the concentration of La and Ce in the shells analyzed in this study are very low (i.e., below the detection limit of all analytical methods used here). Therefore the interference would only occur during calibration and cause a systematic offset between the concentrations measured with each isotope of Ba.

Table 1. Ba isotopes and potentially interfering isotopes.

Isotope	AMU	Natural abundance (%)
Ba^{135}	134.9057	6.592
Ba^{137}	136.9058	11.23
*Ba^{138}	137.9052	71.7
*La^{138}	137.9071	0.09
*Ce^{138}	137.9060	0.25

* interfering isotopes

To test if there are large interferences, Ba^{135}, Ba^{137} and Ba^{138} were recorded on the same run to see if there is a systematic offset between these isotopes. Two *M. edulis* shells were analyzed on 17 June 2004 under typical operating conditions (see Chapter 2). No clear systematic offset was observed for elemental Ba concentrations using any of the isotopes when averaging data over the whole day for each isotope (average data in ppm (= μg/g): Ba^{135} = 7.3; Ba^{137} = 6.9; Ba^{138} = 7.3; data are within the 5 % error expected for this instrument). Moreover, there was no systematic offset at either low or high concentrations (Fig. 1). Finally, there was excellent agreement between the results obtained using the LA-ICP-MS and the Microdrill and SN-HR-ICP-MS (See Section 3.2 and Fig 2G and 2H).

Table 2. Percent relative standard deviation (%RSD) for each Ba isotope measured on the MACS1 (~100 ppm, n = 9) and MACS2 (~1 ppm, n = 8) on 17 June 2004 (ppm = μg/g).

Isotope	MACS1	MACS2
Ba^{135}	8.65	77.2
Ba^{137}	9.05	66.0
Ba^{138}	7.92	10.0

Although there is the possibility of interferences on Ba^{138}, it is still the preferred isotope because this isotope has the highest natural abundance (Table 1) and Ba concentrations in bivalve shells are typically low (~1-3 ppm, Fig. 1). While the concentrations of Ba^{135} and Ba^{137} are high enough at 100 ppm [Ba] for precise measurements, they are not when the analyte contains around 1 ppm [Ba]. This can be illustrated using the %RSD for the MACS1 and MACS2 pellets, which are above 50 % for the less abundant isotopes at 1 ppm (see Table 2).

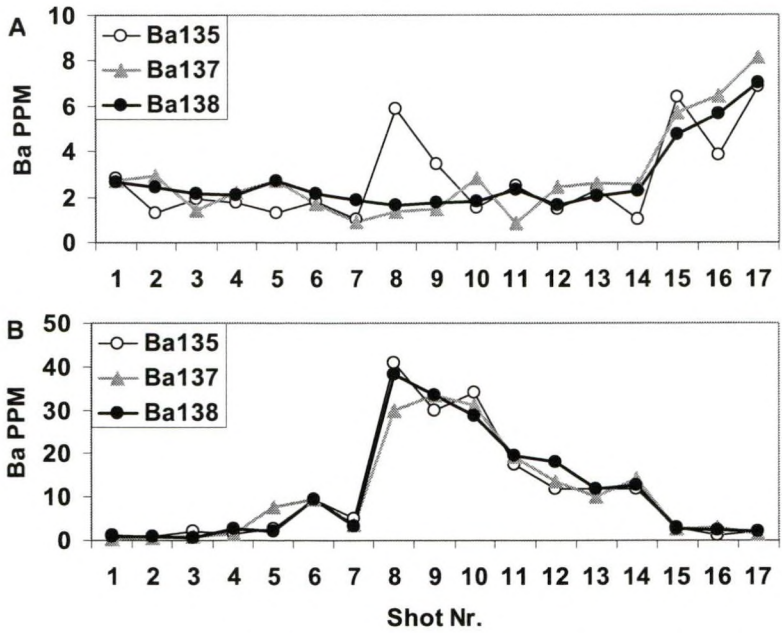

Figure 1. LA-ICP-MS data from a transect along the calcite layer of a *Mytilus edulis* shell analyzed on 17 June 2004. No systematic offset was observed between these isotopes of Ba at either low (A) or high (B) concentrations. Data are total Ba concentrations calculated from each isotope. ppm = μg/g.

In addition, Sr and Kr have masses which cannot be distinguished by this ICP-MS. However, considering the comparison with SN-HR-ICP-MS (see below), this does not seem to be a problem. Here only elements with mass interferences are considered and oxide and doubly charged ion interferences are not discussed.

3.2 LA-ICP-MS validation

Fallon et al. (1999) provide accurate LA-ICP-MS (λ = 193 nm) results by comparing the data with either isotope dilution (ID) - ICP-MS or ID - thermal ionization mass spectrometry (TIMS) measurements. They found that their in-house pressed coral powder disc was a highly accurate calibration standard for LA-ICP-MS for B/Ca, Mg/Ca, Sr/Ca and U/Ca, all of which were within the error of the solution estimate. However, they had a slight offset for their Ba/Ca ratios (~15 %). By combining the USGS synthetic pressed carbonate powder standard, MACS1, and the NIST610 glass standard, a similar precision may possibly be achieved with this LA-ICP-MS system (λ = 266 nm).

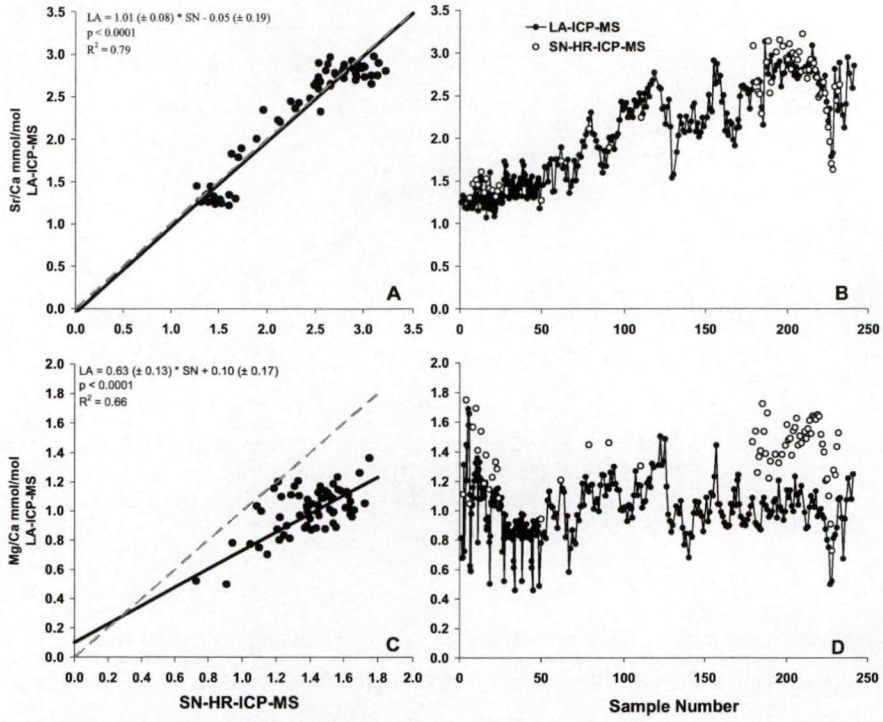

Figure 2. *Continued on next page*

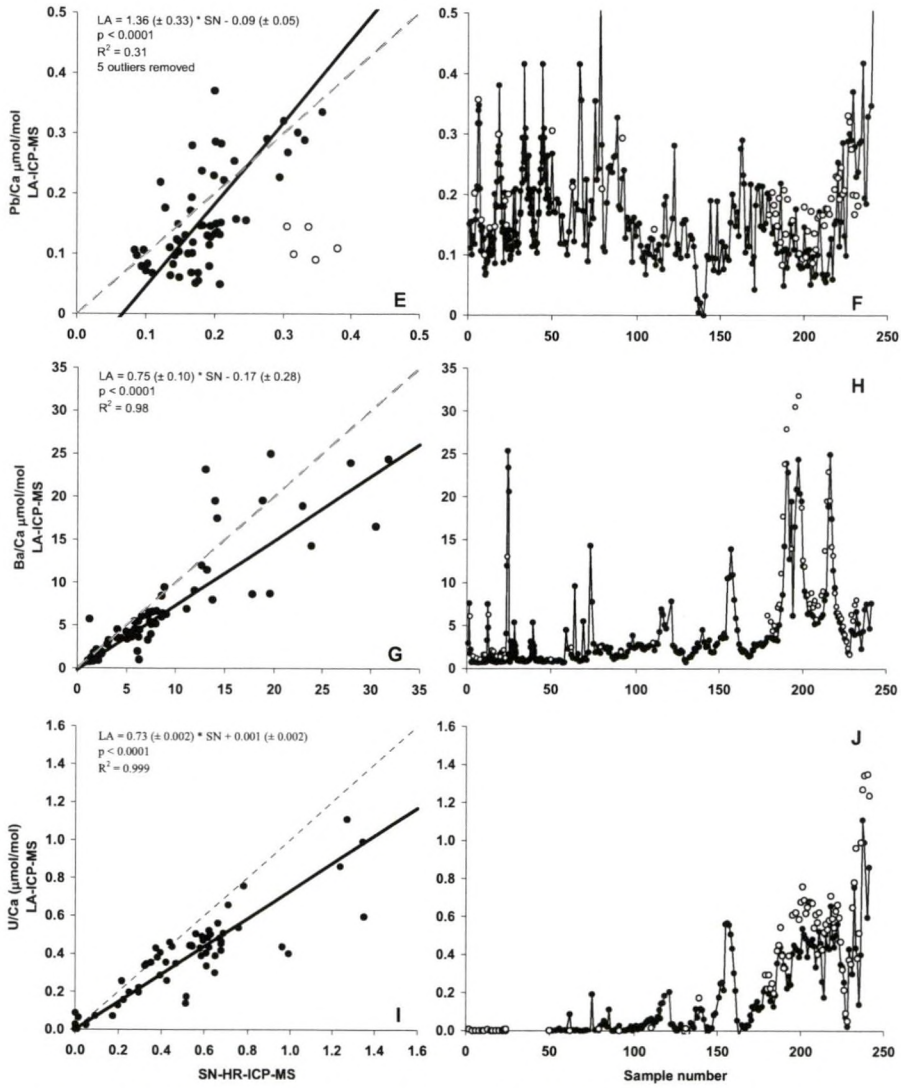

Figure 2. Comparison of LA-ICP-MS data with SN-HR-ICP-MS data from shell B1. Both the BLS regression data (A, C, E, G, and I) (N = 63) as well as the high resolution profile along the shell (sampling is from growing tip to umbo) (B, D, F, H, J) for Sr/Ca, Mg/Ca, Pb/Ca, Ba/Ca, and U/Ca are shown. Note that there are 5 outliers removed from the Pb/Ca regression (E) and U/Ca was not sampled with the LA-ICP-MS for the first 50 samples (J).

After blank subtraction and calibration of shell LA-ICP-MS data, ^{55}Mn, ^{59}Co, ^{65}Cu, and ^{111}Cd all provided concentrations below the detection limit and therefore will not be discussed further. The BLS slope for B/Ca was not significant ($p = 0.19$; $R^2 = 0.05$), with little variation in the LA-ICP-MS data as compared to SN-HR-ICP-MS data (data not shown). Therefore, at this concentration (~ 10 μmol/g), B is not a suitable element to analyze with this instrumental setup.

Overall, there was a good agreement between both methods for the remaining ratios (Fig. 2). Ratios of Sr/Ca were clearly the most reproducible between the methods, with the slope not different from one and the intercept not different from zero (Fig. 2A, B). Ratios of Mg/Ca were not entirely similar between the two methods (BLS slope = 0.63 ± 0.13), with the LA-ICP-MS giving lower ratios (Fig. 2C). Considering the low %RSD and good accuracy using the SN-HR-ICP-MS method (see Chapter 2), the SN-HR-ICP-MS Mg/Ca data are likely more correct. This offset could be a matrix effect problem, as the MACS1 standard does not have an adequate Mg concentration and thus the LA-ICP-MS calibration is more heavily relying on the NIST610 standard alone. Yet, Takesue and van Geen (2004), obtained similar Mg/Ca results (± 10 %) between Flame Atomic Absorption and LA-ICP-MS (λ = 193 nm) data calibrated using only NIST610. Although the LA-ICP-MS Mg/Ca ratios are not accurate, the high resolution profiles do show a similar trend between the two methods, especially when considering the large dip in the Mg/Ca ratios between sample numbers 200 and 250 (Fig. 2D). Therefore, the LA-ICP-MS Mg/Ca data is considered as qualitative. Ratios of Pb/Ca show a lot of scatter when comparing the methods (Fig. 2E); however, the slope is close to one and the trend in the high resolution profile can easily be observed in both profiles (Fig. 2F). Interestingly, the intercept is near zero, indicating a robust LA-ICP-MS calibration, unlike the MACS1 data, which was calibrated with the NIST610 alone (Table 9 of Chapter 2). This indicates that the inclusion of the more similarly matrix matched MACS1 in the calibration reduces the error caused by using the NIST610 alone. Similar to Pb/Ca, there is scatter in the Ba/Ca data (Fig. 2G), but the high resolution profiles match extremely well. The scatter is probably the result of the differences in sample size between the two methods; 50 μm for LA-ICP-MS vs 300 μm for micromilling. Ba/Ca peaks in these shells are very sharp (Fig. 2H), so large differences can easily occur by averaging

different sample sizes. Indeed, most of the deviation in the data is located at higher Ba/Ca ratios (Fig. 2G). Similarly, U/Ca data show some scatter at higher ratios (Fig. 2I), but the profiles show similar trends (Fig. 2J). Therefore, while Sr/Ca ratios can be considered quantitative, Pb/Ca, Ba/Ca, and U/Ca are near-quantitative, and Mg/Ca ratios are semi-qualitative.

In conclusion, considering the large variations of many elemental ratios in bivalve shells (Stecher et al., 1996; Vander Putten et al., 2000; Takesue and van Geen, 2004; Gillikin et al., 2005 a, b; Gillikin et al., in press; Gillikin et al., submitted-a), this LA-ICP-MS is more than adequate for detecting variations in bivalve shell geochemistry.

Chapter 4

Stable carbon and oxygen isotopes in an aragonitic bivalve (*Saxidomus giganteus*): assessing the reproducibility and reliability for environmental reconstruction

Foreword

In this chapter, the most well studied temperature proxy, $\delta^{18}O$, is assessed for the estuarine bivalve *Saxidomus giganteus*. Although there have been countless studies on oxygen isotopes in bivalve shells, many studies still over simplify the problem associated with unknown oxygen isotopic values of the water, which is the main focus here. Additionally, carbon isotope data are also presented, but a more comprehensive discussion on carbon isotopes can be found in the following two chapters.

Publications of the author related to this chapter:

Gillikin, D. P., F. De Ridder, H. Ulens, M. Elskens, E. Keppens, W. Baeyens and F. Dehairs, 2005. Assessing the reproducibility and reliability of estuarine bivalve shells (*Saxidomus giganteus*) for sea surface temperature reconstruction: implications for paleoclimate studies. *Palaeogeography Palaeoclimatology Palaeoecology* doi:10.1016/j.palaeo.2005.03.047

De Ridder, F., R. Pintelon, J. Schoukens and D. P. Gillikin, 2005. Modified AIC and MDL model selection criteria for short data records. *IEEE Transactions on Instrumentation and Measurement* 54 (1): 144-150.

De Ridder, F., J. Schoukens, R. Pintelon, D. P. Gillikin, L. André, W. Baeyens, A. DeBrauwere, and F. Dehairs, 2004. Decoding non-linear growth rates in biogenic archives. *Geochemistry, Geophysics, Geosystems* 5, Q12015, doi:10.1029/2004GC000771.

Abstract

Studies using oxygen isotopes ($\delta^{18}O$) of mollusk shells to determine paleo-temperature need to assume water $\delta^{18}O$ values, which could severely influence calculated temperatures. The aragonitic shells of the Butter Clam, *Saxidomus giganteus* (DeShayes, 1839), were analyzed to determine the reproducibility of the isotopic signal between individuals and to assess how precisely temperature could be calculated given known salinity and temperature. Furthermore, carbon isotopes were also investigated as an environmental proxy. The abundance of well-preserved *S. giganteus* shells in archeological and geological deposits in northwestern North America makes them a particularly suitable species for paleoclimate studies. Seasonally resolved stable oxygen isotope profiles in three *S. giganteus* shells collected from the same site in Puget Sound (Washington, USA) were well correlated ($0.77 < R^2 < 0.87$). Although there were differences up to 0.58 ‰ in high resolution $\delta^{18}O$ profiles of the three shells, the difference between the average $\delta^{18}O$ of each shell was less than half of this (0.19 ‰) and half of what has been reported for between-colony coral variability. Profiles of $\delta^{13}C$ on the other hand were more complex, with shell $\delta^{13}C$ being about 2.5 ‰ lower than expected equilibrium values. However, this roughly conforms to the idea that about 10 % of the shell carbon originates from metabolic CO_2. Both $\delta^{18}O$ and $\delta^{13}C$ indicate that *S. giganteus* do not grow during periods of reduced salinity. Despite the excellent reproducibility of $\delta^{18}O$ between shells, and the fact that salinity effects were duly considered, calculated temperature still differed from instrumental temperature. Applying different salinity - $\delta^{18}O$ water relationships to average shell $\delta^{18}O$, and considering salinity from the shell collection site and a nearby offshore station resulted in calculated average water temperatures ranging from 1.7 to 6.4 °C warmer than measured. Although it could not be determined if *S. giganteus* precipitate their shells in isotopic equilibrium, the difficulty in predicting temperature probably arose from not being able to accurately determine $\delta^{18}O$ of the water at the time of shell precipitation. These data highlight the difficulties inherent to using stable isotope profiles of estuarine biogenic carbonates as environmental proxies.

1. INTRODUCTION

Ever since the pioneering work of Epstein et al. (1953) it has been well known that the oxygen isotopic signature recorded in mollusk shells ($\delta^{18}O_S$) not only reflects the temperature during crystallization, but also the oxygen isotopic ratio of the water ($\delta^{18}O_W$) within which they formed. Despite this, many studies have utilized $\delta^{18}O_S$ as a temperature proxy using assumed $\delta^{18}O_W$ (Weidman et al., 1994; Purton and Brasier, 1997). Carbon isotopes in biogenic carbonates on the other hand, were originally hoped to record the isotopic signature of seawater dissolved inorganic carbon (DIC) (Mook and Vogel, 1968), which can provide information about salinity, anthropogenic carbon inputs and productivity. However, more recent work has shown the complications with this proxy due to the incorporation of metabolic CO_2 (McConnaughey 1989b; McConnaughey et al., 1997; Lorrain et al., 2004a).

Bivalves are beneficial in that they can provide seasonal records of environmental conditions and have a wide geographic distribution, whereas many other proxies, such as corals, are limited in their latitudinal extent. Previous workers have used isotope ratios in bivalve shells as both salinity (Ingram et al., 1996) and temperature proxies (Weidman et al., 1994; Surge et al., 2001). Many paleoclimatic studies (Purton and Brasier, 1997; Dutton et al., 2002; Holmden and Hudson, 2003) rely on the assumption that bivalves fractionate isotopes in accordance with the well-established empirically determined paleotemperature equations for biogenic carbonates (Epstein et al., 1953; Grossman and Ku, 1986; Böhm et al., 2000). However, without species-specific verification with recent specimens, this is a risky practice. As opposed to corals and brachiopods, bivalves do generally secrete their skeletons in equilibrium (cf. Wefer and Berger, 1991), yet this might not always hold true (Owen et al., 2002). In addition, bivalve physiology also plays an important role in the stable isotope ratios recorded in the shells due to the effect of temperature and salinity on growth. Bivalves may be euryhaline or stenohaline and may continue to grow in extreme temperatures or have minimum and or maximum temperature growth hiatuses, all of which will affect the isotopic signal recorded in the shell. The effect of rapidly changing temperature and salinity is especially important in coastal areas and even more so in estuaries.

Coastal settings were important to early people, resulting in numerous shell middens spanning the late Quaternary (e.g., Hetherington and Reid, 2003). It would be beneficial to both archeologists and paleoclimatologists to have well calibrated proxies of temperature in these regions. However, the fact that these regions can be highly dynamic in nature and the stable isotope ratios in carbonates are dependent on the isotope ratio of the water, which co-varies with salinity, make many of these areas difficult for isotope geochemistry.

This study aims to determine the reproducibility of the isotopic signal between individuals and to asses how precisely temperature can be calculated from *Saxidomus giganteus* (DeShayes, 1839) $\delta^{18}O_S$, given known instrumental temperature and salinity. Furthermore, the carbon isotope chemistry is investigated as a proxy of the carbon isotopic signature of DIC ($\delta^{13}C_{DIC}$). The Butter clam, *S. giganteus*, is an aragonitic infaunal marine clam usually inhabiting the intertidal zone, but which can occur at depths in excess of 30 m (Quayle and Bourne, 1972). They are a temperate species, which cannot survive in very cold waters or reduced salinities (Bernard, 1983; Hetherington and Reid, 2003). *S. giganteus* has been continuously present as far north as British Columbia for the past ~12,000 years and probably was an important food source for early peoples as early as 9,000 years BP (Hetherington and Reid, 2003), and continue to be harvested today (Quayle and Bourne, 1972). *S. giganteus* are commonly found in prehistoric midden sites (Hetherington and Reid, 2003; Taylor, 2004) as well as in Pleistocene geologic deposits as well preserved fossils (Kvenvolden et al., 1979), potentially making them a very useful paleo-environmental proxy.

To determine the reliability of *S. giganteus* as a recorder of environmental conditions, three specimens that grew in the same area were analyzed under the premise that if the isotope chemistry of the shells reflects an external environmental forcing, the signal should be similar in each shell. These results were then compared with environmental parameters to ascertain the accuracy and potential problems of using estuarine bivalves as paleo- environmental proxies.

2. MATERIALS AND METHODS

Three specimens of *Saxidomus giganteus* were collected alive from the same area (within ~ 10 m) in Puget Sound, near Carkeek Park, North Seattle, WA, USA (N47°42'45'' W122°22'46'') on 18 September 2001 (Fig. 1). They were collected in gravely mud about 30 cm above mean spring low tide. The shells were carefully opened with a knife and were air-dried after tissue was removed. Sections of the shells were cut with a diamond saw along the axis of maximal growth, rinsed with deionised water, air-dried and mounted on microscopic slides.

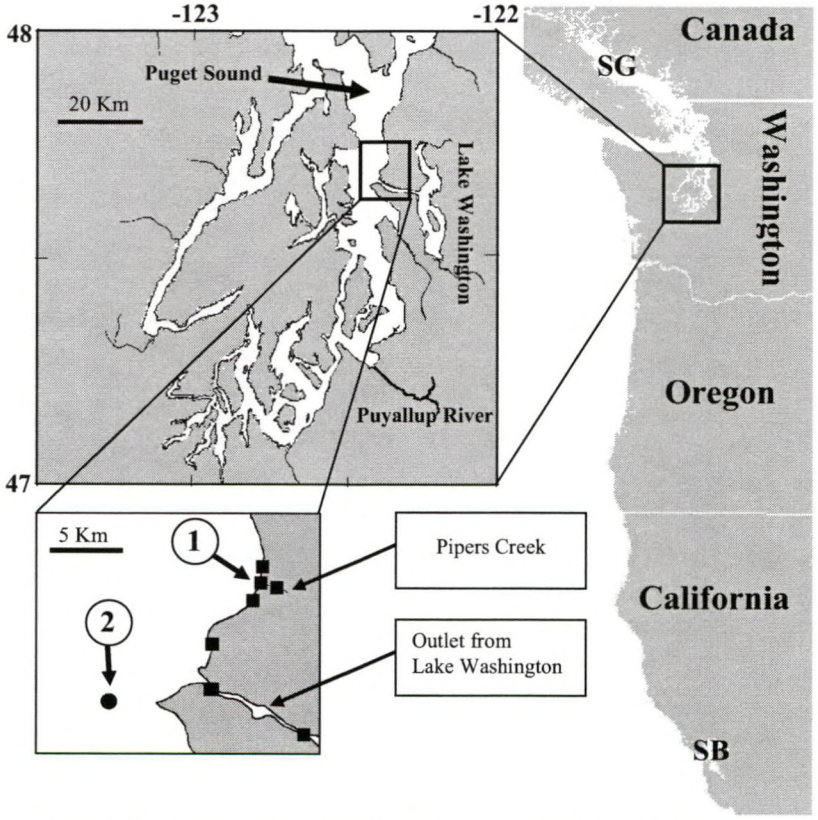

Figure 1. Map of the West Coast of North America with detailed maps indicating the shell collection site (1) and the offshore station PSB003 (2) as well as water sampling sites (squares). The Puyallup River, Strait of Georgia (SG) and San Francisco Bay (SB) are also shown.

Each section cut from a valve represents a series of successive growth increments. The sections were mounted on a computer controlled Merchantek Micromill Sampler (a fixed drill and computer controlled micro positioning device), which allows precise sampling. High resolution profiles were obtained by milling a succession of adjacent grooves 600 μm in length, 200 μm depth and 300 μm width, using a 300 μm bit (325 μm deep spots were used near the umbo due to the thinning of the carbonate layer). Grooves were milled parallel to the growth increments, along a transect from the youngest material (growing tip) to the oldest (umbo) in the aragonite outer layer of the shell section (Fig. 2). Shells were not sampled completely to the umbo because the outer layer became too thin to sample; shell three was only partially sampled. Various drill speeds were tested, as well as manual sampling (scraping with scalpel blade), to see if heating during drilling could have caused mineralogical transformation into calcite (cf. Gill et al., 1995); however, no significant differences were noted in isotope ratios. Additional samples (9 per shell) were collected from the inner layer near the umbo (Fig. 2), which should integrate the isotopic signal over the entire life of the animal.

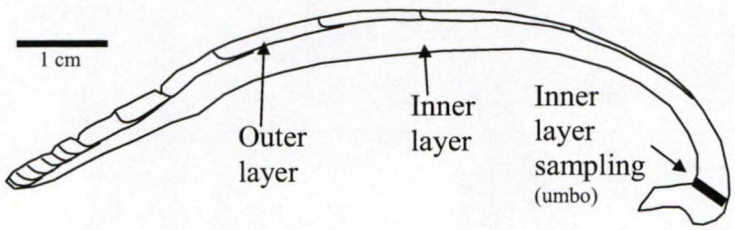

Figure 2. Cross section of *Saxidomus giganteus* shell showing the successive growth increments in the outer layer of the shell.

All isotope analyses were carried out in the Stable Isotope Laboratory of the Vrije Universiteit Brussel, Belgium. Shell oxygen ($\delta^{18}O_S$) and carbon ($\delta^{13}C_S$) isotope analysis was performed using a ThermoFinnigan Kiel III (an automated carbonate preparation device) coupled to a ThermoFinnigan Delta+XL dual inlet isotope ratio mass spectrometer (IRMS). Using anhydrous phosphoric acid, the carbonate of the sample is transformed into CO_2, which is cryogenically purified with liquid nitrogen. The samples were calibrated against the standard NBS-19 ($\delta^{18}O$ = -2.20 ‰, $\delta^{13}C$ =

+1.95 ‰) and data are reported as ‰ VPDB using the conventional delta notation (see Chapter 1). The reproducibility (1σ) of the routinely analyzed carbonate standard (NBS-19) was 0.08 ‰ for $\delta^{18}O$ and 0.04 ‰ for $\delta^{13}C$ (n = 286). Furthermore, the lighter standard, NBS-18 ($\delta^{18}O$ = -23.05 ‰, $\delta^{13}C$ = -5.04 ‰), gave similar precision and was within 0.01 ‰ of the recommended values (n = 22).

As no data on Puget Sound water oxygen isotope chemistry could be found in the literature, nearshore water samples were collected on 29 May 2003 for determination of salinity, $\delta^{18}O$ and $\delta^{13}C_{DIC}$ from the outlet from Lake Washington (Salmon Bay; freshwater) to about 800 m north of Carkeek Park, including Pipers Creek, the small freshwater stream draining into the shell collection area (Fig. 1). Water $\delta^{18}O$ was determined by the conventional CO_2-H_2O equilibration method, similar to Prosser et al. (1991). Precision was better than 0.15 ‰ (1σ) by analysis of seawater standards calibrated against VSMOW. The $\delta^{13}C_{DIC}$ was determined by acidifying 5 ml of water in an 8 ml helium flushed headspace vial and subsequently injecting 400 µl of the headspace into the carrier gas stream of a ThermoFinnigan Delta+XL continuous flow IRMS. Precision of $\delta^{13}C_{DIC}$ was better than 0.2 ‰ based on replicate measurements; data were corrected using calibrated CO_2 gas according to Miyajima et al. (1995) and are given vs. VPDB. Salinity was estimated from Na^+ concentrations (measured by ICP-OES) using the equation:

$$\text{Salinity} = \mu g\ g^{-1}\ Na^+ * 35 / 10783.7 \qquad (1)$$

considering 10783.7 µg g^{-1} Na^+ at a salinity of 35 (DOE, 1994); with an analytical precision of ± 0.25 salinity units.

Monthly measurements of nearshore temperature and salinity from Carkeek Park were obtained from the King County Environmental Laboratory. This data set is not complete and only extends to 1997, while $\delta^{18}O_S$ data suggest these shells started growing in 1991 (see results). To extend the data set, data from an offshore station (station PSB003, situated at approximately 10 km from the sampling area; Fig. 1), monitored since 1971 (also monthly) by the Washington State Department of Ecology's Environmental Information Management System project

(http://www.ecy.wa.gov/eim) were used. The offshore station was sampled at a depth of 0.5 m, but overlies 110 m of water. Water temperature is well correlated between both stations ($R^2 = 0.83$, $p < 0.0001$, $n = 36$; Fig. 3A) allowing us to construct a temperature record back to 1991. However, summer water temperatures are higher at the nearshore station (Carkeek). Salinity is not correlated ($R^2 = 0.14$, $p = 0.062$, $n = 26$) and is generally less variable at the offshore station (Fig. 3B). Average monthly precipitation (1994-2001) for Seattle was obtained from the NOAA (2003) and shows that salinity drops are not always related to precipitation events (Fig. 3B).

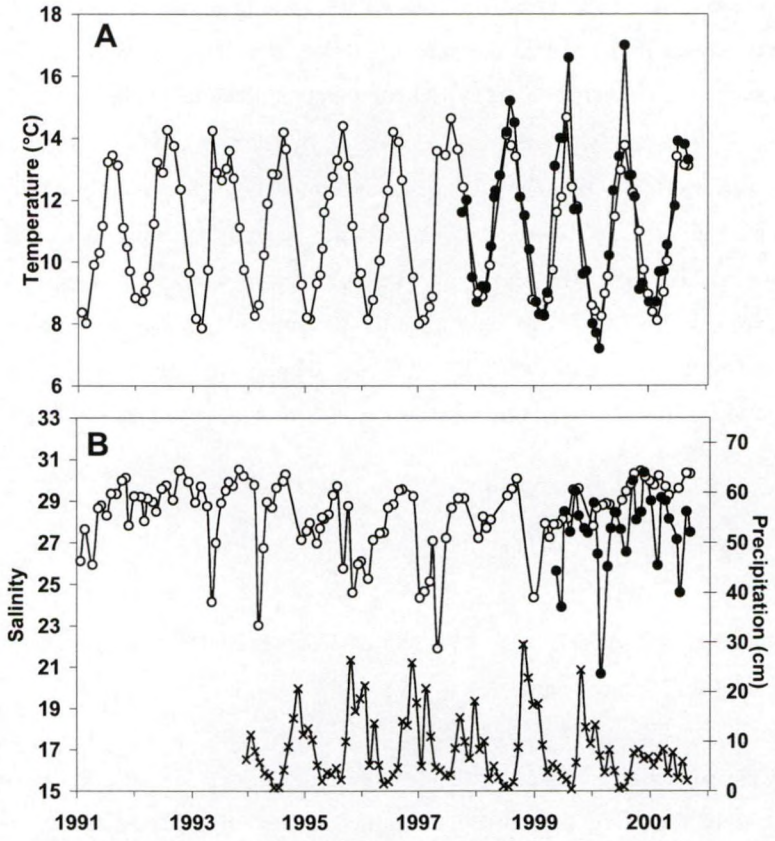

Figure 3. (a) Temperature records at both the shell collection site (Carkeek Park; solid circles) and at the offshore station (PSB003; open circles) and (b) salinity data from both stations (symbols as in a) as well as monthly average precipitation data from Seattle, Washington (crosses).

The aragonite paleotemperature equation of Böhm et al. (2000) was used to estimate temperature from $\delta^{18}O_S$:

$$T\ (°C) = (20.0 \pm 0.2) - (4.42 \pm 0.10) * (\delta^{18}O_S - \delta^{18}O_W);\ \text{for } 3° < T < 28° \qquad (2)$$

which is largely based on the equation of Grossman and Ku (1986) and includes many taxa of aragonite precipitating organisms.

3. RESULTS

When both $\delta^{13}C_{DIC}$ and $\delta^{18}O_W$ are plotted against salinity, the water samples from the outlet of Lake Washington are clearly not following the same mixing lines as the water samples taken nearby the shell collection site (Fig. 4). Excluding the two samples from the outlet of Lake Washington, there are excellent linear relationships between salinity and isotopes, with $\delta^{18}O_W = 0.309 * \text{Salinity} - 10.49$ ($R^2 = 0.998$, $p < 0.0001$, $n = 5$) and $\delta^{13}C_{DIC} = 0.573 * \text{Salinity} - 16.54$ ($R^2 = 0.997$, $p < 0.0001$, $n = 5$).

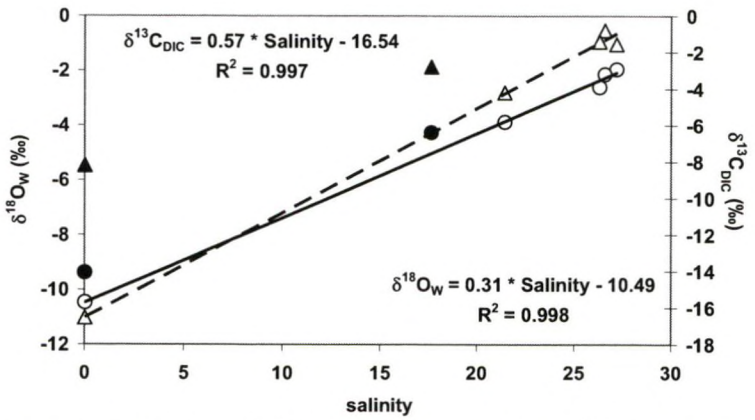

Figure 4. Regressions of $\delta^{18}O_W$ (circles, solid line) and $\delta^{13}C_{DIC}$ (triangles, dashed line) vs. salinity from nearby the collection site (collected on 29 May 2003). Data from the water samples collected from the outlet of Lake Washington were not included in the regression and are shown as solid symbols.

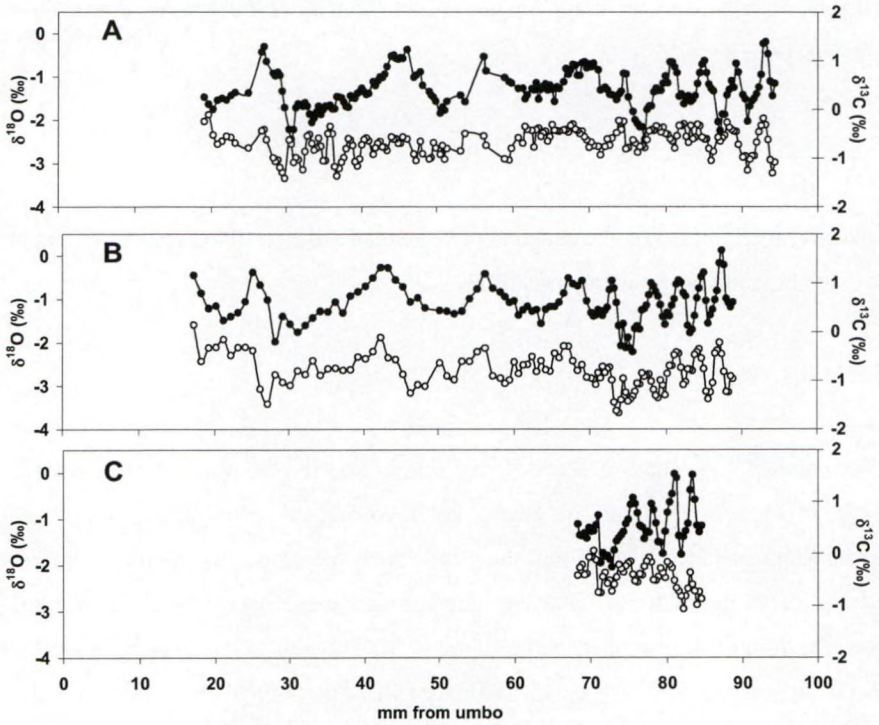

Figure 5. Plots of $\delta^{18}O_S$ (solid circles) and $\delta^{13}C_S$ (open circles) vs. distance from the umbo for the three clams (A: shell 1, B: shell 2, C: shell 3).

Profiles of $\delta^{18}O_S$ and $\delta^{13}C_S$ are plotted against sampling distance from the umbo (oldest carbonate) (Fig. 5). Each shell exhibits a clear seasonal pattern in $\delta^{18}O_S$, with the most negative values representing the warmest summer water temperatures. Shell $\delta^{13}C$ tends to follow a trend of the most negative values falling in the spring or summer (less so in shell 3) (Fig. 5). Averages and ranges of isotope data, as well as results from the inner layer sampling can be found in Table 1. The average high resolution $\delta^{18}O_S$ values were in good agreement between shells, with a maximum difference of 0.19 ‰. Furthermore, the inner layer $\delta^{18}O_S$ represented the average shell well, with a maximum difference of 0.24 ‰. High resolution $\delta^{13}C_S$ on the other hand was variable between the three shells, but was within the same 2 ‰ range for all shells (Fig. 5). Average high resolution $\delta^{13}C_S$ values were within 0.37 ‰ for the three shells and was similar to differences in the inner layer (maximum difference of 0.41 ‰; Table 1). Shell $\delta^{13}C$ and $\delta^{18}O$ exhibit a very weak positive correlation in shells 1 ($R^2 = 0.05$, $p < 0.01$, $n = 190$) and 2 ($R^2 = 0.19$, $p < 0.0001$, $n = 123$) but not in shell

3 (R^2 = 0.01, p = 0.54, n = 55). Growth rates show a strong decrease through ontogeny, typical of bivalves; although the trend is similar for all shells, there are differences of more than 4 mm yr^{-1} (i.e., 1994) between shells (Fig. 6).

Table 1. Average, standard deviation, and minimum and maximum $\delta^{18}O_S$ and $\delta^{13}C_S$ from the three shells as well as the average values obtained from the inner layer near the umbo (see Fig. 2). All data in ‰; n = number of samples.

	Shell 1	Shell 2	Shell 3
Average $\delta^{18}O_S$	-1.29 ± 0.44	-1.10 ± 0.44	-1.16 ± 0.47
Minimum $\delta^{18}O_S$	-2.44	-2.21	-2.04
Maximum $\delta^{18}O_S$	-0.18	0.13	-0.03
Inner layer $\delta^{18}O_S$	-1.08 ± 0.09	-1.34 ± 0.08	-1.23 ± 0.15
Average $\delta^{13}C_S$	-0.67 ± 0.26	-0.81 ± 0.34	-0.44 ± 0.25
Minimum $\delta^{13}C_S$	-1.41	-1.66	-1.06
Maximum $\delta^{13}C_S$	-0.10	0.15	0.06
Inner layer $\delta^{13}C_S$	-0.72 ± 0.15	-1.04 ± 0.29	-0.85 ± 0.18
n*	190	123	55

*Inner layer samples are an average of 9 samples.

To test the reproducibility of the signal recorded in *Saxidomus giganteus* shells, the data first need to be fit on the same time axis to correct for differences in growth rate. Oxygen isotope profiles from shells 1 and 3 were fit to the x-axis of shell 2 (shell 2 arbitrarily chosen) using a phase demodulation method (Fig. 7; see De Ridder et al., 2004). Briefly, this method is based on the periodicity of the signal and uses the side peaks in the Fourier spectrum to model the variations in growth. Once the growth is known, the time axis (x-axis) can be scaled accordingly. Using this method, there is excellent agreement between the three profiles (shell 1 vs. 2, R^2 = 0.87; 1 vs. 3, R^2 = 0.81; 2 vs. 3, R^2 = 0.77; $p < 0.0001$ for all; Fig. 7).

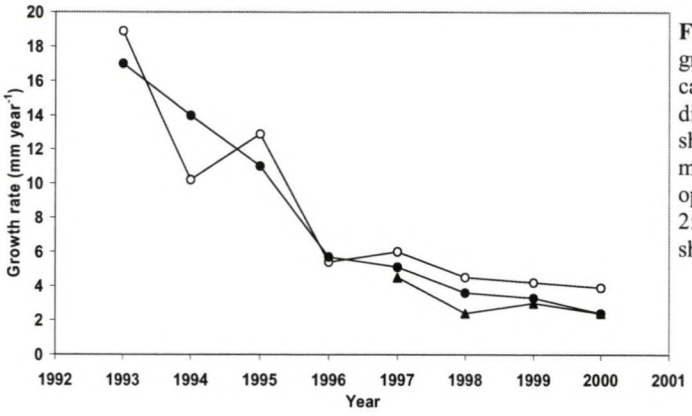

Figure 6. Annual growth rates calculated from the distance along the shell between $\delta^{18}O_S$ maxima (shell 1: open circles, shell 2: solid circles, shell 3: triangles).

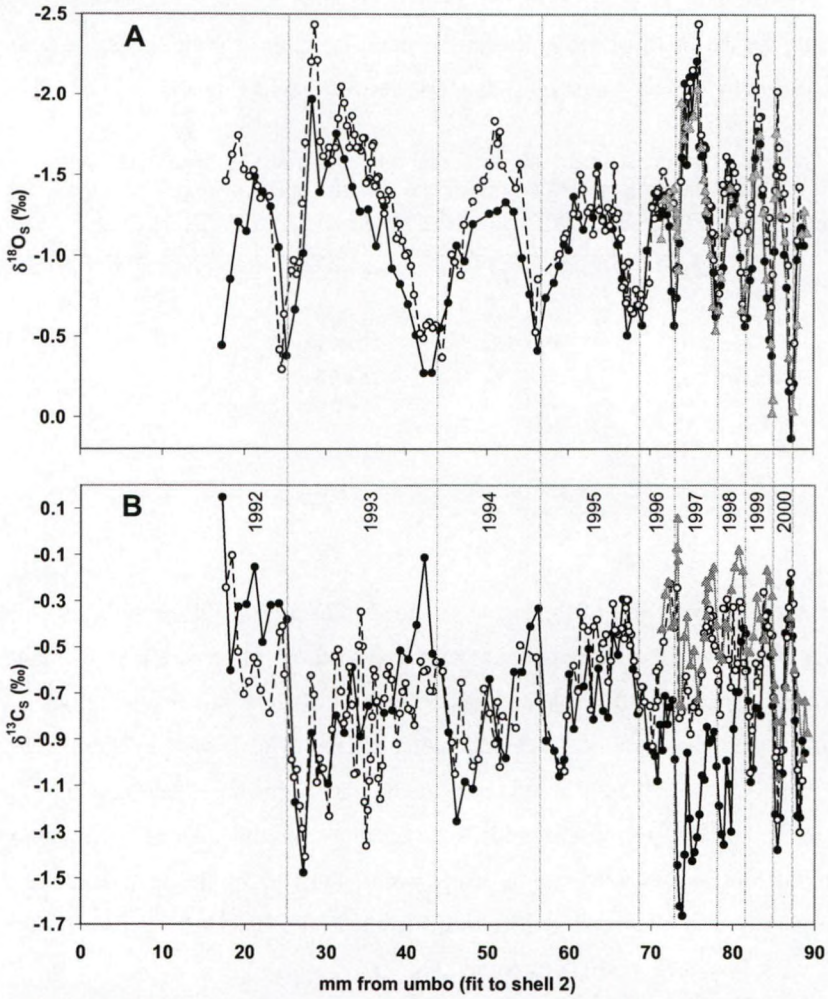

Figure 7. $\delta^{18}O_S$ (A; y-axis inverted) and $\delta^{13}C_S$ (B) of the three shells fit to the x-axis of shell 2 (shell 1: open circles, shell 2: solid circles, shell 3: triangles). Growth years are approximated by dotted lines.

4. DISCUSSION

4.1 Reproducibility

Despite the excellent $\delta^{18}O_S$ correlations between the three shells, there are still important differences of up to 0.58 ‰ (Fig. 7). The offset could be a result of either real differences in $\delta^{18}O_S$ or may be the result of time averaging caused by differences

in growth rate between shells. Time averaging occurs when shell growth slows and sample interval (i.e., drill spacing) remains the same, resulting in the same sample size representing (and averaging) more time. Time averaging will thus bring the amplitude of the $\delta^{18}O_S$ cycle closer to the mean (see Goodwin et al., 2003). Indeed, for the years with the largest $\delta^{18}O_S$ differences (see Fig. 7), the shells exhibit large differences in growth rates (Fig. 6). For example, in the last three years of growth, shell 1 grew 1.4 to 2 times faster than shell 3. This could help explain the reduced summer $\delta^{18}O_S$ values in shell 3, but not the winter difference where shell 3 has the larger amplitude. Furthermore, these differences may be caused by physiological differences between clams, with some clams precipitating their shells during certain hours of the day (e.g., cool mornings; cf. Goodwin et al., 2001). Finally, they might be the result of micro-site conditions being different where the individual clams grew, e.g., groundwater outflow can be limited to very small patches in the intertidal zone (Kohout and Kolipinski, 1967). Whether or not these differences reflect real environmental differences, or are the result of vital effects can not be determined here. The maximum difference between the shells (~ 0.5 ‰) results in a maximum calculated temperature difference of about 2.2 °C. Elliot et al. (2003) found similar differences between *Mercenaria mercenaria* (Linnaeus, 1758) shells grown at the same locale, which they attributed to variation in growth rates between the shells (i.e., an averaging effect). This illustrates the bias that can be expected when working on only one shell. However, it should be noted that the differences between the average $\delta^{18}O_S$ were smaller (Table 1; the maximum difference is 0.19 ‰ between shell 1 and 2) and about half of that recorded in between-colony coral variability (0.4 ‰; Linsley et al., 1999). This suggests that the difference in average calculated temperatures based on different shells in this population is on the order of 0.8 °C.

All $\delta^{13}C_S$ data were within the same 1.9 ‰ range, however were not well correlated overall. It is interesting to note that in the high resolution profiles of $\delta^{13}C_S$, all three shells synchronize during the last two years measured, and shells 1 and 2 show some correlation in the first four years (Fig. 7). However, no adequate explanation could be found for why in some years they synchronize (e.g., 1994-5, 2000-1) and in others they do not.

The similarities between the $\delta^{18}O_S$ averages of the high resolution sampling of the outer layer and the $\delta^{18}O_S$ data from the inner layer (Table 1) confirm that the inner layer may be used to obtain a fast and inexpensive average $\delta^{18}O_S$. Shell $\delta^{13}C$ was also similar between the two methods for shells 1 and 2, but was on average 0.41 ‰ more negative than the high resolution outer layer average of shell 3, which could be an effect of $\delta^{13}C_S$ becoming more positive through ontogeny as was observed in shell 1.

4.2 Oxygen isotopes

When daily growth increments are present, they can easily be used to date the incremental samples (Schöne et al., 2003b; Lorrain et al., 2004a). However, when daily increments are not easily discernible, the usual method used to assign a time scale to the $\delta^{18}O_S$ record is to compare measured and predicted $\delta^{18}O_S$ (Klein et al., 1996a, b; Auclair et al., 2003; Elliot et al., 2003). Predicted $\delta^{18}O_S$ is calculated using a paleotemperature equation (Epstein et al., 1953; Grossman and Ku, 1986; Böhm et al., 2000), where instrumental temperature is known and $\delta^{18}O_W$ usually is calculated from its relationship with salinity.

Understanding the salinity - $\delta^{18}O_W$ relationship is crucial when calculating temperature from $\delta^{18}O_S$, especially in estuarine conditions. For example, only a 0.25 ‰ change in $\delta^{18}O_W$ (or roughly about 1 PSU in this study) results in a 1.1 °C temperature difference. The shortcomings of collecting $\delta^{18}O_W$ data from only one day are acknowledged as $\delta^{18}O_W$ may change seasonally due to changes in the $\delta^{18}O$ of precipitation (and glacial melt water volume). However, there is no published data available from Puget Sound regarding $\delta^{18}O_W$. Carpenter and Lohmann (1995) mistakenly reported the data of Klein et al. (1996a) were from Puget Sound, but they were actually taken 200 km to the north at the northern end of the Strait of Georgia, British Columbia, Canada (see Fig. 1 for location; Klein et al., 1996a). Auclair et al. (2003), working on brachiopods from Puget Sound, used a simple mass balance equation based on marine water (34.5 PSU = 0 ‰) and freshwater (0 PSU = -14 ‰) end members. Due to the fact that the salinity - $\delta^{18}O_W$ relationship from this study might not be robust, other published data from the region were explored. Five regression equations were tested (see Table 2): 1) Klein et al. (1996a) from the Strait

of Georgia, 2) Ingram et al. (1996) from San Francisco Bay, 3) this study, 4) Auclair et al. (2003; see above), and 5) a mixing model based on the freshwater endmember of Coplen and Kendall (2000; $\delta^{18}O_W$ from the Puyallup River, which flows into southern Puget Sound (Fig. 1), measured on several occasions between 1984 and 1987 ($\delta^{18}O_W$ = -12.4 ± 1.3 ‰)) and the marine endmember of Epstein and Mayeda (1953; $\delta^{18}O_W$ of ocean surface water sampled along the Northwest coast (32.6 ± 0.3 PSU; $\delta^{18}O_W$ = -0.95 ± 0.18 ‰)) (hereafter referred to as EM & CK). Using these salinity - $\delta^{18}O_W$ relationships results in a maximum average predicted carbonate difference of 0.77 ‰ (or 3.4 °C) when using the equation of Böhm et al. (2000) (equations are summarized in Table 2 and sampling sites are shown in Fig. 1). The largest difference is between this study and the data of Klein et al. (1996a). However, the use of the salinity - $\delta^{18}O_W$ relationship from this study is not necessarily the best choice. The data of Ingram et al. (1996; San Francisco Bay) and Klein et al. (1996a; Strait of Georgia) were both taken during a full year and bracket the sampling site to the South and North, respectively (see Fig. 1). When considering that $\delta^{18}O$ of precipitation becomes more negative northward along the west coast of North America (IAEA, 2001; Coplen and Kendall, 2000), it is also expected that slopes between salinity and $\delta^{18}O_W$ become larger and intercepts more negative toward the north. Theoretically, the slope and intercept of the salinity - $\delta^{18}O_W$ relationship for Puget Sound should fall between these two equations. Neither the relationship from this study, nor the relationship of Auclair et al. (2003) are bracketed by these equations, whereas the EM & CK equation is (Table 2). This could point to the fact that the Auclair et al. (2003) equation and the equation from this study are not appropriate for Puget Sound. However, when taking a closer look at the predictability of these equations in the salinity range of interest (~20-30 PSU), the 95 % prediction intervals from Klein et al. (1996a) and Ingram et al. (1996) greatly overlap (Fig. 8). This is most likely caused by the large seasonal fluctuations in $\delta^{18}O$ of precipitation and river run-off (IAEA, 2001; Coplen and Kendall, 2000). Therefore $\delta^{18}O_W$ is considered as unknown due to the poor predictability of these equations.

Considering that there is not a well constrained salinity - $\delta^{18}O_W$ relationship for this region, a reliable predicted $\delta^{18}O_S$ cannot be calculated. Furthermore, eq. 2 cannot be solved for $\delta^{18}O_W$ being that the temperature for each $\delta^{18}O_S$ is unknown. Therefore the

only option is to calculate temperature from $\delta^{18}O_S$, using a constant $\delta^{18}O_W$, and to compare this with the instrumental temperature record. We calculated that the average modeled temperature best matched the average instrumental temperature (11.4 °C) when using a $\delta^{18}O_W$ of -3.12 ‰. To reduce the bias of any one shell, an average $\delta^{18}O_S$ profile from the three shells was calculated, using the phase demodulation method of De Ridder et al. (2004), and this was used to calculate temperature, which was fit to the instrumental temperature record using the same technique. This procedure resulted in a reasonable fit with a correlation (R^2) of 83 % ($p < 0.001$; Fig. 9). As there is a good fit between both minima and maxima of many years, *S. giganteus* does not seem to have a growth shut down temperature (temperature where they stop growing) in this temperature range. However, the extreme summer temperatures recorded at Carkeek (which are monthly point measurements) were not recorded in the shell. This could either be the result of *S. giganteus* not precipitating during the warmest summer days or that these warm temperatures last a short time and are averaged with cooler temperatures when sampling the shell. As Bernard (1983) reported that the upper thermal threshold of *S. giganteus* is above 20 °C, and the warmest temperatures here are about 18 °C, the latter seems more likely, but only daily water temperature data could give a definitive answer.

Table 2. West Coast $\delta^{18}O_W$ - salinity relationships from various studies ($\delta^{18}O_W$ = Salinity * b + a).

Location	Relation to study site	Slope (b)	Intercept (a)	Reference
Strait of Georgia	± 200 Km North	0.39	-13.50	Klein et al. (1996a)
Puget Sound	Near collection site	0.31	-10.49	This study
Puget Sound	Theoretical	0.41	-14.00	Auclair et al. (2003)
Puget Sound + Pacific	Nearby collection site (see text)	0.36	-12.44	Epstein & Mayeda (1953) and Coplen and Kendall (2000)
San Francisco Bay	± 1300 Km South	0.32	-10.95	Ingram et al. (1996)

The calculated $\delta^{18}O_W$ which fit best with these data (-3.12 ‰) corresponds to a salinity range of about 21 - 28 (considering the 95 % prediction intervals, Fig. 8), which is the lower range of salinities observed at this site (27.5 ± 2.0; Fig. 3) and 0.5 ‰ more negative than the average $\delta^{18}O_W$ calculated using the EM & KC equation (-2.52 ± 0.72 ‰). This could imply that these bivalves are precipitating out of equilibrium. There are several factors that could cause disequilibrium. Mineralogy is

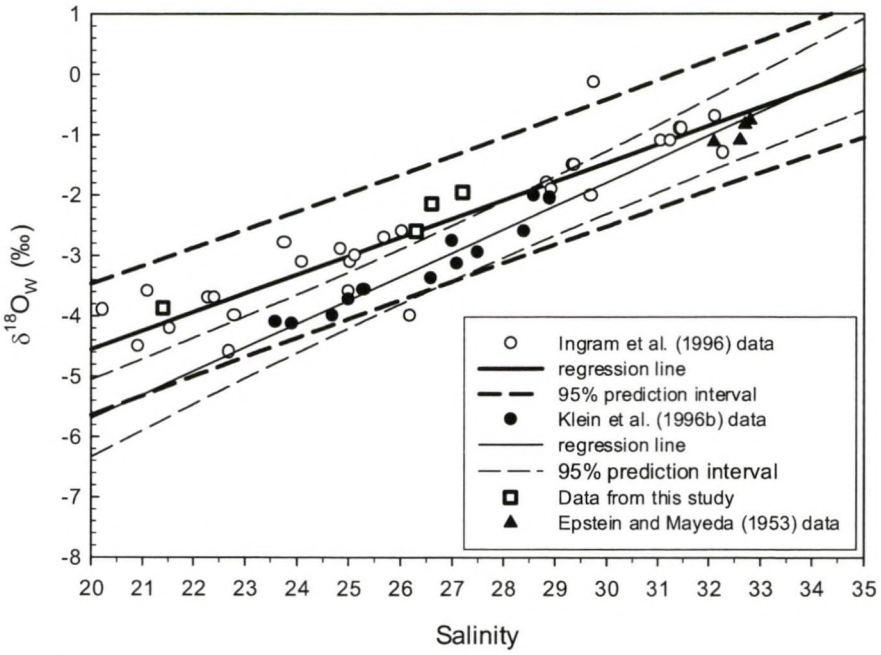

Figure 8. Regressions and 95% prediction intervals of salinity and $\delta^{18}O_W$ for the salinity range of interest. Data from San Francisco Bay (Ingram et al., 1996) and the Strait of Georgia, B.C. (Klein et al., 1996a). Data from Epstein and Mayeda (1953) and data from this study are also plotted.

important as calcite is depleted in ^{18}O by about 0.6 ‰ relative to aragonite (Tarutani et al., 1969); however *S. giganteus* shells are composed almost entirely of aragonite based on XRD analysis and minor element composition (Ulens, 2003; Taylor, 2004; Chapter 8). Kinetic effects can cause depletions in ^{18}O relative to equilibrium when $CaCO_3$ precipitation is fast enough to allow precipitation of HCO_3^- and or CO_3^{2-} before equilibration with H_2O (McConnaughey, 1989b). However, kinetic effects usually act on both carbon and oxygen isotopes; considering the fact that $\delta^{18}O_S$ and $\delta^{13}C_S$ were poorly correlated in all shells, kinetic effects most likely are very small (McConnaughey, 1989b). Differences in pH at the site of calcification can also cause deviations from equilibrium as was noted in both foraminifera (Spero et al., 1997) and corals (Adkins et al., 2003; Rollion-Bard et al., 2003; see also section 3.2.2.1 of Chapter 1). Although there is no data on the pH of *S. giganteus* extrapallial fluid (EPF, where calcification occurs), there is nothing in the limited data available on this animal's physiology (Bernard, 1983) that would suggest it to be greatly different from

other aragonitic Venerids, which do precipitate their shells in equilibrium (Weidman et al., 1994; Elliot et al., 2003). An alternative hypothesis is that the clams, which live buried in the sediment up to 30 cm deep (Qualye and Bourne, 1972), were affected by groundwater incursions (cf. Elliot et al., 2003). Groundwater can be expected to be depleted in ^{18}O as well as to reduce salinity, therefore making the source $\delta^{18}O_W$ more negative.

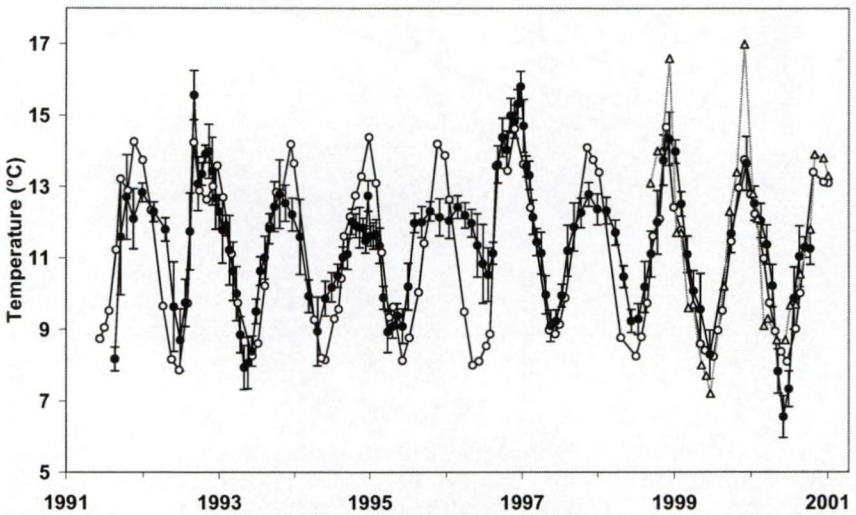

Figure 9. Instrumental temperature from both the offshore station (PSB003; open circles) and the shell collection site (Carkeek Park; triangles) and the modeled temperature obtained from the average $\delta^{18}O_S$ of the three shells (solid circles) using a constant $\delta^{18}O_W$ of -3.12 ‰ and the paleotemperature equation of Böhm et al. (2000); with standard error bars shown.

Often studies employ salinity - $\delta^{18}O_W$ relationships from nearby areas, use theoretical end members to relate salinity to $\delta^{18}O_W$, or assume a constant $\delta^{18}O_W$ (Weidman et al., 1994; Goodwin et al., 2001; Auclair et al., 2003; Elliot et al., 2003). Now that a decent approximation of the date the carbonate was produced is available, the effects of using the different (although not statistically different in this salinity range) salinity - $\delta^{18}O_W$ relationships (Table 2) and the salinities from the two stations can be investigated. All calculations using salinity values from the offshore station (PSB003) resulted in average temperature predictions greater than 3 °C warmer than measured (Table 3, Fig. 10). If it was assumed that this salinity was correct, the shells would be about -1 ‰ out of equilibrium. Elliot et al. (2003) stressed that the offset between their measured and predicted $\delta^{18}O_S$ in some locations was caused by poor salinity -

$\delta^{18}O_W$ relationships and/ or differences in salinity between where the measurement was taken (surface water) and where the clam lived (infaunal). The importance of this is further stressed here. As in this study, it is quite possible that the disequilibrium patterns discussed in Auclair et al. (2003) would be quite different if the actual $\delta^{18}O_W$ and /or salinity at their site were known (they used salinity from a distant station and a theoretical salinity - $\delta^{18}O_W$ relationship). Although Auclair et al. (2003) found their brachiopod shells to be largely out of equilibrium (up to -6 ‰), a shift of 1 ‰ in their data would undoubtedly have changed some of their conclusions.

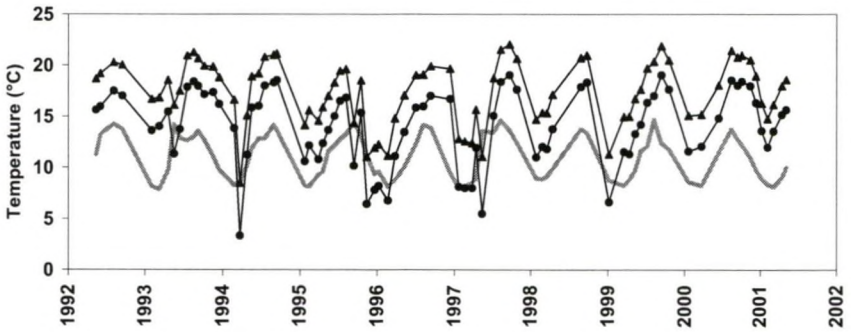

Figure 10. Comparison between instrumental (Inst PSB, grey line) and calculated temperatures. Calculated temperatures were calculated using the average $\delta^{18}O$ from the three shells and salinity from the off-shore station. The most extreme salinity- $\delta^{18}O_W$ relationships were used (Klein et al. (1996b; circles) and data from this study (triangles)); calculations using the other relationships lie between the two extremes.

However, even using the nearshore salinity data, calculated average temperatures are 1.7 to 6.4 °C warmer than measured (based on average $\delta^{18}O_S$ and average instrumental temperature for the period in which the shells grew; Table 3). Averaging the time resolved data can bias the average temperature to warmer temperatures as it can be expected that these shells grow more during the warmer months of the year (i.e., more data points in warmer months will bring the average temperature up). However, both of these sites experience sharp salinity drops, which severely lower the calculated temperature during these periods (See Fig. 10). If these periods are excluded, the difference between calculated and measured temperature becomes slightly larger (Fig. 10). Therefore, Table 3 is an under-estimation of the difference and not an over-estimation. Interestingly, using the paleo-temperature equation of Grossman and Ku (1986), even warmer temperatures are predicted (~ 0.5 °C). Furthermore, the oxygen isotope fractionation between inorganically precipitated

aragonite and water determined by Zhou and Zheng (2003) predicts cooler temperatures than were measured. As stated in their paper, the empirical equations derived for biogenic carbonates reflect a steady-state equilibrium, whereas the inorganic fractionation factors they derived are near thermodynamic equilibrium. As discussed above, equilibrium conditions cannot be tested with these data because the exact $\delta^{18}O_W$ remains unknown. Therefore, it remains unknown if *S. giganteus* precipitates out of 'equilibrium' with surrounding water or if the water available to them (e.g., pore water; cf. Elliot et al., 2003) is different from the measured surface waters. Nevertheless, these data clearly illustrate the complications of working with intertidal estuarine animals for paleoenvironment reconstruction.

Table 3. Difference between average instrumental temperature and average modeled temperature (°C; calculated using the equation of Böhm et al. (2000)) using data from the nearshore collection site (Carkeek, 1999-2001, n = 22) and the offshore station (PSB, 1992-2001, n = 80) for each salinity - $\delta^{18}O_W$ relationship (see text for details). EM & CK is the equation derived from the data of Epstein and Mayeda (1953) and Coplen and Kendall (2000).

Salinity - $\delta^{18}O_W$ relationship	$\Delta T_{Böhm\ PSB\ salinity}$	$\Delta T_{Böhm\ Carkeek\ salinity}$
Klein et al. 1996a	-3.0	-1.7
Ingram et al. 1996	-5.6	-4.4
This study	-6.4	-5.2
Auclair et al. 2003	-3.3	-1.9
EM & CK	-4.0	-2.7

4.3 Carbon isotopes

Early work suggested that the $\delta^{13}C_S$ of biogenic carbonates record $\delta^{13}C_{DIC}$ (Mook and Vogel, 1968), but many more recent reports have shown that vital effects seriously complicate the link between $\delta^{13}C_S$ and $\delta^{13}C_{DIC}$ (Tanaka et al., 1987; McConnaughey, 1989b; McConnaughey et al., 1997; Lorrain et al., 2004a). These authors report that ^{13}C depleted respiratory CO_2 (i.e., metabolic DIC) is incorporated in the skeleton, thus lowering the $\delta^{13}C_S$. McConnaughey et al. (1997) reported that aquatic invertebrates typically incorporate less than 10 % of carbon from metabolic CO_2 resulting in a decrease in $\delta^{13}C_S$ of 2 ‰ or less. According to the inorganic experiments of Romanek et al. (1992), the equilibration ^{13}C fractionation for aragonite relative to HCO_3^- ($\varepsilon_{aragonite\text{-}bicarbonate}$) is $+ 2.7 \pm 0.6$ ‰. Using the salinity data from the Carkeek station (Fig. 3) and the salinity - $\delta^{13}C_{DIC}$ relationship from this study (Fig. 4) an approximate average $\delta^{13}C_{DIC}$ was calculated, and then 2.7 ‰ was added to derive a predicted $\delta^{13}C_S$.

The average predicted $\delta^{13}C_S$ of 1.95 ± 1.15 ‰ is about 2.5 ‰ higher than the average measured $\delta^{13}C_S$, and is close to the depletion reported by others (e.g., 2 ‰, McConnaughey et al., 1997; Owen et al., 2002). Furthermore, using average $\delta^{13}C_{DIC}$, $\delta^{13}C_S$ and temperature and a metabolic CO_2 value of -19 ‰ (*S. giganteus* tissue $\delta^{13}C$ measured by Simenstad and Wissar (1985) in the nearby Hood Canal) a metabolic contribution to the shell of 13 % was calculated (using the equation of McConnaughey et al., 1997). Although strong ontogenic decreases in $\delta^{13}C_S$ are evident in other Venerids (Elliot et al., 2003, Chapter 5), there does not seem to be a strong decrease in $\delta^{13}C_S$ through the lifetime of *S. giganteus* ($\delta^{13}C_S$ actually becomes slightly more positive through ontogeny in shell 1; Fig. 5 and 7). This indicates that the model proposed by Lorrain et al. (2004a), stating that bivalves incorporate increasingly more metabolic DIC through ontogeny, may not be a general model for all bivalves.

As previously stated, the salinity - $\delta^{13}C_{DIC}$ relationship of this study is overly simplistic as $\delta^{13}C_{DIC}$ is known to have large seasonal fluctuations due to respiration, photosynthesis, carbonate dissolution/ precipitation, etc., throughout the year (Mook and Tan, 1991; Hellings et al., 2001; Bouillon et al., 2003). However, in well flushed estuaries with short residence times, $\delta^{13}C_{DIC}$ may follow a simple linear relationship with salinity, especially in salinities above 25 (Mook, 1971; Surge et al., 2001; Fry, 2002; Chapter 6). Furthermore, it is well known that freshwater input is depleted in ^{13}C (see Fig. 4 as well as Hellings et al. (2001) for example). Therefore, a drop in salinity will undoubtedly cause a decrease in $\delta^{13}C_{DIC}$ (of about 4 ‰ at this site; see Fig. 3B and 4). Considering the large occasional drops in salinity at this site (Fig. 3) and the lack of strong depletions in shell ^{13}C and ^{18}O, it is very unlikely that *S. giganteus* precipitates shell material during periods of reduced salinity.

5. Conclusions

Saxidomus giganteus shell oxygen isotopes are clearly controlled by external environmental factors as indicated by the similarities between the three shells. Although there were differences up to 0.5 ‰ in high resolution $\delta^{18}O_S$ profiles, the difference in average $\delta^{18}O_S$ was less than half of this (0.19 ‰) and half of what has

been reported in corals (0.4 ‰; Linsley et al., 1999). This indicates that if $\delta^{18}O_W$ is known, average temperature can be calculated with an uncertainty of ~ 0.8 °C. However, in paleo-environmental studies, $\delta^{18}O_W$ is rarely, if ever, known. Despite the salinity and $\delta^{18}O_W$ data available, temperature could still not be accurately calculated (Table 3). Carbon on the other hand was more complex, although data are roughly conforming to the idea that about 10 % of shell carbon originates from metabolic CO_2 (McConnaughey et al., 1997). Despite this metabolic influence, the general range of $\delta^{13}C_S$ is relatively small (1.9 ‰) and large changes can be expected at this site (up to 4 ‰) indicating $\delta^{13}C_S$ can give an insight into the salinity in which the shells grew. Using both $\delta^{18}O_S$ and $\delta^{13}C_S$ as an indication of salinity, it seems that *S. giganteus* do not grow during periods of reduced salinity. This study could not determine if *S. giganteus* precipitates their shell in isotopic equilibrium with surrounding waters, but these data do clearly highlight some of the problems associated with using intertidal estuarine biogenic carbonates as paleotemperature proxies. Evidentially, salinity independent proxies, or a salinity proxy, are necessary for more precise paleotemperature determinations.

Acknowledgements - I am much indebted to K. Li and S. Mickelson of the King County Department of Natural Resources and Parks, Water and Land Resources Division, Marine Monitoring group (Washington, USA) for collecting the shells and providing water data. I also wish to thank J. Taylor (U. Washington) for providing the XRD data and C. Setterstom for collecting the water samples. A. Van de Maele and M. Korntheuer both assisted with keeping the Kiel III running. Constructive criticism, which greatly improved this Chapter, was given by D. L. Dettman, A. Verheyden, S. Bouillon, A. Lorrain, B.R. Schöne, and anonymous readers.

Chapter 5

Metabolic CO_2 incorporation in aragonitic clam shells (*Mercenaria mercenaria*) and the influence on shell $\delta^{13}C$

Foreword

In the previous chapter metabolic CO_2 incorporation in bivalve shells and its result on the stable carbon isotopic signature of the shell was briefly discussed. Unlike many bivalves, *Saxidomus giganteus* do not exhibit an ontogenic trend of increasing metabolic CO_2 incorporation in their shells (up to 10 years growth); however, previous studies have indicated that *Mercenaria mercenaria* do exhibit such a trend. Therefore, in this chapter the extent of this ontogenic trend is first determined and then an attempt to determine its cause is made. Finally, the possibility of removing this ontogenic trend of metabolic CO_2 incorporation is investigated, with the ultimate goal of being able to determine the $\delta^{13}C$ value of the dissolved inorganic carbon of the water in which the bivalves grew. As the $\delta^{13}C_{DIC}$ in many estuaries is conservative with salinity, having an indication of $\delta^{13}C_{DIC}$ could provide an indication of salinity. Having an indication of salinity would in turn help to reduce some of the errors associated with using $\delta^{18}O$ to calculate temperature, which were demonstrated in the previous chapter.

Abstract

The stable carbon isotopic signature archived in bivalve shells was originally thought to record the $\delta^{13}C$ of seawater dissolved inorganic carbon ($\delta^{13}C_{DIC}$). However, more recent studies have shown that the incorporation of isotopically light metabolic carbon (M) significantly affects the $\delta^{13}C$ signal recorded in biogenic carbonates. If the %M could be corrected for, $\delta^{13}C_{DIC}$ could be estimated from the shell $\delta^{13}C$ values. To assess the M contribution to *Mercenaria mercenaria* shells collected in North Carolina, USA, seawater $\delta^{13}C_{DIC}$, tissue, hemolymph (i.e., blood) and shell $\delta^{13}C$ were sampled. A common decrease, up to 4 ‰, was found in all 8 shells analyzed, including a Pliocene shell, therefore excluding the Suess Effect as being the dominant cause. Furthermore, ontogenic changes in the $\delta^{13}C$ value of respiratory CO_2 could not explain the decreasing shell $\delta^{13}C$ values. Hemolymph $\delta^{13}C$, on the other hand, did exhibit a negative relationship with length ($p < 0.01$, $n = 5$), indicating that respired CO_2 does influence the $\delta^{13}C$ of internal fluids and that the amount of respired CO_2 is related to the age of the bivalve. The percent metabolic C incorporated into the shell (%M) (> 35 %) was significantly higher than has been found in other bivalves, which usually contain less than 10 %M. Attempts to use shell biometrics to predict %M could not explain more than ~60 % of the observed variability, and large differences in the %M between different sites were found. Thus, the metabolic influence cannot adequately be removed from the shell $\delta^{13}C$ to obtain $\delta^{13}C_{DIC}$. However, there does seem to be a common effect of size, as all sites had indistinguishable slopes between the %M and shell length (+0.19 % per mm of shell length) indicating that shell $\delta^{13}C$ may be a potential proxy of bivalve metabolism.

1. INTRODUCTION

Stable isotope geochemistry has become a key tool in paleo-climate and paleo-oceanographic reconstruction. The oxygen isotopic ($\delta^{18}O_S$) signatures of different biogenic carbonates have been used to reconstruct both sea surface temperature and salinity (Jones et al., 1989; Weidman et al., 1994; Ingram et al., 1996; Dettman et al., 2004). On the other hand, carbonate stable carbon isotopic composition ($\delta^{13}C_S$) varies in a more complex manner. Early works suggested that $\delta^{13}C_S$ reflected the $\delta^{13}C$ of dissolved inorganic carbon in seawater ($\delta^{13}C_{DIC}$) (Mook and Vogel, 1968); however, more recent works have suggested that both kinetic and metabolic effects play an important role in determining $\delta^{13}C_S$ (Tanaka et al., 1986; McConnaughey et al., 1997; Dettman et al., 1999; Lorrain et al., 2004a). Kinetic effects generally affect both $\delta^{18}O_S$ and $\delta^{13}C_S$ and result in a good correlation between them (McConnaughey, 1989b). As bivalves generally precipitate in oxygen isotope equilibrium with their surroundings (Epstein et al., 1953; Wefer and Berger, 1991; Chauvaud et al., in press), kinetic effects should be minimal and disequilibrium should be mainly due to metabolic effects. Metabolic effects result from changes in the internal DIC pool, which is a combination of both seawater DIC and metabolic DIC (Dillaman and Ford, 1982; Swart, 1983; McConnaughey et al., 1997). Although the isotopic composition of this internal DIC pool has never been measured in any animal, it is widely assumed that respiration, composed of ^{12}C enriched CO_2, decreases the $\delta^{13}C$ value of it. The $\delta^{13}C$ value of respired CO_2 ($\delta^{13}C_R$) can be assumed to approximately match the $\delta^{13}C$ of the respiring tissue (McConnaughey et al., 1997), but a recent study showed that coral $\delta^{13}C_R$ could be up to 3 ‰ different from tissues (Swart et al., 2005). However, this would only change the percentage of respired carbon in the skeleton by about 3 % when using the equation of McConnaughey et al. (1997) (see discussion). An earlier study suggested that up to 85 % of mollusk shells were composed of metabolic C (Tanaka et al., 1986), but more recently McConnaughey et al. (1997) have shown that this study overestimated the metabolic contribution because it erroneously included the enrichment factor between carbonate and aqueous CO_2. The $\delta^{13}C_{DIC}$ decrease in the internal DIC pool is now generally considered to result in small (< 2 ‰) changes in $\delta^{13}C_S$, or approximately a 10 % contribution from respired CO_2 (McConnaughey et al., 1997).

In bivalves there are varying degrees of $\delta^{13}C_S$ disequilibrium from $\delta^{13}C_{DIC}$. In some species, strong ontogenic decreases in $\delta^{13}C_S$ have been noted (Krantz et al., 1987; Kennedy et al., 2001; Keller et al., 2002; Elliot et al., 2003; Lorrain et al., 2004a), whereas in others there is no discernable decrease (Buick and Ivany, 2004; Gillikin et al., 2005a; Chapter 4). Lorrain et al. (2004a) proposed that the ratio of respired to precipitated carbon, which represents the amount of metabolic carbon available for calcification, increases through ontogeny, thus decreasing $\delta^{13}C_S$. Furthermore, they propose that seawater $\delta^{13}C_{DIC}$ could perhaps be reconstructed from bivalve shells if the metabolic contribution could be removed.

In this study, seawater $\delta^{13}C_{DIC}$, tissue, hemolymph (i.e., bivalve blood) and shell $\delta^{13}C$ from *Mercenaria mercenaria* collected in North Carolina, USA (Fig. 1) were sampled to assess the contribution of metabolic carbon to the shell. *M. mercenaria* is a large aragonite clam, which can obtain an age of nearly 50 years (Peterson, 1986) and is therefore suitable to detect long term ontogenic effects in shell geochemistry. The aim was to 1) determine if *M. mercenaria* has a large ontogenic decrease in $\delta^{13}C_S$ 2) determine what causes the decrease in $\delta^{13}C_S$, and 3) assess if vital effects can be removed in order to estimate $\delta^{13}C_{DIC}$.

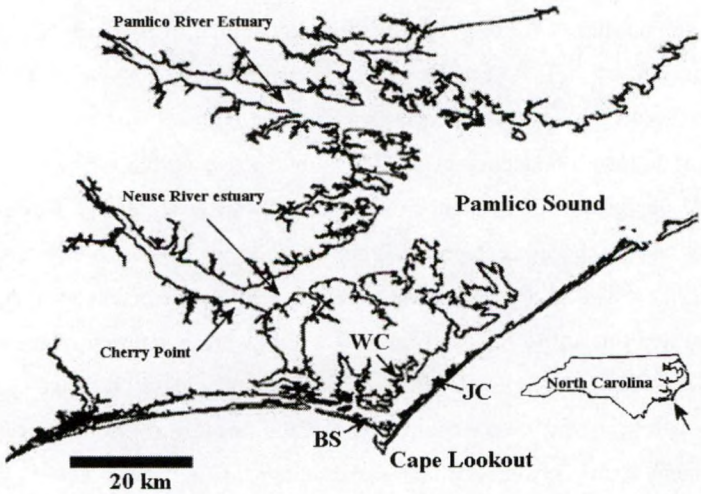

Figure 1. Shell collection sites in eastern North Carolina, USA, near Cape Lookout (BS: Back Sound, JC: Johnson Creek, WC: Wade Creek).

2. METHODOLOGY

Mercenaria mercenaria were collected alive from the Cape Lookout region of North Carolina, USA, from three sites: Jarrett Bay (JB), Johnson Creek (JC), and Back Sound (BS) (Fig. 1) (see Peterson et al., 1983, 1984, and Chapters 8 and 9 for environmental data). In addition, to test if any pattern found in these shells is the result of modern changes in the environment, a Pliocene (~3.2 million years old) shell collected from the Duplin formation in South Carolina (1.5 km northwest of Timmonsville) was analyzed. In JB, an extensive sampling campaign was conducted where the $\delta^{13}C$ of shells of various sizes (12.4 – 99.2 mm), different tissues (gill, mantle, muscle, and foot), hemolymph, water DIC, particulate matter and sediment were sampled (all on 17 Aug. 2004). Only the most recently formed shell material was sampled from clams at this site using a Merchantek MicroMill. Hemolymph was sampled from the adductor muscle using a syringe fitted with a filter and needle and transferred to a sealed He flushed headspace vial containing $HgCl_2$. Similar to water samples, after acidification, the evolved CO_2 gas was injected online into an isotope ratio mass spectrometer (IRMS) (see Gillikin et al., 2005a or chapter 2 for full details). The $\delta^{13}C$ of tissue, sediment and particulate matter were analyzed similar to Bouillon et al. (2004a) and Lorrain et al. (2003) (see also Chapter 2).

Shells were collected from the other sites (JC and BS) in 1980, 1982 and 2002; water samples and muscle tissues from various sized clams (29.3 – 88.8 mm) were collected at JC (Aug. 2003), but not BS. Shells from these sites were sampled in the middle shell layer (see Elliot et al., 2003) at an annual resolution to obtain $\delta^{13}C$ shell profiles using the annual growth lines on the shell, which form in late summer/ early winter in this region (Peterson et al., 1983). Water and shell samples were collected, prepared and analyzed as in Gillikin et al. (2005-a) (see also Chapter 2).

3. RESULTS

All shells, regardless of collection site or time of collection exhibit a large ontogenic decrease in $\delta^{13}C_S$, up to 4 ‰ (Fig. 2), including the Pliocene shell (Fig. 3). The Pliocene shell did not appear to have undergone isotopic diagenesis, as indicated by

both $\delta^{18}O_S$ and $\delta^{13}C_S$ being similar to modern shells and not being well correlated (R^2 = 0.11) ($\delta^{18}O_S$ data are presented in Chapters 8 and 9) (see Elorza and Garcia-Garmilla, 1996, 1998, and Labonne and Hillaire-Marcel, 2000 for discussions on diagenetic indicators).

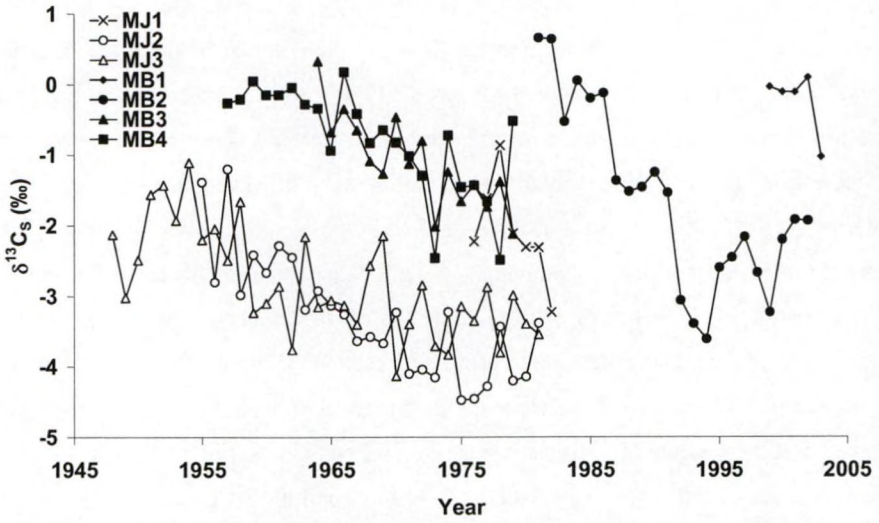

Figure 2. Annual shell $\delta^{13}C$ from *M. mercenaria* shells collected at two sites (Johnson Creek, MJ shells and Back Sound, MB shells) plotted versus year showing the clear ontogenic decrease.

After removing two outliers, the different tissues from JB had significantly different $\delta^{13}C$ values ($p < 0.01$ for all; n = 10), except for mantle (-19.1 ± 0.3 ‰; n = 10) and muscle (-19.1 ± 0.2 ‰; n = 10) tissues (p = 1.0), with gills being the least negative (-18.4 ± 0.3 ‰; n = 10) and the foot the most negative (-19.5 ± 0.03 ‰; n = 10) (Fig. 4). From the JB samples, the only tissue carbon isotopic signature that was significantly correlated to shell length was the foot, with a weak positive correlation (R^2 = 0.45, p = 0.033, n = 10). In contrast, there was a significant strong positive correlation between muscle $\delta^{13}C$ and length (L) in the JC clams ($\delta^{13}C_{muscle}$ = 0.05 (± 0.01) * L – 21.09 (± 0.77), R^2 = 0.98, p = 0.0011, n = 5). Three replicate $\delta^{13}C_{DIC}$ samples taken at JB gave a mean of -0.77 ± 0.20 ‰, which is similar to the average of 13 samples taken in the vicinity of this site the year before (-0.5 ± 0.8 ‰). Johnson Creek $\delta^{13}C_{DIC}$ was more negative at -2.40 ± 0.26 ‰ (n = 3). The muscle tissues of JB clams were -19.1 ± 0.19 ‰ (n = 10) and muscle tissues of JC clams were -18.3 ± 1.2 ‰ (n = 5). Both sediments (-20.3 ± 0.14 ‰) and particulate matter (-21.5 ‰) were

within 2.5 ‰ of tissues (~ 19 ‰) at JB. Only 5 successful hemolymph samples were obtained (many were too small to get an adequate amount of CO_2 for this method). Hemolymph $\delta^{13}C$ was negatively correlated with shell length (Fig. 5A; $R^2 = 0.94$, $p = 0.007$, $n = 5$), but not with tissue or shell $\delta^{13}C$ (Fig. 5B).

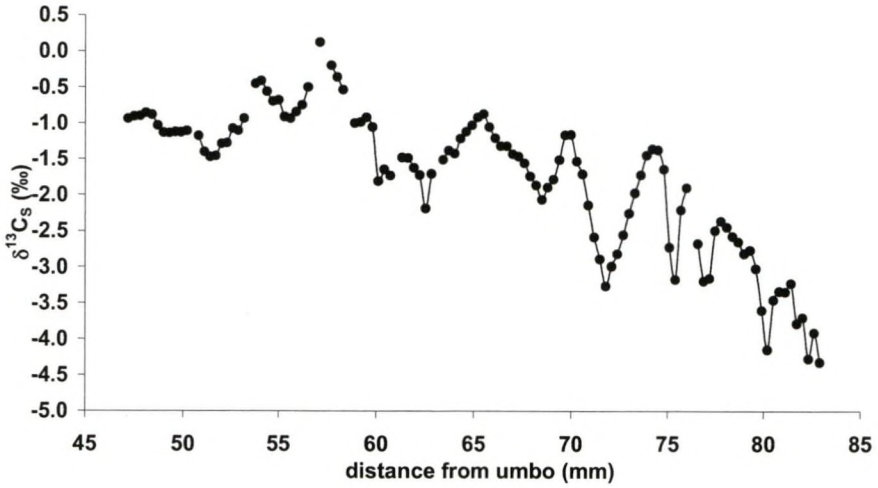

Figure 3. High resolution shell $\delta^{13}C$ profile from a Pliocene *M. mercenaria* shell plotted versus distance from the umbo.

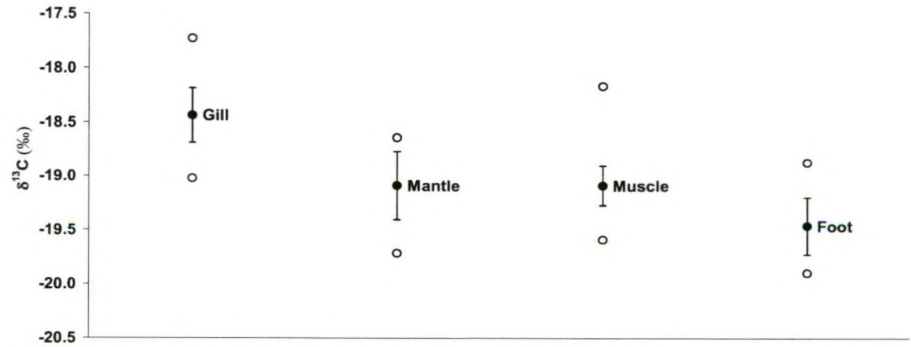

Figure 4. Mean $\delta^{13}C$ values of different *M. mercenaria* tissues from JB, with two 'outliers' removed. Error bars represent standard deviation, $n = 10$.

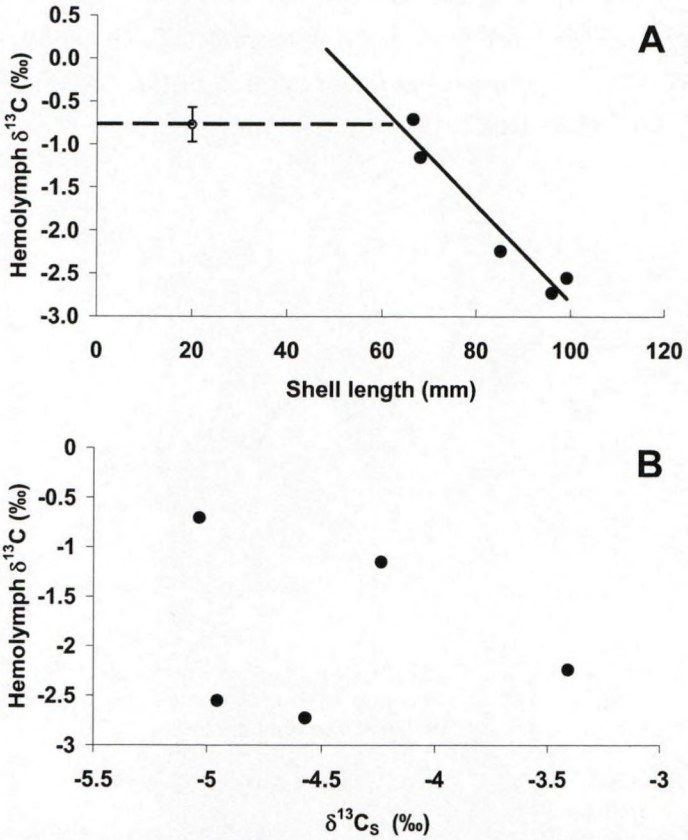

Figure 5. (A) $\delta^{13}C$ values of filtered *M. mercenaria* hemolymph samples plotted versus shell length (L in mm) (closed circles) with the linear relationship: hemolymph $\delta^{13}C$ = -0.055 (±0.027) * L + (2.35 (± 2.28) (R^2 = 0.93, $p < 0.01$, n = 5). The mean $\delta^{13}C_{DIC}$ value (± standard deviation) of the water where the clams were collected is also given (open circle). The dashed line represents smaller clam's hemolymph $\delta^{13}C$ values if it were the same as seawater. (B) The same hemolymph data plotted versus shell $\delta^{13}C$ (the relationship is not significant, p = 0.75).

4. DISCUSSION

4.1 What is the cause of the decreasing $\delta^{13}C_S$?

All *M. mercenaria* shells investigated showed a clear ontogenic decrease in $\delta^{13}C_S$ (Fig. 2). There are several potential causes for this decrease; however, kinetic effects can most definitely be ruled out. Kinetic effects result in a good correlation between $\delta^{18}O_S$ and $\delta^{13}C_S$ (McConnaughey, 1989b, see also introduction), which has not

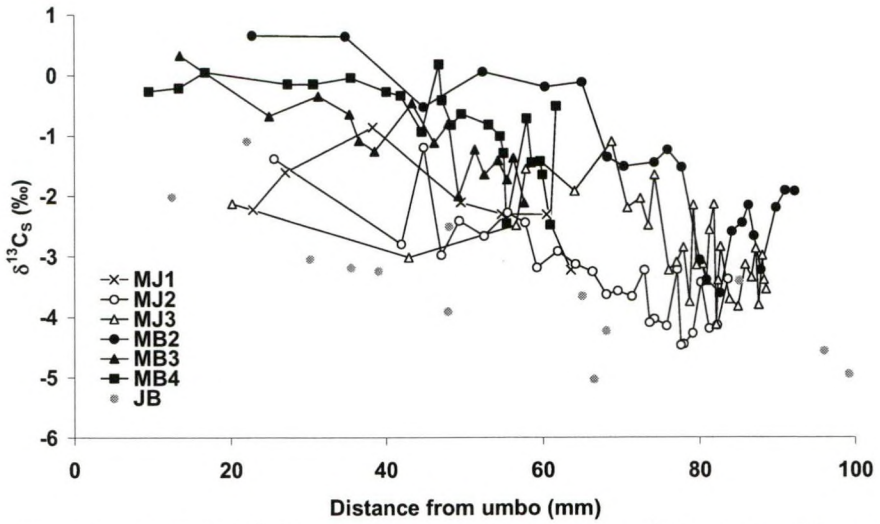

Figure 6. Annual shell $\delta^{13}C$ from *M. mercenaria* shells collected at two sites (Johnson Creek, MJ shells and Back Sound, MB shells) plotted versus shell length. Data from JB shells are also given, but it should be noted that these samples represent less than one year and thus are expected to have a higher variability than the other shells which integrate a full year of growth.

been observed in *M. mercenaria* shells (Elliot et al., 2003; Gillikin, unpublished). Other possible causes for the ontogenic decrease in $\delta^{13}C_S$ can be separated into two main categories: changes in environmental $\delta^{13}C_{DIC}$ and biological changes resulting in a change in the internal DIC pool. Environmental changes include the Suess effect, caused by increasing amounts of anthropogenic ^{13}C depleted CO_2 in the atmosphere, which leads to more negative $\delta^{13}C_{DIC}$ in seawater. This phenomenon has been recorded in sclerosponge skeletons (Druffel and Benavides, 1986; Lazareth et al., 2000), but the change over the past 50 years is on the order of 0.5 ‰, far less than the changes observed in these shells (up to 4 ‰). Additionally, similar decreases in $\delta^{13}C_S$ are noted regardless if the clam was collected in 1980 or 2003 (Fig. 2), and the ontogenic decrease is also evident in the Pliocene shell, which grew well before anthropogenic CO_2 inputs were present (Fig. 3). Thus, changing environmental $\delta^{13}C_{DIC}$ is obviously not the dominant cause. Another possibility is that the clams may live deeper in the sediment as they age and utilize a more negative environmental $\delta^{13}C_{DIC}$ source, as suggested by Keller et al. (2002) and Elliot et al. (2003). Indeed, strong gradients in pore water $\delta^{13}C_{DIC}$ have been observed within the initial 5 cm of sediment due to the remineralization of organic matter (up to -1 ‰ cm^{-1}; McCorkle et

al., 1985). However, this is probably not a cause as Roberts et al. (1989) found that the depth of *M. mercenaria* in the sediment was independent of clam size, and thus different size classes can be considered to use similar water sources. Thus, the most probable cause is a change in the internal DIC pool, which is supported by the negative relationship between shell length and hemolymph $\delta^{13}C$ (Fig. 5).

A change in the internal DIC pool could be due to differences in $\delta^{13}C_R$ caused by food sources with different $\delta^{13}C$ signatures. However, in this study, tissue $\delta^{13}C$ and shell length were generally not correlated. Although some tissues showed a positive relationship, this is opposite to what is observed in the shells (Fig. 6). Thus, a change in food as the animal ages is not likely the cause of the $\delta^{13}C$ trend in the shells. Changes in lipid metabolism can also result in changes in $\delta^{13}C_R$, but this would be expected to be reflected in the tissue $\delta^{13}C$, which it is not. Moreover, lipid content has been shown to be low in *M. mercenaria* tissues, changing the $\delta^{13}C$ value of tissues by ~ 0.5 ‰ (O'Donnell et al., 2003). Changing pH can also affect $\delta^{13}C_S$ (see section 3.2.2.1 of Chapter 1), with increasing pH resulting in decreasing $\delta^{13}C_S$, as has been observed in foraminifera (Spero et al., 1997) and corals (Adkins et al., 2003). However, internal pH has been shown to decrease in older bivalves (Sukhotin and Pörtner, 2001), which would lead to an increase in $\delta^{13}C_S$. Lorrain et al. (2004a) proposed that the increased absolute metabolism in larger bivalves relative to their shell growth rate, leads to a larger availability of metabolic C for $CaCO_3$ precipitation. In other words, the increase in CO_2 production is larger than the demand for calcification, resulting in a larger amount of metabolic C in the internal DIC pool. It is therefore expected that the respired to precipitated carbon ratio (Lorrain et al., 2004a) will also increase through ontogeny in *M. mercenaria*. This indeed seems probable, as *M. mercenaria* has been shown to have a high metabolic rate compared to other bivalves (Hamwi and Haskin, 1969). However, a simple mixture between seawater $\delta^{13}C_{DIC}$ and $\delta^{13}C_R$ might not be occurring; the hemolymph data presented here for an individual 66 mm in length is similar to seawater $\delta^{13}C_{DIC}$ (Fig. 5A), whereas $\delta^{13}C_S$ already decreases with length in individuals with smaller shell sizes (Fig. 6). Therefore, hemolymph $\delta^{13}C$ probably is similar to seawater in smaller individuals (dashed line in Fig. 5A). Furthermore, hemolymph $\delta^{13}C$ may not be a good proxy of the extrapallial fluid (EPF) $\delta^{13}C$, where calcification occurs. The hemolymph is separated from the EPF by a membrane, where enzymatic reactions

(e.g., carbonic anhydrase) facilitate CO_2 diffusion into the EPF (Crenshaw, 1980; McConnaughey, 1989b; Cohen and McConnaughey, 2003), which may be associated with kinetic fractionations (or a pH change), and thus change the $\delta^{13}C_{DIC}$ value. Nevertheless, the hemolymph data prove for the first time that there is a decrease in $\delta^{13}C$ of internal fluids with age (or shell length), which probably can be carried over to the EPF, just not necessarily in absolute terms. Moreover these data generally agree with the respiratory gas exchange model of McConnaughey et al. (1997), where they state that ~90 % of the CO_2 inside aquatic invertebrates derives from the water and ~10 % from respiration (*M. mercenaria* data range from ~0 % to ~10 % CO_2 in hemolymph derived from respiration). However, the positive intercept (+2.35 ‰) in the regression between hemolymph $\delta^{13}C$ and length, and the seawater $\delta^{13}C_{DIC}$ value of ~ -0.8 ‰, implies that either smaller individuals have hemolymph $\delta^{13}C$ values similar to seawater $\delta^{13}C_{DIC}$ (i.e., a nonlinear relationship with an intercept equal to seawater $\delta^{13}C_{DIC}$), or that another source of heavy $\delta^{13}C$ is adding to the pool, but samples from smaller individuals are needed to determine this.

4.2 How much metabolic carbon is in the shells?

The best standing model to calculate the amount of metabolic C in the shell is given by McConnaughey et al. (1997):

$$M * (\delta^{13}C_R) + (1 - M) * \delta^{13}C_{DIC} = \delta^{13}C_s - \varepsilon_{ar\text{-}b} \quad (1)$$

where M is the percent metabolic CO_2 contribution, $\varepsilon_{ar\text{-}b}$ is the enrichment factor between aragonite and bicarbonate (2.7 ‰ in Romanek et al., 1992), and $\delta^{13}C_R$ is approximated from tissue $\delta^{13}C$ (Elliot et al. (2003) have shown that *M. mercenaria* precipitate aragonite shells). At the JB site, where corresponding tissue, water and shell data were available, eq. 1 gave results ranging from 15.8 to 37.8 % M, with a linear relationship between shell length and M (Fig. 7). The $\delta^{13}C$ values from the muscle tissue was used for two reasons: 1) it is the same as the mantle tissue, which is closest to the EPF and should have the largest effect on the internal DIC pool, and 2) the muscle has the slowest turn over time, so integrates the longest time (see Lorrain et al., 2002). For the other sites, tissue or water data to match the carbonate samples for each year are lacking, so the sample taken recently at JC was applied to the entire

JC dataset. Data for BS was assumed. Water at the BS site exchanges with the open ocean (Peterson and Fegley, 1986) so should have a $\delta^{13}C_{DIC}$ value close to oceanic values. Thus it was assumed that $\delta^{13}C_{DIC}$ = -0.5 ‰ and tissues = -19 ‰ (i.e., the mean of the JB site) at the BS site. A maximum error of ~1 ‰ can be expected from these assumptions, which would change M by ~5 % for a 1 ‰ change in $\delta^{13}C_{DIC}$ and ~1 % for a 1 ‰ change in $\delta^{13}C_R$ (i.e., $\delta^{13}C$ of tissues). Using eq. 1 and the assumptions listed above results in M values ranging from 7.4 % to 31.4 % for the BS and JC clams. Correcting for the changes in tissue $\delta^{13}C$ with shell length in JC clams (see results), only changes M by a maximum of 2.3 %. The change in tissue $\delta^{13}C$ with shell length (slope = +0.05 ± 0.01) may be due to larger individuals including microphytobenthos in their diet, which have heavier $\delta^{13}C$ values (~ -15 ‰, Middelburg et al., 2000; Herman et al., 2000) compared to phytoplankton (~ - 20 ‰, see next Chapter). Nevertheless, the change in tissue $\delta^{13}C$ does not greatly contribute to M.

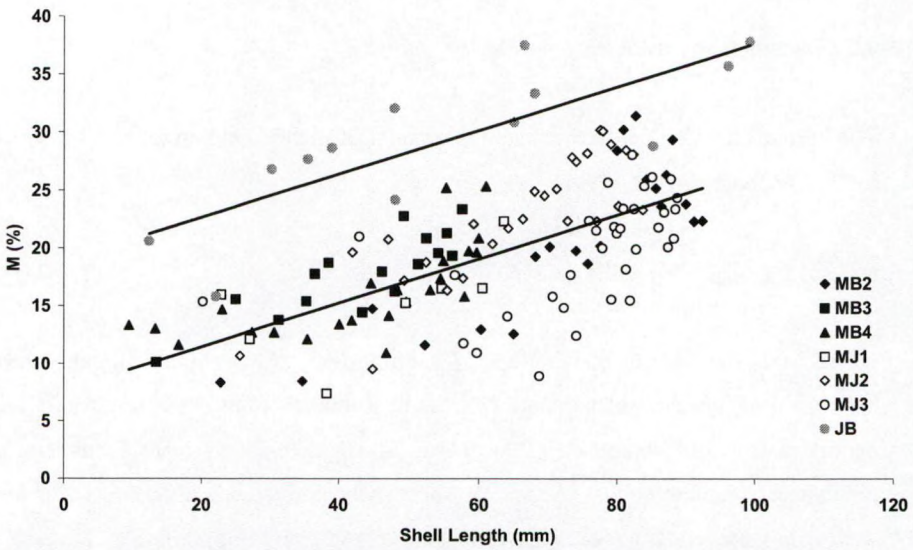

Figure 7. Percent metabolic C (M) from Jarrett Bay clams where tissue, water and shell was sampled for each shell and annual M incorporated into *M. mercenaria* shells collected at two sites (Johnson Creek, MJ shells and Back Sound, MB shells) plotted versus shell length (L in mm). The linear relationship is for the combined Johnson Creek and Back Sound datasets is M (%) = 0.190 (± 0.035) * L + 7.65 (± 2.25) ($p < 0.0001$, $n = 129$, $R^2 = 0.48$). The Jarrett Bay relationship is M (%) = 0.187 (± 0.092) * L + 18.92 (± 5.65) ($p < 0.001$, $n = 13$, $R^2 = 0.64$). The slopes between the two regressions are not statistically different ($p = 0.81$).

At all sites, the M ranges are substantially higher than the proposed 10 % (McConnaughey et al., 1997), even when considering possible errors. Furthermore, there is a linear relationship between M and shell length (Fig. 7), with no significant difference between the slopes or intercepts of the BS and JC sites ($p > 0.05$). The JB site has a similar slope to the other sites ($p = 0.81$), but the intercept is much higher (Fig. 7). This could be the result of different metabolic rates between the sites (cf. Lorrain et al., 2004a). Interestingly, the similarity in slopes suggests that the age effect between populations with apparently different metabolic rates is general, with a change in M of +0.19 % per mm of shell length.

4.3 Can the effect of metabolic carbon be removed?

Being able to predict M would be of great value; with known M, $\delta^{13}C_S$, and tissue $\delta^{13}C$, $\delta^{13}C_{DIC}$ can be calculated using eq. 1. Although tissue $\delta^{13}C$ would not be available for fossil or specimens collected in the past, the shell organic matter $\delta^{13}C$ could be used as a proxy of tissue $\delta^{13}C$. O'Donnell et al. (2003) found that the $\delta^{13}C$ value of organic matter extracted from *M. mercenaria* shells was indistinguishable from tissue $\delta^{13}C$. However, the predictability of M from shell length is weak, with an R^2 of 0.48 for JC and BS clams and 0.64 for JB clams (Fig. 7). An attempt to improve the linear model by including several biometric parameters, in addition to total shell length (i.e., a multiple linear regression with annual growth increment length, annual growth increment weight, and age), was made, but they did not improve the model by more than 4 %. For example, combining age and length to predict M resulted in the highest R^2 (0.52). Additionally, the large difference in intercepts between the two regressions suggests that there is no general relationship between length and M. Thus, unfortunately, there is too much unexplained variability in the data and apparently large differences in metabolic rate between sites, making M predictions difficult and calculating $\delta^{13}C_{DIC}$ highly uncertain. However, as suggested by Lorrain et al. (2004a) $\delta^{13}C_S$ may provide information about metabolic rates for different populations. It would be interesting to understand why the JB clams had higher metabolic rates compared to the other two sites. One possibility is higher organic pollution at this site caused by land run-off, which has been shown to increase respiration rates in bivalves (Wang et al., in press).

Acknowledgements - I thank C.H. Peterson (University of North Carolina, Chapel Hill), who kindly provided the *M. mercenaria* shells collected in the early 1980's; W.C. Gillikin and L. Daniels, who both assisted with sample collection in N.C.; and L. Campbell (University of South Carolina) who kindly provided the Pliocene shell. I express my gratitude to A. Van de Maele and M. Korntheuer for laboratory assistance. A. Verheyden and A. Lorrain gave helpful comments on an earlier version of this chapter.

Chapter 6

The link between salinity, phytoplankton, and $\delta^{13}C$ in *Mytilus edulis*

Foreword

In the previous Chapter, it was demonstrated that the amount of metabolic carbon incorporation into aragonite shells of *Mercenaria mercenaria* changed dramatically through the life of the animal. This chapter focuses on a calcitic bivalve with a much shorter lifespan. With no strong age trend, it is possible that large changes in $\delta^{13}C_{DIC}$, common along many estuaries, would be recorded in the shells and potentially be useful as a salinity indicator.

Abstract

The incorporation of respired ^{13}C depleted carbon into the skeletons of aquatic invertebrates is well documented. The fluid from which these animals calcify is a 'pool' of metabolic CO_2 and external dissolved inorganic carbon (DIC). Typically, less than 10 % of the carbon in the skeleton is metabolic in origin, although higher amounts have been reported. If this small offset is more or less constant, large biogeochemical gradients in estuaries may be recorded in the $\delta^{13}C$ value of bivalve shells. In this study, it is assessed if the $\delta^{13}C$ values of *Mytilus edulis* shells can be used as a proxy of $\delta^{13}C_{DIC}$ and provide an indication of salinity. First the $\delta^{13}C$ values of respired CO_2 ($\delta^{13}C_R$) was considered using the $\delta^{13}C$ values of tissues as a proxy for $\delta^{13}C_R$. Along the strong biogeochemical gradient of the Scheldt estuary, $\delta^{13}C_R$ was linearly related to $\delta^{13}C_{DIC}$ ($R^2 = 0.87$), which in turn was linearly related to salinity ($R^2 = 0.94$). The mussels were highly selective, assimilating most of their carbon from phytoplankton out of the total particulate organic carbon (POC) pool. However, on a seasonal basis, tissue $\delta^{13}C$ varies differently than $\delta^{13}C_{DIC}$ and $\delta^{13}C_{POC}$, most likely due to lipid content of the tissue. All shells contained less than 10 % metabolic C, but ranged from near zero to 10 %, thus excluding the use of $\delta^{13}C$ in these shells as a robust $\delta^{13}C_{DIC}$ or salinity proxy. As an example, an error in salinity of about 5 would have been made at one site. Nevertheless, large changes in $\delta^{13}C_{DIC}$ (>2 ‰) can be determined using *M. edulis* shell $\delta^{13}C$. Preliminary hemolymph $\delta^{13}C$ data are presented and suggest that salinity affects the $\delta^{13}C$ of the internal DIC pool of bivalves independently from the external $\delta^{13}C_{DIC}$.

1. INTRODUCTION

The incorporation of respired ^{13}C depleted carbon into the skeletons of aquatic invertebrates is well documented (Tanaka et al., 1986; McConnaughey et al., 1997; Lorrain et al., 2004a; Swart et al., 2005). The fluid from which these animals calcify is a 'pool' of metabolic CO_2 and external dissolved inorganic carbon (DIC), which both affect the skeletal stable carbon isotopic signature ($\delta^{13}C_S$). The amount of respired carbon ending up in the skeleton is species specific, with most aquatic animals incorporating less than 10 % (or < 2 ‰ offset from $\delta^{13}C_S$ equilibrium with $\delta^{13}C_{DIC}$ in marine settings) (McConnaughey et al., 1997; Kennedy et al., 2001; Lorrain et al., 2004a; Chapter 4), but may be as high as 35 % (Chapter 5). Therefore it is of interest to have a better understanding of what controls the $\delta^{13}C$ value of respired CO_2.

The $\delta^{13}C$ value of respired CO_2 ($\delta^{13}C_R$) can be roughly estimated from the tissue $\delta^{13}C$ value. At the pH of *M. edulis* body fluids (7 – 8; Crenshaw, 1972), more than 90 % of CO_2 hydrates and ionizes to produce HCO_3^-, which should be at most 1 ‰ enriched in ^{13}C compared to the respiring tissue (McConnaughey et al., 1997). Yet, due to other processes affecting the $\delta^{13}C_R$ (e.g., the type of material being respired such as lipids) it can roughly be considered to be 0.5 ‰ heavier than the tissues (McConnaughey et al., 1997). However, a recent study on a zooxanthellate scleractinian coral suggested that $\delta^{13}C_R$ might not always follow tissue $\delta^{13}C$ (Swart et al., 2005). The amount of respired CO_2 in the skeleton can be approximated using the equation of McConnaughey et al. (1997) (see also previous chapter):

$$M(\delta^{13}C_R) + (1 - M) * \delta^{13}C_{DIC} = \delta^{13}C_S - \varepsilon_{cl\text{-}b} \qquad (1)$$

where M is the percent metabolic CO_2 contribution and $\varepsilon_{cl\text{-}b}$ is the enrichment factor between calcite and bicarbonate (1.0 ± 0.2 ‰ in Romanek et al., 1992). Other factors may also play a role in determining the $\delta^{13}C$ value of the internal DIC pool. For example, the enzyme carbonic anhydrase, which catalyses the reaction of bicarbonate to CO_2, which can more easily diffuse through membranes (Paneth and O'Leary, 1985), may add or remove carbon species from this pool (see 3.2.2.1 of Chapter 1).

Considering that many bivalves incorporate only a small amount of respired CO_2, their skeletons should be able to trace large changes in $\delta^{13}C_{DIC}$, as was found by Mook and Vogel (1968) and Mook (1971) for *M. edulis* in the Schelde estuary. This is also true if the offset is constant as was found in a freshwater mussel (Kaandorp et al., 2003). Such data could then be useful for roughly determining the salinity where the animals grew, which could be a valuable addition to the interpretation of shell $\delta^{18}O$ profiles (see Chapter 4). Therefore, the $\delta^{13}C$ values of *M. edulis* shells and mantle tissues, DIC, and particulate organic carbon (POC) were measured across a salinity gradient and over one year. Additionally, a preliminary experiment on the $\delta^{13}C$ of hemolymph was conducted in the laboratory at different $\delta^{13}C_{DIC}$ values and a different salinity.

2. Materials and Methods

2.1 Field data collection

Mussels were collected from the intertidal zone of the Schelde estuary from Knokke (KN) and Hooftplaat (HF) on 17 March 2002 and from Griete (GR) and Ossenisse (OS) on 23 March 2002 (Fig. 1). In addition, mussels were also sampled from HF on 3 May, 28 July, and 29 September and from KN on 3 May and 28 July 2002. Mantle tissues were collected using a scalpel and stored frozen until preparation. During preparation, tissues were dried in an oven at 60 °C for 24 hours, homogenized with a mortar and pestle, and ~1 mg material was placed into a silver cup. 2 - 3 drops of 5 % HCl was added and the cups were allowed to dry in an oven overnight after which they were folded closed. Tissue $\delta^{13}C$ was measured on an Element Analyzer (Flash 1112 Series EA ThermoFinnigan) coupled via a CONFLO III to an IRMS (Delta^{plus}XL, ThermoFinnigan). Using this same instrument and method, Verheyden et al. (2004) report a long term analytical precision for $\delta^{13}C$ of 0.08 ‰ on 214 analyses of the IAEA-CH-6 standard (1σ). Shells were sectioned along the axis of major growth and samples were drilled from the calcite layer along the growth-time axis. Carbonate powders were reacted in a Kiel III coupled to a ThermoFinnigan Delta^{plus}XL dual inlet IRMS with a long-term $\delta^{13}C_S$ precision of 0.039 ‰ (see Chapter 2 for more details).

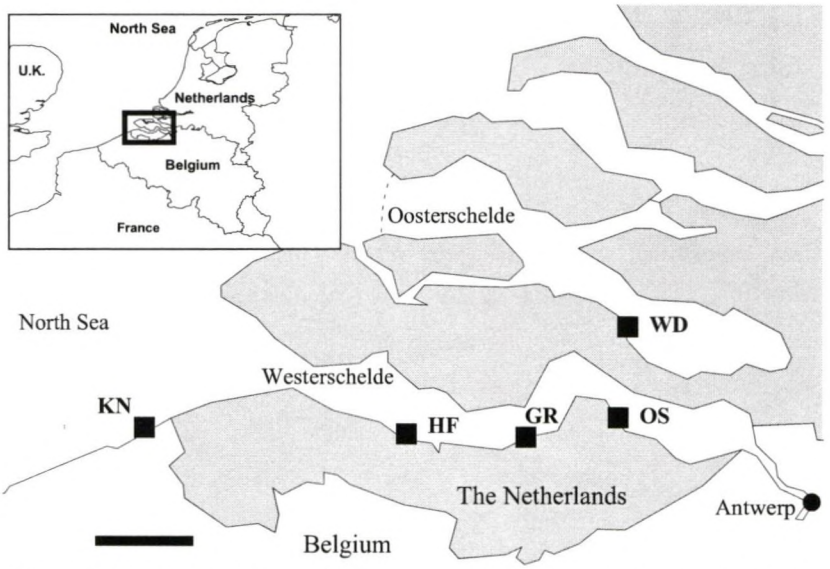

Figure 1. Map of the Westerschelde estuary. The four study sites are indicated Knokke (KN), Hooftplaat (HF), Griete (GR) and Ossenisse (OS). Scale bar = 10 km.

Near-shore water samples were collected at least monthly from Nov. 2001 to Oct. 2002 for chlorophyll *a* concentrations (Chl *a*), $\delta^{13}C_{DIC}$, $\delta^{13}C_{POC}$ and suspended particulate matter (SPM). Chlorophyll *a* was measured using standard protocols (see Chapter 2). The $\delta^{13}C_{DIC}$ was determined by acidifying 5 ml of water in an 8 ml helium flushed headspace vial, overnight equilibration, and subsequently injecting 400 µl of the headspace into the carrier gas stream of the continuous flow IRMS. Precision of $\delta^{13}C_{DIC}$ was better than 0.2 ‰ based on replicate measurements; data were corrected using calibrated CO_2 gas according to Miyajima et al. (1995) (see Chapter 2). The $\delta^{13}C_{POC}$ was measured following Lorrain et al. (2003) (see Chapter 2 for more details) and SPM is based on the dry weights of these filters.

2.2 Laboratory experiment

Mussels were held in four tanks for more than one month and were fed yeast. Three tanks had the same salinity (35) and varying $\delta^{13}C_{DIC}$ values, while one tank had a salinity of 19. The $\delta^{13}C_{DIC}$ of the water in the tanks was measured as described above. Two to five mussels per tank were sampled. Hemolymph samples were drawn from the adductor muscle of the mussels with a sterile needle and syringe, injected into He

flushed 2 ml headspace vials, and were analyzed similar to water $\delta^{13}C_{DIC}$, except 1000 µl was injected into the IRMS.

3. RESULTS

The $\delta^{13}C_{DIC}$ was strongly related to salinity with the linear relationship: $\delta^{13}C_{DIC}$ = Salinity * 0.39 (± 0.03) – 13.71 (± 0.57) (R^2 = 0.94, $p < 0.0001$, n = 63; for the salinity range of ~ 5 to 30) (Fig. 2). To approximate the $\delta^{13}C$ value of phytoplankton, 20 ‰ was subtracted from the $\delta^{13}C_{DIC}$ values (see discussion). There were strong linear relationships between mantle tissue and both $\delta^{13}C_{POC}$ and $\delta^{13}C_{DIC}$ - 20 ‰ ($\delta^{13}C_{DIC-20}$; Fig. 3) for samples collected in March. The slope between mantle tissue and $\delta^{13}C_{DIC-20}$ was not significantly different from one ($p < 0.0001$). Mantle tissue varied considerably throughout the year at HF and KN with a 2 to 3 ‰ decrease between March and September (Fig. 4). In both sites, mantle tissue was least negative in March, just before the phytoplankton bloom, but was more similar to the $\delta^{13}C$ of potential food sources in May, July and September.

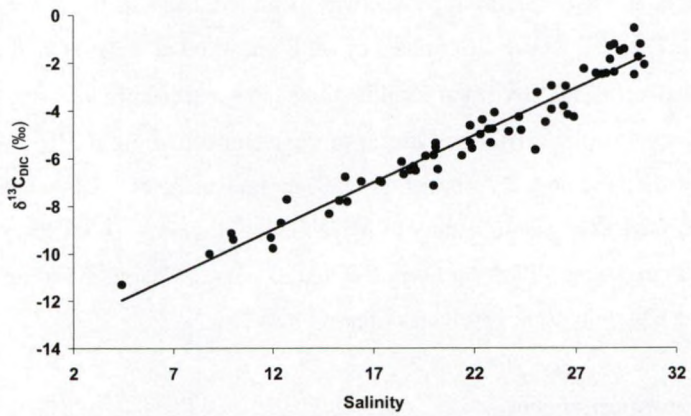

Figure 2. $\delta^{13}C_{DIC}$ versus salinity from samples taken over one year along the Schelde estuary with the relationship: $\delta^{13}C_{DIC}$ = Salinity * 0.39 (± 0.03) – 13.71 (± 0.57) (R^2 = 0.94, $p < 0.0001$, n = 63; for the salinity range of ~ 5 to 30).

Using the $\varepsilon_{cl\text{-}b}$ from Romanek et al. (1992), shells from KN were on average not in equilibrium with $\delta^{13}C_{DIC}$, but the three other sites were (Fig. 5). Although the regression using the mean of all four sites is significant ($p = 0.039$, $R^2 = 0.94$),

removing KN results in a regression line which perfectly bisects the three means (Fig. 5). The intercept of this latter model is 1.65 (± 0.001), which is close to the expected equilibrium value with $\delta^{13}C_{DIC}$ = 0 ‰ (i.e., +1.0 ± 0.2 ‰, Romanek et al., 1992). High-resolution $\delta^{13}C_S$ profiles can be found in Figure 7 of Chapter 10, and show that in general, $\delta^{13}C_S$ is more negative in spring.

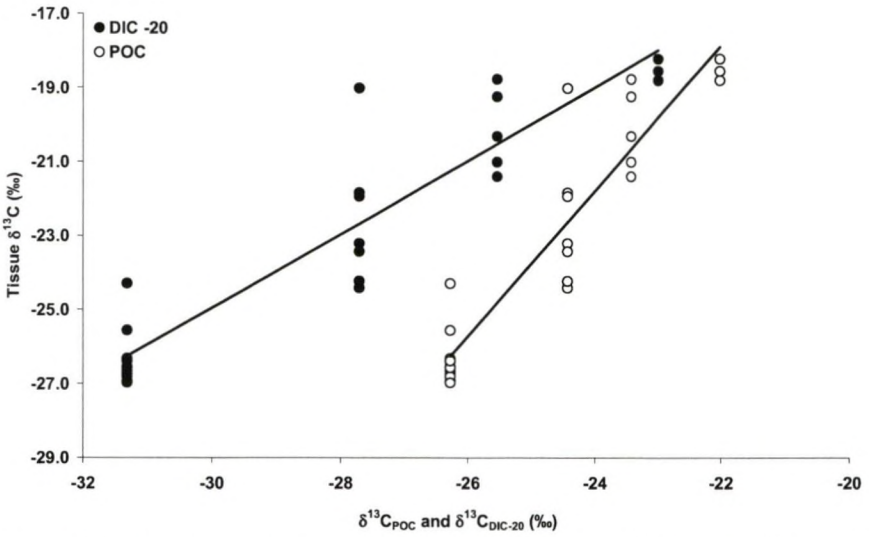

Figure 3. Linear regressions between mantle tissue $\delta^{13}C$ and both $\delta^{13}C_{POC}$ and $\delta^{13}C_{DIC}$ – 20 ‰ from mussels collected in March 2002. N = 27 for all. The relationships are: Tissue $\delta^{13}C = 0.99 (\pm 0.16) * \delta^{13}C_{DIC-20} + 4.89 (\pm 4.48)$ ($R^2 = 0.87$, n = 27, $p > 0.0001$), and Tissue $\delta^{13}C = 1.97 (\pm 0.31) * \delta^{13}C_{POC} + 25.39 (\pm 7.87)$ ($R^2 = 0.87$, n = 27, $p > 0.0001$).

Hemolymph $\delta^{13}C$ values were linear with $\delta^{13}C_{DIC}$ between the three tanks with a salinity of 35, while hemolymph $\delta^{13}C$ values were more negative in the lower salinity tank despite $\delta^{13}C_{DIC}$ being in the same range (Fig. 6). However, these data should be regarded with caution. Although preliminary attempts to determine if there was an effect of using small headspace vials (2 ml; usually, 8 – 20 ml vials are used) suggested that there was no effect, later attempts could not reproduce this. No satisfactory explanation could be found for this. Nevertheless, the fact that there was no effect of vial size during the period that these samples were measured, and the reproducibility between mussels from the same tank, indicates that the more negative hemolymph $\delta^{13}C$ values in the lower salinity tank is probably not an artifact of measurement.

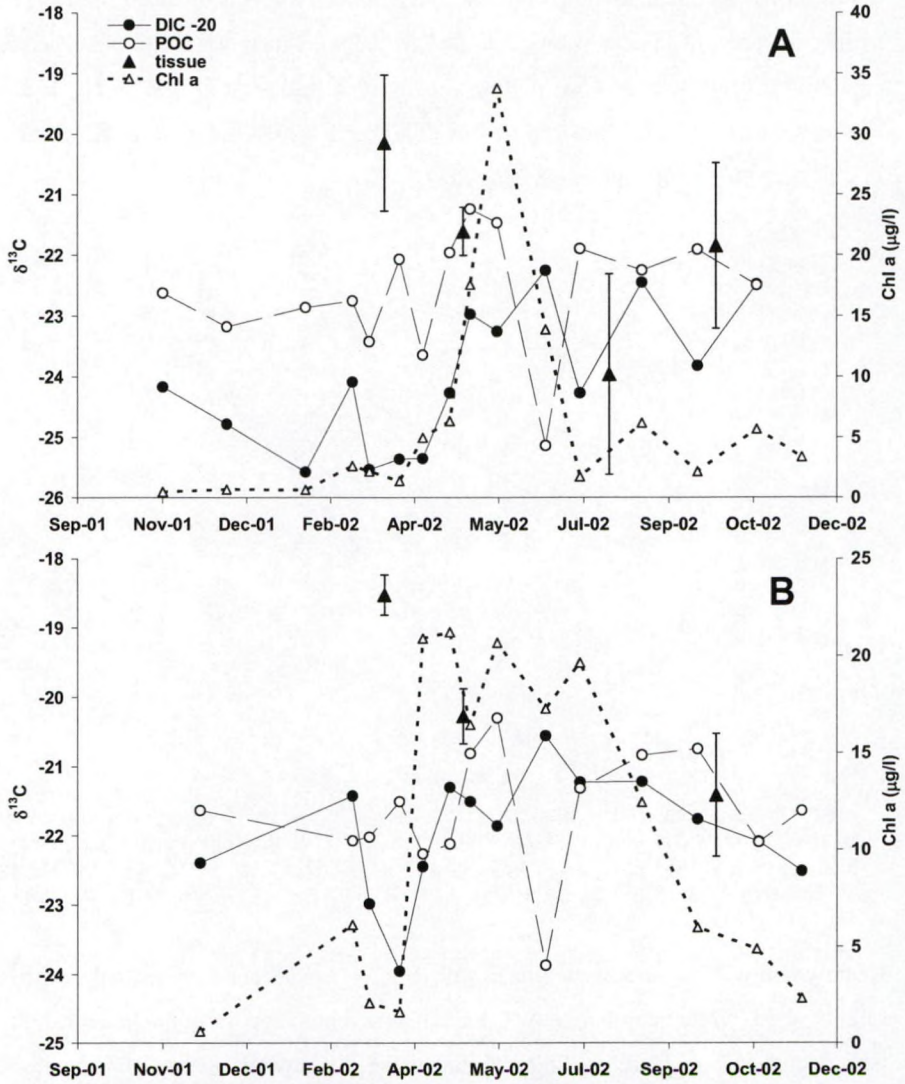

Figure 4. Seasonal samples of mantle tissue $\delta^{13}C$, $\delta^{13}C_{POC}$, $\delta^{13}C_{DIC-20}$, and chlorophyll *a* taken from Hooftplaat (A) and Knokke (B). Error bars represent standard deviations.

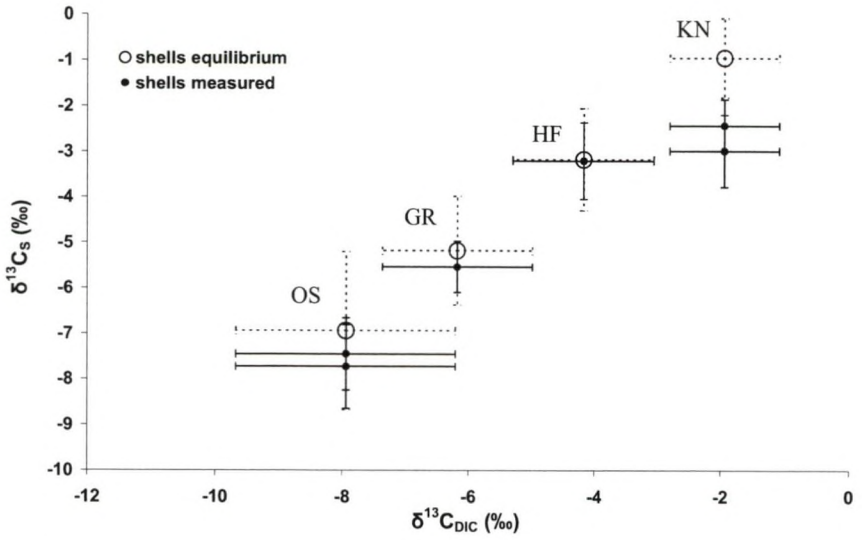

Figure 5. Mean $\delta^{13}C_s$ and $\delta^{13}C_{DIC}$ averaged over the full year for the four sites (noted above data points, see Fig. 1 for description of site codes). High-resolution profiles can be found in Figure 7 of Chapter 10. Also plotted are the expected shell values based on the fractionation factor between $\delta^{13}C_{DIC}$ and calcite (+1.0 ‰; Romanek et al., 1992). Error bars represent standard deviations.

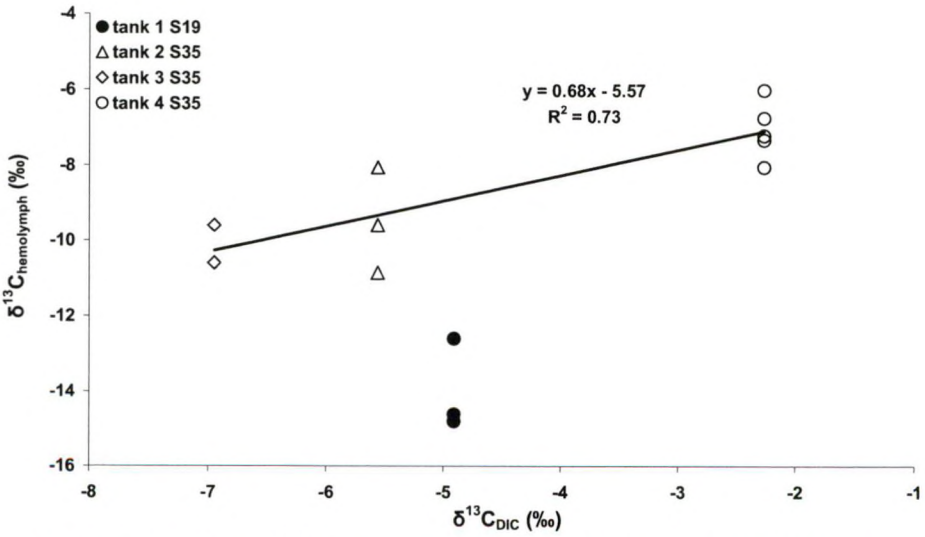

Figure 6. Hemolymph $\delta^{13}C$ from laboratory held mussels. Mussels were held in four tanks, three with a salinity of 35 (Tanks 2, 3 and 4) and one with a salinity of 19 (Tank 1).

4. DISCUSSION

Although it is well established that the carbon isotope fractionation between phytoplankton and DIC is variable (Rau et al., 1992; Hinga et al., 1994; Boschker et al., 2005), a value between 18 and 22 ‰ is often used as an estimate (Cai et al., 1988; Hellings et al., 1999; Fry, 2002; Bouillon et al., 2004b). Therefore, similar to Fry (2002), the average value of 20 ‰ is used. From Fig. 3 it is clear that *M. edulis* is highly selective as the slope between the expected $\delta^{13}C$ of phytoplankton and tissues is not significantly different from one, whereas the slope between $\delta^{13}C$ of tissues and $\delta^{13}C_{POC}$ was 2.0 (±0.3). $\delta^{13}C_{POC}$ and $\delta^{13}C_{DIC}$ were also significantly correlated ($\delta^{13}C_{POC} = 0.42$ (± 0.09) * $\delta^{13}C_{DIC} - 21.0$ (± 0.5); $R^2 = 0.61$, $n = 59$, $p < 0.0001$). The POC is a mixture of different sources of carbon, each with their own $\delta^{13}C$ values, such as phytoplankton, terrestrial carbon (in general, ~ -26 ‰ from C3 plants and ~ -14 ‰ from C4 plants; Mook and Tan, 1991), resuspended sediments (Schelde: ~ -19 to -24 ‰; Middelburg and Nieuwenhuize, 1998; Herman et al., 2000), marine macro-algae detritus (Schelde: green algae ~ -17 ‰, brown algae ~ -25 ‰; Gillikin unpublished data), microphytobenthos (Schelde: ~ -15 ‰; Middelburg et al., 2000; Herman et al., 2000), and other substances from which the mussels must select from. As these samples were taken near the shore, there was probably a large amount of suspended sediments, which is indicated by the high SPM content (range = 13 to 550 mg/l, mean = 86 mg/l). Selection can occur both at the gills (pre-ingestive) and in the gut (post-ingestive) (reviewed in Ward and Shumway, 2004), but using $\delta^{13}C$ as a tracer deals only with assimilated carbon. Moreover, using the selectivity equation from Bouillon et al. (2004b),

$$\text{Selectivity} = (\Delta\delta^{13}C_{tissue} - \Delta\delta^{13}C_{POC} / \Delta\delta^{13}C_{DIC} - \Delta\delta^{13}C_{POC}) * 100\ [\%] \quad (2)$$

where Δ is the overall estuarine gradient in tissue, POC and DIC $\delta^{13}C$ values (assumes that selectivity is similar at all stations, see Bouillon et al., 2004b), suggests that they are ~90 % selective, which further illustrates that they primarily assimilate their carbon from phytoplankton, which in turn obtains its carbon from the DIC. It is generally accepted that the $\delta^{13}C$ value of an organism reflects the $\delta^{13}C$ value of its diet with little (1 ‰) or no change (DeNiro and Epstein, 1978; Fry and Sherr, 1984).

Therefore, the intercept between tissue $\delta^{13}C$ and $\delta^{13}C_{DIC-20}$ should be +1. However, it should be kept in mind that the 20 ‰ fractionation used here is a rough estimate. The intercept of 4.89 ± 4.48 ‰ in Fig. 3 can therefore be explained by an error in the phytoplankton fractionation as well as the individual variation in tissue $\delta^{13}C$. Moreover, errors in this simplified model can arise from the mussels feeding on other food items. Mussels have been shown to feed on dissolved organic carbon (DOC) (Roditi et al., 2000), their own and other bivalve larvae (Lehane and Davenport, 2004), zooplankton (Lehane and Davenport, 2002; Wong et al., 2003), and macroalgae detritus (Levinton et al., 2002); all with different $\delta^{13}C$ values (see above). Nevertheless, as a first approximation, $\delta^{13}C_R$ values should roughly follow DIC, as has been noticed in other bivalves (e.g., Fry, 2002). However, Swart et al. (2005) found that $\delta^{13}C_R$ from a coral significantly deviated from the $\delta^{13}C$ of tissues (both positive and negative deviations of up to 3 ‰), which they attributed to different compounds (e.g., lipids) being respired at different times of the year.

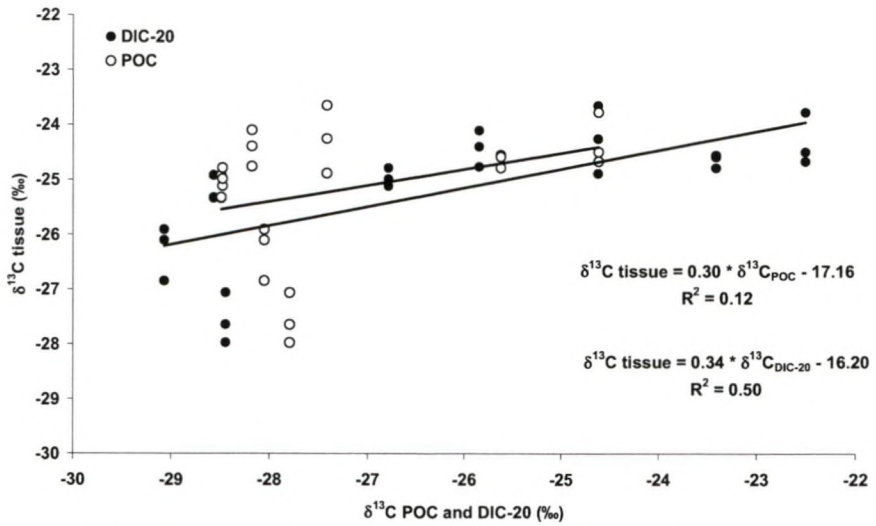

Figure 7. Ribbed mussel (*Geukensia demissa*) bulk tissue $\delta^{13}C$ versus both $\delta^{13}C_{POC}$ and $\delta^{13}C_{DIC-20}$ from mussels collected in August 2004 from along a salinity gradient in a North Carolina salt marsh (N = 24). Data from Gillikin and Bouillon (unpublished).

Although it might seem obvious that the $\delta^{13}C$ of filter feeders that eat phytoplankton, which in turn assimilate their carbon from DIC, would all be related to the $\delta^{13}C_{DIC}$, as is the case with many bivalves (e.g., Fry, 2002), the relationship does not always hold true. For example, despite the linear relationship between salinity and $\delta^{13}C_{DIC}$ in a

North Carolina salt marsh creek ($\delta^{13}C_{DIC}$ = 0.44 * Salinity – 14.45, R^2 = 0.97, n = 15, for the salinity range of 1 – 29; Gillikin and Bouillon, unpublished data), tissues collected from the ribbed mussel, *Geukensia demissa*, did not follow either $\delta^{13}C_{POC}$ or $\delta^{13}C_{DIC-20}$ (Fig. 7). Consequently, no correlation between shell $\delta^{13}C$ and $\delta^{13}C_{DIC}$ was noticed in these specimens (data not shown).

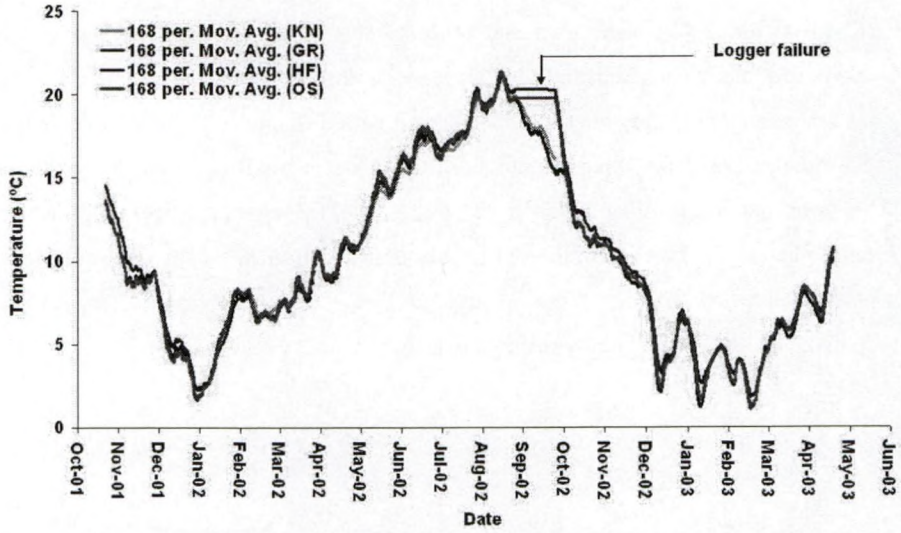

Figure 8. Water temperature recorded hourly using Onset TidBit dataloggers at all four sites. The weekly running average is shown. The loggers failed at two sites for about a month as is indicated on the graph.

From Fig. 4 it is evident that the relationship found in March (Fig. 3) does not necessarily hold true for the whole year. This could be contributed to changing food sources, such as resuspended benthic algae, or variable fractionation between phytoplankton and DIC throughout the year. Indeed, Boschker et al. (2005) found that DIC – diatom fractionation varied from about 16 ‰ to 24 ‰ along this same estuary. Other factors such as temperature and phytoplankton growth rate can also influence the fractionation between phytoplankton and DIC (see Savoye et al., 2003). However, a possible explanation is changing lipid concentration in *M. edulis* tissues. In *M. edulis*, the mantle contains much of the gonad (Morton, 1992); and in this region, *M. edulis* spawning peaks when temperatures exceed approximately 10 °C (Hummel et al., 1989). At all four sites this occurs in mid-March (Fig. 8), approximately at the same time as the tissue samples were collected. In March the mussels have probably just spawned and therefore the tissues have a low lipid content (see de Zwaan and

Mathieu, 1992). Lipids are known to have significantly more negative $\delta^{13}C$ than other biochemical components (Abelson and Hoering, 1961; Tieszen et al., 1983; Focken and Becker, 1998; Lorrain et al., 2002), and the mantle exhibits a sharp drop in lipid content just after spawning (de Zwaan and Mathieu, 1992), thus explaining the more positive tissue $\delta^{13}C$ values in this month. After the phytoplankton bloom, which begins in April or May, the lipid content of the tissues is restored, thus lowering the $\delta^{13}C$ value. Indeed, Lorrain et al. (2002) found that $\delta^{13}C$ of scallop tissues were highest in spring when lipids were low and decreased as lipids increased toward late summer. However in shells, the spawning period is reflected by more negative $\delta^{13}C$ values (Fig. 7 of Chapter 10) although the $\delta^{13}C_{DIC}$ is generally becoming more positive (Fig. 4). This could possibly be explained by high metabolic rates just after spawning, to restore the energy lost during the spawn. Vander Putten et al. (2000) also described these patterns in $\delta^{13}C_S$ in *M. edulis* from the Schelde as being a result of increased respiration associated with periods of high food availability.

Despite the variability in tissue $\delta^{13}C$ throughout the year, the mean shell values roughly match equilibrium values for three of the four sites (Fig. 5). The differences between measured and predicted values vary between sites (Table 1), with salinity apparently having little to do with disequilibrium. According to the hemolymph $\delta^{13}C$ data from the laboratory experiment, salinity affects the internal DIC pool $\delta^{13}C$ value (Fig. 6), which then would be expected to affect $\delta^{13}C_S$. The laboratory hemolymph data show that at a lower salinity, hemolymph $\delta^{13}C$ is more negative, while in opposition, shells from the highest salinity field site (KN) were more negative than equilibrium predicts (Fig. 5). Nevertheless, all shells generally fall within the 10 % metabolic C incorporation suggested to be typical for aquatic marine invertebrates by McConnaughey et al. (1997) (Table 1).

Table 1. Predicted minus measured $\delta^{13}C_S$ (pred – meas, in ‰) and percent metabolic C incorporation (%M) in the shells at each site. %M calculated using average data and the equation of McConnaughey et al. (1997, see eq. 1).

	KN1	KN2	HF	GR	OS1	OS2
Salinity*	29	29	25	20	14	14
pred – meas	2.04	1.49	0.03	0.36	0.51	0.79
%M	10.9	8.0	0.2	2.3	3.0	4.7

*Annual mean.

Although $\delta^{13}C_R$ does not seem to largely affect the $\delta^{13}C_S$ ($\prec$ 10 % incorporation of metabolic CO_2 into the shell), the variability in the percent incorporated is enough to preclude its use as a robust $\delta^{13}C_{DIC}$ proxy, and hence a salinity proxy. For example, if the $\delta^{13}C_S$ values of the KN shell were used to predict $\delta^{13}C_{DIC}$ and salinity, one would conclude that this shell came from a site similar to HF (Fig. 5), even though the salinity difference between these sites is typically around 5. From Fig. 5, it may seem that mussel shells from the same environment could be used to determine $\delta^{13}C_{DIC}$, but *Mercenaria mercenaria* shells collected from similar environments had very different metabolic contributions to their shells (Chapter 5), suggesting this might result in large errors. These data do not provide an explanation why the KN shells were farther from equilibrium than the others, but it could be the result of higher metabolic rates caused by the stronger wave action at this site, which increases water flow and thus food availability. Moderate wave action has been shown to increase growth rates and condition values in *Mytilus* (Steffani and Branch, 2003), which would lead to higher metabolic rates. There are also other possibilities which can increase metabolic rate, such as epibiont cover (such as barnacles (Buschbaum and Saier, 2001), which there are more of at the KN site, see Fig. 9), exposure to predators (Frandsen and Dolmer, 2002), and pollution (Wang et al., in press).

The difference between the results presented here and those from earlier studies on the same species and estuary (i.e., Mook and Vogel, 1968; Mook, 1971), who state that $\delta^{13}C_S$ is a good proxy of $\delta^{13}C_{DIC}$, can be caused by many factors. First, these earlier studies did not separate aragonite and calcite from the shells, which greatly differ in equilibrium $\delta^{13}C$ values with HCO_3^- (i.e., +1 ‰ for calcite and + 2.7 ‰ for aragonite; Romanek et al., 1992). Second, they roasted their samples and found significant differences between roasted and non-roasted δ-values, while Vander Putten et al. (2000) found no difference in calcite from this same species, indicating a possible isotopic alteration in these earlier studies. Finally, these earlier works did not consider metabolic effects and perhaps did not sample populations with markedly different metabolic rates.

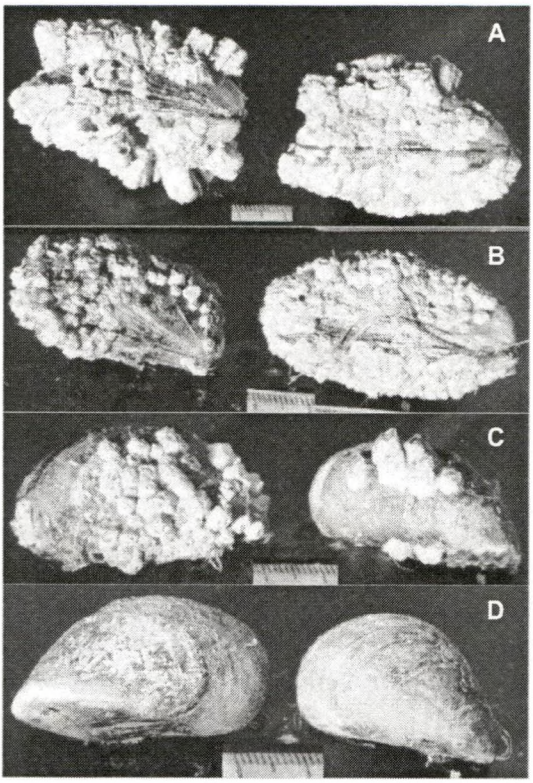

Figure 9. Barnacle cover on caged mussels along the Schelde Estuary from Knokke (A), Hooftplaat (B), Griete (C), and Ossenisse (D). Scales are in mm.

The salinity effect on the $\delta^{13}C$ of the internal DIC pool is an interesting finding, but difficult to explain. It could be the result of increased metabolism in the osmotically stressed mussels, but *M. edulis* is an osmoconformer (Newell, 1989), so this does not seem probable. An alternative hypothesis is that carbonic anhydrase (CA) is being affected by the change in salinity. The enzyme CA is responsible for ion exchange at the gills, and has been shown to correlate with growth in bivalves and to be involved in respiration and acid-base regulation (Duvail et al., 1998). Activity of CA is known to change with salinity in some bivalves, but again, is tied to osmoregulation (Henry and Saintsing, 1983), so does not apply to *M. edulis* since they do not osmoregulate. Therefore, salinity should not affect CA activity in *M. edulis*, but CA activity has been shown to be inhibited by Cl^- ions (Pocker and Tanaka, 1978). A reduction in CA activity could cause a reduction in environmental DIC entering the animal, resulting in a larger ratio of metabolic DIC and more negative $\delta^{13}C$ in the hemolymph.

In conclusion, although $\delta^{13}C_R$ values can closely follow $\delta^{13}C_{DIC}$ values and the percentage of metabolic C incorporated into the shells of *M. edulis* is low, the variability in metabolic C incorporation is too high to allow confident salinity determinations based on $\delta^{13}C_S$. The example presented here could not differentiate between two sites with a salinity difference of 5, which in terms of $\delta^{18}O$ paelothermometry would correspond to about 4 °C (see Chapter 1). Thus $\delta^{13}C_S$ is not a robust proxy of environmental conditions in *M. edulis* calcite, but may be useful for determining metabolic differences between different populations and can still be used as an indicator of large $\delta^{13}C_{DIC}$ (and salinity) differences.

Acknowledgements

I am much indebted to V. Mubiana for assistance with mussel collection and setting up the field experiment. A. Van de Maele and M. Korntheuer both assisted with keeping the Kiel III running. Constructive criticism, which greatly improved this Chapter, was given by A. Lorrain, A. Verheyden, and S. Bouillon.

Chapter 7

Assessing the reproducibility and potential of high resolution trace element profiles in an aragonitic bivalve (*Saxidomus giganteus*) for environmental reconstruction

Foreword

At this stage, the reader should have a clear understanding of the problems associated with stable isotope ($\delta^{13}C$ and $\delta^{18}O$) proxies in estuarine bivalves. Therefore, the need for alternative proxies should also be evident. This Chapter is the first of a series discussing trace element proxies in bivalve shells. In this Chapter, several elements in *S. giganteus* shells are surveyed as proxies and an overview of the problems associated with using trace elements in bivalve shells as environmental records is given. Several hypotheses are discussed for each element and the data from these shells are compared with both coral and sclerosponge data. A few select elements (Sr, Pb, and Ba) are discussed in more detail in the following chapters.

Abstract

Elemental ratios archived in biogenic aragonite can represent a record of past environmental information. While there are numerous studies on corals, bivalves have received less attention despite their widespread occurrence and well preserved fossil shells. The shell chemistry of two *Saxidomus giganteus* from Puget Sound (Washington, USA) has been investigated under the premise that if there is an environmental control (either direct or indirect) on a proxy, then it should be similar between two individuals that grew in the same environment. Data from these two shells were then compared with a third shell that grew under different environmental conditions (Kodiak Island, Alaska, USA). High resolution Sr/Ca, Mg/Ca Ba/Ca, and U/Ca profiles in two *S. giganteus* shells that grew at the same location in Puget Sound vary in a similar fashion. Ratios of Pb/Ca were more dissimilar, but were generally low. The similarities between the two shells may indicate an environmental control on the chemical composition of the shell. However, similar ratios and variations were also noted in the Alaskan shell, despite the different environmental conditions at this location. Therefore, relating the variations in these elemental ratios to environmental parameters is not straightforward. Similarities in the ontogenic decreases in both Sr/Ca and U/Ca from the three shells suggest that similar biological mechanisms may possibly play a role in the incorporation of these elements into the shell. Ratios of Mg/Ca, which have been proposed as a temperature proxy, were similar between shells from Puget Sound, but were in the same range in the Alaskan shell, which grew in cooler waters. Ratios of Ba/Ca display sharp episodic peaks, common in all bivalve species analyzed to date, but could not be correlated to either salinity or phytoplankton production. These results illustrate the difficulties in using trace elements as proxies for environmental conditions and the need for a mechanistic understanding of trace element incorporation into bivalve shell carbonate.

1. INTRODUCTION

Both stable isotopes and elemental ratios archived in bivalve shells can represent a record of environmental and ecological information (Epstein et al., 1953; Dodd, 1965; Jones et al., 1983; Dutton et al., 2002; Holmden and Hudson, 2003; Dettman et al., 2004; Richardson et al., 2004). Although many elemental proxies (e.g., Sr/Ca, Mg/Ca, Pb/Ca, Ba/Ca, U/Ca) have been thoroughly studied in corals (Weber, 1973; Shen and Boyle, 1987; Scott, 1990; Fallon et al., 1999; Cardinal et al., 2001), many have yet to be validated for bivalve species. Bivalve shells are potentially useful archives of environmental information for several reasons. For example, due to their high growth rate, high temporal resolution profiles can easily be obtained, allowing investigation on an intra-annual scale. They generally occur in almost all types of aquatic ecosystems (e.g, deep marine, estuarine, rivers, lakes), from the tropics to the poles. Additionally, many species have a large distribution both in space and environmental tolerance (e.g., a large salinity range). Therefore, bivalve shells can potentially archive environmental information (e.g., sea surface temperature (SST), salinity, productivity) in almost any aquatic environment.

Although there have been high resolution studies on trace element concentrations in bivalve shells (Carriker et al., 1996; Stecher et al., 1996; Klein et al., 1996a; Vander Putten et al., 2000; Lazareth et al., 2003; Richardson et al., 2004), the results have been inconclusive. For example, Klein et al. (1996a) report that Mg/Ca ratios in mussel shells are a robust SST proxy, while Vander Putten et al. (2000) illustrate that Mg/Ca ratios do not track SST in a different species of the same genus. Thus, it is likely that many of these proxies are species-specific, and each proxy should ideally be validated and calibrated for each species.

The Butter clam, *Saxidomus giganteus* (Family: Veneroidea) is an aragonitic infaunal marine clam usually inhabiting the intertidal zone, but which can occur at depths in excess of 30 m (Quayle and Bourne, 1972). They are a temperate species, occurring from Alaska to northern California (Quayle and Bourne, 1972). *S. giganteus* shells are commonly found in prehistoric midden sites (Hetherington and Reid, 2003; Taylor, 2004) as well as in Pleistocene geologic deposits as well preserved fossils

(Kvenvolden et al., 1979), potentially making them a very useful paleo-environmental proxy.

Data on $\delta^{18}O$, $\delta^{13}C$, and Sr/Ca ratios in shells from *S. giganteus* are presented in detail in other Chapters (4 and 8). In this Chapter, Mg/Ca, Pb/Ca, Ba/Ca, and U/Ca are investigated as environmental proxies. First, the elemental ratios from the shells with data from water are compared. Secondly, the reproducibility of the elemental profiles between two shells that grew at the same site (Puget Sound) is assessed. This is done under the premise that if there is an environmental control (either direct or indirect) on a proxy, then it should be similar between two individuals that grew in the same environment. Furthermore, a third shell that grew under different environmental conditions (Kodiak Island, Alaska, USA) was also analyzed and compared with the Puget Sound specimens in order to decipher environmental versus ontogenic (or biological) signals. In addition to the ratios listed above, Sr/Ca ratios are also presented to compare with Mg/Ca ratios, since they have been shown to be related in other carbonates (Carpenter and Lohmann, 1992).

2. METHODS

2.1 Sample collection, preparation and analysis

Two living *Saxidomus giganteus* were collected from Carkeek Park, Puget Sound, Washington, USA (shells B1 and B2; collected Sept. 2001) and one from Old Harbor, Kodiak Island Alaska (shell OH1; collected Jun. 2003). Puget Sound salinities range from 21 to 30 and temperatures from 7 °C to 17 °C, while Old Harbor salinities range from 18 to 32 and temperatures from 0 to 13 °C (see Chapter 8). Gillikin et al. (2005b or Chapter 8) have shown that *S. giganteus* precipitate aragonite shells. Sections of the shells were cut with a diamond saw along the axis of maximal growth, rinsed with deionised water, air-dried and mounted on microscopic slides. These sections were placed directly in the ablation cell of the LA-ICP-MS. The LA-ICP-MS instrumentation and methods used are described in Chapter 2. For this study, the laser was shot directly in the holes of the isotope sampling from Chapter 4 (see also Chapter 3). Samples were taken from the outer shell layer, avoiding the outermost part of the shell which is in contact with the water. Near-shore water samples were

collected on 29 May 2003 from the same vicinity as the clam collection site in Puget Sound.

2.2 Water analysis

Water samples were measured on an inductively coupled plasma-optical emission spectrometer (ICP-OES; Thermo Jarrell Ash Corporation IRIS) using Yt and Au as internal standards (see Chapter 2). The elements analyzed were Ba, Ca, Mg and Sr. Data on Cd, Co, Cu, Pb and Zn concentrations were provided by the King County Department of Natural Resources Water and Land Resources Division, Marine Monitoring group (WA, USA).

2.3 Data treatment

To asses the similarity between the different elemental profiles of the two *S. giganteus* shells, the profiles need to be fit to a common timescale. For this purpose, the $\delta^{18}O$ profiles, obtained from former studies on these shells (Chapter 4), were used. High resolution profiles of $\delta^{18}O_S$ often show a clear annual periodic signal, reflecting the seasonal temperature variation. Using the relation between $\delta^{18}O$ and temperature, shell layers were assigned intra-annual dates. This was achieved by using the phase demodulation method of De Ridder et al. (2004). More details can be found in Gillikin et al. (2005a) and Chapter 4. Considering that the elemental analyses were perfectly aligned with $\delta^{18}O$ analyses (see section 2.1, Gillikin et al., 2005b, and Chapter 8), the fitting of the $\delta^{18}O$ profiles allows a direct comparison of elemental profiles between the two shells. In this study the profiles of shell B1 was fit to shell B2.

Regressions were calculated using bivariate least squares (BLS) statistics. Unlike ordinary least square regressions, the BLS considers errors on both the dependent and independent variables (see Riu and Rius, 1996; Verheyden et al., 2005b). Significance tests for the slope and intercept of the regressions and correlation coefficients are based on the joint confidence interval. Errors of the regression coefficients are given as 95 % confidence intervals.

3. RESULTS AND DISCUSSION

3.1 Comparison between shells and water

Generally, limited elemental discrimination during calcification increases the chance of an elemental proxy faithfully recording variations in water chemistry. This can be quantified using the partition coefficient: $D_{Me} = (Me/Ca)_{shell} / (Me/Ca)_{water}$, where Me refers to a particular element [Note: activity coefficients are not considered here, see Chapter 1, section 3.2.2.1 for more discussion]. For example, many elemental proxies in corals have been successfully calibrated (see previous references), and many of these elements have a D_{Me} close to unity (see Reuer et al., 2003 and Table 1). Figure 1 represents the relationship between elements in *S. giganteus* (using the data from the in-house S-gig standard; see Chapter 2) versus the water (see figure legend for data sources). From this it is clear that Mg and U, and to a lesser extent Sr, Cd, and Zn are discriminated against during uptake, whereas Mn, Co and Pb are preferentially incorporated into the skeleton; Ba and Cu fall either on or close to the 1:1 line and thus have the best potential as proxies. Unfortunately, Cu and Cd were below the detection limit of the LA-ICP-MS and thus are not discussed further. From Table 1 it is clear that bivalve aragonite is very dissimilar from coral, sclerosponge and inorganic aragonite.

Table 1. Partition coefficients (D_{Me}) for *Saxidomus giganteus* (Bivalve) compared with published D_{Me} from zooxanthellate corals, sclerosponge and inorganic aragonite.

Element ratio	Bivalve D_{Me}	Coral D_{Me}	Sclerosponge D_{Me}	Inorganic D_{Me}
Cd/Ca	0.48	~0.8 [A]	~0.08 [I]	--
Co/Ca	7.69	~0.5 [B]	--	--
Cu/Ca	0.99	--	--	--
Pb/Ca	3.89	2.3 [C]	171.85 [J]	--
Zn/Ca	0.15	~1.2 [A]	~3.3 [I]	--
Sr/Ca	0.23	1.1 [D]	1.17 [J]	1.1 [K]
Ba/Ca	0.61	1.27 [E]	0.86 [J]	1.0 [K]
Mg/Ca	0.00022	0.00085 [F]	0.00016 [J]	0.00016 [L]
U/Ca	0.000021	0.95 [G]	2.98 [J]	1.8 to 9.8 [M]
Mn/Ca	2.56	0.1 to 0.5 [H]	~0.2 [I]	--

See legend of Fig. 1 for sources of water data for this study. A, estimated from figure in Reuer et al. (2003); B, Shen and Boyle (1988); C, Shen and Boyle (1987); D, McCulloch et al. (1994); E, Lea et al. (1989); F, Buddemeier et al. (1981); G, Swart and Hubbard (1982); H, Shen et al. (1991); I, S. Verheyden (unpublished); J, Rosenheim et al. (in press); K, Kitano et al. (1971); L, Oomori et al. (1987); M, Meece and Benninger (1993).

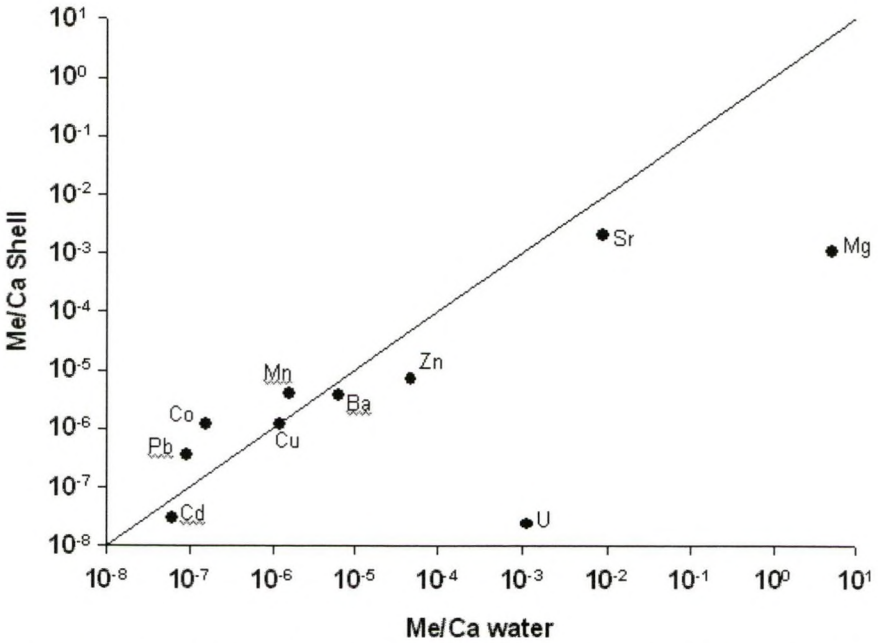

Figure 1. Element/calcium (Me/Ca) ratios for *S. giganteus* shells and seawater (mol/mol). Shell data are from the shell standard (see material and methods) and the water data are referenced in section 2.2 and some are estimated from typical coastal concentrations (Mn/Ca = 4.00 µmol/mol and U/Ca = 0.02 µmol/mol). The diagonal line reflects a partition coefficient (D_{Me}) of 1. Points above this line indicate preferential uptake and those below the line indicate exclusion. Note that this does not account for activity coefficients, which probably is affecting elemental incorporation.

3.2 High resolution profiles

Data from the two *S. giganteus* shells collected from Puget Sound are given in Figure 2, and Figure 3 illustrates the data from the shell from Old Harbor, Kodiak Island, Alaska. The $\delta^{18}O$ axes in Figures 2 and 3 are inverted in order to reflect a relative temperature scale. Gillikin et al. (2005a, see also Chapter 4) found that 83 % of the $\delta^{18}O$ variability in the shells from Puget Sound was due to temperature variations, so salinity effects (i.e., $\delta^{18}O$ of the water) can be considered negligible. Therefore, more positive $\delta^{18}O$ values correspond to winter temperatures and more negative $\delta^{18}O$ values to summer temperatures and thus can be used to delimit seasons of growth. A clear slowing in growth can be seen from the decreasing period of the $\delta^{18}O$ cycles as the distance from the umbo increases (Fig. 2 and 3). Both shells from Puget Sound exhibited similar growth patterns (see Chapter 4), both being about 10 years old, while the Alaskan shell is about 20 years old.

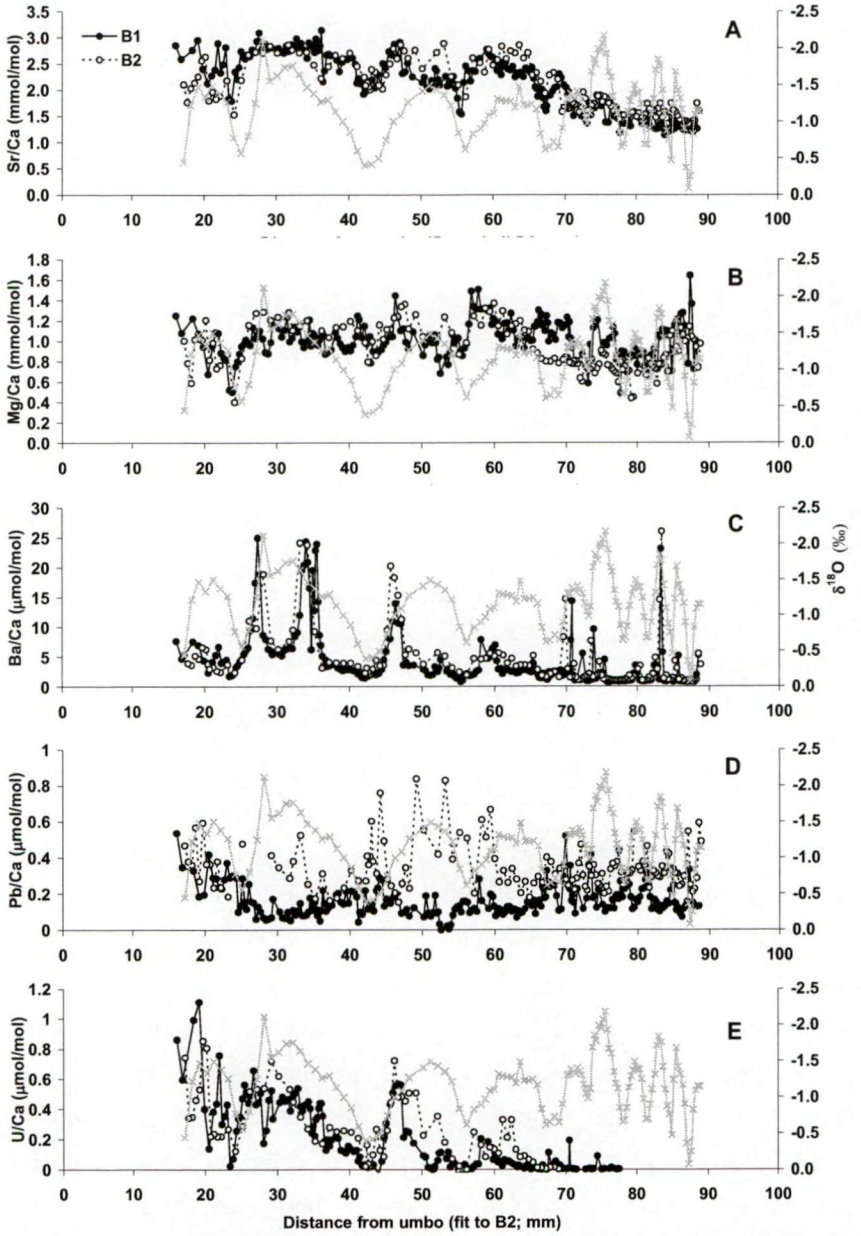

Figure 2. High resolution elemental ratio profiles from the two Puget Sound (Washington, USA) shells measured with LA-ICP-MS fit to shell B2 (see methods). $\delta^{18}O$ data (grey lines) are from Gillikin et al. (2005a) and Sr/Ca data are from Gillikin et al. (2005b). Note that $\delta^{18}O$ axes are inverted.

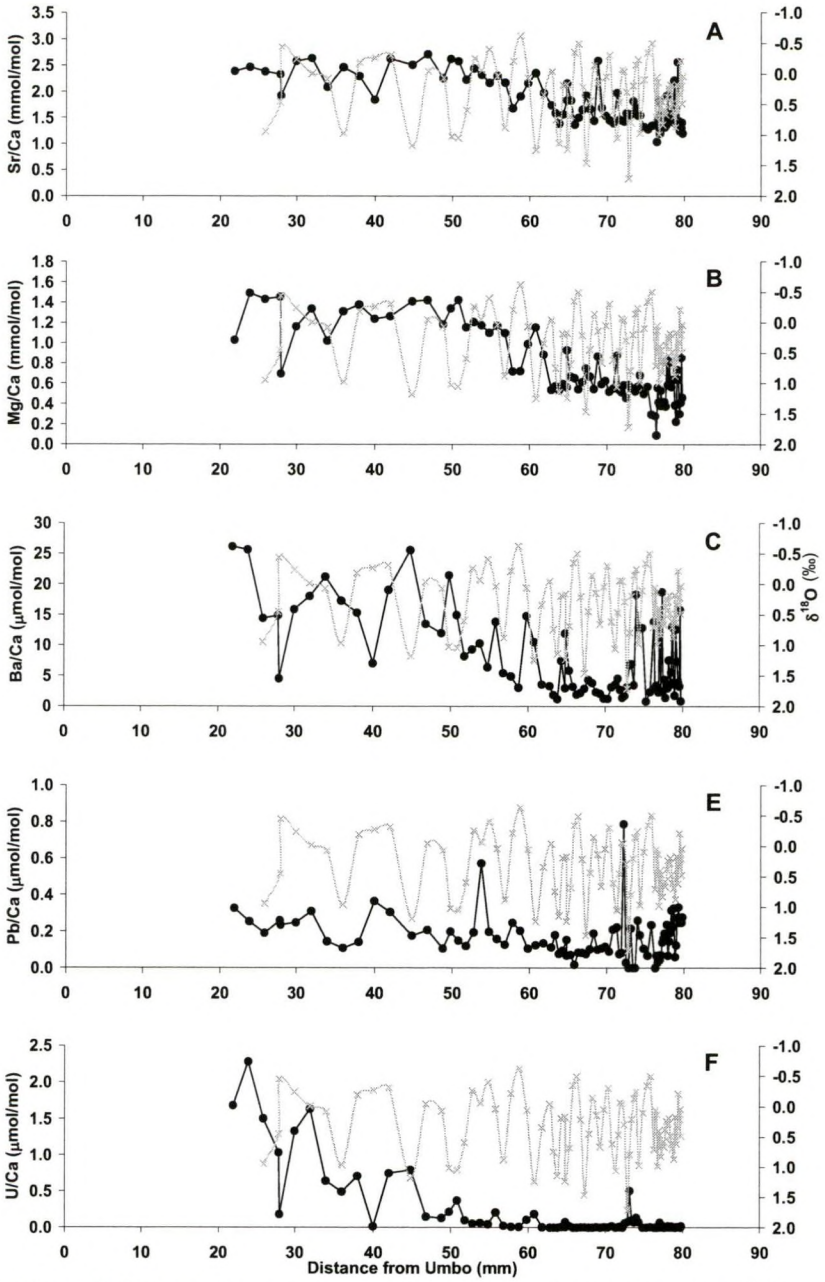

Figure 3. High resolution elemental ratio profiles from the *S. giganteus* shell collected from Old Harbor, Kodiak Island, Alaska, USA, measured with LA-ICP-MS. $\delta^{18}O$ (grey lines) and Sr/Ca data are from Gillikin et al. (2005b). Note that $\delta^{18}O$ axes are inverted.

3.2.1 Sr/Ca ratios

Ratios of Sr/Ca in these shells are discussed in more detail in Chapter 8, where a strong correlation between Sr/Ca and daily growth rate (R^2 = 0.73) was found. Nevertheless, it was hypothesized that growth rate was not the cause of Sr/Ca variations, but that Sr/Ca is controlled by another factor, which is synchronized with growth rate. Although the Sr/Ca profiles are similar between the two Puget Sound shells (Fig. 2A), and Sr/Ca ratios are successfully used as a paleo-temperature proxy in corals (Weber, 1973; Fallon et al., 1999; Cardinal et al., 2001) and sclerosponges (Rosenheim et al., 2004), they could not be related to any environmental parameter in these bivalves (Chapter 8). Ratios of Sr/Ca in these shells (~1 – 3 mmol/mol; and most aragonitic bivalves measured to date) are far from Sr/Ca ratios recorded in inorganic aragonite, corals and sclerosponges (~ 8-10 mmol/mol; Weber, 1973; Kinsman and Holland, 1969; Swart et al., 2002a) indicating strong biological controls dominate Sr incorporation in marine aragonitic bivalves (see also Fig. 1 and Table 1). Despite the strong biological controls on Sr/Ca ratios, they still can be used to obtain detailed (intra-annual) growth rates in *S. giganteus* with some degree of certainty as suggested by Richardson et al. (2004), but this needs to be validated for each species and site (see Gillikin et al., 2005b or Chapter 8).

3.2.2 Mg/Ca ratios

There have been some studies suggesting that Mg/Ca ratios in calcite bivalve shells may be SST proxies (Klein et al., 1996a; Lazareth et al., 2003), and others suggesting that Mg/Ca ratios do not record SST (Vander Putten et al., 2000), or only sometimes do (Freitas et al., 2005). Ratios of Mg/Ca in both corals and foraminifera have been reported to be strongly temperature dependent (Mitsuguchi et al., 1996; Nürnberg et al., 1996), but more recent reports suggest this is not straightforward and may be problematic (Eggins et al., 2004; Meibom et al., 2004). Despite the large deviation from water Mg/Ca ratios (Fig. 1), Mg/Ca ratios in aragonitic bivalve shells (Takesue and van Geen, 2004; this study) are typically within the same range found in corals and sclerosponges (Fallon et al., 1999; Swart et al., 2002a) (See also Table 1).

The Mg/Ca profiles exhibit similarities between the two Puget Sound shells, but are clearly not related to SST (Fig. 2B, using $\delta^{18}O$ as a relative temperature scale). Temperature calculated from shell $\delta^{18}O$ values from Chapter 4 for the Puget Sound

shells was used to test the Mg/Ca – SST relationship, the resultant regressions slope was not significant (Shell B1: $p = 0.89$, B2: $p = 0.60$). Furthermore, variations in Mg/Ca ratios of the water in which they grew cannot be the cause of the variations observed in the shells; salinity remains above 10 at this site (see Chapter 4) and thus water Mg/Ca ratios are therefore constant (Klein et al, 1996a). Comparing the data presented here with other studies, all of which measured Mg/Ca ratios in aragonite bivalves that grew in salinities between 18 and 35 (i.e, ~ constant Mg/Ca ratio in the water), presents largely varying results. For example, Toland et al. (2000) found Mg/Ca ratios of ~ 0.1 to 0.6 mmol/mol in *Arctica islandica* shells, whereas Fuge et al. (1993) obtained much higher values (~ 0.4 to 1.2 mmol/mol) in the same species that grew in similar temperatures. After correcting the LA-ICP-MS data to match SN-HR-ICP-MS data (See Chapter 3), the Mg/Ca ratios ranged from 0.6 to 2.4 mmol/mol in the Puget Sound shells and a similar range was found in the Alaskan shell, which grew in colder waters. Takesue and van Geen (2004), who analyzed *Protothaca staminea* shells from Humbolt Bay in northern California, USA, found a range of ~ 0.7 to 4.0 mmol/mol, despite the fact that their study site has comparable SST and salinities to the Puget Sound site. These results further substantiate that there is no general correlation between Mg/Ca ratios and temperature in aragonitic bivalve shells.

In calcite, Mg/Ca and Sr/Ca have been found to co-vary as a result of crystal deformations, with the smaller Mg ion deforming the crystal, allowing the larger Sr ion to more easily fit in the crystal structure (Mucci and Morse, 1983; Carpenter and Lohmann, 1992), but this is not the case in aragonite (Dietzel et al., 2004). Interestingly, there is a significant strong positive correlation between Sr/Ca and Mg/Ca ratios in the shell from Alaska ($Sr/Ca = 1.41 (\pm 0.16) * Mg/Ca + 0.83 (\pm 0.08)$, $R^2 = 0.84$, $p < 0.0001$, $n = 85$), and weak, but significant correlations in the Puget Sound shells (B1: $Sr/Ca = 0.60 (\pm 0.36) * Mg/Ca + 1.21 (\pm 0.36)$, $R^2 = 0.07$, $p < 0.001$, $n = 236$; B2: $Sr/Ca = 2.60 (\pm 0.32) * Mg/Ca - 0.27 (\pm 0.27)$, $R^2 = 0.24$, $p < 0.0001$, $n = 137$). Considering the large range in slopes and intercepts, this does not seem to be a general phenomenon as is the case for calcite (see Carpenter and Lohmann, 1992). Takesue and van Geen (2004) suggest that in aragonitic bivalve shells, Mg/Ca ratios are dependent on the amount of organic matrix present in the shell, but Sr is incorporated into the crystal and is most likely not associated with the organic matrix

(Walls et al., 1977). Therefore, organic matter cannot cause the correlations between these two elements. Moreover, shell organic matter has been shown to be relatively stable over the year in other bivalves of the Veneroidea family (e.g., 3.5 – 4.0 % in *Spisula subtruncata*; Rueda and Smaal, 2004). Thus the ontogenic decrease in both Sr/Ca and Mg/Ca seen in the Alaskan shell (Fig. 3) is probably not related to shell organic matter. These data suggest that the same biological controls acting on Sr incorporation might also be acting on Mg incorporation to some degree.

Another possibility is that Mg/Ca ratios are related to growth rate, as is the case for Sr/Ca ratios. Indeed a significant relationships between growth rate and Mg/Ca ratios in both Puget Sound shells (Shell B1: $p = 0.012$, B2: $p < 0.0001$) was found, however, unlike Sr/Ca ratios the slopes are significantly different between the two shells ($p < 0.01$; Shell B1: slope = 1.49 ± 1.16, $n = 181$, B2: slope = 7.22 ± 1.81, $n = 118$) and only explain a fraction of the variability (Shell B1: $R^2 = 0.03$; B2: $R^2 = 0.35$). Although this study could not determine the cause of the Mg/Ca variations in these shells, it does not seem that they are recording environmental information, but that biological controls dominate (see also Fig. 1).

3.2.3 Pb/Ca ratios

Ratios of Pb/Ca in biogenic carbonates have been proposed as a proxy of anthropogenic Pb pollution (Shen and Boyle, 1987; Scott, 1990; Lazareth et al., 2000; Yap et al., 2003). In particular, Pitts and Wallace (1994) found a strong linear relationship between dissolved Pb and Pb in shells of the aragonitic clam *Mya arenaria*. Additionally, Pb is preferentially incorporated into aragonite (Fig. 1), with a $D_{Pb} > 1$. Considering the large variability between the Puget Sound shells (Fig. 2D), it seems unlikely that the Pb/Ca ratios in these shells are recording only environmental Pb concentrations. Physiology probably plays a role on Pb incorporation, as was suggested by Vander Putten et al. (2000) for *Mytilus edulis*. In this study, shell B2 is almost consistently exhibiting higher ratios than shell B1, especially between 45 to 60 mm from the umbo (Fig. 2D). Moreover, there is no statistical difference between the means of the Alaskan shell and shell B1, but both are different from B2 (at $p < 0.05$). The Pb/Ca levels in these shells are similar between the two sites, while Puget Sound is expected to have higher environmental Pb concentrations (Paulson and Feely, 1985; USEPA, 1997).

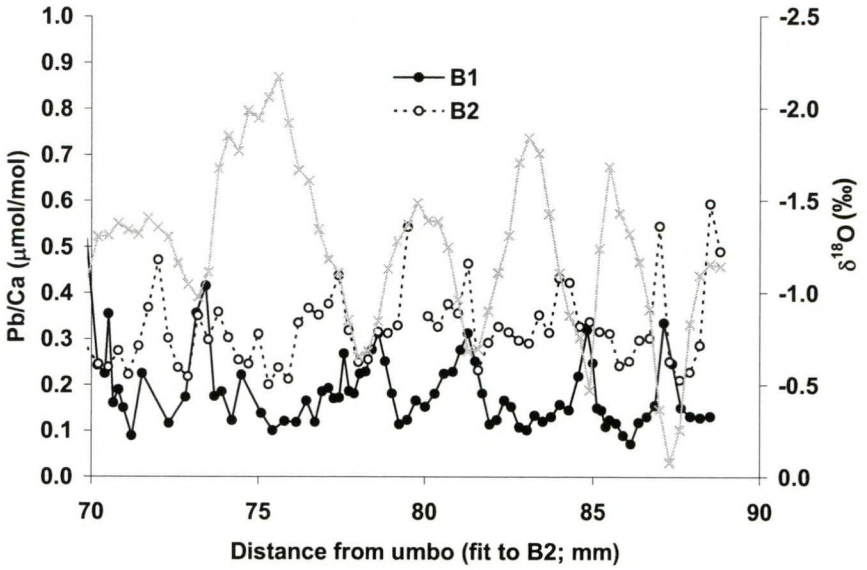

Figure 4. Pb/Ca data from the slow growing region of the Puget Sound (Washington, USA) shells. Data are the same as Figure 2D, but allow a detailed look at the variations in the profile.

Upon a closer inspection of the data (see also Fig. 4) there is a clear pattern in the Pb/Ca signal in shell B1 (Puget Sound), with Pb/Ca peaks occurring every winter. This could be caused by the animal sequestering Pb in its shell to detoxify tissues coupled with reduced winter shell growth, resulting in higher Pb/Ca ratios in the winter. Indeed, many studies have found higher Pb concentrations in bivalve soft tissues during winter (Boalch et al., 1981; Swaileh, 1996). An alternative hypothesis is that there may be higher resuspension of contaminated sediments in the winter or increased Pb inputs during winter, as many studies have found higher water Pb concentrations in winter (e.g., Baeyens, 1998a; Boyle et al., 2005). Nevertheless, this pattern is not found in shell B2, so no conclusions from these data can be drawn. Despite the fact that small temporal and spatial differences in environmental Pb concentrations can probably not be extracted from *S. giganteus* shells, it is not impossible that large scale changes in environmental Pb would be reflected in the shells. The concentrations in these *S. giganteus* shells are generally low, Lazareth et al. (2000) measured ratios as high as 1.2 µmol/mol in a sclerosponge. Therefore, shells that experienced a larger environmental Pb concentration may still be useful

recorders of anthropogenic Pb pollution (Pitts and Wallace, 1994; Richardson et al., 2001; Gillikin et al., in press; Chapter 9).

3.2.4 Ba/Ca ratios

To date, all published records of high resolution Ba profiles in bivalve shells (both aragonite and calcite) have similar characteristics showing a relatively stable background Ba concentration interspaced with sharp episodic Ba peaks (Stecher et al., 1996; Toland et al., 2000; Vander Putten et al., 2000; Lazareth et al., 2003; Gillikin et al., submitted; Chapter 10). Stecher et al. (1996) first proposed that these peaks were the result of the filter feeding bivalves ingesting Ba-rich particles associated with diatom blooms.

The two shells from Puget Sound show a remarkable co-variation, with the Ba/Ca peaks occurring almost exactly at the same time in both shells (Fig. 2C), which strongly suggests an environmental control. Furthermore, this provides an independent proof that the original fitting of the shells, using only $\delta^{18}O$ and the phase demodulation technique of De Ridder et al. (2004), is accurate (see Chapters 4 and 8). To test if there is indeed a relationship between Ba peaks and phytoplankton blooms in *S. giganteus*, the fitting between the $\delta^{18}O$ profile and calendar dates as described in Chapter 4 for the Puget Sound shells were used to match the Ba/Ca data with chlorophyll a (Chl a) data (data from Washington State Dept. of Ecology, http://www.ecy.wa.gov/). From Figure 5 is it evident that there is some coincidence between Chl a and Ba/Ca ratios, but it is not consistent. For example, the large Ba/Ca peak in 1994 actually precedes the Chl a peak. Furthermore, the Ba/Ca peak amplitude does not correspond to the Chl a peak amplitude. On the other hand, it is possible that the clams are selective for certain phytoplankton species that contain higher Ba concentrations, however, the only other pigment data available for this site (pheopigments) did not fit the Ba/Ca data better than Chl a (data not shown). These results suggest that there is not a direct relationship between the two. Additionally, no relationship between Ba/Ca in *Mytilus edulis* shells and Ba ingested as food could be found (Gillikin et al., submitted; Chapter 10). Furthermore, there appears to be an ontogenic effect in the longer lived Alaskan shell (~20 years versus ~10 years for the Puget Sound shells), with a higher background Ba/Ca level towards the umbo (Fig. 3C). Nevertheless, Vander Putten et al. (2000) also found a remarkable coincidence of

the Ba peaks in several mussel shells that grew at the same location, providing further evidence that an environmental parameter controls their occurrence. Remarkably, a similar phenomenon also occurs in corals, with sharp episodic Ba peaks occurring at the same time each year, which are not related to river discharge (Sinclair, in press). Thus, as with corals (Sinclair, in press), there is no suitable hypothesis for these peaks.

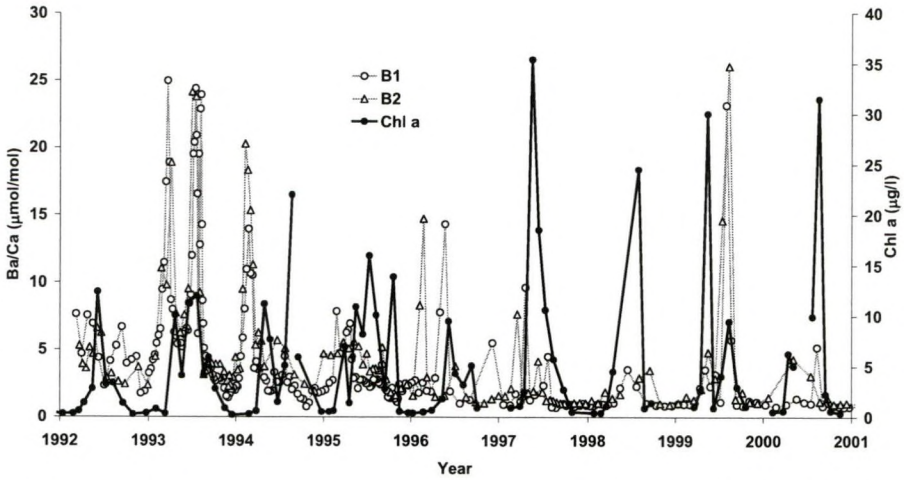

Figure 5. Ba/Ca profiles from the two Puget Sound (Washington, USA) shells and corresponding chlorophyll a data (data from Washington State Dept. of Ecology, http://www.ecy.wa.gov/). The fitting between the $\delta^{18}O$ profile and calander dates, as described in Gillikin et al. (2005a), was used to match the Ba/Ca profiles with chlorophyll a data.

While most research has focused on the Ba-peaks, Gillikin et al., (submitted; Chapter 10) found that the background Ba/Ca level in the shells of another bivalve species (*M. edulis*) could be used as an indicator of Ba/Ca ratios in seawater and hence provide an indication of salinity. Unlike Sr/Ca and Mg/Ca ratios, water Ba/Ca ratios may also alter shell Ba/Ca, as Ba/Ca ratios in the water can change dramatically with salinity (e.g., Gillikin et al., submitted; Chapter 10). According to Figure 1, Ba is the element most likely to faithfully record seawater Ba chemistry. Ratios of Ba/Ca between the two Puget Sound shells are remarkably similar (Fig. 2C). However, in the three *S. giganteus* shells analyzed here, the background Ba/Ca levels are higher near the umbo. Considering that the $\delta^{18}O$ data do not suggest a reduced salinity when the clams were younger (see Chapter 4), this is probably an ontogenic effect.

Unfortunately, this complicates the use of Ba/Ca backgrounds in this species, but does highlight the point that species specific differences in elemental incorporation are important. Nevertheless, despite the ontogenic effect, large temporary salinity changes may still be recorded in the shells. Therefore, this could potentially be a cause of the Ba/Ca peaks in the shells. However, if the relationship between Ba/Ca ratios in water and shells were linear, these peaks would require very large drops in salinity, which did not occur (Gillikin et al., 2005a).

Finally, water temperature is another factor that can affect aragonite Ba/Ca ratios (Zacherl et al., 2003; Dietzel et al., 2004; Elsdon and Gillanders, 2004). However, from comparison with $\delta^{18}O$ and Ba/Ca ratios in these shells it is clear that Ba/Ca ratios do not follow temperature.

3.2.5 U/Ca ratios

Ratios of U/Ca in corals show a negative temperature dependence (Min et al., 1995; Fallon et al., 1999), however, it has been proposed that salinity, alkalinity or variations in uranium speciation in the coral aragonite could also influence the measured U/Ca ratios (Shen and Dunbar, 1995). Although the U/Ca profiles match well between the two Puget Sound shells (Fig. 2E), they are several orders of magnitude lower than in corals (Table 1) and exhibit an opposite relationship with temperature (Fallon et al., 1999; Cardinal et al., 2001), which suggests a biological control on bivalve shell U/Ca ratios (see also Fig. 1). *S. giganteus* shell U/Ca ratios are similar to *M. mercenaria* shells (Kaufman et al., 1996), another aragonitic clam. Interestingly, in the Puget Sound shells, in the first few years of shell growth, U/Ca rises with temperature (inferred from $\delta^{18}O$), but then drops before the temperature maximum.

The regular U/Ca pattern, with its cyclic nature, suggests that early diagenesis is not the cause. If early diagenesis occurred in the older shell section (towards the umbo), which has been exposed to the water the longest, a steady decrease towards the most recent section would be expected. However, the U/Ca ratios near the umbo in the Alaskan shell are twice as high as the Puget Sound shells. This indeed could be the result of early diagenesis, as the shell is older and hence the shell has been exposed to the water for a longer period of time. Clearly there is an ontogenic effect reproducible

in all three shells, but U/Ca does not correlate with growth rate. Additionally, Kaufman et al. (1996) noted a sharp drop in U concentrations from the exterior of the shell to the innermost part in *M. mercenaria*. This could, in part, explain the data presented here. When the shell is young, it is very thin and therefore the juvenile shell section analyzed might have been further towards the exterior of the shell, but again, this does not explain the observed cyclicity.

4. CONCLUSIONS

High resolution Sr/Ca, Mg/Ca Ba/Ca, and U/Ca profiles in two *S. giganteus* shells that grew nearby each other in Puget Sound vary in a similar fashion. Ratios of Pb/Ca were more dissimilar, but were generally low. Despite their similarities, relating the variations in these elemental ratios to environmental parameters is not straightforward. Similarities in the ontogenic decreases in both Sr/Ca and U/Ca from specimens that grew in different environments suggest that similar biological mechanisms may play a role in their incorporation into the shell. Both Mg/Ca and Pb/Ca seem to be influenced by the bivalve's physiology. Profiles of Ba/Ca exhibit sharp episodic peaks, similar to other bivalves, and match extremely well between two shells that grew at the same site, pointing to an environmental control. However, an ontogenic decrease in Ba/Ca was found in the Alaskan shell. Overall, none of the measured elemental ratios could be directly related to environmental parameters. Before bivalve trace element geochemistry can be utilized to obtain accurate environmental information, the extent of biological control on their incorporation must be better understood.

Acknowledgements – I am much indebted to K. Li and S. Mickelson of the King County Department of Natural Resources and Parks, Water and Land Resources Division, Marine Monitoring group (WA, USA) and J. W. Taylor (U. Washington) for collecting the *S. giganteus* shells. I thank A. Van de Maele, M. Korntheuer, and L. Monin for laboratory assistance and H. Ulens who helped with sampling the shells. A. Verheyden and S. Bouillon gave helpful comments on an earlier version of this manuscript and M. Elskens assisted with statistics.

Chapter 8

Can Sr/Ca ratios be used as a temperature proxy in aragonitic bivalves?

Foreword

Ratios of Sr/Ca are one of the most promising paleotemperature proxies in both coral and sclerosponge aragonite. In inorganic calcite, it is well known that precipitation rate is important in Sr incorporation. Studies on bivalve calcite have been inconclusive due to poorly constrained shell growth rate data, but recently Sr/Ca ratios were found to be kinetically controlled in a calcitic bivalve (Lorrain et al., submitted a). However this is not the case for abiogenic aragonite. As briefly illustrated in the previous chapter, Sr/Ca ratios in aragonitic bivalves seem to be growth rate controlled, similar to both abiogenic and biogenic calcite. Here the Sr/Ca data from two aragonitic bivalves are discussed in detail.

Publications of the author related to this chapter:

Gillikin, D. P., A. Lorrain, J. Navez, J. W. Taylor, L. André, E. Keppens, W. Baeyens and F. Dehairs, 2005. Strong biological controls on Sr/Ca ratios in aragonitic marine bivalve shells. *Geochemistry, Geophysics, Geosystems* 6, Q05009, doi: 10.1029/2004GC000874

Lorrain A., D. P. Gillikin, Y.-M. Paulet, L. Chauvaud, J. Navez, A. Le Mercier, L. André, *submitted.* Strong kinetic effects on Sr/Ca ratios in the calcitic bivalve *Pecten maximus*. Submitted to *Geology*

Abstract

It is well known that skeletal remains of carbonate secreting organisms can provide a wealth of information about past environments. Ratios of Sr/Ca have been successfully used as a temperature proxy in corals and sclerosponges. Previous work on aragonitic bivalve shells has not been conclusive, but suggests a major control of growth rate on Sr/Ca ratios. As many studies have used bivalve growth rates to determine temperature, this study tests if Sr/Ca ratios could predict temperature through its relationship with growth rate. Shells from the two species of clams from the same family (Veneroidea) studied here, *Saxidomus giganteus* and *Mercenaria mercenaria*, show vastly different seasonal Sr/Ca profiles. A strong relationship between average annual Sr/Ca ratios and annual growth rate was found in *S. giganteus* shells from both Washington ($R^2 = 0.87$) and Alaska ($R^2 = 0.64$), USA, but not in *M. mercenaria* shells from North Carolina, USA. Furthermore, the Sr/Ca-growth rate relationship was also evident upon a more detailed inspection of sub-annual growth rates in *S. giganteus* ($R^2 = 0.73$). Although there were significant positive correlations between Sr/Ca ratios and temperature (using $\delta^{18}O$ as a relative scale of temperature) in *S. giganteus* shells, the correlations were weak ($0.09 < R^2 < 0.27$) and thus Sr/Ca ratios cannot be used as a reliable temperature proxy in these species of aragonitic bivalves. It is clear from this study that Sr/Ca ratios are not under thermodynamic control in either clam species, since thermodynamics predict a negative correlation between Sr/Ca ratios and temperature in aragonite. This points towards dominance of biological processes in the regulation of Sr^{2+}. This is also reflected by the largely differing Sr/Ca partition coefficients (D_{Sr}) in these shells ($D_{Sr} \approx 0.25$), when compared to inorganic, coral, and sclerosponge studies ($D_{Sr} \approx 1$), all of which show a negative dependence of Sr/Ca on temperature. These data suggest that caution be taken when using Sr/Ca in any biogenic aragonite as a temperature proxy when the D_{Sr} greatly deviates from one, as this indicates the dominance of biological controls on Sr/Ca ratios.

1. INTRODUCTION

Skeletal remains of carbonate secreting organisms potentially offer a wealth of information about past environments. For example, oxygen isotope ratios ($\delta^{18}O$) in biogenic carbonates are a powerful tool for paleotemperature reconstruction. However, interpretation is complicated since the isotopic composition of carbonates is also dependent on the $\delta^{18}O$ of the water, which in itself is related to salinity (see Epstein et al., 1953). This can cause severe problems when attempting to obtain paleo-temperature records from estuarine bivalves (Klein et al., 1996b; Gillikin et al., 2005a; Chapter 4) Alternative sea surface temperature (SST) proxies that are independent of other environmental variables would therefore be of great value.

Ratios of Sr/Ca have been proposed as such a proxy in biogenic aragonite and have been extensively utilized in both corals and sclerosponges with great success (Weber, 1973; Beck et al., 1992; Rosenheim et al., 2004). Ratios of Sr/Ca in inorganic (or abiogenic) aragonite is a function of the Sr/Ca ratio of the solution, expressed as an empirical partition coefficient, $D_{Sr} = (Sr/Ca)_{aragonite} / (Sr/Ca)_{water}$, where Sr/Ca are typically given as molar ratios (Lea and Spero, 1992, 1994). The Sr/Ca ratio of the solution is not of major concern, as for many estuaries the Sr/Ca ratio of the water remains more or less constant above a salinity of about 10 (Dodd and Crisp, 1982), which precludes a large salinity effect for many marine and estuarine species. Inorganic precipitation experiments have shown that D_{Sr} in aragonite is inversely related to temperature (Kinsman and Holland, 1969; Dietzel et al., 2004) and is independent of precipitation rate (Zhong and Mucci, 1989). Mineralogy also significantly affects Sr incorporation, with aragonite typically containing about seven times more Sr than calcite due to the differences in the crystal lattice structure and D_{Sr} being strongly precipitation rate dependent in calcite (Kinsman and Holland, 1969; Tesoriero and Pankow, 1996).

Although many studies have utilized Sr/Ca ratios in corals for paleotemperature reconstruction (Weber, 1973 Beck et al., 1992; McCulloch et al., 1999; and many others), other studies have illustrated some complications with this proxy. For example, significant differences in Sr/Ca - SST relationships between corals growing

at the same site have been reported (de Villiers et al., 1995; Cardinal et al., 2001) and coral Sr/Ca ratios have been found to be inversely related to calcification or growth rate (de Villiers et al., 1995; Ferrier-Pagès et al., 2002; Cohen and McConnaughey, 2003) and to be affected by metabolic processes (Meibom et al., 2003).

Ratios of Sr/Ca in bivalve shells have been less well studied than in corals and there has been much debate over its interpretation. As early as 1956, it was proposed that the Sr/Ca ratio in bivalve shells was dependent on growth rate (Swan, 1956). Later, Dodd (1965) found a large negative correlation between temperature and Sr/Ca ratios in *Mytilus edulis* aragonite. Buchardt and Fritz (1978) found no correlation with either growth rate or temperature and Sr/Ca ratios in a freshwater aragonitic gastropod. Palacios et al. (1996) found that Sr/Ca ratios were more strongly correlated to age than to growth rate in the chondrophores (an internal shell structure located at the hinge) of extinct and extant populations of *Mya arenaria*. They found an increase in Sr/Ca ratios with age in both populations and a decrease with growth rate in the extinct population, but not in the extant population. Based on one shell, Purton et al. (1999) concluded that Sr/Ca ratios were metabolically controlled in aragonitic bivalves, since Sr/Ca ratios increased with decreasing growth rate. However, the results of both Palacios et al. (1996) and Purton et al. (1999) may not be representative because they analyzed the inner layers of the shell, which is known to be repeatedly dissolved and reprecipitated by the animal to buffer internal pH during anaerobic respiration (Crenshaw, 1980) and where biomineralization mechanisms can greatly differ (Wheeler, 1992). Stecher et al. (1996) found that there was a negative correlation between Sr/Ca ratios and $\delta^{18}O$ (therefore positive between Sr/Ca ratios and temperature) in the shell of a modern and a Pleistocene *Mercenaria mercenaria* while there was a positive relationship (negative with temperature) in a *Spisula solidissima* shell, which they attributed to differences in season of maximal growth (i.e., a positive relationship between growth rate and Sr/Ca ratios). Hart and Blusztajn (1998) also found a positive relationship between Sr/Ca ratios and temperature in *Arctica islandica* and applied this relationship to derive SST from hydrothermal vent clams (*Calyptogena magnifica*). Dutton et al. (2002) also found a negative correlation between Sr/Ca ratios and $\delta^{18}O$ in bulk shell samples of the extinct aragonitic bivalve *Cucullaea* sp., however could not find a similar relationship in a shell sampled at high resolution. Finally, Takesue and van Geen (2004) found that Sr/Ca ratios decreased

with decreasing growth rate in the aragonitic shells of *Protothaca staminea*. From this it is clear that there is no consensus on the effect of temperature and/ or growth on aragonitic bivalve Sr/Ca ratios, which therefore may be species specific.

Despite the conflicting reports in the literature, interest in Sr/Ca ratios in bivalve shells as a temperature proxy is still receiving much interest at international congresses (e.g., Tripati et al., 2004; Watanabe et al., 2004; and many others).

Although it seems there is no direct relationship between temperature and Sr/Ca ratios in aragonitic bivalves, but rather a relationship between growth rate and/ or metabolism and Sr/Ca ratios, the latter may still be a useful environmental proxy. In fact, growth rates in bivalves can be dependent on many factors including salinity, temperature and food supply (Lewis and Cerrato, 1997; Witbaard et al., 2003; Strom et al., 2004). In particular there is often a strong correlation between temperature and both shell growth and metabolism (Lewis and Cerrato, 1997; Heilmayer et al., 2004). Indeed, there have been many reports using bivalve shell growth increments to determine SST and other environmental parameters (Schöne et al., 2002; Schöne et al., 2003; Strom et al., 2004). Thus, indirectly, Sr/Ca ratios in bivalve shells may record temperature.

Due to their wide distribution and good preservation, bivalve shells are potentially excellent archives of (paleo)environmental information. Two species that could be particularly suitable for such analyses are *Mercenaria mercenaria* (common along the East coast of North America) and *Saxidomus giganteus* (common along the Northwest coast of North America). These species are well represented in both archaeological and geological deposits (Kvenvolden et al., 1979; Stecher et al., 1996; Hetherington and Reid, 2003) and can live for several decades (Quayle and Bourne, 1972; Peterson, 1986).

To test if Sr/Ca ratios in aragonitic bivalves can indeed provide environmental information, high-resolution sampling techniques are used to measure both $\delta^{18}O$ and Sr/Ca ratios in several specimens of two infaunal clam species from North America, *M. mercenaria* (from North Carolina, USA) and *S. giganteus* (from Washington and Alaska, USA), both belonging to the family Veneroidea. In particular the aim is to

determine whether Sr/Ca ratios are controlled by growth rate and if so, whether growth rate and temperature are coupled tightly enough to allow the use of Sr/Ca ratios as an indirect SST proxy.

2. METHODS

2.1 Sample collection and preparation

Three *Saxidomus giganteus* were collected from Puget Sound, Washington and one from Old Harbor, Kodiak Island, Alaska, USA and nine *Mercenaria mercenaria* were collected from the Cape Lookout region of North Carolina, USA (i.e., Wade Creek, Johnson Creek and Back Sound; full data are listed in Table 1). All specimens were collected alive. Elliot et al. (2003) have shown that *M. mercenaria* precipitate aragonite shells. X-ray diffraction measurements of powdered samples of a *S. giganteus* shell was conducted, which revealed pure aragonite. Sections of the shells were cut with a diamond saw along the axis of maximal growth, rinsed with deionised water, air-dried and mounted on microscopic slides. Carbonate powder was milled from the shell cross-sections using a 300 μm drill bit and Merchantek Micromill (a fixed drill and computer controlled micro positioning device), which allows precise sampling. To avoid shell regions that may have been altered (e.g., the inner layer may have been dissolved and reprecipitated, see introduction, while the outermost layer may have exchanged ions with seawater as they were in direct contact), and to be consistent with other studies, samples were taken from the outer shell layer of *S. giganteus* (which have no middle layer), avoiding the outermost part (see Chapter 2 and 4), and from the middle layer of *M. mercenaria* (see Stecher et al., 1996; Elliot et al., 2003). Various sampling distances were used (150 μm to 1 mm) depending on growth rate (i.e., fewer samples in regions of high growth). High resolution Sr/Ca profiles were obtained using a laser ablation system (see Sample Analysis, section 2.3). As the three *M. mercenaria* sampled at high resolution did not show expected results (see Discussion), six more *M. mercenaria* were sampled at low resolution (annual) using the growth lines on the shells, which are formed annually in late August to late September in this region (Peterson et al., 1985). Annual sampling (low resolution) was carried out by milling lines across the annual growth increment, thus providing average annual Sr/Ca ratios for these six shells.

Table 1. List of samples and environmental data.

Species	Shell name	Location	Sediment	SST range (°C)	Salinity range	Date collected	Clam Age (yr)	Nr. of years sampled
Saxidomus giganteus	B1	Puget Sound, WA	Gravely mud	7 - 17	21 - 30	18 Sept 01	11	10
	B2	Puget Sound, WA	Gravely mud	7 - 17	21 - 30	18 Sept 01	11	10
	B3	Puget Sound, WA	Gravely mud	7 - 17	21 - 30	18 Sept 01	11	5
	OH1	Old Harbor, Kodiak Is., AK	Gravely mud	0 - 13	18 - 32	28 June 03	21	19
Mercenaria mercenaria	MW1	Jarrett Bay, NC	Mud	1 - 35	23 - 37	15 Sept 02	9	4.5
	MW2	Wade Creek, NC	Mud	1 - 35	23 - 37	20 Aug 03	7	7
	MB1	Back Sound, NC	Sandy	2 - 30[1]	28 - 34[1]	23 Aug 03	4.5	4.5
	MB2	Back Sound, NC	Sandy	2 - 30[1]	28 - 34[1]	23 Aug 03	23	‡22
	MB3	Back Sound, NC	Sandy	2 - 30[1]	28 - 34[1]	May 1980	16	‡16
	MB4	Back Sound, NC	Sandy	2 - 30[1]	28 - 34[1]	May 1980	24	‡23
	MJ1	Johnson Cr., NC	Mud	2 - 30[1]	28 - 34[1]	1982	7	‡7
	MJ2	Johnson Cr., NC	Mud	2 - 30[1]	28 - 34[1]	1982	28	‡27
	MJ3	Johnson Cr., NC	Mud	2 - 30[1]	28 - 34[1]	1982	34	‡33

‡ Sampled at an annual resolution; [1]Based on Peterson et al. (1987).

2.2 Environmental data

Both SST and salinity data from Puget Sound, Washington (sampled monthly from Oct. 1997 to Sept. 2001) were provided by the King County Environmental Laboratory. Hourly SST data (Sept. 2002 to Aug. 2004) from Kodiak Island, Alaska, are from the NOAA (http://co-ops.nos.noaa.gov/data_retrieve.shtml?input_code =001000111pan&station=9457292+Kodiak+Island+,+AK) and salinity is from Taylor (2004) and references therein. Hourly SST from Wade Creek, North Carolina, was recorded for one year (Sept. 2002 to Aug. 2003) using a temperature logger (Onset Computer Corporation, StowAway TidbiT), while salinity was measured sporadically over a two year period using a WTW multiline P4 conductivity meter. Data from Back Sound are from Peterson et al. (1987). Although no data were available from Johnson Creek, it probably experiences SST and salinities similar to Back Sound. Average monthly SST data are represented in Figure 1. For all samples, salinity was well above 10 and hence Sr/Ca ratios in the water can be considered more or less constant (Dodd and Crisp, 1982; Klein et al., 1996b). Unfiltered water samples were also collected from both sites.

2.3 Sample analysis

Oxygen and carbon isotope analysis was performed using a ThermoFinnigan Kiel III coupled to a ThermoFinnigan Delta+XL dual inlet isotope ratio mass spectrometer

(IRMS). The samples were calibrated against the NBS-19 standard ($\delta^{18}O$ = -2.20 ‰, $\delta^{13}C$ = +1.95 ‰) and data are reported as ‰ VPDB using the conventional delta notation. The reproducibility (1σ) of the routinely analyzed carbonate standard is better than 0.1 ‰ for both $\delta^{18}O$ and $\delta^{13}C$ (more details can be found in Chapter 2).

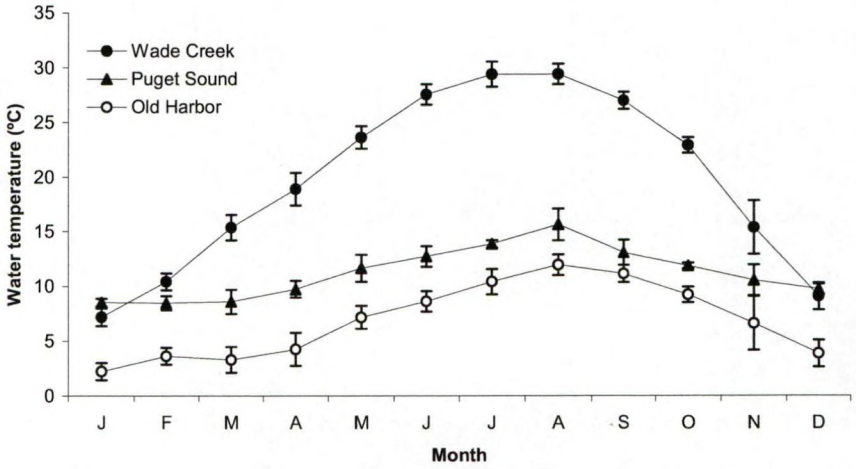

Figure 1. Monthly average SST and standard deviations from the three locations in this study. Data from Puget Sound, Washington are averages of monthly temperature data collected between Oct. 1997 and Sept. 2001. Data from Old Harbor, Kodiak Island, Alaska represent averaged data collected hourly between Sept. 2002 and Aug. 2004. Wade Creek, North Carolina data are averaged hourly temperature data, recorded between Sept. 2002 and Aug. 2003.

High resolution Sr/Ca sampling and analysis of all shells was carried out on a laser-ablation inductively coupled plasma-mass spectrometer (LA-ICP-MS) and data were calibrated using both the NIST 610 (values from Pearce et al. (1997)) and the USGS MACS1 (values from S. Wilson, USGS, unpublished data, 2004). The laser was shot (~50 μm spots) directly in the holes of the isotope sampling allowing direct alignment of Sr/Ca and isotope profiles (cf. Toland et al., 2000). Calibration (including blank subtraction and drift correction) was performed offline following Toland et al. (2000). Reproducibility of Sr/Ca ratios measured by LA-ICP-MS over the entire sampling period (> 1 yr) was better than 0.1 mmol/mol (1σ) based on replicate measurements of shell material. Details of LA-ICP-MS operating conditions can be found in Lazareth et al. (2003). Briefly, the system consists of a Fisons-VG frequency quadrupled Nd-YAG laser (266 nm) coupled to a Fisons-VG PlasmaQuad II+ mass spectrometer. Water samples were analyzed for Sr/Ca ratios on an ICP-OES (see Chapter 2).

Data from LA-ICP-MS were validated with solution nebulization high resolution ICP-MS (SN-HR-ICP-MS; Finnigan MAT Element2). Sampling for SN-HR-ICP-MS analysis was performed by drilling directly beneath the isotope sample, thus removing surface contamination (see section 2.1). Carbonate powders from the high resolution LA-ICP-MS validation and low resolution annual samples (~ 150 µg) were dissolved in a 1 ml 5 % HNO_3 solution containing 1 µg l^{-1} of In and Bi, which were used as internal standards. Reproducibility for Sr/Ca ratios measured with SN-HR-ICP-MS over the entire sampling period was better than 4 % (1σ) based on replicate measurements of two reference materials (CCH1, n=36, Sr/Ca = 0.359 mmol/mol (values from Govindaraju (1994)) and MACS1, n=18, Sr/Ca = 0.255 mmol/mol). Considering the low Sr concentrations in these two standards, an in-house standard produced from a *S. giganteus* shell was also analyzed (approximately 25 mg of milled carbonate was dissolved in 50 ml of 5 % HNO_3, diluting this four times at the time of analysis provided similar concentrations to the samples). The higher concentration of the in-house standard provided better reproducibility (2.6 % (1σ), Sr/Ca = 1.99 ± 0.05, n = 9) and is more indicative of the reproducibility of the samples. There was a significant linear correlation between LA-ICP-MS and SN-HR-ICP-MS results from the B1 shell, with the slope not significantly different from one (slope = 0.99, R^2 = 0.90, $p < 0.0001$, n = 63, intercept not significant (p = 0.62)); note that sample sizes are different, 50 µm for LA vs. 300 µm for micromilling, so this can also include small-scale spatial variability in the sample itself. Therefore, the LA-ICP-MS calibration method can be considered robust. Additionally, this illustrates that the sample size difference between drilling (300 µm; SN-HR-ICP-MS and $\delta^{18}O$ sampling) and LA (50 µm) does not influence the Sr/Ca profiles and thus allows direct comparison of Sr/Ca ratios and $\delta^{18}O$ values.

2.4 Data treatment

To asses the similarity between the Sr/Ca profiles of the three *S. giganteus* shells collected from the same location (Puget Sound), the $\delta^{18}O$ profiles of shell B1 and B3 were fit to shell B2. This was achieved by using a phase demodulation method (see De Ridder et al., 2004). Briefly, this method models the intra-annual variation in growth rate by using Fourier analysis. Once the variation in growth rate of each shell

is known, the time axes (x-axes) can be scaled accordingly and the $\delta^{18}O$ profiles of the three shells can be fit to one scale. Considering that the Sr/Ca analyses were perfectly aligned with $\delta^{18}O$ analyses (see section 2.3), the fitting of the $\delta^{18}O$ profiles now allows a direct comparison of Sr/Ca profiles between the three shells. Similarly, this method was used to fit the $\delta^{18}O$ calculated temperature to the instrumental temperature (see Chapter 4 for full details), which is used here to derive daily growth rates (see section 4.1).

2.5 Terminology

Considering that these results are discussed in the context of calcification processes, the distinction between growth rates and calcification rates should be made. In this study, the term growth rate is defined as the linear extension of the shell per unit time (or growth increment per time). It must be noted that variations in this growth rate may differ from variations in the calcification rate (or crystal growth rate), which can be difficult to estimate (see Lorens (1981) and Carpenter and Lohman (1992) for discussions on this). It is well known that growth rates (i.e., linear shell extension rates) in bivalves decrease through ontogeny (e.g., Peterson, 1986; Schöne et al., 2002), and vary within one year (Peterson et al., 1986; Lorrain et al., 2004a). Since decreasing shell growth rate is usually accompanied by a thickening of the shell, variations in the total $CaCO_3$ precipitated by the animal each year and linear shell growth rate may not necessarily correlate (e.g. Lorrain et al., 2004a). On the other hand, along linear transects, as sampled in this study, we may expect calcification rate and shell growth rates to vary in a similar fashion. Unlike corals, bivalve shell density should not change dramatically along the shell. Therefore, differences in linear growth can result either from constant calcification rates and non continuous growth over the year, or varying calcification rates and continuous growth. Considering that both of these species apparently grow for most of the year (Peterson and Fegley, 1986; Gillikin et al., 2005a; Chapter 4), it seems highly unlikely that calcification rates remain constant.

3. RESULTS

High resolution oxygen isotope profiles obtained from all seven shells sampled at a high resolution show a clear, relatively smooth, annual cyclicity (Figs. 2 and 3). The $\delta^{18}O$ axes in Figures 2 and 3 are inverted in order to reflect a relative temperature scale. More positive $\delta^{18}O$ values correspond to winter temperatures and more negative $\delta^{18}O$ values to summer temperatures. Sharp, episodic drops in the $\delta^{18}O$ profiles, indicative of short-term freshwater discharge extremes, are absent. As reported in Chapter 4, the three *S. giganteus* shells from Puget Sound show remarkably similar $\delta^{18}O$ ($0.77 < R^2 < 0.87$) recording the full range of temperatures at this site (i.e., there was no shell growth shutdown temperature); the average $\delta^{18}O$ from the three Puget Sound specimens are given in Figure 4. The shell from Alaska has more positive $\delta^{18}O$ indicative of the cooler temperatures this clam experienced (Fig. 2D). Growth lines in *S. giganteus* shells were not annual in nature (up to three lines in one year) and were not systematically located in a particular season (data not shown). Values of $\delta^{18}O$ in *M. mercenaria* cover the range of $\delta^{18}O$ measured in the four *S. giganteus* shells (Fig. 3), undoubtedly due to the large range of temperatures at the North Carolina sites (see Table 1 and Fig. 1). The annual growth lines in *M. mercenaria* shells occurred in late summer as has been previously shown for this location (Peterson et al., 1985).

As there is a negligible salinity effect on the $\delta^{18}O$ variability in these *S. giganteus* (Chapter 4) and *M. mercenaria* (Elliot et al., 2003) shells, $\delta^{18}O$ is presumed to be primarily temperature controlled. Using the $\delta^{18}O$ profiles as a relative temperature scale, Sr/Ca profiles also show an annual cyclicity near the umbo in shell B1 and B2 (Fig. 2 and 4). However, in the slow growing parts of the shell (most recently formed), the cyclicity becomes unclear. This is most easily seen in the Sr/Ca profile of shell B3, in which only the slow growing part of the shell was sampled (Fig. 2C; compare x-axes). The annual Sr/Ca cyclicity was not observed in the *S. giganteus* shell collected in Alaska, nor in any of the three *M. mercenaria* shells analyzed at high resolution. Detailed inspection of the profiles shows that there is an annual Sr/Ca cycle for both species only in years when annual growth rates were above about 10 mm yr^{-1}, but this is not always the case (Figs. 2 and 3). There were no distinct changes in the Sr/Ca profiles in the organic rich regions of shell growth lines for either species.

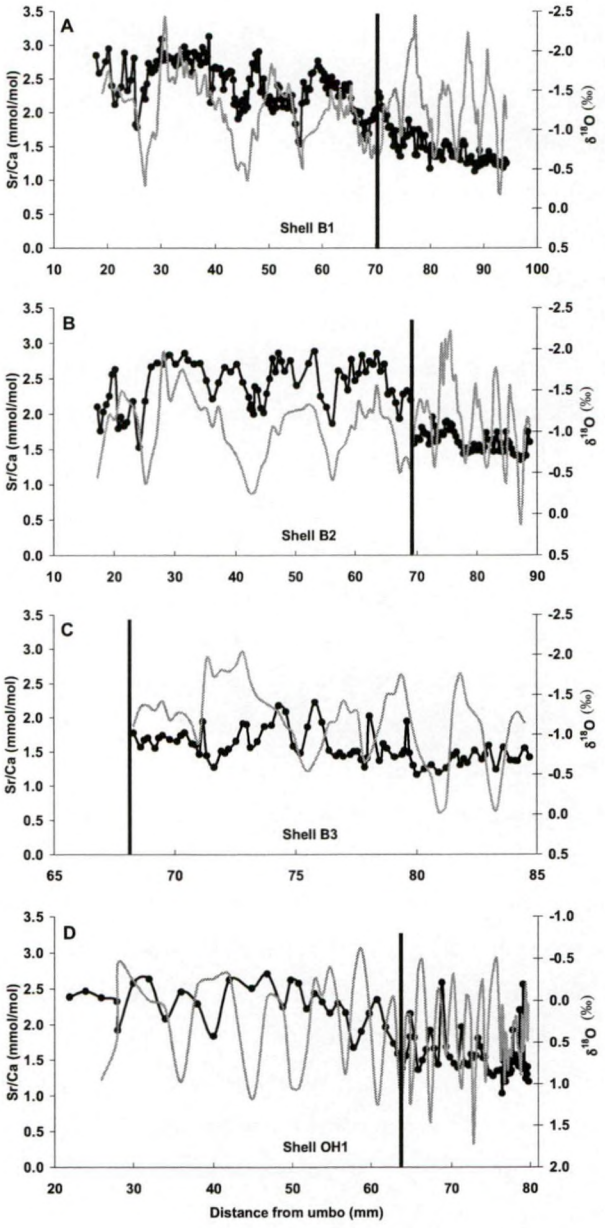

Figure 2. Ratios of Sr/Ca (black lines and circles) and $\delta^{18}O$ (grey lines) from the three *S. giganteus* shells from Puget Sound, Washington (A, B and C) and the specimen from Old Harbor, Kodiak Island, Alaska (D). Note that the $\delta^{18}O$ axes are inverted and x-axes vary. See Table 1 for more details about each site. Vertical lines indicate the separation of slow and fast growth (see Table 2). The resolution of the $\delta^{18}O$ samples is identical to the Sr/Ca samples.

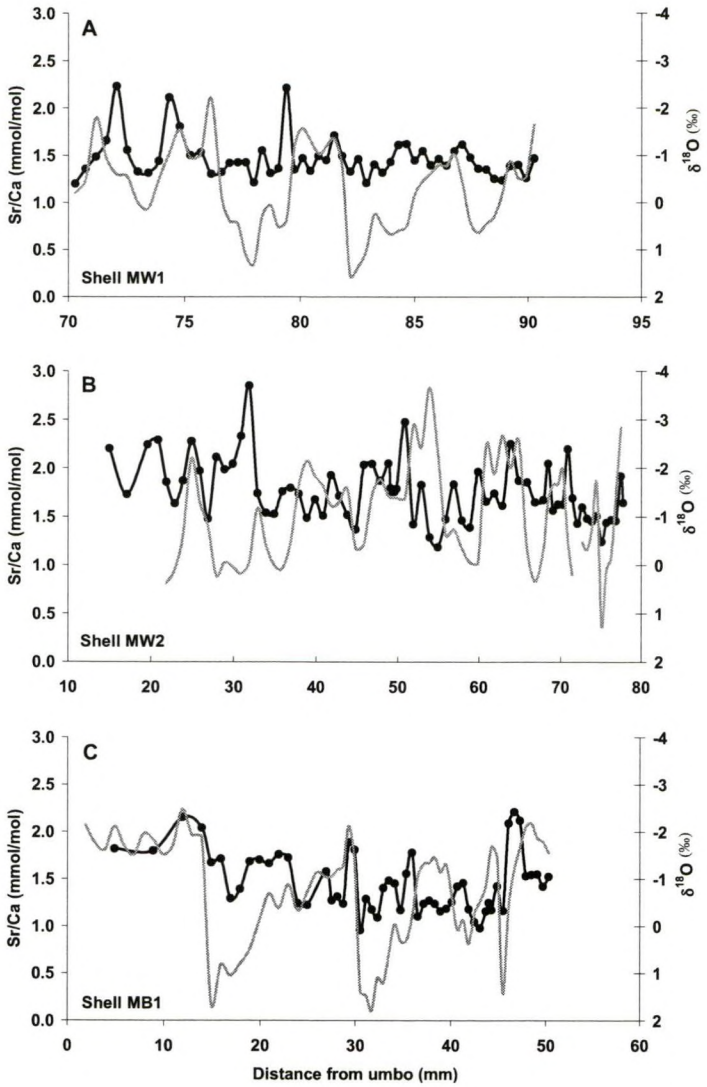

Figure 3. Ratios of Sr/Ca (black lines and circles) and $\delta^{18}O$ (grey lines) from the three *M. mercenaria* shells from North Carolina. Shells MW1 and MW2 (A and B) are from more estuarine sites with muddy sediments, while shell MB1 (C) is from a more marine site with sandy sediments. Note that the $\delta^{18}O$ axes are inverted and x-axes vary. See Table 1 for more details about each site. The resolution of the $\delta^{18}O$ samples is identical to the Sr/Ca samples.

Table 2. Regression data for Sr/Ca ratios and $\delta^{18}O$ in *S. giganteus*. Data are separated between regions of fast and slow growth. The separation between fast and slow growth was chosen based on the $\delta^{18}O$ profile (see Fig. 2).

Shell and growth	Slope	R^2	p <	n
B1 fast	-0.42	0.21	0.0001	120
B1 slow	-0.11	0.09	0.05	62
B2 fast	-0.44	0.22	0.001	56
B2 slow	-0.16	0.27	0.0001	63
B3 slow	-0.09	0.03	n.s.	54
OH1 fast	0.06	0.01	n.s.	31
OH1 slow	0.23	0.13	0.01	52

n.s. = not significant at $\alpha = 0.05$. Shells B1-3: Puget Sound, WA; OH1: Kodiak Island, AK.

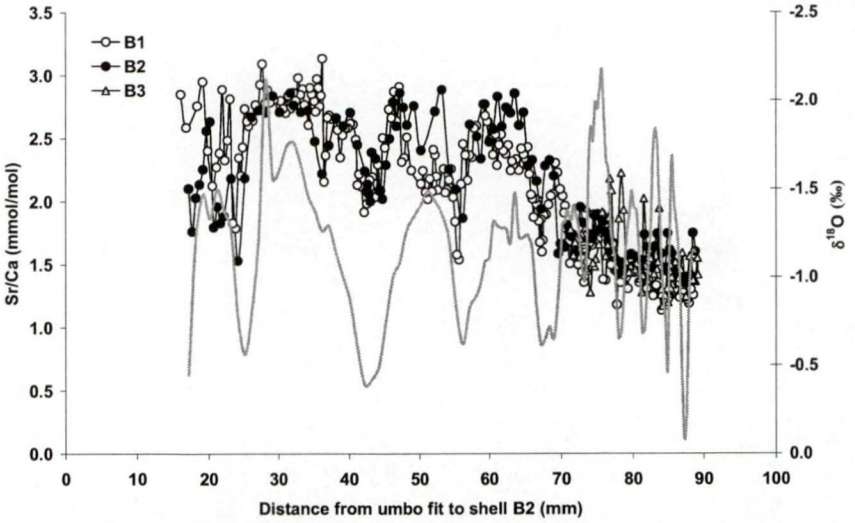

Figure 4. Ratios of Sr/Ca (black lines with symbols) and average $\delta^{18}O$ (grey line) from the three *S. giganteus* shells from Puget Sound, Washington (Fig. 2 A-C). Data were fit to the x-axis of shell B2 using a phase demodulation method (see Methods). Note that the $\delta^{18}O$ axis is inverted.

All *S. giganteus* shells show a clear decrease in Sr/Ca ratios through ontogeny, starting around 2 - 3 mmol/mol, decreasing to 1 – 2 mmol/mol as the clams age (Fig. 2). Figure 4 illustrates the good correlation between Sr/Ca ratios in the shells from Puget Sound (between B1 and B2: $R^2 = 0.73$, slope not different from one, $p < 0.0001$). As the negative relationship between shell and temperature is well known (Epstein et al., 1953), the $\delta^{18}O$ data were used to delimit annual growth for each shell sampled at high resolution. Simply, the shell $\delta^{18}O$ maximum was used as a winter mark and the distance between each of these points was considered as the annual

growth rate. The Sr/Ca data between two successive winter marks were then averaged. Combining the 21 years sampled from the three *S. giganteus* shells from Puget Sound resulted in a significant relationship between Sr/Ca ratios and growth rate ($p < 0.0001$) with $R^2 = 0.87$ (Fig 5A). The partially sampled shell (B3) had a lower R^2 (0.69, n = 4) as compared to the other two shells (B1: $R^2 = 0.88$, n = 8; B2: $R^2 = 0.92$, n = 9), undoubtedly due to the small sample size and reduced growth rate range. The shell from Kodiak Island also shows a significant relationship between these parameters, albeit not as strongly as the Puget Sound specimens ($R^2 = 0.64$, $p < 0.0001$, Fig 5A). As can be seen in the high resolution profiles, *M. mercenaria* shells do not show a significant relationship between growth rate and Sr/Ca ratios ($R^2 = 0.04$, $p = 0.56$, Fig 5B). Likewise, the 128 annual growth increments sampled at an annual resolution from six *M. mercenaria* shells do not show a consistent trend with growth rate (Fig 6). Only two of the six shells were found to have a significant positive relationship between annual growth and average annual Sr/Ca ratios, however, growth rate explained only 30 and 56 % of the Sr/Ca variation in these shells (Table 3).

Table 3. Regression data of Sr/Ca ratios and annual growth rate in *M. mercenaria* sampled at an annual resolution.

Site	Shell	Slope	R^2	p <	n
Back	MB2	0.00	0.00	n.s.	22
Sound	MB3	0.03	0.56	0.001	16
	MB4	0.02	0.13	n.s.	23
Johnson	MJ1	-0.01	0.03	n.s.	7
Creek	MJ2	-0.01	0.06	n.s.	27
	MJ3	0.01	0.30	0.01	33

n.s. = not significant at $\alpha = 0.05$

It is clear that the overall relationship between Sr/Ca ratios and $\delta^{18}O$ is weak in all shells. There are, however, significant correlations between $\delta^{18}O$ and Sr/Ca ratios in *S. giganteus* shells when regions of fast and slow growth are separated (Table 2, see also Fig. 2). Although the correlations are weak (maximum $R^2 = 0.27$), the slopes of the fast and slow growing regions were similar between shells B1 and B2 (Table 2). *M. mercenaria* shells on the other hand do not exhibit this trend. There is no discernable relationship between $\delta^{18}O$ and Sr/Ca ratios, nor was an ontogenic decrease noted (Fig. 3).

Water samples collected from various locations around the North Carolina sites gave a mean Sr/Ca ratio of 8.40 ± 0.09 mmol/mol (n = 56, salinity range = 14 to 33). The Puget Sound samples had a mean Sr/Ca ratio of 8.64 ± 0.19 mmol/mol (n = 4, salinity range = 22 to 28). Both of which are close to the open ocean value of 8.55 ± 0.04 mmol/mol (de Villiers, 1999).

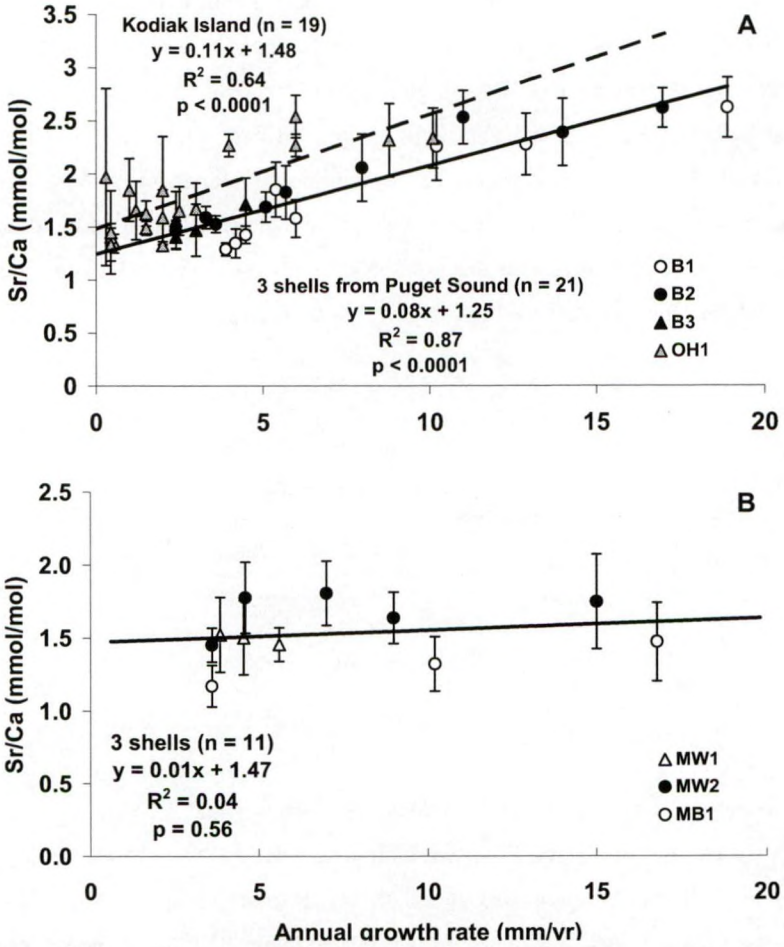

Figure 5. Average annual Sr/Ca ratios versus annual growth rates (from data in Figs. 2 and 3). The three *S. giganteus* shells from Puget Sound, Washington are included in the same regression (solid line) and are compared with the regression of the 19 year old specimen from Kodiak Island Alaska (dashed line) (A). The three *M. mercenaria* shells are included in the same regression (B). Error bars represent standard deviations; n = number of annual growth increments included in each regression

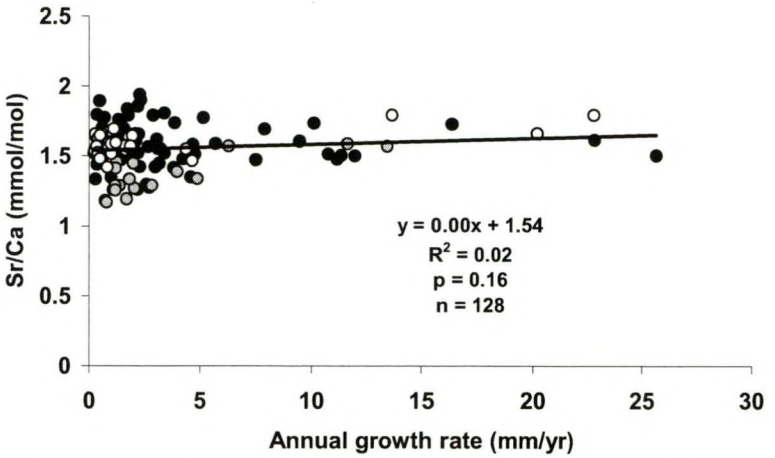

Figure 6. Annual Sr/Ca ratios from the six *M. mercenaria* shells sampled at an annual resolution. Shells MB3 and MJ3, which had significant correlations with growth rate (see Table 3), are represented by the grey and white symbols, respectively. All data are included in the regression; n = number of annual growth increments included in the regression.

4. DISCUSSION

It is becoming increasingly clear that many proposed proxies in biogenic carbonates are complicated by the influence of the physiology of the animal precipitating the carbonate (Klein et al., 1996b; Stecher et al., 1996; Purton et al., 1999; Vander Putten et al., 2000; Zacherl et al., 2003; Lorrain et al., 2004a). However, an animal's physiology is often strongly dependent on the environmental conditions it experiences (see Introduction). For elements to reach the site of calcification, they must first pass through biological membranes which can alter the original seawater chemistry (Wheeler, 1992), possibly in a predictable manner. Although the elemental contents of the external water may influence the elemental contents of the shell to some degree, it is highly unlikely that variations in the external seawater Sr/Ca ratios are responsible for the approximately 50 to 200 % Sr/Ca variations observed in the shells in this study. As previously stated, seawater Sr/Ca ratios should have remained relatively constant in the areas where these bivalves grew. Although some shells experienced low salinities (see Table 1), the $\delta^{18}O$ profiles do not show sharp episodic peaks to more negative values as would be expected if the clams were growing during periods of reduced salinity (Figs. 2 and 3).

4.1 Are Sr/Ca ratios controlled by growth rate?

On an annual scale, using $\delta^{18}O$ maxima as winter markers, annually averaged Sr/Ca ratios are strongly correlated to annual growth rate in *S. giganteus* shells from Puget Sound and to a slightly lesser extent in the *S. giganteus* shell from Alaska (Fig. 5A). However, using annual growth rates does not account for sub-annual variations in growth rate, which is undoubtedly occurring in these shells (Peterson and Fegley, 1986; Elliot et al., 2004). To determine if Sr/Ca ratios are related to growth rate on a sub-annual scale, which would rule out a purely ontogenic effect (see Palacios et al., 1994), sub-annual growth rate data are required. This is possible considering that temperature calculated from $\delta^{18}O$ in the shells of *S. giganteus* from Puget Sound covers the full range of instrumental temperature at this site (see Chapter 4), indicating these shells very likely grew throughout the year. Therefore, calendar dates can be assigned to each sample from these shells with some degree of confidence. This can be done using the method outlined in Klein et al. (1996b), where the calculated temperature (here using the empirical equation of Böhm et al. (2000)) from each sample is fit with the instrumental temperature, for which the calendar dates are known (see section 2.4). Then with the sample distance and the time difference between the samples, a daily growth rate can be calculated. Comparing Sr/Ca ratios and daily growth rates in the three *S. giganteus* shells (B1, B2 and B3) resulted in a significant positive relationship between both factors (Fig. 7; $R^2 = 0.73$, $p < 0.0001$, $n = 350$). The relationship was not as good in the shell where only the slow growing section was sampled (shell B3: $R^2 = 0.31$, $p < 0.0001$, $n = 53$) as compared to the fully sampled shells (shell B1: $R^2 = 0.73$, $p < 0.0001$, $n = 179$; shell B2: $R^2 = 0.70$, $p < 0.0001$, $n = 118$). Thus, even at a more detailed level, growth rate explains much of the variability of Sr/Ca in these *S. giganteus* shells (with the slope and intercept not significantly different from the annual growth rate-Sr/Ca regression). Therefore, the relationship between Sr/Ca ratios and growth rate is not caused by an age effect as was noted by Palacios et al. (1994).

In opposition, Sr/Ca ratios in *M. mercenaria* shells were not significantly correlated to growth rate in seven of the nine shells analyzed (Figs. 5B and 6, Table 3). Two factors may account for the discrepancy between the Sr/Ca patterns in *M. mercenaria* shells in this study as compared to the *M. mercenaria* shells analyzed by Stecher et al.

(1996). First, Stecher et al. (1996) sampled their modern clam from a marine site with sandy sediment (Delaware, USA), which could imply differences in Sr controls between the same species depending on habitat. However, even though the nine clams sampled here are from both estuarine muddy sediments and sandy marine sediments, the data were not comparable to Stecher et al. (1996) for *M. mercenaria*. A second possibility for the difference may be that growth rates in the shells analyzed by Stecher et al. (1996) were generally higher than the growth rates of the *M. mercenaria* analyzed in this study, which could imply that differences in nutrient availability or other site-specific differences could be responsible for the discrepancy. Finally, population genetics may play a role. However, no satisfactory explanation based on our current knowledge of Sr incorporation into bivalve shells could be found.

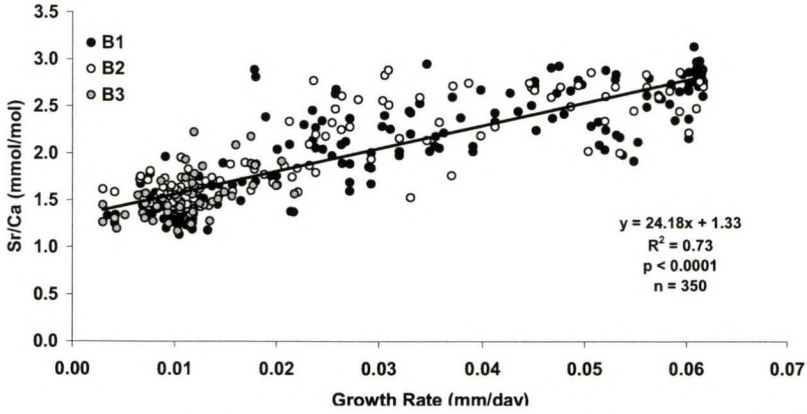

Figure 7. All Sr/Ca data from the three *S. giganteus* shells from Puget Sound, Washington, versus calculated daily growth rate (see text). The same regression calculated with annual growth rates gives: $y = 0.07x + 1.33$, similar to Fig. 5A. All data are included in the regression; n = number of samples included in the regression.

Despite the good correlation between growth and Sr/Ca ratios in *S. giganteus*, the fact that there is no precipitation rate effect in inorganic aragonite (Zhong and Mucci, 1989), and that the *M. mercenaria* shells analyzed in this study do not consistently show a relationship between growth rate and Sr/Ca ratios, implies that Sr/Ca ratios are not under direct control of growth rate. Therefore, there is no general mechanism that can answer the question of whether Sr/Ca ratios are controlled by growth rate.

4.2 Can Sr/Ca ratios be used as a temperature proxy?

The inverse relationship between $\delta^{18}O$ in shells and temperature is well established (Epstein et al., 1953). Elliot et al. (2003) and Gillikin et al. (2005a) have shown that variations of $\delta^{18}O$ in the shells of both species used in this study are largely temperature controlled, with temperature explaining most of the $\delta^{18}O$ variability in the *S. giganteus* shells used in this study ($R^2 = 0.83$, see Gillikin et al., (2005a)). Therefore, if Sr/Ca ratios are under thermodynamic control, there should be a negative relationship between Sr/Ca ratios and temperature, and a positive relationship between Sr/Ca ratios and $\delta^{18}O$. However, positive correlations between $\delta^{18}O$ and Sr/Ca ratios were not found in either species (correlations between Sr/Ca ratios and $\delta^{18}O$ in these shells are negative), aside from a very weak, but significant positive correlation in the *S. giganteus* shell from Kodiak Island ($R^2 = 0.13$, $p < 0.01$, Table 2). This further stresses that Sr/Ca ratios are not under thermodynamic control and that biological effects on Sr incorporation dominate in these bivalves.

If Sr/Ca ratios are correlated with growth rate, and growth rate is correlated with temperature, then Sr/Ca ratios should correlate fairly well with $\delta^{18}O$. However, despite the evidence that Sr/Ca ratios are tightly coupled with growth rate in *S. giganteus* (Fig. 7), and growth rate is often following temperature in bivalves (see introduction), Sr/Ca ratios are not very well correlated with $\delta^{18}O$ ($0.09 < R^2 < 0.27$, see Table 2). Therefore, disappointingly, Sr/Ca ratios cannot be used as a reliable temperature proxy in these bivalves. Although the good correlation between Sr/Ca ratios between the different shells of *S. giganteus* that grew in Puget Sound (Fig. 4) could indicate an environmental control on Sr/Ca ratios, the correlation is probably the result of the clams having similar ages and growth rate being correlated between them.

The discussion above suggests that there is a biological control on Sr/Ca ratios in bivalve shells. Additional evidence for this is given by comparing the D_{Sr} of inorganic, coral, and sclerosponge aragonite with the D_{Sr} of aragonitic bivalves. The D_{Sr} of inorganic, coral, and sclerosponge aragonite is typically around 1 (McCulloch et al., 1999; Dietzel et al., 2004; Rosenheim et al., 2004), while in aragonitic bivalves it is around 0.25 (Palacios et al., 1994; Stecher et al., 1996; Takesue and van Geen,

2004; this study), indicating a strong biological regulation of Sr in aragonitic bivalves. This was also found by Zacherl et al. (2004), who analyzed Sr/Ca in two aragonitic structures of a gastropod. They found that the D_{Sr} of slow growing (~0.8 μm d^{-1}) statoliths was near 1 and Sr/Ca and temperature were inversely correlated, as in corals and inorganic aragonite, whereas the fast growing (~19 μm d^{-1}) protoconch was more similar to bivalves in both D_{Sr} (~0.35) and Sr/Ca-temperature relationship (positive). This again illustrates that when D_{Sr} is far from unity, strong biological controls dominate. Although biogenic aragonites with Sr/Ca ratios far from expected equilibrium values (i.e., D_{Sr} = 1) may still be faithful recorders of the environment, it is stressed that care should be taken when using these carbonates due to the high probability of dominating biological controls on shell Sr/Ca ratios.

4.3 Previous hypotheses on Sr incorporation

Changes in Sr/Ca ratios in fish otoliths have been attributed to the onset of gametogenesis and energy relocation for spawning (Kalish, 1991). However, *S. giganteus* starts to spawn around 3-5 years (3.5-4 cm) (Quayle and Bourne, 1972) and the sharp drop in Sr/Ca ratios noted in these shells occurred around the 6th year (7 cm). Similarly, *M. mercenaria* can become sexually mature at one year (Eversole et al., 1980) and Stecher et al. (1996) found Sr/Ca ratios to drop at around four years of age. So, this is not a plausible explanation for the observed trends.

Lewis and Cerrato (1997) noted increases in shell transparency with increased metabolism in the aragonite shells of *Mya arenaria*, which could imply differences in crystallization. Differences in crystal morphology and alignment could lead to differences in Sr/Ca ratios. For example, Paquette and Reeder (1995) showed that Sr had largely different partition coefficients for different faces in calcite crystals at similar crystal growth rates to these clams (~ 10–40 μm day^{-1}). Differences in element partitioning between crystal faces in aragonite may be even greater due to the lower symmetry of aragonite as compared to calcite (aragonite should have more crystallographically distinct crystal faces; see Allison and Finch (2004)). Although no consistent differences in Sr/Ca ratios were noted in opaque or translucent growth lines in *M. mercenaria* shells in this study, the overall crystal morphology in these clams

may differ and explain some of the results presented here. Unfortunately, no studies have as yet dealt with this issue. It could also be argued that differences in organic matrix in the shell could be partially responsible for the variations in Sr/Ca ratios (cf. Vander Putten et al., 2000). However, almost all the Sr in *M. mercenaria* shells is incorporated into the crystal lattice and is most likely not associated with the organic matrix (Walls et al., 1977), which is probably similar in *S. giganteus* shells. Furthermore, this is supported by the lack of correlation between Sr/Ca profiles and the organic rich growth lines in the shells of both species. Moreover, a preliminary experiment showed that Ca concentrations did not change along a *S. giganteus* shell (within the analytical error of 5 %) (Gillikin, unpublished). This is also supported by other studies that have shown that shell organic matrix only changes up to 0.5 % over the year (Rueda and Smaal, 2004). Thus, the decrease in Sr/Ca ratios in *S. giganteus* shells cannot be due to changing organic matter content.

4.4 What controls Sr/Ca ratios in aragonitic bivalves?

Biomineralization in bivalves takes place in the extrapallial fluid (EPF), a thin film of liquid between the calcifying shell surface and the mantle epithelium (Wheeler, 1992). The central EPF is where the inner shell layer is precipitated, whereas the outer and/ or middle shell layer is precipitated from the marginal EPF. Typically the EPF is isolated from seawater and therefore may have different elemental concentrations than seawater. Direct measurements of the marginal EPF are difficult and there are few reports, if any, of marginal EPF elemental concentrations. There are, however, limited data available on the central or inner EPF elemental concentrations (Crenshaw, 1972; Wada and Fujinuki, 1976). Elements may move into the EPF through the epithelial mantle cells via active (i.e., intracellular transport) or inactive processes (i.e., paracellular (or intercellular) transport through, e.g., 'gap' junctions) (see Crenshaw, 1980; Wheeler, 1992; Klein et al., 1996b). In the marginal mantle epithelium (where the shell areas analyzed here are formed) it is believed that active processes dominate (Crenshaw, 1980).

Two enzymes which have been determined to be of great importance in calcification are Ca^{2+}-ATPase and carbonic anhydrase (CA). The enzyme Ca^{2+}-ATPase pumps Ca^{2+} to the EPF while removing $2H^{+}$, and CA catalyses the reaction of bicarbonate to

CO_2, which can then easily diffuse through membranes (Crenshaw, 1980; Cohen and McConnaughey, 2003). The link between CA activity and calcification rate is slightly ambiguous. For example, in the scallop *Pecten maximus*, CA activity is more closely linked with tissue growth than shell growth and is mainly involved in respiration, acid-base regulation and ionic transport (Duvail et al., 1998). Furthermore, CA activity does not change seasonally (Duvail et al., 1998) although shell growth rate certainly does (Lorrain et al., 2004a). However, Cohen and McConnaughey (2003) state that CA is important in counteracting CO_2 depletion, ensuring an abundant supply of CO_2 for calcification. The enzyme Ca^{2+}-ATPase not only supplies Ca^{2+} to the site of calcification, but helps concentrate CO_3^{2-} at the calcification site by pumping protons away (Cohen and McConnaughey, 2003). It is therefore logical that when Ca^{2+}-ATPase activity increases, so do calcification rates (and presumably shell growth or extension rates increase as well). Ferrier-Pagès et al. (2002) found that both Ca and Sr in corals were inhibited by a calcium channel blocker, illustrating that both elements can use similar pathways. However, the enzyme Ca^{2+}-ATPase does have a higher affinity for Ca^{2+} (Yu and Inesi, 1995). Therefore, increased Ca^{2+}-ATPase activity increases calcification rate and decreases Sr/Ca ratios by increasing Ca^{2+} disproportional to Sr^{2+}, so Sr/Ca ratios and growth rates should be inversely correlated. This inverse correlation is observed in corals (de Villiers et al., 1995; Ferrier- Pagès et al., 2002), but *S. giganteus* displays the opposite (Fig. 7).

In the calcite shell of *Mytilus trossulus*, Klein et al. (1996b) found higher Sr/Ca ratios in a younger faster growing mussel as compared to an older slow growing mussel, thus indicating a positive relationship between Sr/Ca ratios and growth rate, which they attributed to metabolic effects. They proposed a model where Sr^{2+} enters the EPF via paracellular transport and is excluded from intracellular transport. Therefore, when metabolic pumping through intracellular pathways is high, the Ca^{2+} concentration in the EPF will increase disproportional to Sr^{2+}, resulting in a lower Sr/Ca ratio in the EPF and subsequently in the shell; which is similar to the Ca^{2+}-ATPase discussion above. They then explain the positive relationship between Sr/Ca ratios and growth rate in their shells using the work of Rosenberg and Hughes (1991), which states that growth rate is inversely proportional to mantle metabolic efficiency (measured as glucose consumption). However, in light of the above discussion, this contradicts the logical notion that increased metabolic pumping (which implies

increased Ca^{2+}-ATPase activity) would increase growth rates and not decrease them. Moreover, in the model of Klein et al. (1996b), increased metabolic pumping should both decrease Sr/Ca ratios and lead to more negative $\delta^{13}C$ of the EPF and shell (by addition of ^{12}C enriched metabolic CO_2). Nevertheless, in spite of a threefold Sr/Ca decrease in *S. giganteus* shells (Fig 5A), there was no decrease in $\delta^{13}C$ (data not shown, see Chapter 4), whereas $\delta^{13}C$ strongly decreased through ontogeny in *M. mercenaria* shells (up to 4 ‰ in one shell, see Meng (2004) and Chapter 5), but Sr/Ca ratios did not (Fig. 5B). Thus a mechanism other than metabolic pumping must control Sr/Ca ratios in bivalve aragonite.

Contrary to the Ca^{2+}-ATPase discussion above, Wada and Fujinuki (1976) found that Sr/Ca ratios in the central EPF of two aragonitic bivalves was higher in summer than in winter and that elemental concentrations were slightly more concentrated during periods of rapid shell growth (summer) and slightly diluted during periods of slow or no shell growth (winter) as compared to the ambient seawater. Although the central EPF is not relevant for this study, this illustrates a biological accumulation of Sr^{2+} in the central EPF during periods of high growth. If this were also the case for the marginal EPF, this could help explain the results from *S. giganteus* shells and other works who found a positive effect of growth rate on aragonitic bivalve shell Sr/Ca ratios (Stecher et al., 1996; Takesue and van Geen, 2004). However, the Sr/Ca ratios of the EPF measured by Wada and Fujinuki (1976) did not differ from that of seawater enough to produce aragonite with such low Sr/Ca ratio, which has more recently been confirmed for another aragonitic bivalve (Lorrain et al., 2004b). This implies that Sr^{2+} discrimination in aragonitic bivalve shells occurs during shell crystallization, at the crystal surface, and not at biological membranes. Indeed, there is strong evidence that there are biological controls on crystal formation (e.g., Falini et al., 1996), which could possibly also regulate Sr/Ca ratios in the shell.

5. CONCLUSIONS

It is clear from this study that Sr/Ca ratios are not under thermodynamic control and that biological processes dominate. Growth rate explained much of the variability in *S. giganteus* shells, but there was no discernable pattern in the Sr/Ca profiles of *M.*

mercenaria shells. However, Stecher et al. (1996) found a seasonal periodicity in *M. mercenaria* shell Sr/Ca ratios from Delaware Bay which was related to growth rate. Thus either Sr^{2+} is governed by another factor, occasionally correlated to growth rate, or Sr^{2+} incorporation biology is site specific. Although there were significant positive correlations between Sr/Ca ratios and temperature ($0.09 < R^2 < 0.27$; using $\delta^{18}O$ as a relative scale of temperature) in *S. giganteus* shells, the correlations were weak and therefore Sr/Ca ratios cannot be used as a reliable temperature proxy in these species of aragonitic bivalves. The strong biological regulation of Sr/Ca ratios can be seen from the deviation of D_{Sr} in these shells ($D_{Sr} \approx 0.25$) from expected equilibrium values (i.e., $D_{Sr} \approx 1$). Inorganic, coral, and sclerosponge aragonite all show a negative dependence of Sr/Ca ratios on temperature, the opposite of what is typically found in bivalves. Considering this strong biological regulation on Sr/Ca ratios, it also seems unlikely that these shells would record changes in seawater Sr/Ca ratios. It is suggested that caution be taken when using Sr/Ca ratios in any biogenic aragonite as a temperature proxy when the D_{Sr} greatly deviates from one, as this indicates the dominance of biological controls on Sr/Ca ratios.

Although this study could not determine what controls Sr/Ca ratios in these aragonitic bivalves, possible hypotheses have been discredited and new hypotheses have been proposed. If a mechanistic understanding is to be achieved, future research needs to focus on the biochemistry of the elemental pathway through the organs, body fluids, and incorporation into the shell.

Acknowledgements – I am much indebted to K. Li and S. Mickelson of the King County Department of Natural Resources and Parks, Water and Land Resources Division, Marine Monitoring group (WA, USA) for collecting the *S. giganteus* shells and providing water data. W.C. Gillikin and L. Daniels both assisted with sample collection in N.C. C.H. Peterson (University of North Carolina, Chapel Hill) kindly provided *M. mercenaria* collected in the early 1980's. L. Meng, T. Haifeng, and H. Ulens assisted in sampling the shells. I thank A. Van de Maele, M. Korntheuer, and L. Monin for laboratory assistance. A. Verheyden, S. Bouillon, R. K. Takesue, an anonymous reviewer and L. D. Labeyrie (editor G^3) gave helpful comments on an earlier version of this manuscript, and F. De Ridder assisted with the phase demodulation technique.

Chapter 9

Are aragonitic bivalve shells useful archives of anthropogenic Pb pollution?

Foreword

In Chapter 7 it was shown that intra-annual Pb/Ca ratios in an aragonitic clam were highly variable and probably did not only reflect environmental Pb. Here the shells of another species are investigated, both intra-annually and inter-annually, covering the period of 1949 to 2002.

Publication of the author related to this chapter:

Gillikin, D.P., F. Dehairs, W. Baeyens, J. Navez, A. Lorrain and L. André, *In press*. Inter- and intra-annual variations of Pb/Ca ratios in clam shells (*Mercenaria mercenaria*): a record of anthropogenic lead pollution? *Marine Pollution Bulletin*

Abstract

In this study, the use of bivalve shells as a proxy of lead pollution is re-assessed. Previous studies have stressed that shells display little variability compared to soft tissues and thus are better for pollution biomonitoring. However, in this chapter it is illustrated that there is large inter- and intra-annual Pb variability between shells of the clam *Mercenaria mercenaria* collected in North Carolina, USA. Therefore, year to year, as well as intra-annual variations in Pb/Ca ratios should be interpreted with caution. Despite this variability, an annual Pb chronology from 1949 to 2002 was obtained using 11 shells collected at different times which clearly exhibited the late 1970's peak in Pb from leaded gasoline use. This indicates that when enough specimens are pooled together, bivalve shells can be used for long term Pb records. The data from this study compare well with other studies of aragonite clams from unpolluted sites. From this it is concluded that the Cape Lookout region of North Carolina has not received extensive pollution over the 1949-2002 period. The 1949-1976 period was not significantly different from the 1982-2002 period, although other proxies suggest that it should be considerably higher. Therefore, the data presented here suggest that there is still a modern source of Pb in the coastal North Carolina environment.

1. INTRODUCTION

Coastal and estuarine environments are important natural resources supporting recreational activities and commercial fishing as well as providing a host of ecological services. The pollution of these regions can have serious adverse effects and thus has been closely monitored in the past several decades. For example, the Mussel Watch program, where soft tissues of bivalves have been used to monitor pollution in the coastal zone (Goldberg, 1975; Claisse, 1989) has been monumental. Nevertheless, pre-1970 data are scarce (Cantillo, 1998) and data are limited to certain estuaries. For example, there are currently only seven Mussel Watch sites along the entire North Carolina (USA) coast (Lauenstein et al., 2002). However, there are other substrates that can retrospectively extend the record back through time and into other locations such as sediments (Chow and Patterson, 1962; Chillrud et al., 2003; Kim et al., 2004), tree rings (Kardell and Larsson, 1978; Baes and McLaughlin, 1984; Watmough et al., 1999) and biogenic carbonates (Shen and Boyle, 1987; Pitts and Wallace, 1994; Lazareth et al., 2000).

Each substrate has its advantages and drawbacks. For example, sediments may be bioturbated and often provide low resolution profiles (Benninger et al., 1979; Sharma et al., 1987; Cooper et al., 2004). On the other hand, biogenic carbonates can provide high resolution profiles and once incorporated, the proxy remains more or less stable as long as diagenetic processes do not occur. However, biology of the animal may affect the record (Vander Putten et al., 2000). Both corals and sclerosponges have been shown to accurately trace anthropogenic Pb inputs in tropical and subtropical waters (Shen and Boyle, 1987; Lazareth et al., 2000; Swart et al., 2002a; Ramos and Ohde, 2004), but long term chronologies (> 50 years) based on bivalve shells have not been attempted.

Similar to sclerosponges, bivalve carbonate may be a superior recorder of Pb because bivalves accumulate higher Pb concentrations in their skeletons. Sclerosponge skeletons contain 10 to 35 times more Pb than corals (based on the 1970's Pb peak; Shen and Boyle, 1987; Lazareth et al., 2000; Swart et al., 2002a). Bivalve shell Pb/Ca ratios from polluted sites have been reported to be higher than 7 μmol/mol (Price and

Pearce, 1997), whereas corals from polluted sites can have Pb/Ca ratios up to 0.23 μmol/mol (Fallon et al., 2002).

There have been many studies on trace metal concentrations in bivalve shells. However, many of these studies did not include Pb due to its low levels (Szefer et al., 2002; Nicholson and Szefer, 2003; Cravo et al., 2004). Of the studies that did measure Pb, many analyzed whole shells (Koide et al., 1982; Yap et al., 2003), thus averaging several years of shell growth and including the outer layer of the shell which may exchange with the external medium. Other studies that separated the most recently formed shell material have shown that shell Pb concentrations are linearly related to both tissue and particulate Pb concentrations (Bourgoin, 1990), and dissolved Pb concentrations (Pitts and Wallace, 1994). However, Bourgoin (1990) analyzed the inner nacreous shell layer and Pitts and Wallace (1994) analyzed the last formed section of the shell. This could affect the Pb levels they measured because Pb concentrations were found to vary by a factor of more than 10 between inner and outer shell layers (Fuge et al., 1993; Raith et al., 1996). Richardson et al. (2001) analyzed Pb concentrations in *Modiolus modiolus* shells from a polluted and non-polluted site covering 10 years of growth. They observed elevated levels in shells from the polluted site, as well as a decrease of concentrations through time, which they attributed to the decline in pollution at the polluted site. However, they could not deconvolve age and time, and age has been shown to influence Pb concentrations in some mollusks (Hirao et al., 1994).

In order to test if indeed bivalve shells can provide a long term record of anthropogenic Pb pollution, Pb/Ca ratios in several *Mercenaria mercenaria* shells from North Carolina, USA, were analyzed in order to construct a chronology from 1949 to 2002 with an annual resolution. As no data are available on Pb concentrations in the environment, the profile is compared with an expected profile based on data from a Caribbean sclerosponge, a coral from Florida and US Pb emissions. Furthermore, high resolution sub-annual Pb/Ca profiles were analyzed to asses the intra-annual variability. Finally, a fossil Pliocene shell was analyzed with the aim of obtaining pristine background Pb/Ca ratios.

2. MATERIALS AND METHODS

2.1 Expected Pb curve

The expected Pb curve presented in Figure 1 was constructed using data from a sclerosponge (*Ceratoporella nicholsoni*) from the Bahamas (Lazareth et al., 2000), a scleractinian coral (*Montastrea annularis*) from the Florida Keys (Shen and Boyle, 1987), and total national US Pb emissions (EPA, 2000). The difference in the Pb maxima (i.e., US Pb emissions: 1972, coral: 1977, and sclerosponge: 1979) is likely due to the reservoir effect of the ocean (see Shen and Boyle, 1987). The decrease observed in the Pb emission caused by the use of unleaded gasoline should thus be delayed by approximately 5 – 7 years. Therefore, like the coral and sclerosponge, the clams in this study are expected to show a peak around 1977 – 1979. The Pb emissions start to level off at around 3 % of the 1970 values in 1986, so the shells are expected to show a leveling off around the years 1991 – 1993.

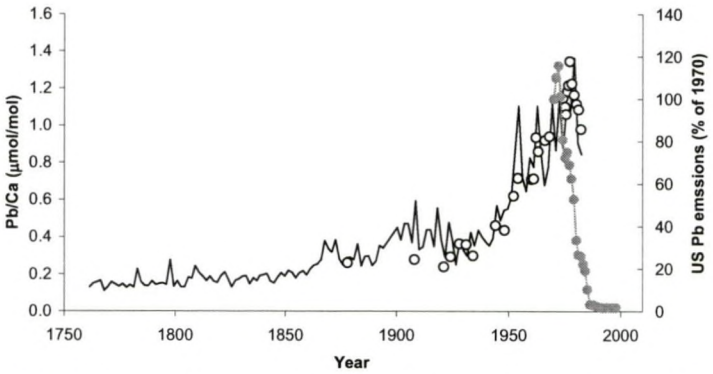

Figure 1. Expected lead curve based on data from a sclerosponge (solid line, Lazareth et al., 2000), coral (open circles, data multiplied by 30, Shen and Boyle, 1987) and US Pb emissions (grey line and circles, EPA, 2000)

2.2 Sample collection, preparation and analysis

Living *M. mercenaria* were collected from the Cape Lookout region of North Carolina, USA at about 1 meter water depth (Fig. 2; full data are listed in Table 1, more data on environmental conditions can be found in Peterson et al., 1985;

Peterson, 1986, 2002; Gillikin et al., 2005b). The Pliocene (~3.2 million years old) shell was collected from the Duplin formation in South Carolina (1.5 km northwest of Timmonsville). Elliot et al. (2003) have shown that *M. mercenaria* precipitate aragonite shells. Sections of the shells were cut with a diamond saw along the axis of maximal growth, rinsed with deionised water, air-dried and mounted on microscopic slides. To avoid shell regions that may have been altered (e.g., the inner layer may have been dissolved and re-precipitated, while the outermost layer may have exchanged ions with seawater as they were in direct contact), samples were taken from the middle layer of the shell (see Elliot et al., 2003).

Table 1. List of samples and environmental data.

Shell name	Site	Sediment Type[2]	SST range (°C)	Salinity range	Date collected	Clam Age (yr)	Years sampled
MW1	Wade Creek	Mud	1 - 35	23 - 37	15 Sept 02	9	‡ 99-01
MW2	Wade Creek	Mud	1 - 35	23 - 37	20 Aug 03	7	‡ 98-02
MW3	Wade Creek	Mud	1 - 35	28 - 37	15 Sept 02	7	00-01
MW4	Wade Creek	Mud	1 - 35	28 - 37	15 Sept 02	20	84-02
MB1	Back Sound	Sandy	2 - 30[1]	28 - 34[1]	23 Aug 03	4.5	‡ 00-02
MB2	Back Sound	Sandy	2 - 30[1]	28 - 34[1]	23 Aug 03	23	81-02
MB3	Back Sound	Sandy	2 - 30[1]	28 - 34[1]	May 1980	16	64-79
MB4	Back Sound	Sandy	2 - 30[1]	28 - 34[1]	May 1980	24	58-79
MJ1	Johnson Cr.	Mud	2 - 30[1]	28 - 34[1]	1982	7	76-82
MJ2	Johnson Cr.	Mud	2 - 30[1]	28 - 34[1]	1982	28	55-80
MJ3	Johnson Cr.	Mud	2 - 30[1]	28 - 34[1]	1982	34	49-81
P1	Duplin Form., SC	N/A	N/A	N/A	N/A	~12	‡ 9 yrs

‡ Sampled at high resolution; N/A = unknown; [1]Based on Peterson et al. (1987); [2]estimated.

For annual Pb/Ca ratios, carbonate powder was milled from the shell cross-sections using a 300 μm drill bit and Merchantek Micromill (a fixed drill and computer controlled micro positioning device), using the growth lines as year markers that are formed annually in late August to late September in this region (Peterson et al., 1985). Before the sample was taken, 100 μm of the surface was milled and vacuumed off to remove surface contamination. The sample was then milled from the same groove. Sample depth varied with growth rate in order to produce approximately 300 – 400 μg of carbonate powder. Samples were transferred to 2 ml acid washed polystyrene containers and capped. At the time of analysis, samples were dissolved in 1 ml 5 % bi-distilled HNO_3 containing 1 μg l^{-1} of In and Bi, which were used as internal standards. Due to the small sample sizes, acid digestion was rapid. Multi-element calibration standards were prepared from certified single element stock solutions. The

isotope ^{208}Pb was analyzed in low resolution and ^{43}Ca in medium resolution on a high resolution - inductively coupled plasma - mass spectrometer (HR-ICP-MS; Finnigan MAT Element2). Two reference materials were run with the samples MACS1, a synthetic carbonate standard developed by the USGS, and an in-house shell standard. The in-house standard was produced from an aragonitic bivalve shell (*Saxidomus giganteus*). Reproducibility over the entire sampling period, as determined from the in-house shell standard, was 9.8 % relative standard deviation (%RSD; Pb/Ca = 0.36 ± 0.04 µmol/mol, n = 9) and MACS1 was within 4 % of the recommended value (n = 18) (values from S. Wilson, USGS, unpublished data, 2004). The detection limit (3 σ) was approximately 0.0011 µmol/mol, which is similar to other studies using an equivalent instrument (e.g., Barbante et al., 1999).

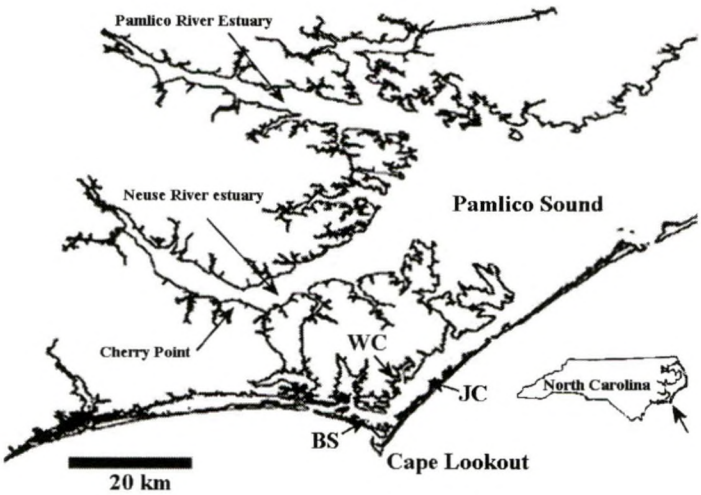

Figure 2. Shell collection sites in eastern North Carolina, near Cape Lookout (BS: Back Sound, JC: Johnson Creek, WC: Wade Creek).

The Pliocene and three modern shells were also measured at high resolution to trace intra-annual Pb/Ca variations. High resolution Pb/Ca profiles were obtained using a laser ablation system (LA-ICP-MS). Data were calibrated using both the NIST 610 (values from Pearce et al., 1997) and the USGS MACS1. The laser was shot (~50 µm spots) directly in the holes of the isotope sampling (see further) allowing direct alignment of Pb/Ca and isotope profiles (cf. Toland et al., 2000). Signal intensities of ^{26}Mg, ^{43}Ca, ^{55}Mn, ^{86}Sr, ^{138}Ba, ^{208}Pb, and ^{238}U were recorded. Calibration (including

blank subtraction and drift correction) was performed offline, following Toland et al. (2000). Reproducibility of Pb/Ca ratios measured by LA-ICP-MS was 6.8 % (%RSD) based on replicate measurements of MACS1 (n = 25) [note that %RSD is lower than the HR-ICP-MS because of the high Pb/Ca ratio in this standard (59.6 μmol/mol versus 0.36 μmol/mol in the HR-ICP-MS standard)]. Details of LA-ICP-MS operating conditions can be found in Lazareth et al. (2003). Briefly, the system consists of a Fisons-VG frequency quadrupled Nd-YAG laser (λ = 266 nm) coupled to a Fisons-VG PlasmaQuad II+ mass spectrometer. The detection limit (3 σ) was approximately 0.01 μmol/mol. All data are given as means ± standard error unless otherwise noted.

For shells sampled at high resolution, oxygen isotopes ($\delta^{18}O$) were also measured to provide a relative temperature scale, and from this, an intra-annual time scale (see Elliot et al. (2003) for discussion on $\delta^{18}O$ in *M. mercenaria* shells and temperature). Carbonate powders were milled from the shell in a similar manner as for HR-ICP-MS sampling (except for removal of the surface), producing ~ 100 μg of sample. Samples were reacted in a ThermoFinnigan Kiel III coupled to a ThermoFinnigan Delta+XL dual inlet isotope ratio mass spectrometer (IRMS). The samples were calibrated against the NBS-19 standard ($\delta^{18}O$ = -2.20 ‰) and data are reported as ‰ VSMOW using the conventional delta notation. The reproducibility (1σ) of the routinely analyzed carbonate standard was better than 0.1 ‰ (more details can be found in Gillikin et al. (2005a) or Chapter 2).

3. RESULTS

3.1 Diagenic indicators in the fossil shell

The $\delta^{18}O$ values of the Pliocene shell are within the values obtained from the modern shells (Fig. 3) indicating minimal recrystallization, if any (c.f., Labonne and Hillaire-Marcel, 2000). Generally, during diagenesis, a number of other chemical changes occur and these changes can be used to identify altered carbonates. High trace element contents of Mn, U, and Fe usually indicate some degree of diagenetic alteration, especially if they are accompanied by low Sr and Mg contents (Brand and Veizer, 1980; Kaufman et al., 1996). Table 2 clearly illustrates that Mn, U and Fe are elevated

and Mg is low in the Pliocene shell, however, Sr is high. Higher Sr (and lower Mg) in non-recrystallized, diagenically altered *M. mercenaria* shells was also found by Walls et al. (1977). Therefore, there has undoubtedly been some diagenetic alteration on this shell, and thus the Pb/Ca data from this shell is probably not a true indication of pristine conditions.

Table 2. Comparison of elemental ratios (mean ± standard deviation) between Pliocene (n = 82) and modern shell (n = 43) and results of t-tests.

Ratio	Modern	Pliocene	p
Mg/Ca (mmol/mol)	0.41 ± 0.13	0.23 ± 0.06	<0.001
Mn/Ca (μmol/mol)	0.51 ± 0.43	3.73 ± 2.57	<0.001
Fe/Ca (mmol/mol)	0.04 ± 0.02	0.22 ± 0.14	<0.001
Sr/Ca (mmol/mol)	1.56 ± 0.16	2.26 ± 0.39	<0.001
Ba/Ca (μmol/mol)	6.87 ± 5.04	34.96 ± 19.98	<0.001
Pb/Ca (μmol/mol)	0.10 ± 0.06	0.12 ± 0.05	0.073
U/Ca (μmol/mol)	0.01 ± 0.02	0.08 ± 0.04	<0.001

3.2 High resolution Pb/Ca profiles

There were large variations in Pb/Ca ratios throughout the year in these shells, ranging from < 0.01 to 0.52 umol/mol (Fig. 3). There are no clear ontogenic trends in the data, nor consistent seasonal trends. There was a significant correlation between $\delta^{18}O$ and Pb/Ca ratios in shell MW1 ($R = 0.58$, $p < 0.0001$, $n = 52$), but not in the other shells. Data from the Pliocene shell are higher or similar to the modern shells further indicating altered Pb/Ca ratios in this shell. Coefficient of variation (standard deviation / mean * 100) values ranged from 36.9 to 111.6 % (shell MW1 = 36.9 %, MW2 = 53.6 %, MB1 = 111.6 %, P1 = 38.8 %). Counting the number of points within one year, the resolution corresponds to approximate monthly for most shells.

3.3 Annual Pb/Ca profile: 1949 - 2002

Seven data were below the detection limit (5.7 % of all samples) and were removed from the dataset. From Figure 4 it is clear that there is a large variation between shells. However, averaging all data from the time periods 1949-1976, 1977-1981, and 1982-2002 results in significantly different means. The 1977-1981 period has

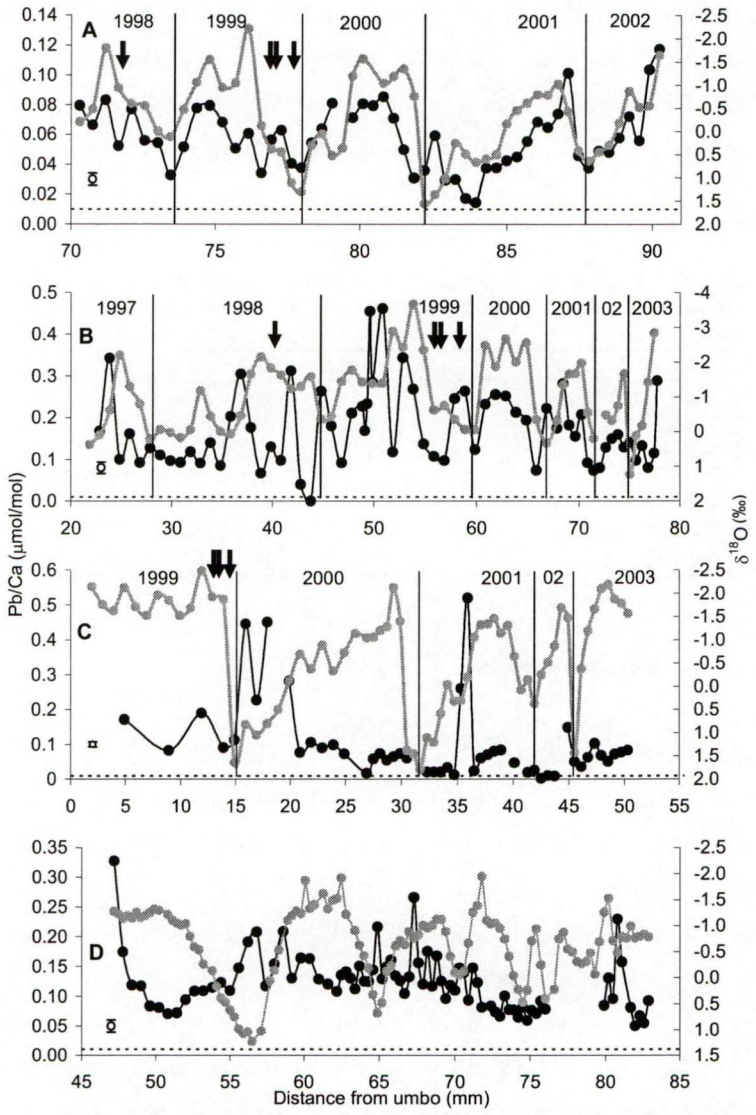

Figure 3. High resolution Pb/Ca ratios (thin black lines and circles) and oxygen isotopes (thick grey line and circles) of three modern shells (A, MW1; B, MW2; C, MB1) and the fossil Pliocene shell (D, P1) (see Table 1 for shell codes). Years are delimited on modern shells using the winter oxygen isotope value (most positive). Analytical precision is given on the left of each graph as the open symbol with error bars (based on mean Pb/Ca for each shell, %RSD = 6.8) and the detection limit is represented by the dashed line. Arrows mark approximate location of hurricanes.

significantly higher Pb/Ca ratios (0.157 ± 0.017 μmol/mol, n = 20) than the 1949-1976 period (0.098 ± 0.005 μmol/mol, n = 79) and 1982-2002 period (0.083 ± 0.007 μmol/mol, n = 52) (t-tests, $p < 0.001$ for each). However, the 1949-1976 and 1982-2002 periods were not different from each other (t-test, $p = 0.08$). There was a significant difference between mean Pb/Ca ratios in shells from Johnson Creek and Back Sound for the 1949-1976 period (t-test, $p < 0.001$) with Johnson Creek having higher ratios (Johnson Creek Pb/Ca = 0.112 ± 0.007 μmol/mol, n = 50; Back Sound Pb/Ca = 0.074 ± 0.005 μmol/mol, n = 29). There was no difference between Back Sound and Wade Creek shells during 1982 – 2002 (t-test, $p = 0.08$) nor Johnson Creek and Back Sound during 1977 – 1981 (t-test, $p = 0.25$). There was no relationship between age and Pb/Ca ratios when all shells were pooled together ($p = 0.23$, $R = 0.09$, n = 151). Hurricanes, which can increase resuspension of potentially contaminated sediments, did not visually correlate with increased Pb/Ca ratios (Fig. 4).

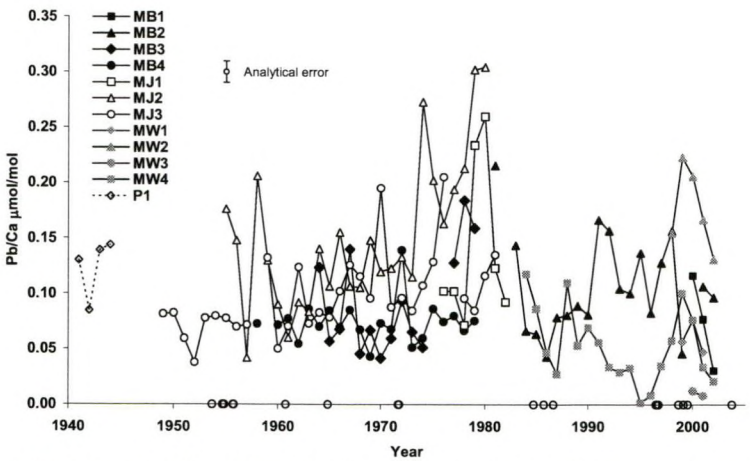

Figure 4. Annually sampled Pb/Ca ratios from the 11 *M. mercenaria* shells (see Table 1 for shell codes). The open symbols on the x-axis represent hurricane years (data from NCSO, 2004). The analytical error is based on 9.8% of the mean Pb/Ca ratio (0.101 ± 0.0099 μmol/mol). The Pliocene shell (P1) is also shown for comparison (dashed line, 1941-1944).

4. DISCUSSION

One test to asses if a proxy is primarily driven by environmental conditions is to determine its variability among individuals that grew under the same environmental conditions. Many studies have proposed that bivalve shells are better than soft tissues for monitoring pollution because the degree of trace metal variation is lower (Bourgoin, 1990; Yap et al., 2003; Cravo et al., 2004). However, a high variability between shells was found (Fig. 4), as well as a high intra-annual variability (Fig. 3). Other studies have also reported high intra-annual Pb/Ca variability (Price and Pearce, 1997; Vander Putten et al., 2000; Richardson et al., 2001); however, the cause of this variability is not straightforward and may be due to many factors.

In the first place, the intra-annual variability may be caused by variations in environmental Pb concentrations, which could be the result of increased terrestrial run off from heavy rains and /or sediment resuspension. Hurricanes can both increase terrestrial runoff and increase sediment resuspension, which can alter the biogeochemistry of the water column for several months (Paerl et al., 2001). However, Pb/Ca ratios do not seem related to hurricanes in these shells. The high resolution profiles include 4 hurricanes (Bonnie, 26 Aug. 1998; Dennis, 4 Sept. 1999; Floyd, 16 Sept. 1999; and Irene, 17 Oct. 1999). By inspecting Fig. 3, it is clear that Pb/Ca ratios are not elevated during the late summer in 1998 and 1999, despite the three hurricanes that occurred in 1999. Additionally, no clear correlation between hurricanes and annual Pb/Ca ratios is evident (Fig. 4). A possible reason for the lack of response may be that the clams stop calcifying during these stressful times. Moreover, hurricanes usually occur between August and October, which are months when *M. mercenaria* are already exhibiting reduced growth (Peterson and Fegley, 1986). Alternatively, biological regulation on Pb uptake can influence the shell Pb/Ca ratio as shell formation is a biological process. Although Vander Putten et al. (2000) could not determine the cause of seasonal Pb/Ca variations in *Mytilus edulis* shells, they suggested that perhaps it is regulated by seasonal variations in the distribution of the organic matrix. However, this study does not support this, as the organic rich growth lines did not exhibit higher Pb/Ca ratios (growth lines occur in late summer/ early fall, before the winter mark in Fig. 3).

The inter-shell variability may be the result of small scale spatial differences in environmental Pb concentrations. These small scale differences could be caused by groundwater seepage sites. Groundwaters can be highly contaminated with Pb (Landmeyer et al., 2003) and groundwater outflow can be limited to very small patches in the intertidal zone (Kohout and Kolipinski, 1967). Alternatively, pore-water Pb concentrations can also be highly variable, changing 10 fold over a few centimeters depth (Leermakers et al., in press), which could help explain the observed variability in these shells. The difference between Back Sound and Johnson Creek shells may be due to sediment type. It is well known that organic rich sediments contain higher Pb concentrations as compared to sandy sediments (Church et al., 1986; Kim et al., 2004). Indeed, Johnson Creek clams had higher Pb concentrations and were collected from muddy sediments, whereas the Back Sound clams were collected from sandy sediments. Other sources may include acute pollution from boats using leaded gasoline, which have been present up until recently (pers. obs.). Again, biology may be the cause as several studies have illustrated that the physiological state of bivalves is related to soft tissue Pb concentration (e.g., Lares and Orians, 1997). Thus, perhaps the shell Pb/Ca ratio is also related to the condition of the bivalves. However, this cannot be determined from the data presented here.

It has been demonstrated that Pb concentrations in soft tissues of *M. mercenaria* are not related to body weight (Boyden, 1974) and hence size, unlike many *Mytilus* spp. (Boalch et al., 1981; Saavedra et al., 2004). The fact that there was no relationship between Pb/Ca ratios and age (and thus shell size) agrees with this. Considering that *M. mercenaria* have been shown not to bioaccumulate Pb in their tissues, but reach an equilibrium with their environment (Alcutt and Pinto, 1994), should make them an excellent pollution indicator. Unfortunately, the high variability in the data complicates interpretation.

However, this high variability does not exclude *M. mercenaria* shells from being used as a Pb pollution record. The data are significantly higher during the 1977 – 1981 period, which is expected from other anthropogenic lead proxies (see Fig. 1). After averaging the data from all sites and shells, the expected anthropogenic profile is evident (Fig. 5). In fact, the profile from 1949 to 1987 is what would be expected.

There is a significant increase from 1949 to 1976 at 1.49 ± 1.15 nmol/mol per year (R = 0.46, p = 0.013, n = 28), then a peak in 1980 and the sharp decrease afterwards. The main difficulty is to interpret the 1986 to 2002 period. First, based on regional sediment cores (Cooper et al., 2004) as well as the expected trend (Fig. 1), the 1986 – 2002 period should be much lower than the pre-1970 period (sediment cores from the Pamlico River estuary (Fig. 2) show a ~20 % reduction in Pb concentrations; Cooper et al., 2004). Secondly, no adequate explanation could be found for the two peaks observed in this section (i.e., 1990 and 1998, see Fig. 5), which again, do not correlate with hurricane years. In addition to hurricanes, boat traffic can also cause sediment resuspension and considering the exponential rise in the local population (see Cooper et al., 2004), this has most probably increased in recent times and may explain the 1986 -2002 period with higher than expected Pb/Ca ratios.

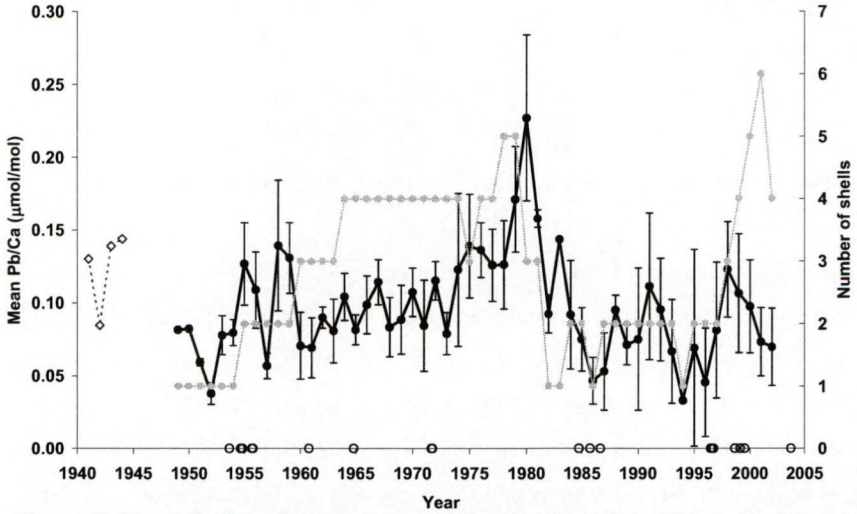

Figure 5. Mean Pb/Ca ratios (black line and circles, data from Fig 4). Error bars represent standard error. The grey line and circles show the number of *M. mercenaria* shells each mean is based on. The open symbols on the x-axis represent hurricane years (data from NCSO, 2004). The Pliocene shell (P1) is also shown for comparison (dashed line and diamonds, 1941-1944).

Unfortunately, the fossil shell did not provide pre-pollution Pb/Ca levels (see section 3.1 and Table 2). Therefore, the data presented here is compared with other studies of aragonite clams (Veneroidea). Bourgoin and Risk (1987) measured Pb in fossil *Mya truncate* shells (8200 BP) which had higher Pb/Ca ratios (0.28 µmol/mol) than the diagenetically altered shell analyzed in this study (see Table 2 and Fig. 3). Although

they determined that the original mineralogy of the aragonite shell was preserved, they did not chemically determine if there was diagenesis, so like with the fossil shell used here, this value may be erroneously high. Pitts and Wallace (1994) measured Pb in several fossil (1600 BP) *Mya arenaria* shells and found Pb/Ca ratios varying from 0.01 to 0.03 μmol/mol, about 10 times less than the modern *M. mercenaria* shells from this study. Using data from another species may not be appropriate, but their Pb/Ca ratios from a relatively unpolluted site (covering 1988 to 1989; 0.06 ± 0.004 μmol/mol) closely match the data from these same years in this study (0.08 ± 0.01 μmol/mol). Therefore, in general, the Cape Lookout region of North Carolina has apparently received little Pb pollution. This is surprising considering this region is just south of the highly polluted Pamlico Sound (cf. Cooper et al., 2004) and is in close proximity to the US Marine Corps Air Station at Cherry Point (Fig. 2).

Studies to determine the partition coefficient between environmental Pb (dissolved and particulate) and *M. mercenaria* shells are needed to validate the accuracy of using shells to trace pollution events. Nevertheless, it is recommended to use several shells to reduce the variability in the data. Due to this high variability, sub-annual data are probably not reliable. Marchitto et al. (2000a) created a master temperature chronology spanning 154 years from *Arctica islandica* shell growth increments and hypothesized that a 1000 year chronology would be feasible. Sampling these shells for Pb/Ca ratios could extend temperate records of Pb pollution back over the past millennium on an annual scale at different latitudes.

Acknowledgements - I thank C.H. Peterson (University of North Carolina, Chapel Hill), who kindly provided the *M. mercenaria* shells collected in the early 1980's; W.C. Gillikin and L. Daniels, who both assisted with sample collection in N.C.; and L. Campbell (University of South Carolina) who kindly provided the Pliocene shell. I express my gratitude to L. Monin for laboratory assistance, T. Haifeng who helped with sampling the shells, and to C.E. Lazareth for providing the sclerosponge data. A. Verheyden and S. Bouillon gave helpful comments on an earlier version of this manuscript.

Chapter 10

Barium uptake into the shells of the common mussel (*Mytilus edulis*) and the potential for estuarine paleo-chemistry reconstruction

Foreword

Vander Putten et al. (2000) clearly demonstrated that Mg/Ca, Sr/Ca, and Pb/Ca in *Mytilus edulis* shells from the Schelde estuary were not directly providing environmental information. Therefore, although full oceanographic data were collected in this study, along with the field data presented in this chapter, the ratios mentioned above will not be discussed in this chapter. As briefly discussed in Chapter 1, Mg/Ca and Sr/Ca should remain more or less constant in the salinities where *M. edulis* lives, so changes in water chemistry would not be incorporated into the shell. Indeed, trends related to salinity in Mg/Ca, Sr/Ca, and Pb/Ca ratios could not be detected any in the shells collected along the Schelde estuary in this study. Moreover, Sr/Ca ratios were under strong kinetic effects in calcite shells of another bivalve (Lorrain et al., submitted a). Therefore, it was decided to focus on the one element that Vander Putten et al. (2000) had the most faith in, barium.

Publication of the author related to this chapter:

Gillikin, D. P., F. Dehairs, A. Lorrain, D. Steenmans, L. André, J. Navez and W. Baeyens (*Under revision*). Barium uptake into the shells of the common mussel (*Mytilus edulis*) and the potential for estuarine paleo-chemistry reconstruction. *Geochemica et Cosmochimica Acta.*

Abstract

Environmental proxies stored in biogenic carbonates are a major source of our knowledge of the Earth's past climate. However, a rigorous validation and calibration is a prerequisite to extract meaningful information from these proxies. Here it is tested if calcite shells of the common mussel, *Mytilus edulis*, contain barium in proportion to the water in which they grew. Both laboratory and field experiments verify that there is a direct relationship between background $[Ba/Ca]_{shell}$ and $[Ba/Ca]_{water}$ in *M. edulis* shells. The field calibration provided a Ba/Ca partition coefficient (D_{Ba}) of 0.071 (± 0.001), which is similar to the D_{Ba} determined from inorganic calcite studies. There was no discernable effect of growth rate or temperature on D_{Ba}. These data suggest that *M. edulis* shells can be used as an indicator of $[Ba/Ca]_{water}$. Thus fossil or archaeological *M. edulis* shells can be used to extend knowledge of estuarine and coastal dissolved Ba throughputs back in time. Moreover, considering the inverse relationship between $[Ba/Ca]_{water}$ and salinity, $[Ba/Ca]_{shell}$ data could be used as an indicator of salinity. In addition, both the laboratory and field experiments indicate, contrary to previous hypotheses, that the frequently observed sharp episodic peaks found in most high resolution Ba/Ca profiles in bivalve shells are clearly not simply related to phytoplankton production.

1. INTRODUCTION

Both stable isotopes and elemental ratios archived in bivalve shells have been used for paleo-environmental reconstruction (e.g., Torres et al., 2001; Dettman et al., 2004), however, many of these proxies have certain drawbacks associated with them. For example, although oxygen isotopes ($\delta^{18}O$) in shells are a robust sea surface temperature (SST) proxy, unknown water $\delta^{18}O$ can significantly complicate interpretation, especially in estuaries (e.g., Gillikin et al., 2005a; Chapter 4). On the other hand, some proxies in carbonates may be seriously affected by vital effects, such as stable carbon isotope ratios ($\delta^{13}C$) (McConnaughey et al., 1997; Lorrain et al., 2004a) and Sr/Ca ratios (Stecher et al., 1996; Gillikin et al., 2005b; Chapter 8), which are often species specific. Therefore, each proxy should ideally be validated and calibrated for each species.

The oceanic barium cycle has received much attention over the past several decades (Chan et al., 1977; Dehairs et al., 1980; 1992; Paytan and Kastner, 1996; McManus et al., 2002; Jacquet et al., 2005). This is due in part to the use of Ba as a paleoproductivity and paleoalkalinity proxy (Dymond et al., 1992; Lea, 1993; McManus et al., 1999). Barium enters the oceans from river or ground water inputs, which pass through estuaries and the coastal zone (Carroll et al., 1993; Guay and Falkner, 1997; 1998; Shaw et al., 1998). These Ba inputs are important for the oceanic Ba cycle as shown by many studies (Edmond et al., 1978; Moore and Edmond, 1984; Coffey et al., 1997; Guay and Falkner, 1997; 1998); however, historical records of riverine inputs are lacking. Having a proxy of Ba inputs from estuaries or the coastal zone, which can be extended back in time, would be highly valuable.

Barium / calcium ratios have been proposed as a proxy of dissolved seawater Ba/Ca in aragonitic corals (McCulloch et al., 2003), calcitic foraminifera (Lea and Boyle, 1989; 1991) and vesicomyid clam shells (Torres et al., 2001) providing information on salinity, nutrient and alkalinity distributions in past oceans. Furthermore, a temperature dependence on the Ba/Ca partition coefficient ($D_{Ba} = (Ba/Ca)_{carbonate} / (Ba/Ca)_{water}$) has also been observed in both biogenic and abiogenic aragonites (Lea et

al., 1989; Zacherl et al., 2003; Dietzel at al., 2004) and a precipitation rate effect was found in abiogenic calcite (Tesoriero and Pankow, 1996).

To date, all published records of high resolution Ba profiles in bivalve shells (both aragonite and calcite) have similar characteristics with a more or less stable background Ba concentration, interspaced with sharp episodic Ba peaks (Stecher et al., 1996; Toland et al., 2000; Vander Putten et al., 2000; Torres et al., 2001; Lazareth et al., 2003). Stecher et al. (1996) first proposed that these peaks were the result of the filter feeding bivalves ingesting Ba-rich particles associated with diatom blooms, as either phytoplankton (see Fisher et al., 1991), or barite (Stecher and Kogut, 1999). It is well known that primary productivity and barite formation are closely associated (Dehairs et al., 1980; 1987). Once inside the digestive tract Ba may be metabolized and moved via the hemolymph to the extrapallial fluid (EPF), where shell precipitation occurs (Wilbur and Saleuddin, 1983). Vander Putten et al. (2000) found a remarkable coincidence of the Ba peaks in several mussel shells collected at the same site, providing further evidence that an environmental parameter controls their occurrence. However, this hypothesis remains untested. Furthermore, there are no studies reporting D_{Ba} for bivalves and the only study suggesting that bivalves record dissolved Ba may possibly have included the effects of these Ba extremes (see Torres et al., 2001).

The aim of this study was to assess the D_{Ba} for the bivalve *Mytilus edulis*, as well as to investigate if indeed particulate Ba could be the cause of the aforementioned Ba peaks in the shell. To validate this proxy, Ba concentrations in the shells, soft tissues and hemolymph of mussels exposed to different levels of dissolved Ba in the laboratory as well as fed diets with varying Ba concentrations were measured. To calibrate the proxy on natural populations, a field study along the Westerschelde Estuary, The Netherlands (NL) was conducted where mussels were grown while elemental concentrations and physico-chemical water parameters were regularly monitored. This experimental setup allowed us to compare data from both culture and natural situations.

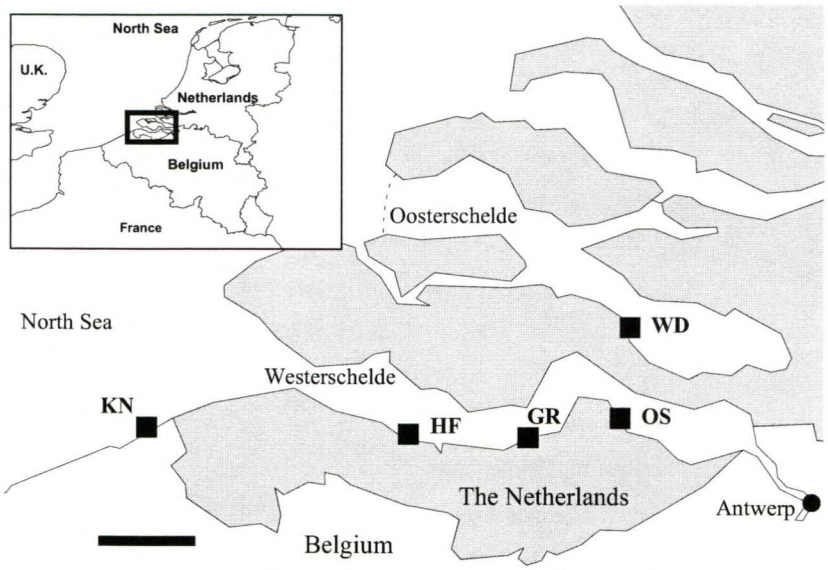

Figure 1. Map of the Westerschelde and Oosterschelde estuaries. The mussel collection site at Wemmeldinge (WD) and the four study sites are indicated Knokke (KN), Hooftplaat (HF), Griete (GR) and Ossenisse (OS). Scale bar = 10 km.

2. Materials and Methods

2.1 Laboratory experiments

Mytilus edulis were collected from the Oosterschelde estuary near Wemmeldinge, the Netherlands (salinity ~ 35; temperature ~ 8 °C) in March 2004 (Fig. 1). Epibionts were gently removed and the mussels were acclimated to laboratory conditions at 9.2 ± 0.3 °C (mean ± standard deviation) for 7 days, then another 14 days at 14.7 ± 0.2 °C (i.e., 21 days acclimation; temperature monitored hourly with a TidBit data logger, Onset Computer Corp.). During acclimation, mussels were fed three times per week with 12 mg of dried yeast per animal per week (Artemic Systems, LANSY PZ). After the acclimation period, 40 mussels (2.8 ± 0.3 cm length) were selected for the 'dissolved Ba' experiment and were stained with calcein (200 mg l^{-1}; $C_{30}H_{26}N_2O_{13}$; Sigmal Chemical) for 20 hours to mark the beginning of the experiment in the shell (see Rowley and Mackinnon, 1995). Afterwards, 10 mussels were placed in each of four aquaria containing 10 l of filtered (10 μm) North Sea water spiked with

approximately 0, 110, 220 and 440 nmol l^{-1} of Ba (as $BaCl_2$) (Table 1). Water was continuously circulated through acid washed plastic filters (except during feeding periods, see further) and was aerated. Mussels were fed the same quantities of yeast as during the acclimation period. Feeding took place for three hours, three times per week. Mussels were fed in their separate aquaria during which the filtration pumps were turned off. This experiment ran for 36 days, during which the water in all tanks was changed weekly (similar to Lorens and Bender, 1980) and was maintained at 16.4 ± 0.6 °C with a pH of 7.9 ± 0.1 and salinity of 36.4 ± 0.9 (on occasion salinity was adjusted with MilliQ water (>18MΩ cm^{-1}) to compensate for evaporation; pH and salinity were measured with a WTW multiline P4 multimeter). Water samples were taken two times per week for $[Ba/Ca]_{water}$ using syringe filters (Macherey-Nagel; Chromafil A45/25; cellulose mixed esters; 0.45 µm pore size, 25 mm diameter), once just before and after a water change, and were acidified with trace metal grade HCl to ~ pH 3. Procedural blanks were also taken by filtering MilliQ water (>18MΩ cm^{-1}).

Table 1. Summary of average seawater $[Ba/Ca]_{water}$ (µmol/mol; ± SE) for each laboratory $[Ba/Ca]_{water}$ treatment group. N = 8 water samples per treatment, spread over the experiment.

Tank	Treatment *	$[Ba/Ca]_{water}$ (µmol/mol)
1	Ambient	5.08 ± 0.22
2	+110 nmol l^{-1}	19.38 ± 0.71
3	+220 nmol l^{-1}	36.34 ± 0.91
4	+440 nmol l^{-1}	65.05 ± 2.37
5	Feeding*	4.61 ± 0.45

*see text

To assess the effect of Ba being ingested as food, a feeding experiment was conducted. In a fifth aquarium, two plastic mesh baskets, each with 10 mussels were held under the same conditions, except that there was 20 l of water to compensate for the higher density of animals and they were fed differently. These mussels were fed in separate aquaria with different foods. One batch was fed a slurry of living phytoplankton (*Chlamidomonas reinhardii*) grown in a 'normal' Tris-Acetate-Phosphate (TAP) medium (hereafter referred to as phyto +0) with the phytoplankton containing 5.87 ± 0.51 nmol g^{-1} dry weight (DW) Ba (n = 3), whereas the other batch were fed the same phytoplankton species, which were grown in a Ba rich TAP medium (spiked with 730 nmol l^{-1} Ba; hereafter referred to as phyto +100; see Steenmans (2004) for more details regarding phytoplankton culturing) with [Ba] =

14.56 ± 0.95 nmol g^{-1} DW (n = 3). Both batches were fed for 1 hour per day, five days per week, with a total of 18 mg phytoplankton (DW) per animal per week. This provided three levels of Ba in food given to mussels maintained in normal seawater Ba concentrations (i.e., yeast (with [Ba] = 3.35 ± 0.32 nmol g^{-1} DW (n = 3)), phyto +0 and phyto +100). After feeding, mussels were returned to their aquarium. This experiment was run for 29 days; water maintenance and sampling was similar to the dissolved Ba experiment.

After the experiments were completed, mussels were removed from their aquaria one at a time and were sampled for hemolymph, soft tissues and shells. Hemolymph was sampled by blotting the shell dry, and then gently prying open the valves with a scalpel, draining the mantle cavity and then sampling the hemolymph from the adductor muscle with a sterile 5 ml syringe and needle. Procedural blanks were prepared by drawing MilliQ water into a new syringe and injecting it into a micro-centrifuge tube. Whole tissues were dissected from the valves using a scalpel. Samples (hemolymph and tissues) were transferred to micro-centrifuge tubes and were immediately frozen to -20 °C until analysis. Shells were rinsed with MilliQ water (>18MΩ cm^{-1}) and were air dried.

A condition index was used to compare mussel health at the end of the experiments ([shell length / shell width] / tissue dry weight) to mussels health at the end of the acclimation period (beginning of experiments), which indicated that all animals were healthy (ANOVA, LSD test, $p > 0.05$ for all).

2.2 Field experiment

Mytilus edulis (~ 3 cm) were collected from the Oosterschelde (The Netherlands; Fig. 1). The Oosterschelde estuary was dammed in the late eighties and now has more or less marine salinities (S > 30; Gerringa et al., 1998). Mussels were transported back to the laboratory where epibionts were removed. They were then stained with calcein as in the previously described experiments. Within the next week (on 24 Oct. 2001), 50 mussels were placed into four stainless steel cages and these were deployed along an estuarine salinity gradient in the Westerschelde estuary (Fig. 1; see Baeyens et al., 1998b for a general description of the Westerschelde). Cages were attached at the

same tidal level as the highest density of 'local' mussels at Ossenisse (OS; the most upstream occurrence of wild *Mytilus* populations), Griete (GR), Hooftplaat (HF), and Knokke (KN; Fig. 1). Water temperature was monitored at each site hourly using a TidBit data logger. Water was sampled monthly for one year (Nov. 2001- Nov. 2002) and every two weeks between March and May for salinity, dissolved Ba/Ca, particulate Ba , and chlorophyll a (hereafter, Chl a). Salinity was measured *in situ* with a WTW multiline P4 multimeter. $[Ba/Ca]_{water}$ was sampled by filtering 250 to 500 ml of seawater through 0.4 μm polycarbonate filters (Osmonics poretics). The filtrate was acidified with trace metal grade HNO_3 to ~ pH 3. Blanks were prepared by filtering MilliQ water (>18MΩ cm^{-1}) through the same system and blank filter. Phytoplankton pigments were sampled by filtering 200 to 500 ml of seawater through GF-F filters. Filters were wrapped in aluminum foil and placed in liquid nitrogen; three replicates were taken at each sampling. Upon return to the laboratory, samples were transferred to a –85 °C freezer until analysis.

Mussels were collected on four different dates (29 Sept. 02, 9 Dec. 02, 20 Feb. 03 and 21 Apr. 03). Mussels transplanted to OS did not survive (undoubtedly due to the salinity shock) and therefore local mussels from this site were used. Similarly, the wave action at KN repeatedly destroyed cages and all mussels were lost; so again at this site, mussels from the local population were used.

2.3 Sample preparation and analysis

All water samples for dissolved Ba and Ca analysis were diluted with MilliQ water (>18MΩ cm^{-1}) to assure a salt concentration less than 0.2 %. Barium was measured on a VG PlasmaQuad II+ inductively coupled plasma mass spectrometer (ICP-MS) using In as an internal standard. Calcium was measured with an IRIS Thermo Jarrell Ash Corp. ICP- optical emission spectrometer (ICP-OES) using Yt and Au as internal standards. Certified reference materials (CRM) were also run to check for precision and accuracy. The reproducibility of the SLRS-3 water standard was < 4 % (%RSD) for both Ba and Ca and mean values were within 5 % of the recommended values for both elements (n = 8). Phytoplankton pigments were analyzed at NIOO-CEME, Yerseke, NL, using reverse-phase HPLC (Gieskes et al., 1988) with a reproducibility of 2.7 % (or 0.3 μg/l; 1σ) for Chl a, based on an in-house standard (n = 7).

Hemolymph samples were defrosted and 150 µl of sample was pipetted into a clean Teflon beaker. The sample was digested by adding 150 µl HNO_3 and 150 µl H_2O_2 (trace metal grade) and allowing the reaction to take place in the sealed beaker at 60 °C for more than 12 hours. Indium and Re were used as internal standards to control instrument fluctuations. Samples were analyzed for Ba and Ca on a Finnigan Element2 High Resolution-Inductively Coupled Plasma-Mass Spectrometer (HR-ICP-MS). Samples were diluted 20 times with milliQ water (>18MΩ cm^{-1}) to assure a salt concentration less than 0.2 %. Reproducibility of seawater and hemolymph samples was < 5 % for both Ba and Ca ($[Ba/Ca]_{hemolymph}$ = 3.8 ± 0.2 µmol/mol, n = 9, and $[Ba/Ca]_{water}$ = 65.1 ± 2.1 µmol/mol, n = 9).

Three animals from each laboratory treatment were randomly selected and their tissues were digested following the protocol of Blust et al. (1988). Briefly, samples were digested in 2 ml of bi-distilled HNO_3 for at least 12 hours and were then microwave digested with the addition of 1 ml of Ultrapure H_2O_2. The digested tissue samples were then analyzed for Ba and Ca with a HR-ICP-MS in the same manner as hemolymph. Reproducibility was established by running different CRMs, the DORM-2 Dogfish muscle (National Research Council of Canada) and the NIST 1566a oyster tissue. For DORM-2, reproducibility was 4.8 % ([Ba/Ca] = 1.16 ± 0.05 mmol/mol, n = 5), while it was 7.6 % for 1566a oyster tissue ([Ba/Ca] = 0.22 ± 0.02 mmol/mol, n = 7). Neither of these CRMs are certified for Ba concentrations, but values obtained for NIST 1566a were within 10 % of previously published values (see Buckel et al., 2004).

Shells were sectioned along the axis of maximal growth using a wet diamond saw. Thick sections were viewed under an optical microscope with UV light and calcein marks were mapped for each shell. Only shells from the laboratory experiments with greater than 70 µm new growth were used (the laser ablation spot is 50 µm in diameter, see further). Unfortunately, mussels from the feeding experiment were not exposed to calcein for a long enough period (4 hours). Therefore, the new growth could not be assessed and these shells could not be analyzed for Ba/Ca ratios. Shells from the field experiment were first sampled for stable isotopes. Carbonate powder was milled from the shell cross-sections using a 300 µm drill bit and a Merchantek

Micromill (a fixed drill and computer controlled micro positioning device), which allows precise sampling. Samples were milled from the outer calcite shell layer. Various sampling distances were used (150 μm to 1 mm) depending on growth rate (i.e., fewer samples in regions of high growth). Oxygen and carbon isotope analysis was performed using a ThermoFinnigan Kiel III coupled to a ThermoFinnigan Delta+XL dual inlet isotope ratio mass spectrometer (IRMS). The samples were calibrated against the NBS-19 standard ($\delta^{18}O$ = -2.20 ‰, $\delta^{13}C$ = +1.95 ‰) and data are reported as ‰ VPDB using the conventional delta notation. The reproducibility (1σ) of the routinely analyzed carbonate standard is better than 0.1 ‰ for both $\delta^{18}O$ and $\delta^{13}C$ (more details can be found in Gillikin et al., 2005a and Chapter 2). High resolution Ba/Ca profiles from field grown shells were obtained using either solution nebulization HR-ICP-MS (SN-HR-ICP-MS) on micromilled powders (powders were milled directly beneath the isotope sample to assure proper alignment of the data and to remove surface contamination) or by laser ablation ICP-MS (LA-ICP-MS; see below). All shells from the dissolved Ba experiment with adequate growth were analyzed for Ba/Ca using the LA-ICP-MS.

Carbonate powders for Ba/Ca analyses (~ 150 μg) were dissolved in a 1 ml 5 % HNO_3 solution containing 1 ppb of In and Re, which were used as internal standards. Ba/Ca reproducibility over the sampling period was 6.6 % (1σ; or 0.06 μmol/mol) based on replicate measurements of a *M. edulis* in-house reference material ([Ba/Ca] = 0.96 μmol/mol; n = 8). Accuracy was assessed using the USGS MACS1 carbonate standard ([Ba/Ca] = 84.76 μmol/mol) and was found to be within 1 % of the recommended value (n = 6; values from S. Wilson, USGS, unpublished data, 2004).

Data from LA-ICP-MS analyses were calibrated using both the NIST 610 (values from Pearce et al. (1997)) and the USGS MACS1 (values from S. Wilson, USGS, unpublished data, 2004). The laser was shot (~50 μm spots) directly in the holes of the isotope sampling allowing direct alignment of Ba/Ca and isotope profiles for the field experiment (cf. Toland et al., 2000). All shells from the laboratory experiment were analyzed in front of the calcein mark (one analysis per shell, if growth was less than 50 μm, the shell was not sampled). Calibration (including gas blank subtraction, ^{43}Ca normalization, and drift correction) was performed offline following Toland et

al. (2000). Reproducibility of Ba/Ca ratios over the sampling period was 0.11 μmol/mol (1σ; or 12.8 %) at the 1 μg/g level (MACS2, mean = 0.9 μmol/mol, n = 17) and 5.9 μmol/mol (1σ; or 7.3 %) at the 80 μg/g level (MACS1, mean = 80.5 μmol/mol, n = 47), which covers the full range of Ba/Ca values encountered in this study (see results). Accuracy was assessed using MACS2; as there is no recommended value available for MACS2, the value from SN-HR-ICP-MS analyses was used (MACS2 = 0.90 ± 0.07 μmol/mol (n = 5)), which indicate a robust LA-ICP-MS calibration. Details of operating conditions can be found in Lazareth et al. (2003). Briefly, the system consists of a Fisons-VG frequency quadrupled Nd-YAG laser (266 nm) coupled to a Fisons-VG PlasmaQuad II+ mass spectrometer.

The background or baseline $[Ba/Ca]_{shell}$ was selected by first omitting obvious peaks (e.g., ~15 – 22 mm from the umbo in shell KN200203), then omitting all data that was greater than 50 % of the (peak-less) mean. This was repeated until the change in mean $[Ba/Ca]_{shell}$ was less than 5 %. This provided an objective criterion for selecting background $[Ba/Ca]_{shell}$ data.

3. RESULTS

3.1 Laboratory experiments

3.1.1 Hemolymph

In the dissolved Ba experiment, *Mytilus edulis* $[Ba/Ca]_{hemolymph}$ was only slightly different from the $[Ba/Ca]_{water}$, with the linear least squares regression

$$[Ba/Ca]_{hemolymph} = 0.86 (\pm 0.04) * [Ba/Ca]_{water} + 2.26 (\pm 1.49) \quad (1)$$

(in μmol/mol; $R^2 = 0.98$, $p < 0.0001$, n = 36) (Fig 2). The errors of the regression coefficients reported above (and hereafter) represent the 95 % confidence intervals. Despite the Ba difference in foods offered (3.35 to 14.56 nmol g^{-1} DW Ba), hemolymph was similar between the three treatments of the feeding experiment (Fig. 2, inset).

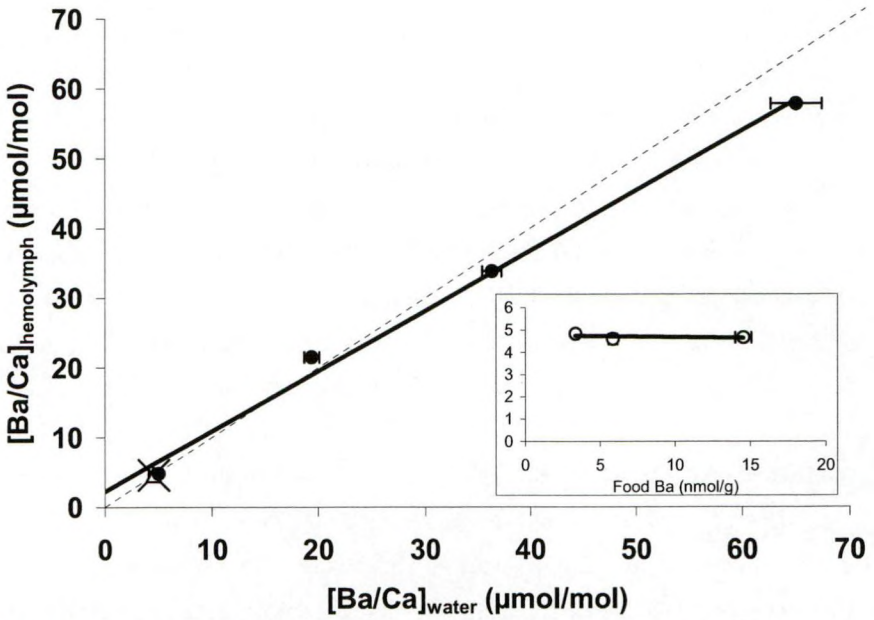

Figure 2. Mean Ba/Ca ratios (± SE) in hemolymph of laboratory grown *Mytilus edulis* versus Ba/Ca ratios of culturing water (± SE; solid circles). The solid line shows the linear least squares regression, with the relationship $[Ba/Ca]_{hemolymph}$ = 0.86 (± 0.04) * $[Ba/Ca]_{water}$ + 2.26 (± 1.49) (R^2 = 0.98, $p < 0.0001$, n = 36). The 1:1 line is also shown (dashed). Data from the feeding experiment, where the mussels were fed food enriched in Ba are shown as the X and diamond. The inset graph illustrates that food [Ba] does not influence hemolymph Ba/Ca ratios (y-axis legend is the same as the main graph).

3.1.2 Tissues

In the dissolved Ba experiment, tissue Ba/Ca was slightly enriched as compared to $[Ba/Ca]_{water}$ in the ambient treatment but was reduced by almost half in the highest $[Ba/Ca]_{water}$ treatment, with the intermediate treatments having a 1:1 relationship between tissue and water (Fig. 3). This resulted in an exponential fit between water and tissue

$$[Ba/Ca]_{tissue} = 35.36\ (\pm\ 2.19) * (1\text{-}\exp^{(-0.07\ (\pm\ 0.01)\ *[Ba/Ca]water)}) \qquad (2)$$

(in µmol/mol; R^2 = 0.99, $p < 0.0001$, n = 11) (Fig. 3). Although there is not enough data for statistics, it is clear that there is a trend of increasing tissue Ba/Ca with increasing food Ba (Fig. 3, inset) in the feeding experiment.

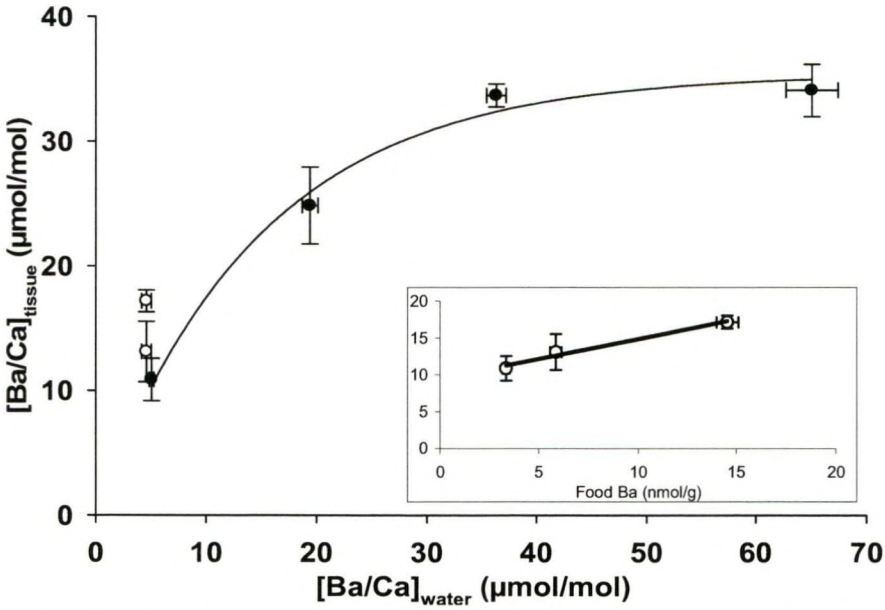

Figure 3. Mean Ba/Ca ratios (± SE) in bulk tissue of laboratory grown *Mytilus edulis* versus Ba/Ca ratios of culturing water (± SE; solid circles). The solid line shows the exponential fit, with the relationship $[Ba/Ca]_{tissue} = 35.36\ (\pm\ 2.19) * (1\text{-}exp^{(-0.07\ (\pm\ 0.01) * [Ba/Ca]water)})$ ($R^2 = 0.99$, $p < 0.0001$, $n = 11$). Data from the feeding experiment, where the mussels were fed food enriched in Ba are shown as the open symbols. The inset graph illustrates that food [Ba] clearly does influence tissue Ba/Ca ratios (y-axis legend is the same as the main graph).

3.1.3 Shells

Between six to nine shells were analyzed for each Ba treatment. In the dissolved experiment, $[Ba/Ca]_{shell}$ was directly proportional to $[Ba/Ca]_{water}$ with the linear relationship

$$[Ba/Ca]_{shell} = 0.10\ (\pm\ 0.02) * [Ba/Ca]_{water} + 1.00\ (\pm\ 0.68) \qquad (3)$$

(in µmol/mol; $R^2 = 0.84$, $p < 0.0001$, $n = 28$) (Fig 4). To calculate the partition coefficient (D_{Ba}), many studies force the regression through zero (see Zacherl et al., 2003), however, considering that the intercept is well above zero (range = 0.32 to 1.68), it was decided not to force through the origin, resulting in a D_{Ba} of 0.10 ± 0.02 (95 % CI). However, forcing through the origin does not significantly change the D_{Ba} (0.12 ± 0.01; 95 % CI) (t-test, $p = 0.38$).

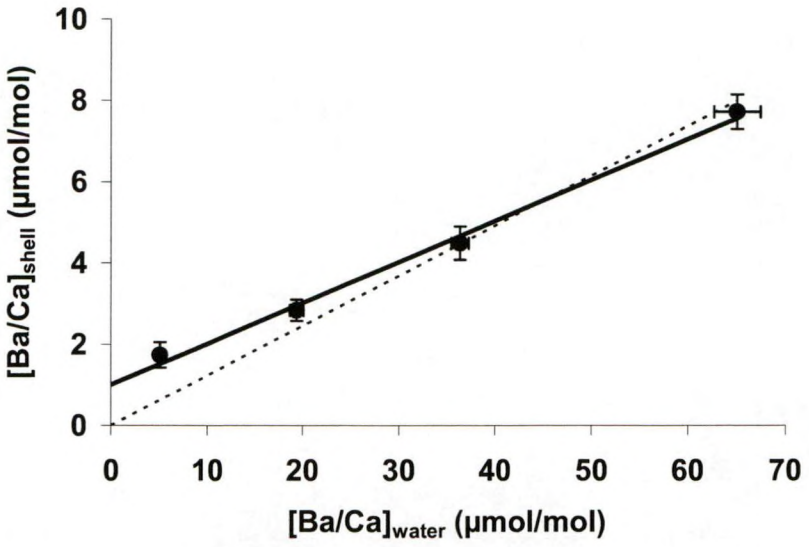

Figure 4. Mean Ba/Ca ratios (± SE) in shells of laboratory grown *Mytilus edulis* versus Ba/Ca ratios of culturing water (± SE). The solid line shows the linear least squares regression, with the relationship $[Ba/Ca]_{shell} = 0.10 (\pm 0.02) * [Ba/Ca]_{water} + 1.00 (\pm 0.68)$ ($R^2 = 0.84$, $p < 0.0001$, $n = 28$). The dashed line represents the regression forced through zero.

3.2 Field experiment

3.2.1 Environmental parameters

All four sites had significantly different salinity and $[Ba/Ca]_{water}$ values (Fig. 5A, B; ANOVA, $p < 0.0001$; post hoc LSD test, all $p < 0.01$) and there was a highly significant negative relationship between $[Ba/Ca]_{water}$ and salinity (Fig. 6; in µmol/mol; $R^2 = 0.73$, $n = 55$, $p < 0.0001$) with the linear relationship

$$[Ba/Ca]_{water} = -1.22 (\pm 0.21) * \text{Salinity} + 46.05 (\pm 4.57) \quad (4)$$

There was no overall difference between Chl a concentrations at any of the stations (ANOVA, p = n.s.), with the phytoplankton bloom starting in April and ending in late summer at all sites (Fig. 5C). The temperature profiles from the four sites were remarkably similar, with an annual range of 20 °C (see Fig. 8 of Chapter 6). Near-shore particulate Ba was dominated by lithogenic Ba, so no biological signal could be deduced and the data were not used [lithogenic Ba was estimated based on sample Al

content and a Ba/Al molar ratio of 0.00128 for shale (Taylor and McLennan, 1985)] (data not shown).

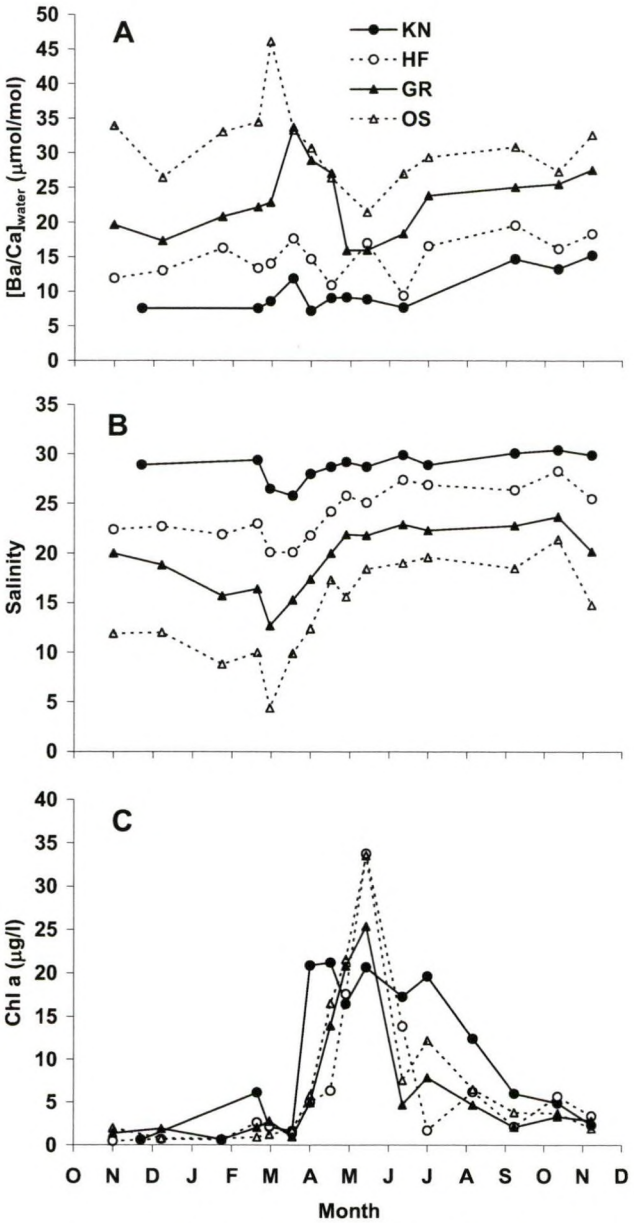

Figure 5. Dissolved $[Ba/Ca]_{water}$ (A), salinity (B) and Chl a (C) at the four Schelde sites measured over one year (Nov. 2001 - Nov. 2002).

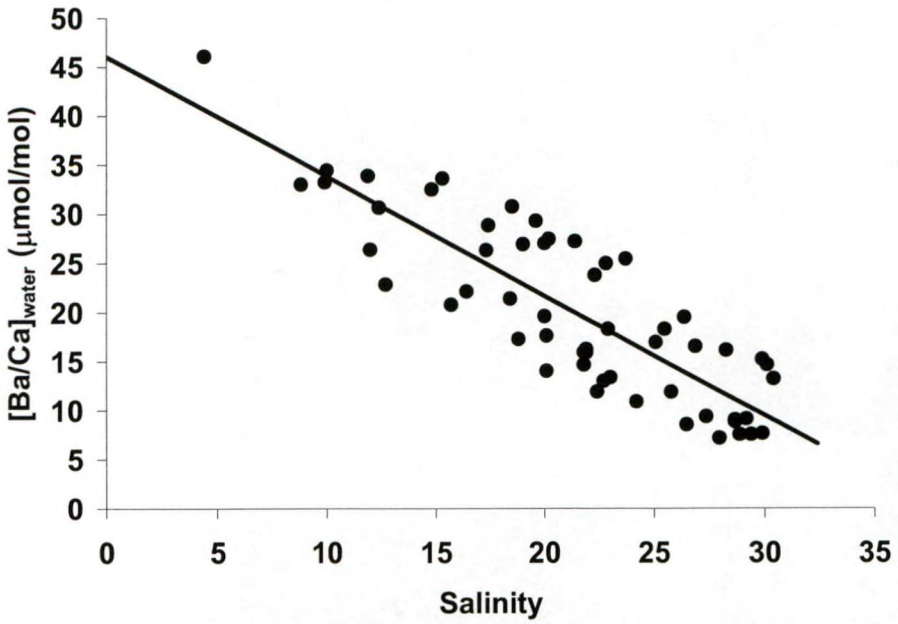

Figure 6. Salinity versus $[Ba/Ca]_{water}$ including data from all sites and sampling dates. The linear relationship ($R^2 = 0.73$, $n = 55$, $p < 0.0001$) is $[Ba/Ca]_{water} = -1.22 (\pm 0.21) * Salinity + 46.05 (\pm 4.57)$.

3.2.2 Shells

Profiles of $\delta^{18}O$, $\delta^{13}C$ and $[Ba/Ca]_{shell}$ are plotted against distance from the umbo for the six shells analyzed in Fig. 7. Again, all profiles are characterized by the typical background $[Ba/Ca]_{shell}$, interrupted by sharp episodic peaks (aside from one shell from OS, Fig. 7). Moreover, using the inverted $\delta^{18}O$ scale as a temperature and season indicator (i.e., positive $\delta^{18}O$ in winter), it is clear that these Ba peaks in the shell occur during spring when SST started to rise. The two shells which were transplanted from the Oosterschelde (sites HF and GR) showed clear calcein marks in their shells, which coincided with abrupt changes in the stable isotope profiles. The change in the $\delta^{13}C$ profile is most pronounced in the GR shell as this site has a much lower salinity (Fig. 5B) and hence more negative $\delta^{13}C$, compared to the Oosterschelde, where these animals were collected.

Figure 7. (see next page) High resolution $\delta^{18}O$, $\delta^{13}C$, and $[Ba/Ca]_{shell}$ profiles from the six shells. Black filled symbols denote data selected as background $[Ba/Ca]_{shell}$ data. Vertical lines correspond to the time of transplantation (HF and GR shells only, see text) as determined from the calcein stain. Shell codes represent collection site and date (format: ddmmyy). Note that the isotope axes are inverted.

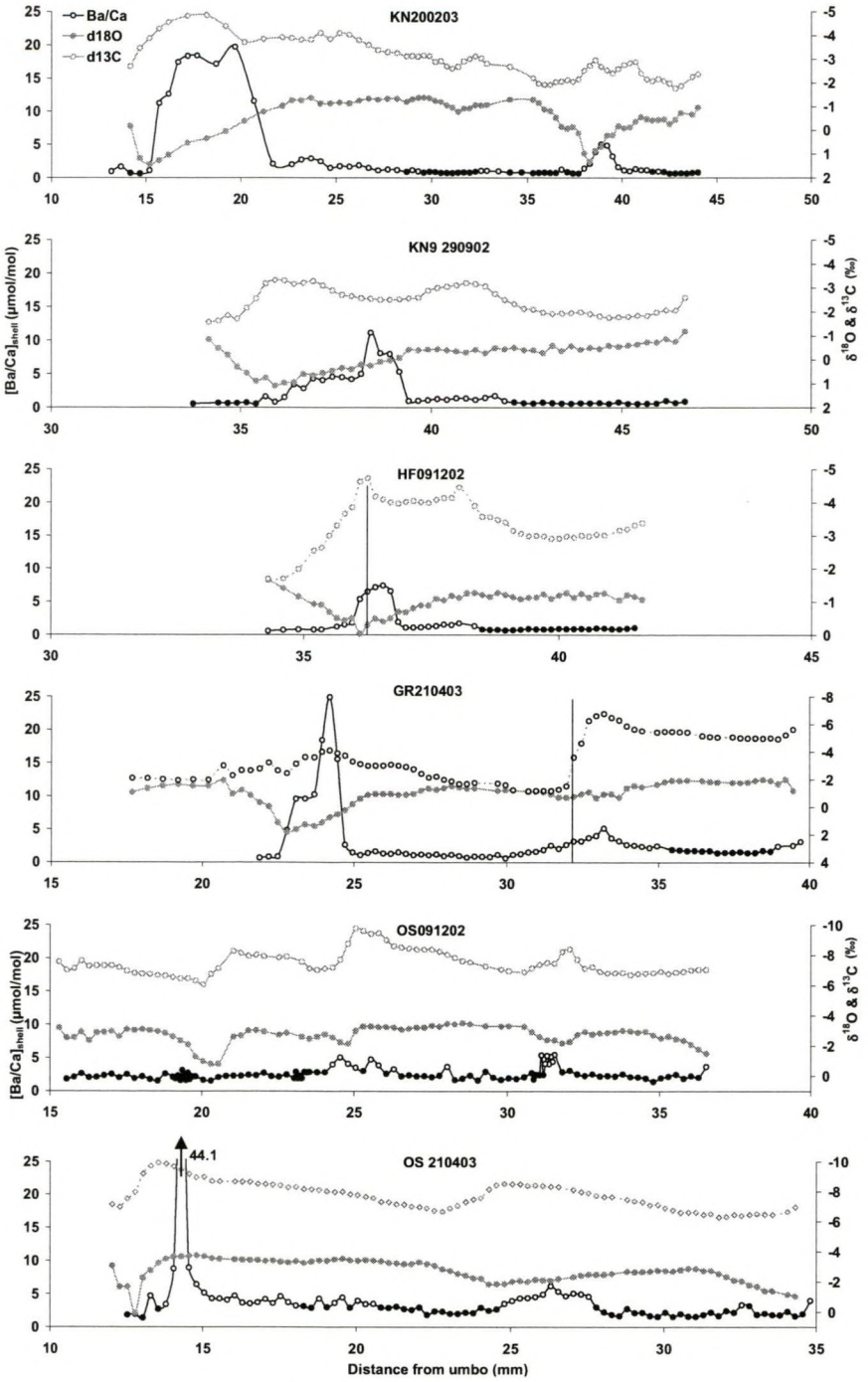

Figure 7. Legend on previous page

After selecting only the background $[Ba/Ca]_{shell}$ data from the shells (filled circles in Fig. 7), there was a highly significant linear relationship between $[Ba/Ca]_{shell}$ and average $[Ba/Ca]_{water}$ data

$$[Ba/Ca]_{shell} = 0.071\ (\pm\ 0.001) * [Ba/Ca]_{water} \quad (5)$$

(in µmol/mol; $R^2 = 0.96$, $p < 0.0001$, $n = 228$ [data of 6 shells from 4 sites]; Fig. 8). As opposed to the laboratory data, these data do include zero in the intercept, which was found to be not significant ($p = 0.8$) and was therefore not included in the regression. Thus the D_{Ba} determined from the field experiment is 0.071 (± 0.001), which is significantly different from the D_{Ba} determined in the laboratory (Fig. 8; t-test, $p < 0.001$).

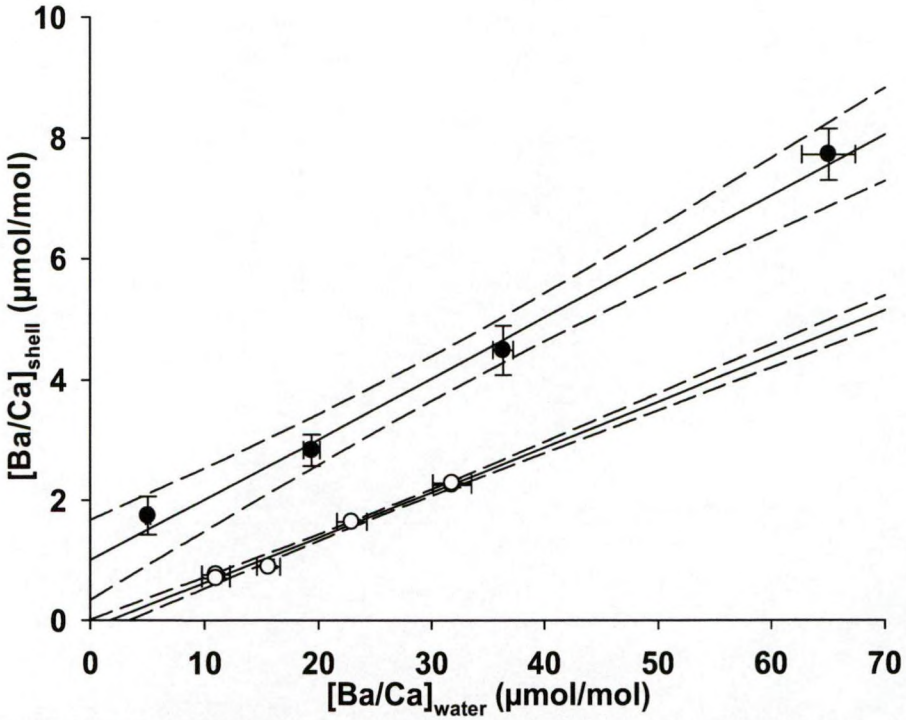

Figure 8. Mean Ba/Ca ratios (± SE) in shells of laboratory grown (closed symbols; based on 28 shells) and field grown (open symbols; based on multiple data from 6 shells) *Mytilus edulis* versus Ba/Ca ratios of water (± SE). The solid line shows the linear least squares regressions and the dashed lines the 95 % CI. Slopes are significantly different (t-test) at $p < 0.0001$.

4. DISCUSSION

4.1 Pathway of barium incorporation into the shell

Biomineralization in bivalves takes place in the extrapallial fluid (EPF), a thin film of liquid between the calcifying shell surface and the mantle epithelium (Wheeler, 1992). The central EPF is where the inner aragonite shell layer is precipitated, whereas the outer calcite shell layer is precipitated from the marginal EPF (i.e., the layer analyzed in this study). The EPF is isolated from seawater and therefore may have different elemental concentrations than seawater. Direct measurements of the marginal EPF are difficult and to my knowledge only one report provides marginal EPF elemental concentrations, but unfortunately Ba was not measured (Lorens, 1978). However, there does not seem to be a difference in Ba concentrations between hemolymph and central EPF in other bivalve species (Lorrain et al., subm. b). Elements move into the EPF through the epithelial mantle cells which are supplied from the hemolymph (Wilbur and Saleuddin, 1983). Ions enter the hemolymph of marine mollusks primarily through the gills, although they may also enter via the gut (see Wilbur and Saleuddin, 1983 and references therein). The relative contributions of Ba to the shell from food versus environment are unknown, however, in light of the above discussion and the fact that mollusk guts are known to contain high Ba concentrations (Lobel et al., 1991; Lorrain et al., subm. b), it is probable that the gut is a source of Ba in mollusk shells. However, although mussels were fed food with different Ba concentrations, which was taken up in the bulk tissues (Fig. 3), hemolymph Ba concentrations did not increase (Fig. 2), indicating that food is not a major source of Ba in the shell. Furthermore, the fact that the regression between $[Ba/Ca]_{shell}$ and $[Ba/Ca]_{water}$ in field specimens go through zero, also provides an empirical verification that food is not a major source of Ba in the shell, at least for the background $[Ba/Ca]_{shell}$ data (see also section 4.4).

4.2 Mytilus edulis D_{Ba}

Both the laboratory and field experiment verify that there is a direct relationship between $[Ba/Ca]_{shell}$ and $[Ba/Ca]_{water}$ in *M. edulis*. A possible explanation for the

difference in slopes between the laboratory and field experiment $[Ba/Ca]_{shell}$ vs. $[Ba/Ca]_{water}$ could be that the stress of handling and the suddenly increased Ba concentration caused a saturation of the ionoregulatory ability of the animal. Lorens and Bender (1980) found that elemental ratios in shells increased in laboratory held *M. edulis* for a short while, which they termed the "transition zone calcite" (or TZC), then decreased. They proposed that this was caused by the stress of capture and the adjustment to a new environment. Although these animals were acclimated to laboratory conditions for three weeks, the change to the experimental conditions may have caused stress and the TZC may have been included in the analyses. This could explain the higher D_{Ba} in the laboratory cultured mussels. Furthermore, the fact that the regression does not go through the origin supports this. As in the field population, it can be expected that when there is zero Ba in the water, there should be zero Ba in the shell. Interestingly, as the hemolymph can be expected to represent the crystallization fluid better than seawater, when a regression between hemolymph and shell is performed (laboratory experiment), the regression does go through the origin (intercept not significant, $p = 0.07$). The D_{Ba} calculated using hemolymph, 0.134 (± 0.006) ($R^2 = 0.95$, $n = 25$, $p < 0.0001$), is also more similar to that for planktonic foraminifera (see further). Nevertheless, the field experiment does represent a more natural situation, which suggests that this is the more correct D_{Ba} for *M. edulis*, 0.071 (± 0.001).

It should be noted that incorporation of elements in calcite with ionic radii larger than calcium (such as Ba) are expected to be strongly affected by external factors, such as temperature or salinity (Pingitore and Eastman, 1984; Morse and Bender, 1990). Temperature is unlikely to affect D_{Ba} in calcite (see section 4.3), however, it could not be determined if salinity has an effect or not. The strong relationship in the field between $[Ba/Ca]_{water}$ and salinity makes it difficult to deconvolve the effects, whereas in the laboratory salinity was similar in all treatments. Therefore, this could be another reason for the difference in slopes between the two experiments.

Abiogenic experiments on the D_{Ba} in calcite have provided a range of values, which is probably due to unconstrained precipitation rates in many of the experiments (Tesoriero and Pankow, 1996). For the range of *M. edulis* shell precipitation rates estimated by Lorens (1981), D_{Ba} is expected to range between 0.03 and 0.05

according to the abiogenic calcite experiments of Tesoriero and Pankow (1996), with the upper value not being too far off from ours (i.e., 0.07). Planktonic foraminifera, on the other hand have higher D_{Ba} than *M. edulis*, ranging from 0.09 to 0.19 (Lea and Boyle, 1991; Lea and Spero, 1992; 1994), whereas benthic foraminifera have an even higher D_{Ba} in both laboratory (0.20 – 0.5; Havach et al., 2001) and field based studies (0.37; Lea and Boyle, 1989). It can generally be considered that when the partition coefficient of a particular element (D_{Me}) is far from inorganically determined D_{Me}, then other factors most likely influence D_{Me}, such as the physiology of the organism or other biological factors. For example, Sr/Ca in corals has been shown to be an excellent SST proxy and the D_{Sr} is close to one (mmol/mol) (e.g., McCulloch et al., 1999), which is similar to abiogenic aragonite (Dietzel et al., 2004), whereas in aragonitic bivalve shells it is around 0.25 and there is no link with SST (Gillikin et al., 2005b; Chapter 8). Considering that foraminifera Ba/Ca has successfully been used as a proxy of dissolved Ba/Ca, and that the foraminifera D_{Ba} is farther from expected values than *M. edulis*, further implies that Ba/Ca ratios in *M. edulis* shell have a great potential as a robust proxy of dissolved seawater Ba/Ca as there should be an even smaller biological effect in *M. edulis* calcite.

To further test the robustness of this proxy, the data for the period preceding transplantation from shell GR210403 was used. These data should be representative of Oosterschelde conditions with salinity above 30 (see section 2.2). The background $[Ba/Ca]_{shell}$ before transplantation is 0.98 ± 0.05 (n = 13), which corresponds to a $[Ba/Ca]_{water}$ of 13.8 ± 0.73 when using the D_{Ba} of 0.071. A Ba/Ca value of 13.8 ± 0.73 is reasonable for a salinity of about 30 (Fig. 6) and provides additional evidence that even at low $[Ba/Ca]_{water}$, this is a good indicator of $[Ba/Ca]_{water}$.

4.3 Kinetic and thermodynamic effects on D_{Ba}

At the typical shell growth rates of *M. edulis* (Lorens, 1981), D_{Ba} is expected to be strongly dependent on growth rates (Tesoriero and Pankow, 1996), which is not evident in this study. If the D_{Ba} was increasing at higher shell growth rates, then shells with different growth rates would not plot on the same regression line. For example, the two transplanted shells (GR and HF) both grew about 0.45 mm $month^{-1}$ after transplantation (using $\delta^{18}O$ and calcein marks to approximate a time line), whereas the

shell from KN (shell KN200203) exhibits a growth rate of about 1.88 mm month^{-1} based on the full year that was sampled (Fig. 7). As these shells do not deviate from the regression line in a predictable manner (Fig. 8), this study does not support the existence of a precipitation rate effect on *M. edulis* shell Ba incorporation. However, the slightly elevated non-peak and non-background regions may be the results of higher growth rates when this shell section is formed (see section 4.4).

Considering the 20 °C temperature range at these sites, and the stable background [Ba/Ca] ratios observed in these shells, it does not seem likely that there is a major temperature effect on D_{Ba} in *M. edulis*. This is most probably true for all bivalves as well, as the stable Ba background in all published data is evident and temperature almost always has a seasonal cyclicity. Similarly, Lea and Spero (1994) did not find an influence of temperature on D_{Ba} in foraminifera, and this may possibly be the case for all biogenic calcites.

4.4 High resolution barium profiles

The results presented here confirm the general Ba profiles recorded in other bivalves (see Introduction), with a stable background signal interrupted by sharp episodic peaks, generally occurring in the spring (using $\delta^{18}O$ as a relative temperature scale). The unstable background Ba in OS shells probably reflects the highly variable salinity at this site. Another striking feature of the profiles is that the peak amplitude seems to be correlated to animal size, with smaller (younger) specimens having larger peaks. For example, shell KN200203 has a large Ba/Ca peak ~ 20 µmol/mol at 15 – 22 mm of growth, while in the same shell at 38 – 40 mm the peak only reaches ~ 5 µmol/mol (Fig. 7). This is reproduced in the other shells as well, with a large peak around 24 mm in shell GR210403 and small peaks around 35 – 40 mm in shells KN9 290902 and HF091202 (Fig. 7). This trend was also found by Vander Putten et al. (2000), who collected their *M. edulis* shells from the same estuary in 1997, suggesting it is not an environmental signal. This could be an averaging effect, with the sample size integrating more growth time as shell growth slows when the animal is older (see Goodwin et al., 2001), but considering the width of the peaks, this does not seem probable and is more likely a physiological effect of ageing (see further).

There are several hypotheses which could explain the $[Ba/Ca]_{shell}$ peaks. The hypothesis of Stecher et al. (1996), that either Ba-rich phytoplankton or barite formed in decaying phytoplankton flocs are ingested by the filter feeding bivalve and eventually the Ba is sequestered in the shell is plausible. Although the data from the feeding experiment do not support this, further experiments using a larger range of [Ba] in food are necessary to be conclusive. The lack of a $[Ba/Ca]_{shell}$ peak in the shell OS 091202 (Fig. 7) and the large Chl a peak at this site (Fig. 5C) suggest that phytoplankton blooms are not the cause. However, this does not exclude barite ingestion as a reason. It is possible that barite formation only occurs downstream from the OS site, which could explain the large sharp peak in the KN shells (Fig. 7) despite the lower broad Chl a peak at this site (Fig. 5C) (see Stecher and Kogut, 1999), but particulate Ba data from the Schelde estuary, which show a peak at mid salinities in spring, do not agree with this scenario (Zwolsman and van Eck, 1999). Increases in $[Ba/Ca]_{water}$ is highly unlikely to be the cause as the 20 – 25 μmol/mol $[Ba/Ca]_{shell}$ peaks would require $[Ba/Ca]_{water}$ to be around 300 μmol/mol, which is clearly not the case (Fig 5A). An alternative hypothesis may be that Ba is remobilized from tissue stores during spawning, which also occurs in the spring. The lack of a peak in the OS shell could possibly be due to this mussel not spawning. Osmotic stress may have required a large part of this animals' energy budget, leaving no energy for spawning (cf. Hummel et al., 2000; Qiu et al., 2002; Gillikin et al., 2004). It is also interesting to note that the $\delta^{13}C$ profiles coincide with changes in $[Ba/Ca]_{shell}$. This is most evident in shells KN9 290902 and HF092102, where the $\delta^{13}C$ is more negative when the $[Ba/Ca]_{shell}$ deviates from background concentrations and more positive when the $[Ba/Ca]_{shell}$ is at background levels (Fig. 7). Bivalve shell $\delta^{13}C$ is known to be influenced by the incorporation of metabolically derived light carbon (i.e., ^{12}C) (see Chapters 4, 5 and 6). Furthermore, it has been shown that increased metabolism in larger bivalves, relative to growth rate, leads to a larger availability of metabolic C for $CaCO_3$ precipitation and therefore results in a more negative $\delta^{13}C$ in the shell (Lorrain et al., 2004a). Using this rationale, higher metabolic rates from either spawning or seasonally increased growth, caused by an increase in food supply, would also result in a more negative shell $\delta^{13}C$. This could explain the pattern seen in these shells, and also agrees with a metabolic control on $[Ba/Ca]_{shell}$ peak amplitude as described above. However, data from the scallop, *Pecten maximus*, do not confirm this hypothesis, with their $[Ba/Ca]_{shell}$ peaks not being correlated with spawning (Lorrain,

2002). Finally, it can be argued that the $[Ba/Ca]_{shell}$ peaks can be caused by higher organic matter content in the shell. Bivalve shells can contain up to 5 % organic matter (see Marin and Luquet, 2004, and references therein) and Ba is known to be associated with organic matter (Lea and Boyle, 1993). However, neither Hart et al. (1997) nor Sinclair (in press) found a relationship between organic matter and Ba concentrations in other biogenic carbonates (i.e., corals).

Remarkably, a similar phenomenon also occurs in corals, with sharp episodic Ba peaks occurring at the same time each year, which are not related to river discharge (Sinclair, in press). However, unlike bivalves, Sinclair (in press) found that the timing of the peaks differed between coral colonies, even when they grew within 20 km of each other. The main conclusion of Sinclair (in press) regarding the cause of these peaks in corals was that there is currently no satisfactory hypothesis to explain them. This is also the case for bivalves. However, the similarities between corals and bivalves points at a common cause for these peaks. This in itself is amazing considering the large difference in biology, ecology, and biomineralization between these two phyla of invertebrates.

4.5 Implications for estuarine and coastal paleo-seawater chemistry

This study clearly illustrates that *M. edulis* shells may be used as a proxy of dissolved $[Ba/Ca]_{water}$. However, it should be clear that only high resolution profiles covering an adequate amount of growth may be used to assure the correct background $[Ba/Ca]_{shell}$ is selected. This selection can also be aided using the $\delta^{18}O$ and $\delta^{13}C$ profiles. Selecting the mid-summer growth region (or the most negative $\delta^{18}O$) along with the most positive $\delta^{13}C$ should result in a good selection of background $[Ba/Ca]_{shell}$. Obviously whole shell analyses are not suitable to determine $[Ba/Ca]_{water}$. Once the correct background $[Ba/Ca]_{shell}$ is obtained, the $[Ba/Ca]_{water}$ may be estimated using the D_{Ba} of 0.071 ($\pm$ 0.001). These data can be useful for giving a relative indication of salinity (different estuaries can be expected to have different salinity - $[Ba/Ca]_{water}$ relationships (Coffey et al., 1997)), which could assist with $\delta^{18}O$ interpretations (see Gillikin et al., 2005a (or Chapter 4) for more explanation). Furthermore, if $[Ba/Ca]_{water}$ was extended back through geologic time for the worlds large estuaries, the overall change in the oceanic Ba budget could be better constrained.

5. CONCLUSIONS

In the laboratory, it was verified that Ba/Ca in *Mytilus edulis* shells may be used as a proxy of dissolved $[Ba/Ca]_{water}$. This was then calibrated on shells grown under field conditions, resulting in a D_{Ba} of 0.071 (± 0.001), which is not far off from the expected D_{Ba} range determined from inorganic calcite studies (Tesoriero and Pankow, 1996). These data suggest that there are no temperature or growth rate effects on D_{Ba} in *M. edulis* and that these shells may be used to calculate $[Ba/Ca]_{water}$. This proxy can be used as a relative indicator of salinity, as well as to extend our knowledge of estuarine Ba cycling back through time by using fossil or archaeological shells.

Acknowledgements - I thank P. Dubois and H. Ranner (Université Libre de Bruxelles) for the use of their cold room and assistance with the laboratory experiment. V. Mubiana (U. Antwerp) kindly assisted with mussel collection, gave advice on mussel husbandry and helped setting up the field experiment and acid digesting the tissue samples. I am grateful for the HPLC expertise offered by J. Sinke and J. Nieuwenhuize (NIOO-CEME, Yerseke, NL). H.A. Stecher, D.W. Lea, A. Verheyden, S. Bouillon and two anonymous reviewers gave helpful comments on an earlier version of this manuscript. M. Elskens assisted with statistics and together with N. Brion collected the many liters of North Sea water.

Chapter 11

A note on elemental uptake in calcite bivalve shells

Foreword

In the previous chapters of this dissertation, the potential of trace elements as proxies of environmental conditions has mainly been discussed in terms of the element partition coefficients with respect to the surrounding seawater. However, as mentioned in the Introduction (Chapter 1), ideally, the partition coefficient should be calculated using the element ratio of the EPF (see section 2 and 4.1 of Chapter 1). In the present chapter, the auxiliary data from the barium laboratory experiment (Chapter 10) are presented. The partition coefficients presented here are the first to use an internal fluid as the source water for several of the elements. In addition, the possibility of food as a source of ions for the shell, a relatively unexplored field, is also investigated. Since the experimental design did not intend for these data to be obtained, certain aspects may appear ill planned, but nevertheless, considering the little information available on these topics, I feel that these data cannot be left unmentioned and that they may inspire future studies.

1. INTRODUCTION

Biomineralization in bivalves takes place in the extrapallial fluid (EPF), a thin film of liquid between the calcifying shell surface and the mantle epithelium (Wheeler, 1992; see also Chapter 1). There are several routes that ions can follow to the EPF. The hemolymph can supply ions, which move into the EPF through the epithelial mantle cells (Wilbur and Saleuddin, 1983). Ions enter the hemolymph of marine mollusks primarily through the gills, although they may also enter via the gut (see Wilbur and Saleuddin, 1983 and references therein). Once inside the digestive tract, elements may be metabolized and moved via the hemolymph to the EPF (Wilbur and Saleuddin, 1983). Ions can potentially also move directly from seawater through the periostracum into the EPF as suggested by Hickson et al. (1999). The relative contributions from these sources remain largely unknown, but it is often assumed that inorganic ions in the EPF are derived from the hemolymph (e.g., Nair and Robinson, 1998).

Direct measurements of the marginal EPF are difficult due to the small volume (Lorrens, 1978). There are some reports of central EPF elemental concentrations (where the inner shell layer is precipitated) (Crenshaw, 1972; Wada and Fujinuki, 1976; Lorrain et al., subm. b); however, to my knowledge only one report provides marginal EPF elemental concentrations (where the outer and/or middle shell layer is precipitated), but unfortunately only Na, Mg and Ca were measured and the author suggested to treat the data with caution due to sampling problems (Lorens, 1978). If elements enter the EPF via the hemolymph, the hemolymph might give an indication of EPF concentrations, or at least provide information about an alternative source of ions (other than water) for the EPF. It should be kept in mind that the EPF and hemolymph are considered separate compartments. Indeed, on a study of central EPF, Lorrain et al. (subm. b) found that the scallop *Pecten maximus* had different elemental concentrations in hemolymph and central EPF for many elements. However, in the same study, the clam *Ruditapes phillipinarum* was shown to have similar concentrations between the two compartments. Likewise, in another clam, *Mercenaria mercenaria*, Mg/Ca ratios were similar between hemolymph and central EPF (Crenshaw, 1972). Carrying this over to the marginal EPF, it seems that no generalizations can be made, and that differences or similarities between hemolymph

and EPF are species specific. Ignoring the periostracum route, of which little is known, ions can be conceptualized to pass two important membrane barriers: from the gills (or gut) to the hemolymph and from the hemolymph to the EPF and finally into the shell. Therefore, hemolymph elemental concentrations can provide information about what happens at the first barrier. Although some data are available for fish otoliths (reviewed in Campana, 1999), little or no data are available for bivalves. Thus, as a preliminary step, an elemental characterization of *Mytilus edulis* hemolymph, soft tissues, shell, and the water in which they grew is presented.

2. MATERIALS AND METHODS

The data presented in this chapter are auxiliary data from the laboratory experiment described in Chapter 10, where detailed materials and methods can be found, as well as a discussion on Ba (which is not included here). Also, precision and accuracy of reference materials can be found in Chapter 2.

Briefly, in this experiment, mussels were exposed to different levels of Ba dissolved in the water, with Tank 1 having the lowest (Ba/Ca = 5.1 ± 0.2 µmol/mol; i.e., nothing added to North Sea water) and Tank 4 containing the highest (Ba/Ca = 65.1 ± 2.4 µmol/mol). Tank 2 and 3 had intermediate values: Ba/Ca = 19.4 ± 0.7 µmol/mol and Ba/Ca = 36.3 ± 0.9 µmol/mol, respectively. Tank 5 contained two batches of mussels (recognizable as Tank 5 and Tank 5.5 in Fig. 1) that grew in water similar to Tank 1, but were fed phytoplankton grown in different cultures and containing different amounts of Ba, whereas the mussels in Tanks 1 - 4 were fed yeast. Some elements were measured in these foods and can be found in Table 2. Unfortunately, shells from Tank 5 could not be analyzed (see Chapter 10). Shells, seawater, tissues and hemolymph were investigated for ten elements: Mg, Pb, B, Co, Sr, U, Mn, Cu, Zn, and Cd. (as a ratio to Ca in shells, seawater, and hemolymph). For elements that were below the detection limit of the LA-ICP-MS, HR-ICP-MS data from a shell that grew at Knokke, Belgium was used (placed at position 0.5 on the x-axis in Fig 1). Water at Knokke should not be greatly different from the North Sea water used in the experiment, but does have a slightly lower salinity (~ 29). Therefore, comparisons with the Knokke shells should be treated with caution.

In addition to comparing shell, hemolymph, water and tissue concentrations to gain insight into the possible routes ions can follow, partition coefficients (D_{Me}) are provided, calculated as $D_{Me} = (Me/Ca)_{shell} / (Me/Ca)_{water}$ (calculated from mussels in Tank 1). However, it must be noted that the hemolymph probably has very different activity coefficients than the water, as the hemolymph contains high concentrations of organic molecules (see Misogianes and Chasteen, 1979; Nair and Robinson, 1998; Falini et al., 1996). The presence of organic compounds and polysulfides can severely alter activity coefficients, and make their calculations nearly impossible (Morse and Bender, 1990) [Note: activity coefficients indicate the fraction of ions available for chemical interactions]. If activity coefficients are not considered when calculating the partitioning of elements between two phases, the results can be misleading (Morse and Bender, 1990). Therefore, the partition coefficients presented here should not be considered absolute thermodynamic distribution coefficients (K_D; see Mucci and Morse, 1990 and section 4.1 of Chapter 1).

3. Results and Discussion

3.1 Trace and minor element partition coefficients in Mytilus edulis *calcite*

Figure 1 illustrates the element to calcium ratios in the shells, seawater, and hemolymph for ten elements (tissues are in ppb, or μg/kg). These variations can not be attributed to variations in hemolymph Ca, since hemolymph Ca only varied 6 % (%RSD) among all samples.

Ratios of Sr/Ca were consistently slightly higher in hemolymph as compared to water (Fig. 1), but were much lower in the shells, in accordance with a Sr partition coefficient (D_{Sr}) of 0.14 (for both hemolymph and water), which is very similar to the D_{Sr} determined by Lorens and Bender (1980) for *M. edulis* (0.13; Table 1). Magnesium also matches the results of Lorens and Bender (1980) very well, and is the same for both sources (Table 1). Uranium is substantially lower in both hemolymph and shells compared to water ($D_U = 0.03$), but falls close to the range of D_U measured in inorganic calcites which range from 0.04 to 0.26 (Kitano and Oomori, 1971). Partition coefficients for Cd, Mn, and Co (and Sr) were determined to be

strongly precipitation rate dependent in calcite (Lorens, 1981). At the approximate crystal growth rate of *M. edulis*, the expected partition coefficients are ~5 for Mn, ~10 for Cd, and ~2 for Co (Lorens, 1981). Depending on whether the water or the hemolymph is taken, the results presented here roughly agree with this (Table 1). However, it could be expected that the hemolymph would be a better indication of the source of ions for the calcite (see introduction). The expected D_{Mn} is found when using hemolymph as the source, but Co and Cd are farther from expected. Nevertheless, this could have to do with the availability of the ions in the hemolymph. For example, Cd is known to be bound to proteins (Nair and Robinson, 2000), which could make it more difficult to pass into the EPF. Similar to Mg, B is also apparently strongly regulated, since B/Ca was about 3500 times lower in the shell compared to the water and hemolymph. When considering the inorganic D_B, the shell has about 10 times less B than expected (Table 1). Similarly, Co/Ca ratios were also lower in the shell compared to the hemolymph (Fig. 1, Table 1).

Table 1. Partition coefficients (D_{Me}) between *M. edulis* calcite and water (Water D_{Me}), and *M. edulis* calcite and hemolymph (Hemo D_{Me}) compared with both inorganic expected D_{Me} (i Exp D_{Me}) and biogenic expected D_{Me} (b Exp D_{Me}).

Me	Pb	U*	B*	Mg	Mn*	Co*	Cu*	Zn*	Sr	Cd*
Water D_{Me}	3.14	0.03	0.00026	0.0012	17.07	2.24	0.73	2.28	0.14	0.26
Hemo D_{Me}	0.69	0.16	0.00024	0.0012	7.42	0.060	0.030	0.15	0.14	0.0061
i Exp D_{Me}	17.2	0.26	~0.003	0.017	~5	~2	~23	~4.5	0.25	~10
b Exp D_{Me}		0.01	~0.004	0.0013				~9	0.13	~1

*shell data from Knokke shell; **i Exp D_{Me}** (inorganic expected D_{Me}) from Lorens, 1981 (Cd, Mn, and Co); Kitano and Oomori, 1971 (U); Hemming et al., 1995 (B, recalculated); Mucci, 1987 (Mg); Carpenter and Lohman, 1992 (Sr); Kitano et al., 1980 (Cu); Rimstidt et al., 1998 (Pb); Dardenne (1967) (Zn) and **b Exp D_{Me}** (biogenic) from Lorens and Bender, 1980 (Sr and Mg from *M. edulis* calcite); Vengosh et al., 1991 (B, recalculated); Marechal-Abram et al., 2004 (Cd in benthic foraminifera) Russell et al., 2004 (U in planktonic foraminifera); Marchitto et al., 2000b (Zn in benthic foraminifera).

Lead in bivalve shells has been suggested to be an excellent indicator of pollution (see Chapter 9 for references), with a bioconcentration factor of 10,000 (versus water) being noted in some bivalves (Pitts and Wallace, 1994). However, when considering hemolymph as the source of Pb for the shell, it appears that Pb is actually not concentrated in the shell, but is excluded (Fig. 1), in opposition to what is expected from inorganic calcite (Table 1).

Ratios of Mn/Ca, Cu/Ca, and Zn/Ca were all also considerably higher in the hemolymph as compared to the water and thus must come from the food or are concentrated physiologically (i.e., ionoregulation or bioaccumulation). Copper, Zn, and Mn are important biological ions; for example, Cu is the oxygen carrier in invertebrate hemolymph (compared with Fe in mammal blood), where as Mn is associated with organic molecules (Mathew et al., 1996). Therefore, some of these elements are expected to be higher in the hemolymph than the water.

At first sight, some elements with consistent D_{Me} between other studies and hemolymph and water (e.g., Sr and Mg) might seem promising proxies of environmental conditions (cf. Campana, 1999). However, there are other problems associated with these proxies. For example, Sr is highly precipitation rate dependent in calcite (Lorens, 1981), which has recently been shown in biogenic calcite as well (Lorrain et al., subm. a). Furthermore, Mg is often associated with the shell organic matrix (Takesue and van Geen, 2004) and does not track temperature in *M. edulis* shells (Vander Putten et al., 2000). These elements however may roughly record variations in water concentrations as was shown by Lorens and Bender (1980), but *M. edulis* do not survive in salinities below ~10 (see Chapter 10 and Qiu et al., 2002) and Mg/Ca and Sr/Ca usually remain constant above this salinity (Dodd and Crisp, 1982). Therefore, the usefulness of this is extremely limited.

3.2 Is food a source of ions to the shell?

Out of the few elements measured in food (Table 2), Mg, Mn and Ca are higher in phytoplankton as compared to the yeast. The increased Mg in the phytoplankton (Table 1) is reflected in the higher tissue concentrations, but not in the hemolymph (Fig. 1), which can be assumed to be the route to the shell. This suggests that Mg from food is not an important source for the shell. Although Mn is regulated at higher level in the hemolymph compared to water, similar to other bivalve species (Mathew et al., 1996), there is no sign of increased Mn in the hemolymph, nor tissues, with elevated Mn in food. This also implies that there is no link between Mn ingested as food and shell Mn/Ca ratios, as was hypothesized by Vander Putten et al. (2000) and Lazareth et al. (2003). Ratios of Co/Ca were generally low in the shell, tissues and water, but were higher in the hemolymph compared to water in mussels fed yeast and lower in

mussels fed phytoplankton. Unfortunately, Co was not measured in the food, so no concrete conclusions can be drawn, but Co from food does seems to enter the hemolymph based on these limited data. Copper was much higher in the phytoplankton than yeast; however, the opposite was observed in the hemolymph. Uranium and Sr were not drastically different in the two diets offered and no substantial differences were noted in the tissues or hemolymph. One phytoplankton treatment had high Pb (Table 1), but this is not reflected in the tissues or hemolymph (Fig. 1).

Table 2. Elemental concentrations (mean ± s.d., n = 3) in food items (ppm or μg/g).

Food	Ca	Mg	Pb	Sr	U	Mn	Cu
Yeast	545±3	947±28	0.19±0.08	2.1±0.2	0.03±0.00	6.0±0.3	4.2±0.3
Phyto+0	1109±24	2616±65	5.4±0.2	3.3±0.1	0.03±0.00	73.0±2.3	148±1
Phyto+100	1046±27	1777±41	0.26±0.01	1.2±0.03	0.01±0.00	50.2±2.0	25.0±0.3

See Chapter 10 for description of phytoplankton batches phyto+0 (Tank 5) and phyto+100 (Tank 5.5).

3.3 The interaction of other ions (Ba) on D_{Me}

This experiment was designed to determine Ba uptake in the shells, but this also allowed us to test the effect of increased Ba on other elements. Clearly there is an effect as in Tanks 1 and 2, water, hemolymph and shells have similar Mg/Ca ratios, but at higher Ba concentrations (Tanks 3 and 4), there are higher shell Mg/Ca ratios, although not in the water or hemolymph (Tank 1 had high variation and thus was not statistically different from 3 and 4, but Tank 2 was lower than 3 and 4 (ANOVA, $p < 0.05$)). This could be an effect of Ba interfering with the physiological regulation of Mg into the EPF, or a physical effect of Ba incorporation into the crystal lattice. The effect of Ba in the crystal lattice is not supported by the high-resolution profiles of shell sections, where Mg/Ca ratios do not change when Ba/Ca ratios peak (see Chapter 10 and Vander Putten et al., 2000). On the other hand, it has been hypothesized that *M. edulis* strongly regulate Mg entering the EPF (Lorens and Bender, 1977) in order to produce low-Mg calcite (notice that shell Mg/Ca ratios are 1000 times lower than water and hemolymph). Thus it is possible that Ba interferes with this physiological mechanism.

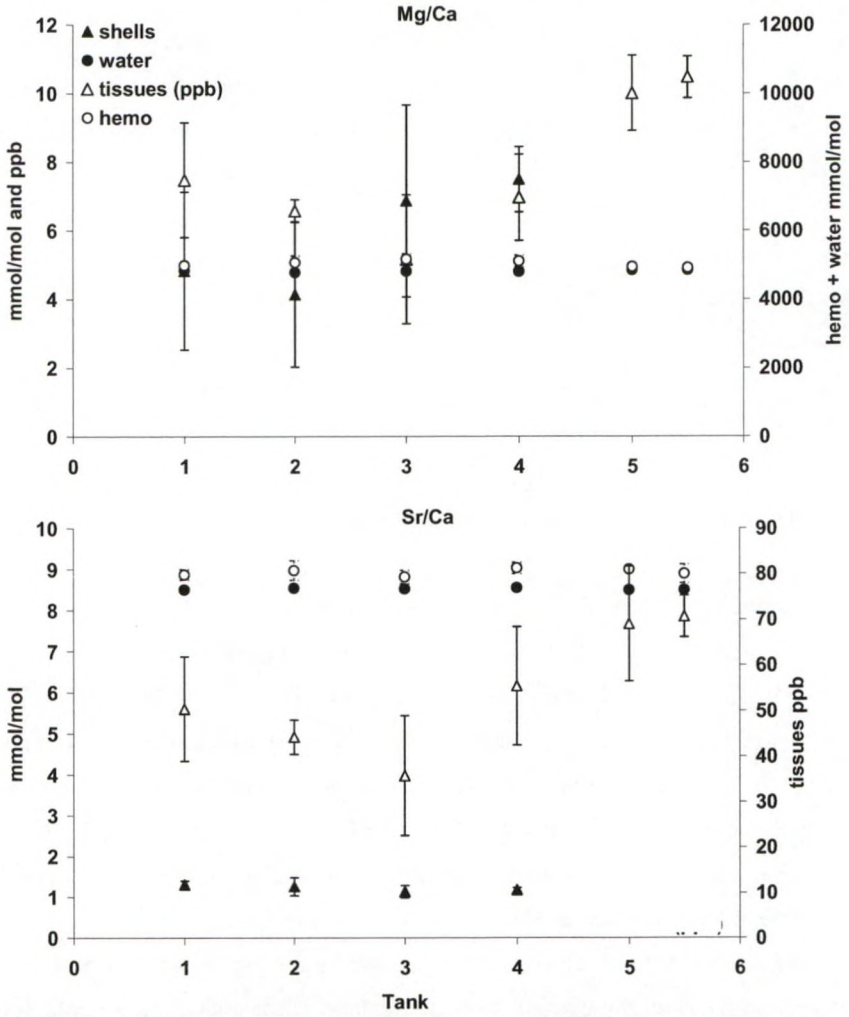

Figure 1. Element to calcium ratios in shells (n = 6 to 9), water (n = 2), and hemolymph (hemo; n = 6 to 9), and elemental concentrations in tissues (n = 3). n refers to the number of samples per treatment. Tanks 1 through 4 had the same conditions aside from different Ba concentrations (Ba/Ca = T1: 5.1, T2: 19.4, T3: 36.3, T4: 65.1 µmol/mol). Tank 5 had the same conditions as Tank 1, but mussels were fed phytoplankton with low (Tank 5) and high (illustrated as Tank 5.5) Ba concentrations, instead of yeast. The shell at position 0.5 is the average and standard deviation from the Knokke shell (see Materials and Methods). Error bars represent standard deviation. Note that the left y-axis is for all parameters unless a second y-axis is given (parameters for second y-axis listed on axis).

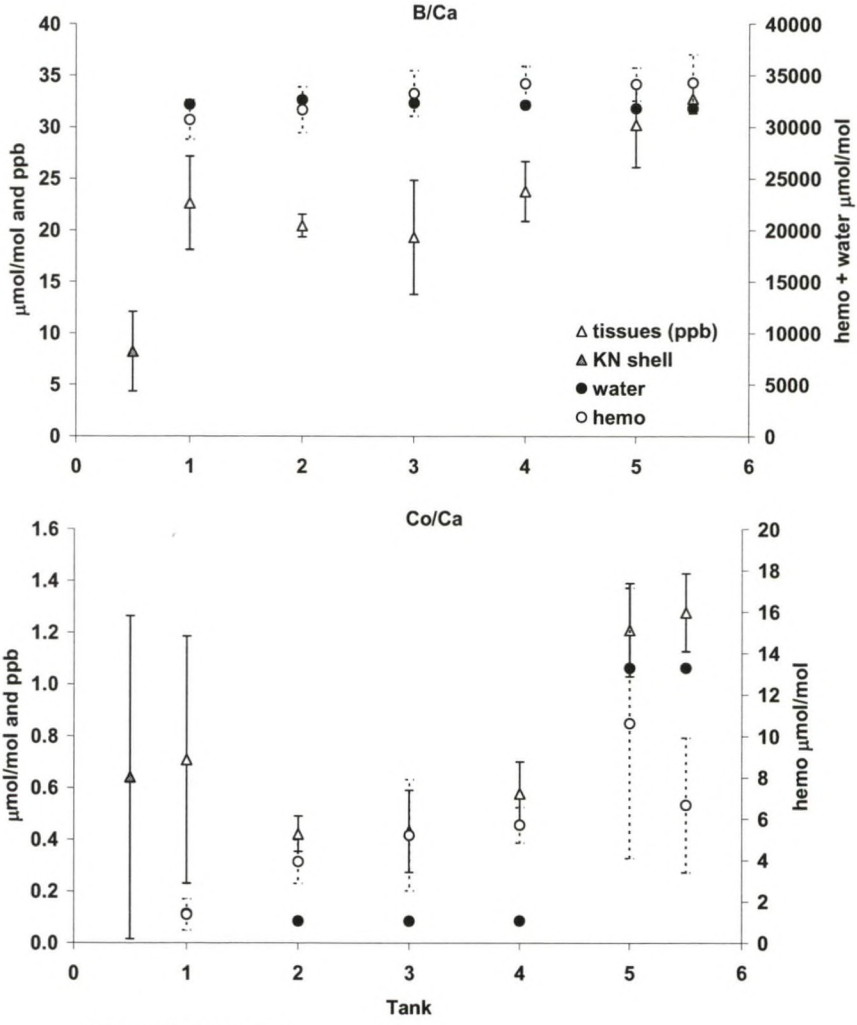

Figure 1. *Continued.*

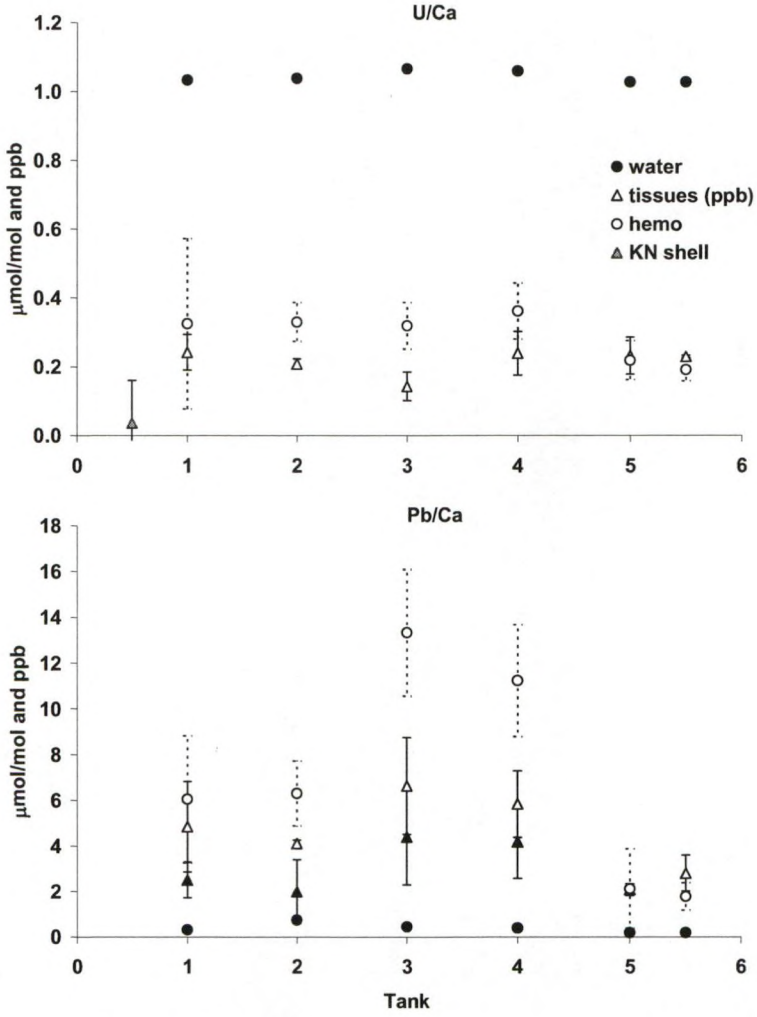

Figure 1. *Continued.*

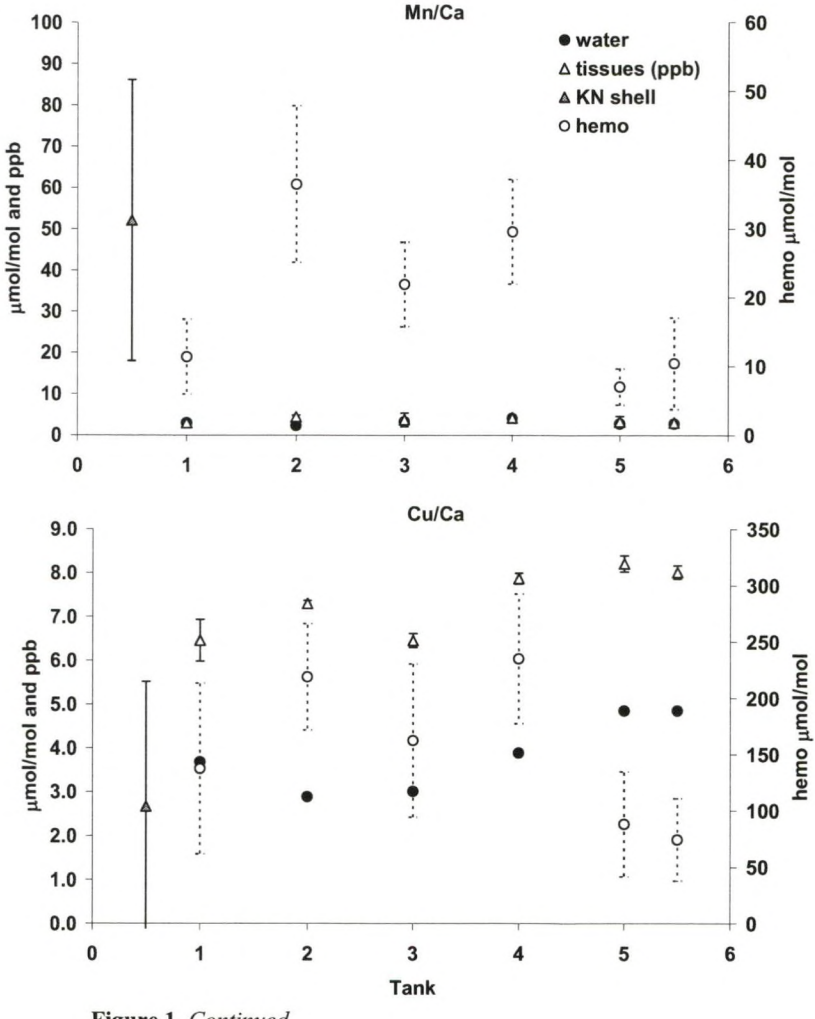

Figure 1. *Continued.*

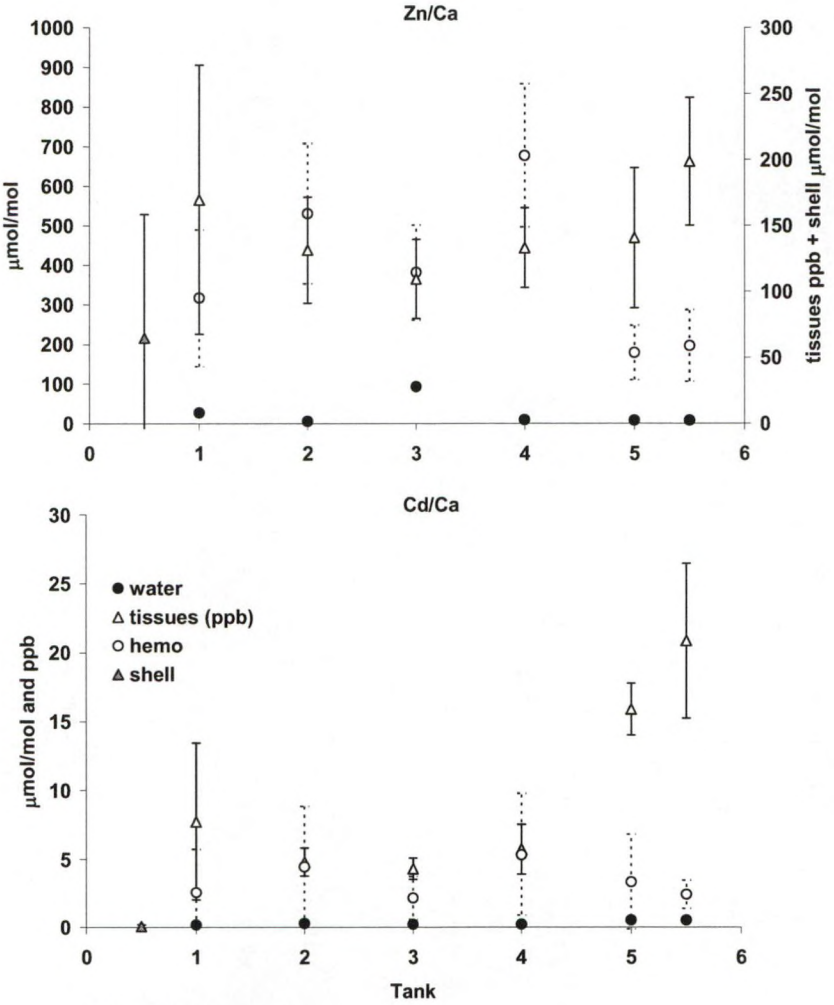

Figure 1. *Continued*

A similar trend is also seen in the Pb/Ca data, with shells from Tank 1 and 2 being lower than 3 and 4 (all significant at $p < 0.05$ (ANOVA), except 1and 4), but here the hemolymph is also elevated.

Interestingly, hemolymph B/Ca and Co/Ca ratios also show positive correlations with Ba/Ca water concentrations (Fig. 1; B/Ca slope = 0.0048 ± 0.0011, $p < 0.001$, $R^2 = 0.34$; and Co/Ca slope = 6.02 ± 1.04, $p < 0.001$, $R^2 = 0.50$), possibly indicating that Ba is also influencing the physiological regulation of these elements or the incorporation of these elements in the shell.

Spangenberg and Cherr (1996) noted adverse effects of Ba on *M. edulis* embryos. At 100 µg/l there were severe adverse developmental effects as well as abnormal shell calcification. Although the concentrations used in the present study were lower (maximum ~ 70 µg/l) and adult mussels were used, minor cellular damage or impairment still may have occurred at the higher Ba levels. This could explain the effect of Ba concentration found on Mg, Pb, B, and Co discussed above. Using the hemolymph D_{Me} of these elements as an indication of regulation to the EPF, Mg, Pb, B, and Co all seem to be physiologically excluded from the EPF. Thus this physiological mechanism could possibly have been disrupted by the toxicity of Ba.

It could be argued that ions may enter the hemolymph from the gut and quickly be moved from the hemolymph to the EPF or elsewhere. However, this would require a fast turn-over rate of the hemolymph. In a preliminary experiment, high levels of calcein (determined visually) was still present three days after calcein incubation even though the mussels were in calcein-free seawater. This suggests that hemolymph turnover rates are slow and that the sampling design would have captured any ions entering the hemolymph from the gut.

3.4 General remarks and recommendations

Although these data do not allow many concrete conclusions to be drawn, there are some interesting points. Firstly, partition coefficients are provided for many elements for the first time, and in addition D_{Me} calculated using internal and external water sources are compared (Table 2). Partition coefficients between water and shell and

hemolymph and shell give very different values (except for B, Mg, and Sr), with one often suggesting a concentration effect and the other the opposite. It was found that the physiology regulating Mg, Pb, B, and Co may be affected by other ions (in this case Ba), and hence could affect shell concentrations. Additionally, food does not seem to be an important source for Mg and Mn in *M. edulis* calcite. In conclusion, these data shed light on some aspects of *M. edulis* trace element incorporation, but highlight the complexities involved in using marine bivalves as paleoenvironmental proxies. Using the results presented here as a basis from which to draw new ideas, similar experiments should be conducted to bring us closer to a mechanistic understanding of trace element incorporation in bivalve shells.

Chapter 12

Conclusions

Previous studies have given mixed conclusions about the potential of bivalves as environmental proxies. It has been illustrated that **$\delta^{18}O$** is an excellent proxy of sea surface temperature (SST) in deep sea marine bivalves (e.g., Weidman et al., 1994; Schöne et al., 2004), but the data from estuarine and coastal bivalves have been difficult to interpret. As described in Chapters 1 and 4, the $\delta^{18}O$ of bivalve shells ($\delta^{18}O_S$) is dependent on both the $\delta^{18}O$ of the water ($\delta^{18}O_W$) and the water temperature at the time of crystallization. Thus large errors can be made when calculating SST from $\delta^{18}O_S$ of estuarine species and even from oceanic bivalves if incorrect assumptions are made about the changes in past $\delta^{18}O_W$. A prime example of this is illustrated in Chapter 4, where it is shown that even with detailed salinity data and some indications of the salinity-$\delta^{18}O_W$ relationship, errors in calculated average water temperatures ranged from 1.7 to 6.4 °C warmer than measured. Considering that we are attempting to determine small SST changes, for example, on the order of 1 °C over the past millennium (Mann et al., 1998; Briffa, 2000), these proxies must be robust. Therefore, to overcome the difficulties inherent to the $\delta^{18}O$ proxy, either a salinity independent (i.e., temperature only) proxy or a salinity proxy are needed, especially for estuarine and coastal bivalves, which were the focus of this dissertation.

One of the earliest salinity indicators proposed was **$\delta^{13}C$** in carbonates ($\delta^{13}C_S$) (Mook and Vogel, 1968; Mook, 1971). This was primarily through the assumption that $\delta^{13}C$ in carbonates reflects the $\delta^{13}C$ of the dissolved inorganic carbon ($\delta^{13}C_{DIC}$), which is often conservative along the upper salinity gradient in estuaries (e.g., Fry, 2002; Hellings et al., 2001; Chapter 6). However, more recent works have illustrated that metabolic CO_2 interferes with this signal (Tanaka et al., 1986; McConnaughey et al., 1997; Lorrain et al., 2004a). The ontogenic decrease in shell $\delta^{13}C$ observed in many species of bivalves has been hypothesized to be caused by increased absolute metabolism in larger individuals resulting in an increase of internal metabolic $^{12}CO_2$ available for calcification (Lorrain et al., 2004). The *Mercenaria mercenaria*

hemolymph $\delta^{13}C$ data presented in this work are negatively correlated with shell length, and therefore agree with this hypothesis (Chapter 5). Nevertheless, this effect is generally considered to be small in aquatic animals, with ~ 10 % metabolic CO_2 being incorporated, usually changing the shell $\delta^{13}C$ less than 2 ‰ (McConnaughey et al., 1997). In contrast, Chapter 5 illustrates that this effect can be rather large in relatively long lived bivalves, with *Mercanaria mercenaria* shells containing up to 35 % metabolic CO_2. Furthermore, it was shown that this is species specific, with another member of the same family of clams (*Saxidomus giganteus*) containing the expected < 10 % metabolic CO_2, even over 10 years growth (Chapter 4). However, despite these results, there is still the possibility that the metabolic effect can be removed when certain variables are known. McConnaughey et al. (1997) propose an equation where the % metabolic CO_2 incorporated in the shell (%M) can be calculated if $\delta^{13}C_{DIC}$, $\delta^{13}C$ of respiring tissues and $\delta^{13}C_S$ are known. Therefore, if a proxy to determine %M could be developed, $\delta^{13}C_{DIC}$ could be determined (both $\delta^{13}C$ of respiring tissues and $\delta^{13}C_S$ can be extracted from fossil shells – see Chapter 5). However, attempts to use shell biometrics (e.g., length) did not result in good enough correlations to accurately predict %M. Alternatively, large changes in $\delta^{13}C_{DIC}$ could possibly be identified in shell $\delta^{13}C$ if the %M is constant enough in a particular bivalve species. Unfortunately, this also did not give promising results as bivalves that grew in salinities differing by 4 could not be separated using $\delta^{13}C_S$ data (Chapter 6). Thus, $\delta^{13}C_S$ cannot confidently be used to determine salinity, although it can be used to provide a rough indication of $\delta^{13}C_{DIC}$ and salinity.

There have been many successful reports of salinity independent proxies in other biogenic carbonates, such as foraminiferal calcite (Mg/Ca; Nürnberg et al., 1996; Lea et al., 1999; Elderfield and Ganssen, 2000; Shevenell et al, 2004; Pak et al., 2004), coral aragonite (Sr/Ca; Weber, 1973; Beck et al., 1992; McCulloch et al., 1994, 1999; Sinclair et al., 1998; Fallon et al., 1999; Swart et al., 2002b) and sclerosponge aragonite (Sr/Ca; Swart et al., 2002a; Haase-Schramm et al., 2003; Rosenheim et al., 2004, 2005). In fact, these proxies have been shown to be so robust that many studies have used the salinity independent SST proxy to deconvolve $\delta^{18}O_W$ from the $\delta^{18}O$ carbonate record and use salinity-$\delta^{18}O_W$ relationships to determine changes in salinity (corals: Ren et al., 2003; foraminifera: Schmidt et al., 2004; Stott et al., 2004; and

sclerosponges: Rosenheim et al., 2005). Thus, one would expect that these proxies would also be useful in bivalves.

Temperature exerts a strong influence on **Mg/Ca** ratios in inorganic **calcite** (Mucci, 1987; Oomori et al., 1987), and formaniferal calcite (Nürnberg et al., 1996; Lea et al., 1999). Thus, similar to Sr/Ca in aragonite, we would expect Mg/Ca ratios in bivalve calcite to record SST. Indeed, there have been several reports that Mg/Ca is related to SST in bivalve calcite (Dodd, 1965; Klein et al., 1996a; Lazareth et al., 2003; De Ridder et al., 2004). However, other reports have shown that the relationship does not hold over the year (Vander Putten et al., 2000) or that ontogenic effects interfere in older specimens (Freitas et al., 2005). Considering that Vander Putten et al. (2000) clearly demonstrated the poor relationship between Mg/Ca and temperature in *M. edulis* (the calcitic bivalve used in this study), the field Mg/Ca data were not presented here (which are in agreement with Vander Putten et al., 2000). Data from the laboratory suggest that Mg is strongly regulated by *M. edulis* (Chapter 11) as proposed by Lorens and Bender (1977), with the shell containing about 10 times less Mg than inorganic calcite. Lorens and Bender (1977) suggest that *M. edulis* biologically regulates the amount of Mg entering the EPF to produce low-Mg calcite. The data in Chapter 11 illustrate that the partition coefficients (D_{Mg}) between water and shell and hemolymph and shell are the same (0.0012) (and are the same as reported by Lorens and Bender (1980), 0.0013); thus the regulation does not occur at the boundary between water and hemolymph, but likely at the hemolymph – EPF boundary. Indeed, similar to Lorens and Bender (1977), an apparent regulatory breakdown in this mechanism was noted (in this study caused by high levels of Ba – see Chapter 11). Therefore, it is probably this strong biological regulation that obscures the Mg/Ca – SST relationship in bivalve calcite.

Mg/Ca ratios in coral **aragonite** have been shown to track temperature fluctuations (Mitsuguchi et al., 1996; Sinclair et al., 1998; Fallon et al., 1999), but more recent reports have shown that Mg is under strong biological control in corals, being correlated to the fine scale structure of the skeleton (Meibom et al., 2004). Ratios of Mg/Ca in bivalve aragonite have been shown to be correlated with SST in some species (R^2 = 0.71; Takesue and van Geen, 2004), and not at all in others (slope not

significant; Chapter 7). In Chapter 7 a review of the literature is provided, which demonstrates the inconsistencies in the Mg/Ca-SST relationship between and among species, suggesting that there is no general correlation between Mg/Ca ratios and temperature in aragonitic bivalve shells.

In inorganic **calcite**, it has been demonstrated that **Sr/Ca** ratios are kinetically controlled, fluctuating as a function of precipitation rate with little to no effect of temperature (Lorens, 1981; Morse and Bender, 1990; Tesoriero and Pankow, 1996). Reports of Sr/Ca ratios in calcitic bivalves have been inconclusive, with some suggesting that Sr/Ca ratios track changes in salinity (Klein et al., 1996b), whereas others have suggested metabolic and or kinetic effects dominate (Vander Putten et al., 2000; Lazareth et al., 2003; Freitas et al., 2005). However, our group has clearly demonstrated for the first time that Sr/Ca ratios are under kinetic controls in the calcitic bivalve *Pecten maximus* (Lorrain et al., subm. a). Nevertheless, this does not necessarily render Sr/Ca ratios in calcite useless, as the same effect has been used to determine productivity in coccolith calcite (Stoll and Schrag, 2000; Stoll and Bains, 2003), and can probably be used as a proxy of calcification rates in bivalves. However, it should be kept in mind that the Sr/Ca partition coefficient (D_{Sr}) in *P. maximus* (0.20 ± 0.01) is closer to the inorganic D_{Sr} (0.25; Carpenter and Lohman, 1992) than *Mytilus edulis* calcite (0.13 – 0.14; Lorens and Bender, 1980; Chapter 11), which might suggest that other biological factors play a role in *M. edulis* calcite Sr/Ca.

Contrary to inorganic calcite, inorganic **aragonite Sr/Ca** is not largely affected by precipitation rates and exhibits a strong inverse relationship with temperature (Kinsman and Holland, 1969; Zhong and Mucci, 1989); hence its great success in coral and sclerosponge aragonite. However, bivalves apparently do not incorporate Sr into their shells in the same manner. Stecher et al. (1996) was one of the first to illustrate that high-resolution Sr/Ca profiles were roughly positively correlated with growth rate (similar to calcite). They measured Sr/Ca in two species of aragonitic clams, *Mercenaria mercenaria* and *Spisula solidissima*. They found that Sr/Ca ratios were positively correlated with temperature in *M. mercenaria* and negatively in *S. solidissima*. Considering that *M. mercenaria* exhibits highest growth in summer and

S. solidissima in winter, they attributed the Sr/Ca ratio variations to growth rate. Nevertheless, their results have repeatedly been mis-cited as being a temperature control (Holmden and Hudson, 2003; Martin et al., 2004; Freitas et al., 2005). In Chapter 8 it is shown that the growth rate effect noted for *M. mercenaria* by Stecher et al. (1996) does not always hold. In the nine specimens analyzed in this thesis, none exhibited a strong relationship between annual growth rate and Sr/Ca ratios. However, similar to Stecher et al. (1996), a strong positive relationship between annual growth rate and Sr/Ca ratios was found in *S. giganteus* shells (R^2 = 0.73) (Chapter 8). Considering that the calcification fluid (extrapallial fluid, EPF) of aragonite bivalves is not greatly different from seawater (Wada and Fujinuki, 1976; Lorrain et al., 2004b), it is hypothesized that Sr^{2+} discrimination in aragonitic bivalve shells occurs during shell crystallization, at the crystal surface, and not at biological membranes. Indeed, there is strong evidence that there are biological controls on crystal formation (e.g., Falini et al., 1996), which could possibly also regulate Sr/Ca ratios in the shell. Therefore, Sr/Ca ratios in aragonitic bivalves should only be used as a proxy with great caution, if at all.

Ratios of U/Ca have also received some attention as a temperature proxy in coral aragonite (Sinclair et al., 1998; Fallon et al., 1999; Cardinal et al., 2001), but little has been published on bivalve aragonite. Although, the data presented here do not suggest that this is a SST proxy in bivalve aragonite (Chapter 7), more species need to be sampled before this can be considered conclusive.

Unlike Mg/Ca and Sr/Ca ratios in seawater, **Ba/Ca** ratios in seawater strongly vary with salinity (Dodd and Crisp, 1982; Chapter 10). Consequently, Ba/Ca ratios have been proposed as a proxy of dissolved seawater Ba/Ca in aragonitic corals (Tudhope et al., 1996; McCulloch et al., 2003; Sinclair and McCulloch, 2004), calcitic foraminifera (Lea and Boyle, 1989; 1991) and vesicomyid clam shells (Torres et al., 2001) providing information on salinity, nutrient and alkalinity distributions in past oceans. However, there are 'anomalous' Ba/Ca peaks in coral aragonite that cannot be explained by environmental parameters (Sinclair, in press). Despite the fact that inorganic aragonite and calcite behave differently in their Ba incorporation (temperature dependence in aragonite (Dietzel et al., 2004) and precipitation rate

effects in calcite (Tesoriero and Pankow, 1996)), both bivalve **calcite and aragonite** have a near-ubiquitous Ba/Ca pattern in their shells, with a more or less stable background Ba concentration, interspaced with sharp episodic Ba peaks (Stecher et al., 1996; Toland et al., 2000; Vander Putten et al., 2000; Torres et al., 2001; Lazareth et al., 2003; Chapter 7 and 10). Stecher et al. (1996) first proposed that these peaks were the result of the filter feeding bivalves ingesting Ba-rich particles associated with diatom blooms, as either phytoplankton, or barite. Both calcite and aragonite bivalve shells show highly reproducible Ba/Ca profiles in shells from the same site (Vander Putten et al., 2000; Chapter 7), indicative of an external factor controlling the patterns. The peaks roughly correspond to the start of the phytoplankton bloom (Vander Putten et al., 2000; Chapter 7), but not all peaks coincide with a Chl a peak (Chapter 7). The feeding experiments conducted here were inconclusive (Chapter 10), but the limited data, combined with data from the field (Chapter 7 and 10), indicate the link between phytoplankton abundance and the Ba/Ca peaks are not straightforward. Nevertheless, their reproducibility suggests that in the future they may prove to be a reliable proxy for some environmental parameter. Unlike the peaks, the background Ba/Ca levels in *M. edulis* calcite could be related to the Ba/Ca ratio of the water in which they grew (Chapter 10). There was a highly significant correlation between water and shell Ba/Ca in both animals grown in the field and laboratory, with the field data providing a D_{Ba} of 0.07, similar to the inorganic D_{Ba} of 0.05 (Tesoriero and Pankow, 1996). This suggests that background Ba/Ca ratios in bivalve shells are potentially a proxy of the Ba/Ca ratio of estuarine water. However, it was also found that the background Ba/Ca levels in the aragonite shells of *S. giganteus* exhibited a decrease through ontogeny. Considering aragonite should not have a precipitation rate effect (see above), this is probably a biological control on background Ba/Ca ratios. This provides another good example why all proxies should be considered species specific. Nevertheless, Ba/Ca ratios in bivalve shells seem to contain environmental information and future research should focus on this proxy.

Both corals and sclerosponges have been shown to trace anthropogenic Pb inputs into the ocean (Shen and Boyle, 1987; Lazareth et al., 2000; Swart et al., 2002a). Similarly, the use of bivalve shells as continuous recorders of **pollution** has also received considerable attention over the past few decades. However, many studies

have analyzed whole shells (Koide et al., 1982; Yap et al., 2003), and not high-resolution time series. Vander Putten et al. (2000) analyzed high-resolution **Pb/Ca** profiles in *M. edulis* shells and found that there was a metabolic influence on Pb/Ca ratios. The data presented in Chapter 7 and 9 confirm what Vander Putten et al. (2000) found for *M. edulis* for two other bivalve species, that intra-annual variations in Pb/Ca are not solely related to environmental Pb. However this does not exclude the possibility that large changes in environmental Pb concentrations would be recorded in the shells. Indeed, Richardson et al. (2001) analyzed Pb concentrations in *Modiolus modiolus* shells from a polluted and non-polluted site covering 10 years of growth and found elevated levels in shells from the polluted site, as well as a decrease of concentrations through time. They attributed the decreasing Pb in the shells to the decline in pollution at the polluted site. However, they could not deconvolve age and time, and age has been shown to influence Pb concentrations in some mollusks (Hirao et al., 1994). Nevertheless, Pb/Ca ratios from a chronology of several *M. mercenaria* shells illustrated that there was no clear age effect on Pb/Ca ratios in the shells. Furthermore, although there was considerable variation in the data, the anthropogenic Pb profile could be seen in the 54 year chronology. This indicates that although bivalve shells may not be the most suitable substrate for tracking Pb pollution, they can provide information when enough individuals are sampled.

Although many of the results presented in this dissertation are negative (summarized in Table 1), many interesting data have been provided. There are three main points which can be concluded from this work:

1. Factors determining elemental incorporation in bivalve carbonate is species specific;
2. Bivalves strongly regulate elemental incorporation for many (most) elements; and
3. In bivalve carbonate, $\delta^{18}O$, Ba/Ca and possibly Pb/Ca seem to be useful proxies, while $\delta^{13}C$, Sr/Ca, Mg/Ca and U/Ca are strongly influenced by vital effects.

Table 1. Overview of potential and problems of proxies measured in this study (based on literature and results from this study). Subscripts A and C refer to aragonite and calcite, respectively. SST = sea surface temperature; SSS = sea surface salinity, partic. = particulate; '→ SSS' indicates that the proxy could give an indication of salinity. Ch. denotes the chapters where the proxy is discussed (in addition to Chapter 1).

Proxy	of	Bivalve $CaCO_3$	Problems	Ch.
$\delta^{18}O_{A+C}$	SST	Excellent, little to no vital effects	Unknown $\delta^{18}O_W$ can cause very large errors	4
$\delta^{13}C_{A+C}$	$\delta^{13}C_{DIC}$ → SSS	Only large changes	Metabolic CO_2 interferes with signal and effect is highly variable	4, 5, 6
Mg/Ca_A	SST	Only sometimes weakly correlated with SST[1]	Strong vital effects, problems of association with organic matrix[1]	7
Mg/Ca_C	SST	Species specific and inconclusive[2]	Vital effects	11 +
Sr/Ca_A	SST	Sometimes cyclic, but not temperature controlled	Strong vital effects	8
Sr/Ca_C	SST	Sometimes cyclic, but not temperature controlled	Kinetic effects	11 *
Ba/Ca_A	Ba/Ca_{water} → SSS	Background Ba/Ca exhibits ontogenic effects	Vital effects, more work needed	7
Ba/Ca_C	Ba/Ca_{water} → SSS	Excellent correlation with background Ba/Ca	More work needed before this can be considered a robust proxy	10
Ba/Ca_A	$Ba/Ca_{partic.}$	Peaks reproducible, but direct link with $Ba/Ca_{partic.}$ remains elusive	Inconclusive	7
Ba/Ca_C	$Ba/Ca_{partic.}$	Peaks reproducible, but direct link with $Ba/Ca_{partic.}$ remains elusive	Inconclusive	10 +
Pb/Ca_A	Pb/Ca_{water}	Large changes evident	Vital effects, intra-annual data highly variable	7, 9
Pb/Ca_C	Pb/Ca_{water}	Intra-annual data highly variable	Vital effects	11 +
Pb/Ca_A	$Pb/Ca_{partic.}$	Large changes evident	Vital effects, intra-annual data highly variable	7, 9
Pb/Ca_C	$Pb/Ca_{partic.}$	Intra-annual data highly variable	Vital effects	11 +
U/Ca_A	SST, SSS, alkalinity	Strong ontogenic effects	Vital effects	7
U/Ca_C	SST, SSS, alkalinity	??	Low concentrations	11

* Lorrain et al. (submitted); + See also Vander Putten et al., 2000; [1]Takesue and van Geen, 2004; [2]see also Freitas et al., 2005

RECOMMENDATIONS FOR FUTURE RESEARCH

1. Laboratory experiments, similar to those in Chapter 10 & 11 are needed. Properly designed experiments would give a better mechanistic understanding of proxy incorporation in bivalve carbonate. In these experiments, smaller mussels with higher growth rates should be used to avoid the problem of slow growth encountered. Mussels of around 1 cm would probably be the best. Chapter 11 suggests many interesting hypothesis which should be tested. For example, does food contribute to shell elemental concentrations? Can bivalves regulate their internal chemistry? Etc.
2. Frequent collections (at least weekly) of specimens from the field from *in situ* populations, in conjunction with water sampling should be carried out to gain a better understanding of proxy incorporation in natural settings.
3. More research is needed to understand the promising Ba/Ca proxy (both background and peaks). Frequent collections of water, tissue, hemolymph and shell might shed light on a possible mechanism.
4. The newer field of 'non-traditional' isotopes need to be studied in bivalve shells – such as δCa, δMg, δLi, δB, etc.
5. Moving away from environmental reconstruction, understanding what controls trace element incorporation in bivalve shells is an interesting subject that could add to our knowledge of biomineralization and/ or bivalve paleo-ecology.

References

Abelson PH, & Hoering TC (1961) Carbon isotope fractionation in the formation of amino acids by photosynthetic organisms. *Proceedings of the National Academy of Sciences* 47: 623-632.

Addadi L, & Weiner S (1997) Biomineralization - A pavement of pearl. *Nature* 389: 912-912.

Adkins JF, Boyle EA, Curry WB, & Lutringer A (2003) Stable isotopes in deep-sea corals and a new mechanism for "vital effects". *Geochimica et Cosmochimica Acta* 67: 1129-1143.

Alcutt F, & Pinto JT (1994) Glutathione concentrations in the hard clam, *Mercenaria mercenaria*, following laboratory exposure to lead (a potential model system for evaluating exposure to carcinogens and toxins). *Comparative Biochemistry and Physiology C-Pharmacology Toxicology and Endocrinology* 107: 347-352.

Alibert C, Kinsley L, Fallon SJ, McCulloch MT, Berkelmans R, & McAllister F (2003) Source of trace element variability in Great Barrier Reef corals affected by the Burdekin flood plumes. *Geochimica et Cosmochimica Acta* 67: 231-246.

Allam B, Paillard C, & Auffret M (2000) Alterations in hemolymph and extrapallial fluid parameters in the Manila clam, *Ruditapes philippinarum*, challenged with the pathogen *Vibrio tapetis*. *Journal of Invertebrate Pathology* 76: 63-69.

Allison N, & Finch AA (2004) High-resolution Sr/Ca records in modern *Porites lobata* corals: Effects of skeletal extension rate and architecture. *Geochemistry Geophysics Geosystems* 5, Q05001, doi:10.1029/2004GC000696.

Anderson TF & Arthur MA (1983) Stable isotopes of oxygen and carbon and their application to sedimentologic and paleoenvironmental problems: SEPM Short Course, *Society of Sedimentary Geology* 151 pp.

Antajan E & Gasparini S (2004) Assessment of Cryptophyceae ingestion by copepods using alloxanthin pigment: a caution. *Marine Ecology-Progress Series* 274: 191-198.

Antajan E (2004) Responses of calanoid copepods to changes in phytoplankton dominance in the diatom - *Phaeocystis globosa* - dominated Belgium coastal waters. *PhD Thesis*, Vrije Universiteit Brussel, 139 pp.

Antajan E, Chretiennot-Dinet M-J, Leblanc C, Daro M-H, & Lancelot C (2004) 19'-hexanoyloxyfucoxanthin may not be the appropriate pigment to trace occurrence and fate of *Phaeocystis*: the case of *P. globosa* in Belgian coastal waters. *Journal of Sea Research* 52: 165-177.

Arthur MA, Williams DF, & Jones DS (1983) Seasonal temperature-salinity changes and thermocline development in the Mid-Atlantic Bight as recorded by the isotopic composition of bivalves. *Geology* 11: 655–659.

Auclair AC, Joachimski MM, & Lecuyer C (2003) Deciphering kinetic, metabolic and environmental controls on stable isotope fractionations between seawater and the shell of *Terebratalia transversa* (Brachiopoda). *Chemical Geology* 202: 59-78.

Baes CF, & McLaughlin SB (1984) Trace elements in tree rings: evidence of recent and historical air pollution. *Science* 224: 494-497.

Baeyens W, Elskens M, Gillain G, & Goeyens L (1998a) Biogeochemical behaviour of Cd, Cu, Pb and Zn in the Scheldt estuary during the period 1981–1983. *Hydrobiologia* 366: 15-44.

Baeyens W, van Eck B, Lambert C, Wollast R, & Goeyens L (1998b) General description of the Scheldt estuary. *Hydrobiologia* 366: 1-14.

Barbante C, Cozzi G, Capodaglio G, Van de Velde K, Ferrari C, Boutron C, & Cescon P (1999) Trace element determination in alpine snow and ice by double focusing inductively coupled plasma mass spectrometry with microconcentric nebulization. *Journal of Analytical Atomic Spectrometry* 14: 1433-1438.

Barranguet C, Herman PMJ, & Sinke JJ (1997) Microphytobenthos biomass and community composition studied by pigment biomarkers: importance and fate in the carbon cycle of a tidal flat. *Journal of Sea Research* 38: 59-70.

Bassett MV, Wendelken SC, Dattilio TA, Pepich BV, & Munch DJ (2002) The application of tris buffer and copper sulfate for the preservation of phenylurea pesticides analyzed using US EPA method 532 in the UCMR survey. *Environmental Science & Technology* 36: 1809-1814.

Bath GE, Thorrold SR, Jones CM, Campana SE, McLaren JW, & Lam JWH (2000) Strontium and barium uptake in aragonitic otoliths of marine fish. *Geochimica et Cosmochimica Acta* 64: 1705-1714.

Beck JW, Edwards R, Ito E, Taylor FW, Recy J, Rougerie F, Joannot P, & Henin C (1992) Sea-surface temperature from coral skeletal strontium calcium ratios. *Science*, 257: 644–647.

Becker BJ, Fodrie FJ, McMillan PA, & Levin LA (2005) Spatial and temporal variation in trace elemental fingerprints of mytilid mussel shells: A precursor to invertebrate larval tracking. *Limnology and Oceanography* 50: 48-61.

Bemis BE, Spero HJ, Bijma J, & Lea DW (1998) Reevaluation of the oxygen isotopic composition of planktonic foraminifera: Experimental results and revised paleotemperature equations. *Paleoceanography* 13: 150-160.

Benninger LK, Aller RC, Cochran JK, & Turekian KK (1979) Effects of biological sediment mixing on the ^{210}Pb chronology and trace metal distribution in a Long Island Sound sediment core. *Earth and Planetary Science Letters* 43: 241-259.

Benway HM, & Mix AC (2004) Oxygen isotopes, upper-ocean salinity, and precipitation sources in the eastern tropical Pacific. *Earth and Planetary Science Letters* 224: 493-507.

Bernard FR (1983) Physiology and the mariculture of some Northeastern Pacific bivalve molluscs. *Canadian Special Publication of Fisheries and Aquatic Sciences* 63, 1-24.

Bigg GR, & Rohling EJ (2000) An oxygen isotope dataset for marine waters. *Journal of Geophysical Research – Oceans* 105 (C4): 8527-8535.

Blust R, Van der Linden A, Verheyen E, & Decleir W. (1988) Evaluation of microwave heating digestion and graphite furnace atomic absorption spectrometry with continuum source background correction for the determination of iron, copper and cadmium in brine shrimp. *Journal of Analytical Atomic Spectrometry* 3: 387-393.

Boalch R, Chan S, & Taylor D (1981) Seasonal variation in the trace-metal content of *Mytilus edulis*. *Marine Pollution Bulletin* 12: 276-280.

Böhm F, Joachimski MM, Dullo WC, Eisenhauer A, Lehnert H, Reitner J, & Worheide G (2000) Oxygen isotope fractionation in marine aragonite of coralline sponges. *Geochimica et Cosmochimica Acta* 64: 1695-1703.

Boschker HTS, Kromkamp JC, & Middelburg JJ (2005) Biomarker and carbon isotopic constraints on bacterial and algal community structure and functioning in a turbid, tidal estuary. *Limnology and Oceanography* 50: 70–80.

Bouillon S (2002) Organic carbon in a southeast Indian mangrove ecosystem: sources and utilization by different faunal communities. *PhD Thesis*, Vrije Universiteit Brussel, 334 pp.

Bouillon S, Frankignoulle M, Dehairs F, Velimirov B, Eiler A, Abril G, Etcheber H, & Borges AV (2003) Inorganic and organic carbon biogeochemistry in the Gautami Godavari estuary (Andhra Pradesh, India) during pre-monsoon: The local impact of extensive mangrove forests. *Global Biogeochemical Cycles* 17: 1114, doi: 10.1029/2002GB002026.

Bouillon S, Koedam N, Baeyens W, Satyanarayana B, & Dehairs F (2004b) Selectivity of subtidal benthic invertebrate communities for local microalgal production in an estuarine mangrove ecosystem during the post-monsoon period. *Journal of Sea Research* 51: 133-144.

Bouillon S, Moens T, Overmeer I, Koedam N, & Dehairs F (2004a) Resource utilization patterns of epifauna from mangrove forests with contrasting inputs of local versus imported organic matter. *Marine Ecology Progress Series* 278: 77-88.

Bourgoin BP (1990) *Mytilus edulis* shell as a bioindicator of lead pollution - considerations on bioavailability and variability. *Marine Ecology-Progress Series* 61: 253-262.

Bourgoin BP, & Risk MJ (1987) Historical changes in lead in the eastern Canadian arctic, determined from fossil and modern *Mya truncata* shells. *Science of the Total Environment* 67: 287-291.

Boyden CR (1974) Trace-element content and body size in mollusks. *Nature* 251: 311-314.

Boyle EA, Bergquist BA, Kayser RA, & Mahowald N (2005) Iron, manganese, and lead at Hawaii Ocean Time-series station ALOHA: Temporal variability and an intermediate water hydrothermal plume. *Geochimica et Cosmochimica Acta* 69: 933-952.

Brand U, & Veizer J (1980) Chemical diagenesis of a multi-component carbonate system-1. Trace elements. *Journal of Sedimentary Petrology* 50: 1219-1236.

Briffa KR (2000) Annual climate variability in the Holocene: interpreting the message of ancient trees. *Quaternary Science Reviews* 19: 87-105

Broecker WS & Peng T-H (1982) *Tracers in the Sea*. Eldigio Press, 690 pp.

Brown RJC & Milton MJT (2005) Analytical techniques for trace element analysis: an overview. *TrAC Trends in Analytical Chemistry* 24: 266-274.

Buchardt B, & Fritz P (1978) Strontium uptake in shell aragonite from the freshwater gastropod *Limnaea stagnalis*. *Science* 199: 291-292.

Buckel JA, Sharack BL, & Zdanowicz VS (2004) Effect of diet on otolith composition in *Pomatomus saltatrix*, an estuarine piscivore. *Journal of Fish Biology* 64: 1469-1484.

Buddemeier RW, Schneider RC, & Smith SV (1981) The alkaline earth chemistry of corals. *Proceedings of the 4th International Coral Reef Symposium,* Manila. pp. 81 - 85.

Buick DP, & Ivany LC (2004) 100 years in the dark: longevity of Eocene bivalves from Antarctica. *Geology* 32: 921-924.

Buschbaum C, & Saier B (2001) Growth of the mussel *Mytilus edulis* L. in the Wadden Sea affected by tidal emergence and barnacle epibionts. *Journal of Sea Research* 45: 27-36.

Cai DL, Tan FC, & Edmond JM (1988) Sources and transport of particulate organic carbon in the Amazon River and estuary. *Estuarine Coastal and Shelf Science* 26: 1-14.

Campana SE (1999) Chemistry and composition of fish otoliths: pathways, mechanisms and applications. *Marine Ecology-Progress Series* 188: 263-297.

Cantillo AY (1998) Comparison of results of mussel watch programs of the United States and France with worldwide mussel watch studies. *Marine Pollution Bulletin* 36: 712-717.

Capasso G, & Inguaggiato S (1998) A simple method for the determination of dissolved gases in natural waters. An application to thermal waters from Vulcano Island. *Applied Geochemistry* 13: 631-642.

Cardinal D, Hamelin B, Bard E, & Patzöld J (2001) Sr/Ca, U/Ca and $\delta^{18}O$ records in recent massive corals from Bermuda: relationships with sea surface temperature. *Chemical Geology* 176: 213-233.

Carignan J, Cardinal D, Eisenhauer A, Galy A, Rehkamper M, Wombacher F, & Vigier N (2004) A reflection on Mg, Cd, Ca, Li and Si isotopic measurements and related reference materials. *Geostandards and Geoanalytical Research* 28: 139-148.

Carpenter SJ, & Lohmann KC (1992) Sr/Mg ratios of modern marine calcite: Empirical indicators of ocean chemistry and precipitation rate. *Geochimica et Cosmochimica Acta* 56: 1837-1849.

Carpenter SJ, & Lohmann KC (1995) $\delta^{18}O$ and $\delta^{13}C$ values of modern brachiopod shells. *Geochimica et Cosmochimica Acta* 59: 3749-3764.

Carriker MR, Swann CP, Ewart J, & Counts CL (1996) Ontogenetic trends of elements (Na to Sr) in prismatic shell of living *Crassostrea virginica* (Gmelin) grown in three ecologically dissimilar habitats for 28 weeks: A proton probe study. *Journal of Experimental Marine Biology and Ecology* 201: 87-135.

Carroll J, Falkner KK, Brown ET, & Moore WS (1993) The role of the Ganges-Brahmaputra mixing zone in supplying barium and Ra-226 to the Bay of Bengal. *Geochimica et Cosmochimica Acta* 57: 2981-2990.

Chan LH, Drummond D, Edmond JM, & Grant B (1977) On the barium data from the Atlantic GEOSECS expedition. *Deep-Sea Research* 24: 613-649.

Chang VT-C, Williams RJP, Makishima A, Belshawl NS, & O'Nions RK (2004) Mg and Ca isotope fractionation during $CaCO_3$ biomineralisation. *Biochemical and Biophysical Research Communications* 323: 79–85.

Chauvaud L, Lorrain A, Dunbar RB, Paulet Y-M., Thouzeau G, Jean F, Guarini J-M, & Mucciarone D (in press) The shell of the Great Scallop *Pecten maximus* as a high frequency archive of paleoenvironmental change. *Geochemistry, Geophysics, Geosystems*

Chauvaud L, Thouzeau G, & Paulet Y-M (1998) Effects of environmental factors on the daily growth rate of *Pecten maximus* juveniles in the Bay of Brest (France). *Journal of Experimental Marine Biology and Ecology* 227: 83-111.

Chillrud SN, Hemming S, Shuster EL, Simpson HJ, Bopp RF, Ross JM, Pederson DC, Chaky DA, Tolley L-R, & Estabrooks F (2003) Stable lead isotopes, contaminant metals and radionuclides in upper Hudson River sediment cores: implications for improved time stratigraphy and transport processes. *Chemical Geology* 199: 53-70.

Chow TJ, & Patterson CC (1962) The occurrence and significance of lead isotopes in pelagic sediments. *Geochimica et Cosmochimica Acta* 26: 263-308.

Claisse D (1989) Chemical contamination of French coasts - the results of a 10 years mussel watch. *Marine Pollution Bulletin* 20: 523-528.

Clark DL (1971) Arctic Ocean ice cover and its Late Cenozoic history. *Geological Society of America Bulletin* 82: 3313–3324.

Clark GR (1968) Mollusk shell: Daily growth lines. *Science* 161: 800–802.

CoBabe E, & Pratt LM (1995) Molecular and isotopic compositions of lipids in bivalve shells: a new prospect for molecular paleontology. *Geochimica et Cosmochimica Acta* 59: 87-95.

CoBabe E, & Ptak AJ (1999) Comparison of in situ mineral associated lipid compositions in modern invertebrate skeletons: preliminary evidence of dietary and environmental influence. *Paleobiology* 25: 201-211.

Coffey M, Dehairs F, Collette O, Luther G, Church T, & Jickells T (1997) The behaviour of dissolved barium in estuaries. *Estuarine, Coastal and Shelf Science* 45: 113-121.

Cohen AL, & McConnaughey TA (2003) Geochemical perspectives on coral mineralization. In Dove PM, De Yoreo JJ, & Weiner S (eds.) *Biomineralization. Reviews in Mineralogy & Geochemistry* 54. pp. 151-187.

Cook ER, Esper J, & D'Arrigo RD (2004) Extra-tropical Northern Hemisphere land temperature variability over the past 1000 years. *Quaternary Science Reviews* 23: 2063-2074.

Cooper SR, McGlothlin SK, Madritch M, & Jones DL (2004) Paleoecological evidence of human impacts on the Neuse and Pamlico Estuaries of North Carolina, USA. *Estuaries* 27: 617-633.

Coplen TB (1996) New guidelines for reporting stable hydrogen, carbon, and oxygen isotope - ratio data. *Geochimica et Cosmochimica Acta* 60: 3359-3360.

Coplen TB, & Kendall C (2000) Stable hydrogen and oxygen isotope ratios for selected sites of the U.S. Geological Survey's NASQAN and benchmark surface-water networks. *U.S. Geological Survey Open File Report. 00-160*, 1-424.

Craig CA, Jarvis KE, & Clarke LJ (2000) An assessment of calibration strategies for the quantitative and semi-quantitative analysis of calcium carbonate matrices by laser ablation-inductively coupled plasma-mass spectrometry (LA-ICP-MS). *Journal of Analytical Atomic Spectrometry* 15: 1001-1008.

Craig H (1953) The geochemistry of stable carbon isotopes. *Geochimica et Cosmochimica Acta* 3: 53-92.

Cravo A, Bebianno MJ, & Foster P (2004) Partitioning of trace metals between soft tissues and shells of *Patella aspera*. *Environment International* 30: 87-98.

Crenshaw MA (1972) Inorganic composition of molluscan extrapallial fluid. *Biological Bulletin* 143: 506-512.

Crenshaw MA (1980) Mechanisms of shell formation and dissolution. In Rhoads DC & Lutz RA (eds.) *Skeletal Growth of Aquatic Organisms: Biological Records of Environmental Change*, Plenum Press, New York, pp. 115-132.

Crenshaw MA, & Neff JM (1969) Decalcification at the mantle – shell interface in molluscs. *American Zoologist* 9: 881-885.

Dansgaard W (1981) Ice core studies - dating the past to find the future. *Nature* 290: 360-361.

Dansgaard W, & Tauber H (1969) Glacier oxygen-18 content and Pleistocene ocean temperatures. *Science* 166, 499–502.

Dardenne M (1967) Étude experimentale de la distribution de zinc dans les carbonates de calcium. *Bulletin des Recherches Géologiques et Minières* 5: 75.

D'Arrigo RD, Cook ER, Mann ME, & Jacoby GC (2003) Tree-ring reconstructions of temperature and sea-level pressure variability associated with the warm-season Arctic Oscillation since AD 1650. *Geophysical Research Letters* 30 (11): 1549.

Davenport CB (1938) Growth lines in fossil pectens as indicators of past climates. *Journal of Paleontology* 12: 514-515.

De Ridder F, Pintelon R, Schoukens J, Gillikin DP, André L, Baeyens W, de Brauwere A, Dehairs F (2004) Decoding nonlinear growth rates in biogenic environmental archives. *Geochemistry Geophysics Geosystems* 5, Q12015, doi:10.1029/2004GC000771.

De Ridder F, Pintelon R, Schoukens J, Navez J, André L, & Dehairs F (2002) An improved multiple internal standard normalisation for drift in LA-ICP-MS measurements. *Journal of Analytical Atomic Spectrometry* 17: 1461-1470.

de Villiers S (1999) Seawater strontium and Sr/Ca variability in the Atlantic and Pacific oceans. *Earth and Planetary Science Letters* 171: 623-634.

de Villiers S, Nelson BK, & Chivas AR (1995) Biological-controls on coral Sr/Ca and $\delta^{18}O$ reconstructions of sea-surface temperatures. *Science* 269: 1247-1249.

de Villiers S, Dickson JAD, & Ellam RM (2005) The composition of the continental river weathering flux deduced from seawater Mg isotopes. *Chemical Geology* 216: 133-142.

de Zwaan A, & Mathieu M (1992) Cellular biochemistry and endochrinology. In: Gosling E (ed.) *The mussel Mytilus: Ecology, Physiology, Genetics and Culture. Developments in Aquaculture and Fisheries Science*. Vol. 25, Elsevier, pp. 223-307.

Degens ET (1965) *Geochemistry of Sediments – a Brief Survey*. Prentice Hall, New Jersey, USA. 342 pp.

Dehairs F, Baeyens W, & Goeyens L (1992) Accumulation of suspended barite at mesopelagic depths and export production in the Southern Ocean. *Science* 258: 1332-1335.

Dehairs F, Chesselet R, & Jedwab J (1980) Discrete suspended particles of barite and the barium cycle in the open ocean. *Earth and Planetary Science Letters* 49: 528-550.

Dehairs F, Lambert CE, Chesselet R, & Risler N (1987) The biological production of marine suspended barite and the barium cycle in the Western Mediterranean Sea. *Biogeochemistry* 4: 119–139.

Delaney ML, Linn LJ, & Druffel ERM (1993) Seasonal cycles of manganese and cadmium in coral from the Galapagos Islands. *Geochimica et Cosmochimica Acta* 57: 347-354.

DeNiro M, & Epstein S (1978) Influence of diet on the distribution of carbon isotopes in animals. *Geochimica et Cosmochimica Acta* 42: 495–506.

Dettman DL, Flessa KW, Roopnarine PD, Schöne BR, & Goodwin DH (2004) The use of oxygen isotope variation in shells of estuarine mollusks as a quantitative record of seasonal and annual Colorado River discharge. *Geochimica et Cosmochimica Acta* 68: 1253-1263.

Dettman DL, Reische AK, & Lohmann KC (1999) Controls on the stable isotope composition of seasonal growth bands in aragonitic fresh-water bivalves (unionidae). *Geochimica et Cosmochimica Acta* 63, 1049-1057.

Dietzel M, Gussone N, & Eisenhauer A (2004) Co-precipitation of Sr^{2+} and Ba^{2+} with aragonite by membrane diffusion of CO_2 between 10 and 50 degrees C. *Chemical Geology* 203: 139-151.

Dillaman RM, & Ford SE (1982) Measurement of calcium-carbonate deposition in mollusks by controlled etching of radioactively labeled shells. *Marine Biology* 66: 133-143.

Dodd JR (1965) Environmental control of strontium and magnesium in *Mytilus*. *Geochimica et Cosmochimica Acta* 29: 385-398.

Dodd JR, & Crisp EL (1982) Non-Linear variation with salinity of Sr/Ca and Mg/Ca ratios in water and aragonitic bivalve shells and implications for paleosalinity studies. *Palaeogeography, Palaeoclimatology, Palaeoecology* 38: 45-56.

DOE, 1994. Handbook of methods for the analysis of the various parameters of the carbon dioxide system in sea water; version 2. In: Dickson AG, & Goyet C (eds.) ORNL/CDIAC-74.

Druffel ERM (1997) Geochemistry of corals: Proxies of past ocean chemistry, ocean circulation, and climate. *Proceedings of the National Academy of Sciences of the United States of America* 94: 8354-8361.

Druffel ERM, & Benavides LM (1986) Input of excess CO_2 to the surface ocean based on $^{13}C/^{12}C$ ratios in a banded Jamaican sclerosponge. *Nature* 321: 58-61.

Dutton AL, Lohmann KC, & Zinsmeister WJ (2002) Stable isotope and minor element proxies for Eocene climate of Seymour Island, Antarctica. *Paleoceanography* 17 (2), doi: 1016, 10.1029/2000PA000593.

Duvail L, Moal J, & Fouchereau-Peron M (1998) CGRP-like molecules and carbonic anhydrase activity during the growth of *Pecten maximus*. *Comparative Biochemistry and Physiology C-Pharmacology Toxicology & Endocrinology* 120: 475-480.

Dymond J, Suess E, & Lyle M (1992) Barium in deep-sea sediment: A geochemical proxy for paleoproductivity. *Paleoceanography* 7: 163-181.

Edmond J M, Boyle ED, Drummond D, Grant B, & Mislick T (1978) Desorption of barium in the plume of the Zaire (Congo) River. *Netherlands Journal of Sea Research* 12: 324-328.

Eggins SM, Sadekov A, & De Deckker P (2004) Modulation and daily banding of Mg/Ca in *Orbulina universa* tests by symbiont photosynthesis and respiration: a complication for seawater thermometry? *Earth and Planetary Science Letters* 225: 411-419.

Elderfield H, & Ganssen G (2000) Past temperature and $\delta^{18}O$ of surface ocean waters inferred from foraminiferal Mg/Ca ratios. *Nature* 405: 442-445.

Elliot M, deMenocal PB, Linsley BK, & Howe SS (2003) Environmental controls on the stable isotopic composition of *Mercenaria mercenaria*: potential application to paleoenvironmental studies. *Geochemistry Geophysics Geosystems* 4, 1056, doi: 10.1029/2002GC000425.

Elorza J, & GarciaGarmilla F (1996) Petrological and geochemical evidence for diagenesis of inoceramid bivalve shells in the Plentzia formation (upper Cretaceous, Basque-Cantabrian region, northern Spain). *Cretaceous Research* 17: 479-503.

Elorza J, & Garcia-Garmilla F (1998) Palaeoenvironmental implications and diagenesis of inoceramid shells (Bivalvia) in the mid-Maastrichtian beds of the Sopelana, Zumaya and Bidart sections (coast of the Bay of Biscay, Basque Country). *Palaeogeography, Palaeoclimatology, Palaeoecology* 141: 303-328.

Elsdon TS, & Gillanders BM (2004) Fish otolith chemistry influenced by exposure to multiple environmental variables. *Journal of Experimental Marine Biology and Ecology* 313: 269-284.

Emiliani C (1954) Temperatures of Pacific bottom waters and polar superficial waters during the Tertiary. *Science* 119: 853-855.

EPA (2000) National air pollutant emission trends: 1900 – 1998. *U.S. Environmental Protection Agency report 454/R-00-002*.

Epstein S, & Mayeda T (1953) Variation of ^{18}O content of waters from natural sources. *Geochimica et Cosmochimica Acta* 4: 213-224.

Epstein S, Buchsbaum R, Lowenstam HA, & Urey HC (1953) Revised carbonate - water isotopic temperature scale. *Bulletin of the Geological Society of America* 64: 1315-1326.

Erez J, & Luz B (1983) Experimental paleotemperatures equation for planktonic foraminifera. *Geochimica et Cosmochimica Acta* 47: 1025–1031.

Eversole AG, Michener WK, & Eldridge PJ (1980) Reproductive cycle of *Mercenaria mercenaria* in a South Carolina estuary *Proceedings of the National Shellfish Association* 70: 20-30.

Fairbanks RG, & Dodge RE (1979) Annual periodicity of the O^{18}/O^{16} and C^{13}/C^{12} ratios in the coral *Montastrea annularis*. *Geochimica et Cosmochimica Acta* 43: 1009-1020.

Falini G, Albeck S, Weiner S, & Addadi L (1996) Control of aragonite or calcite polymorphism by mollusk shell macromolecules. *Science* 271: 67-69.

Fallon SJ, McCulloch MT, van Woesik R, & Sinclair DJ (1999) Corals at their latitudinal limits: laser ablation trace element systematics in Porites from Shirigai Bay, Japan. *Earth and Planetary Science Letters* 172: 221-238.

Fallon SJ, White JC, McCulloch MT (2002) Porites corals as recorders of mining and environmental impacts: Misima Island, Papua New Guinea. *Geochimica et Cosmochimica Acta* 66: 45-62.

Ferrier-Pages C, Boisson F, Allemand D, & Tambutte E (2002) Kinetics of strontium uptake in the scleractinian coral *Stylophora pistillata*. *Marine Ecology Progress Series* 245: 93-100.

Finch AA, Shaw PA, Weedon GP, & Holmgren K (2001) Trace element variation in speleothem aragonite: potential for palaeoenvironmental reconstruction. *Earth and Planetary Science Letters* 186: 255-267.

Fisher NS, Guillard RRL, & Bankston DC (1991) The accumulation of barium by marine-phytoplankton grown in culture. *Journal of Marine Research* 49: 339-354.

Focken U, & Becker K (1998) Metabolic fractionation of stable carbon isotopes: implications of different proximate compositions for studies of the aquatic food webs using $\delta^{13}C$ data. *Oecologia* 115: 337– 343.

Frandsen RP, & Dolmer P (2002) Effects of substrate type on growth and mortality of blue mussels (*Mytilus edulis*) exposed to the predator *Carcinus maenas*. *Marine Biology* 141: 253-262.

Freitas P, Clarke LJ, Kennedy H, Richardson C, & Abrantes F (2005) Mg/Ca, Sr/Ca, and stable-isotope ($\delta^{18}O$ and $\delta^{13}C$) ratio profiles from the fan mussel *Pinna nobilis*: Seasonal records and temperature relationships. *Geochemistry Geophysics Geosystems* 6, Q04D14, doi:10.1029/2004GC000872.

Friedman I, & O'Neil JR (1977) Compilation of stable isotope fractionation factors of geochemical interest. In: Fleischer M (ed.) *Data of geochemistry* (6th edition): U.S. Geological Survey Professional Paper 440-KK, p. 1–12.

Fritts HC, Blasing TJ, Hayden BP, & Kutzbach JE (1971), Multivariate techniques for specifying tree-growth and climate relationships and for reconstructing anomalies in paleoclimate. *Journal of Applied Meteorology* 10: 845–864.

Fry B (2002) Conservative mixing of stable isotopes across estuarine salinity gradients: A conceptual framework for monitoring watershed influences on downstream fisheries production. *Estuaries* 25: 264-271.

Fry B, & Sherr EB (1984) ^{13}C measurements as indicators of carbon flow in marine and freshwater ecosystems. *Contribution to Marine Science* 27: 13– 47.

Fryer BJ, Jackson SE, & Longerich HP (1995) Design, operation and role of the laser-ablation microprobe coupled with an inductively-coupled plasma - mass-spectrometer (LAM-ICP-MS) in the earth-sciences. *Canadian Mineralogist* 33: 303-312.

Fuge R, Palmer TJ, Pearce NJG, Perkins WT (1993) Minor and trace element chemistry of modern shells: a laser ablation inductively coupled plasma spectrometry study. *Applied Geochemistry supplement* 2: 111-116.

Furla P, Galgani I, Durand I, & Allemand D (2000) Sources and mechanisms of inorganic carbon transport for coral calcification and photosynthesis. *Journal of Experimental Biology* 203: 3445–3457.

Furst M, Lowenstam HA, & Burnett DS (1976) Radiographic study of distribution of boron in recent mollusk shells. *Geochimica et Cosmochimica Acta* 40: 1381-1386.

Fyhn HJ, & JD Costlow (1975) Anaerobic sampling of body-fluids in bivalve mollusks. *Comparative Biochemistry and Physiology A-Physiology* 52: 265-268.

Gaetani GA, & Cohen AL (2004) Experimental investigation of elemental paleothermometers: how and why they work. In: *ICP VIII, 8th International Conference on Paleoceanography: An Ocean View of Global Change*, Biarritz, France, 2004, p. 219 (abstract).

Gerringa LJA, Hummel H, & Moerdijk-Poortvliet TCW (1998) Relations between free copper and salinity, dissolved and particulate organic carbon in the Oosterschelde and Westerschelde, Netherlands. *Journal of Sea Research* 40: 193-203.

Gieskes WWC, Kraay GW, Nontji A, Setiapennana D, & Sutomo (1988) Monsoonal alternation of a mixed and layered structure in the phytoplankton of the euphotic zone of the Banda Sea (Indonesia), a mathematical analysis of algal pigment fingerprints. *Netherlands Journal of Sea Research* 22: 123-137.

Gill I, Olson JJ, & Hubbard DK (1995) Corals, paleotemperature records, and the aragonite-calcite transformation. *Geology* 23: 333-336.

Gillikin DP, De Ridder F, Ulens H, Elskens M, Keppens E, Baeyens W, & Dehairs F (2005a) Assessing the reproducibility and reliability of estuarine bivalve shells (*Saxidomus giganteus*) for sea surface temperature reconstruction: implications for paleoclimate studies. *Palaeogeography Palaeoclimatology Palaeoecology* doi: 10.1016/j.palaeo.2005.03.047

Gillikin DP, De Wachter B, & Tack JF (2004) Physiological responses of two ecologically important Kenyan mangrove crabs exposed to altered salinity regimes. *Journal of Experimental Marine Biology and Ecology* 301: 93-109.

Gillikin DP, Dehairs F, Baeyens W, Navez J, & André L (in press) Inter- and intra-annual variations of Pb/Ca ratios in clam shells (*Mercenaria mercenaria*): a record of anthropogenic lead pollution? *Marine Pollution Bulletin.*

Gillikin DP, Dehairs F, Lorrain A, Steenmans D, Baeyens W, & André L (submitted) Barium uptake into the shells of the common mussel (*Mytilus edulis*) and the potential for estuarine paleo-chemistry reconstruction. *Geochimica et Cosmochimica Acta*

Gillikin DP, Lorrain A, Navez J, Taylor JW, André L, Keppens E, Baeyens W, & Dehairs F (2005b) Strong biological controls on Sr/Ca ratios in aragonitic marine bivalve shells. *Geochemistry, Geophysics, Geosystems* 6, Q05009, doi:10.1029/2004GC000874.

Goldberg ED (1975) The mussel watch - A first step in global marine monitoring. *Marine Pollution Bulletin* 6: 111.

Goodwin DH, Flessa KW, Schöne BR, & Dettman DL (2001) Cross-calibration of daily growth increments, stable isotope variation, and temperature in the Gulf of California bivalve mollusk *Chione cortezi*: implications for paleoenvironmental analysis. *Palaios* 16: 387-398.

Goodwin DH, Flessa KW, Tellez-Duarte MA, Dettman DL, Schöne BR, & Avila-Serrano GA (2004) Detecting time-averaging and spatial mixing using oxygen isotope variation: a case study. *Palaeogeography, Palaeoclimatology, Palaeoecology* 205: 1– 21.

Goodwin DH, Schöne BR, & Dettman DL (2003) Resolution and fidelity of oxygen isotopes as paleotemperature proxies in bivalve mollusc shells: models and observations. *Palaios* 18: 110-125.

Govindaraju K (1994) 1994 Compilation of working values and sample description for 383 geostandards. *Geostandards Newsletter* XVIII Special issue: 1-158.

Grossman EL, & Ku TL (1986) Oxygen and carbon isotope fractionation in biogenic aragonite - temperature effects. *Chemical Geology* 59: 59-74.

Guay C K, & Falkner KK (1997) Barium as a tracer of Arctic halocline and river waters. *Deep-Sea Research II* 44: 1543-1569.

Guay CK, & Falkner KK (1998) A survey of dissolved barium in the estuaries of major Arctic rivers and adjacent seas. *Continental Shelf Research* 18: 859-882.

Gueiros BB, Machado W, Lisboa SD, & Lacerda LD (2003) Manganese behavior at the sediment-water interface in a mangrove dominated area in Sepetiba Bay, SE Brazil. *Journal of Coastal Research* 19: 550-559.

Guillong M, & Gunther D (2002) Effect of particle size distribution on ICP-induced elemental fractionation in laser ablation-inductively coupled plasma-mass spectrometry. *Journal of Analytical Atomic Spectrometry* 17: 831-837.

Günther D, & Hattendorf B (2005) Solid sample analysis using laser ablation inductively coupled plasma mass spectrometry. *TrAC Trends in Analytical Chemistry* 24: 255-265.

Gussone N, Eisenhauer A, Heuser A, Dietzel M, Bock B, Böhm F, Spero HJ, Lea DW, Bijma J, & Nagler TF (2003) Model for kinetic effects on calcium isotope fractionation (δ^{44}Ca) in inorganic aragonite and cultured planktonic foraminifera. *Geochimica et Cosmochimica Acta* 67: 1375-1382.

Haase-Schramm A, Bohm F, Eisenhauer A, Dullo WC, Joachimski MM, Hansen B, & Reitner J (2003) Sr/Ca ratios and oxygen isotopes from sclerosponges: Temperature history of the Caribbean mixed layer and thermocline during the Little Ice age. *Paleoceanography* 18 (3): 1073 doi:10.1029/2002PA000830.

Hall JK (1979) Sediment waves and other evidence of paleo-bottom currents at two locations in the deep Arctic Ocean. *Marine Geology* 23: 269–299.

Hart SR, and Blusztajn J (1998) Clams as recorders of ocean ridge volcanism and hydrothermal vent field activity. *Science* 280: 883-886.

Hart SR, Cohen AL, & Ramsay P (1997) Microscale analysis of Sr/Ca and Ba/Ca in Porites, *Proceedings of the 8th International Coral Reef Symposium* 2: 1707-1712.

Havach SM, Chandler T, Wilson-Finelli A, & Shaw TJ (2001) Experimental determination of trace element partition coefficients in cultured benthic foraminifera. *Geochimica et Cosmochimica Acta* 65: 1277-1283.

Heilmayer O, Brey T, & Pörtner HO (2004) Growth efficiency and temperature in scallops: a comparative analysis of species adapted to different temperatures. *Functional Ecology* 18: 641-647.

Hellings L, Dehairs F, Tackx M, Keppens E, Baeyens W, 1999. Origin and fate of organic carbon in the freshwater part of the Scheldt Estuary as traced by stable carbon isotopic composition. *Biogeochemistry* 47: 167– 186.

Hellings L, Dehairs F, Van Damme S, & Baeyens W (2001) Dissolved inorganic carbon in a highly polluted estuary (the Scheldt). *Limnology and Oceanography* 46: 1406-1414.

Hemming NG, & Hanson GN (1992) Boron isotopic composition and concentration in modern marine carbonates. *Geochimica et Cosmochimica Acta* 56: 537-543.

Hemming NG, Reeder RJ, & Hanson GN (1995) Mineral-fluid partitioning and isotopic fractionation of boron in synthetic calcium-carbonate. *Geochimica et Cosmochimica Acta* 59: 371-379.

Henderson LM, & Kraček FC (1927) The fractional precipitation of barium and radium chromates. *Journal of the American Chemical Society* 49: 739-749.

Henry RP, & Saintsing DG (1983) Carbonic-anhydrase activity and ion regulation in 3 species of osmoregulating bivalve mollusks. *Physiological Zoology* 56: 274-280.

Herman PMJ, Middelburg JJ, Widdows J, Lucas CH & Heip CHR (2000) Stable isotopes as trophic tracers: combining field sampling and manipulative labelling of food resources for macrobenthos. *Marine Ecology Progress Series* 204: 79-92.

Hetherington R, & Reid RGB (2003) Malacological insights into the marine ecology and changing climate of the late Pleistocene - early Holocene Queen Charlotte Islands archipelago, western Canada, and implications for early peoples. *Canadian Journal of Zoology* 81: 626-661.

Hickson JA, Johnson ALA, Heaton THE, & Balson PS (1999) The shell of the Queen Scallop *Aequipecten opercularisis* (L.) as a promising tool for palaeoenvironmental reconstruction: evidence and reasons for equilibrium stable-isotope incorporation. *Palaeogeography Palaeoclimatology Palaeoecology* 154: 325-337.

Hinga KR, Arthur MA, Pilson MEQ, & Whitaker D (1994) Carbon isotope fractionation by marine phytoplankton in culture: the effects of CO_2 concentration, pH, temperature, and species. *Global Biogeochemical Cycles* 8: 91-102.

Hirao Y, Matsumoto A, Yamakawa H, Maeda M, Kimura K (1994) Lead behavior in abalone shell. *Geochimica et Cosmochimica Acta* 58: 3183-3189.

Hoefs J (2004) *Stable Isotope Geochemistry*. Springer-Verlag, 5th edition, 244pp.

Holmden C, & Hudson JD (2003) $^{87}Sr/^{86}Sr$ and Sr/Ca investigation of Jurassic mollusks from Scotland: Implications for paleosalinities and the Sr/Ca ratio of seawater. *Geological Society of America Bulletin* 115: 1249-1264.

Hong SM, Candelone JP, Turetta C, & Boutron CF (1996) Changes in natural lead, copper, zinc and cadmium concentrations in central Greenland ice from 8250 to 149,100 years ago: Their association with climatic changes and resultant variations of dominant source contributions. *Earth and Planetary Science Letters* 143: 233-244.

Hönisch B, Hemming NG, Grottoli AG, Amat A, Hanson GN, & Bijma J (2004) Assessing scleractinian corals as recorders for paleo-pH: Empirical calibration and vital effects. *Geochimica et Cosmochimica Acta* 68: 3675-3685.

Hudson JH, Shinn EA, & George RY (1978) Oxygen and carbon isotopic growth record in a reef coral from Florida Keys and a deep-sea coral from Blake Plateau. *Science* 202: 627-629.

Hummel H, Bogaards RH, Bachelet G, Caron F, Sola JC, & Amiard-Triquet C (2000) The respiratory performance and survival of the bivalve *Macoma balthica* (L.) at the southern limit of its distribution area: a translocation experiment. *Journal of Experimental Marine Biology and Ecology* 251: 85-102.

Hummel H, Fortuin AW, Bogaards RH, Wolf L, de Meijboom A (1989) Changes in *Mytilus edulis* in relation to short-term disturbances of the tide. In: Klekowski, R., Styczynska-Jurewicz, E., Falkowski, L. (eds.), *Proc. 21st European Marine Biological Symposium*, Warsaw, Ossolineum, pp. 77– 89.

IAEA (2001) GNIP Maps and Animations. *International Atomic Energy Agency*, Vienna. Accessible at http://isohis.iaea.org.

Ingram BL, Conrad ME, & Ingle JC (1996) Stable isotope and salinity systematics in estuarine waters and carbonates: San Francisco Bay. *Geochimica et Cosmochimica Acta* 60: 455-467.

IPCC (Intergovernmental Panel on Climate Change) (2001) *IPCC Third Assessment Report: Climate Change 2001*. Watson RT, & the Core Writing Team (eds.) IPCC, Geneva, Switzerland. pp. 184. Available online at http://www.ipcc.ch/

Ivany LC, Wilkinson BH, & Jones DS (2003) Using stable isotopic data to resolve rate and duration of growth throughout ontogeny: An example from the surf clam, *Spisula solidissima*. *Palaios* 18: 126-137.

Jacquet SHM, Dehairs F, Cardinal D, Navez J, & Delille B (2005) Barium distribution across the Southern Ocean frontal system in the Crozet–Kerguelen Basin. *Marine Chemistry* 95: 149-162.

Johnsen SJ, Clausen HB, Dansgaard W, Langway CC (1972) Oxygen isotope profiles through Antarctic and Greenland ice sheets. *Nature* 235: 429-434.

Johnson KS (1982) Carbon dioxide hydration and dehydration kinetics in seawater. *Limnology and Oceanography* 27: 849-855.

Jones DS, Arthur MA, & Allard DJ (1989) Sclerochronological records of temperature and growth from shells of *Mercenaria mercenaria* from Narragansett Bay, Rhode Island. *Marine Biology* 102: 225-234.

Jones DS, Williams DF, Arthur MA 1983. Growth history and ecology of the Atlantic surf clam, *Spisula solidissima* (Dillwyn), as revealed by stable isotopes and annual shell increments. *Journal of Experimental Marine Biology and Ecology* 73: 225-242.

Jones TL, & Kennett DJ (1999) Late Holocene Sea temperatures along the central California coast. *Quaternary Research* 51: 74-82.

Kaandorp RJG, Vonhof HB, Del Busto C, Wesselingh FP, Ganssen GM, Marmol AE, Pittman LR, & van Hinte JE (2003) Seasonal stable isotope variations of the modern Amazonian freshwater bivalve *Anodontites trapesialis*. *Palaeogeography Palaeoclimatology Palaeoecology* 194: 339-354.

Kaehler S, & McQuaid CD (1999) Use of the fluorochrome calcein as an in situ growth marker in the brown mussel *Perna perna*. *Marine Biology* 133: 455-460.

Kalish JM (1991) Determinants of otolith chemistry - seasonal-variation in the composition of blood-plasma, endolymph and otoliths of bearded rock cod *Pseudophycis barbatus*. *Marine Ecology Progress Series* 74: 137-159.

Kardell L, & Larsson J (1978) Lead and cadmium in oak tree rings (*Quercus robur* L). *Ambio* 7: 117-121.

Katz A, Sass E, Starinski A, & Holland HD (1972) Strontium behaviour in the aragonite-calcite transformation: An experimental study at 40-98°C. *Geochimica et Cosmochimica Acta* 36: 481-496.

Kaufman A, Ghaleb B, Wehmiller JF, & Hillaire-Marcel C (1996) Uranium concentration and isotope ratio profiles within *Mercenaria* shells: Geochronological implications. *Geochimica et Cosmochimica Acta* 60: 3735-3746.

Keller N, Del Piero D, & Longinelli A (2002) Isotopic composition, growth rates and biological behaviour of *Chamelea gallina* and *Callista chione* from the Gulf of Trieste (Italy). *Marine Biology* 140: 9-15.

Kennedy H, Richardson CA, Duarte CM, & Kennedy DP (2001) Oxygen and carbon stable isotopic profiles of the fan mussel, *Pinna nobilis*, and reconstruction of sea surface temperatures in the Mediterranean. *Marine Biology* 139: 1115-1124.

Killingley JS, & Berger WH (1979) Stable isotopes in a mollusc shell: Detection of upwelling events. *Science* 205: 186–188.

Kim G, Alleman LY, & Church TM (2004) Accumulation records of radionuclides and trace metals in two contrasting Delaware salt marshes. *Marine Chemistry* 87: 87-96.

Kim ST & O'Neil JR (1997) Equilibrium and nonequilibrium oxygen isotope effects in synthetic carbonates. *Geochimica et Cosmochimica Acta* 61: 3461-3475.

Kinsman DJJ, & Holland HD (1969) The co-precipitation of cations with $CaCO_3$ - IV. the co-precipitation of Sr^{2+} with aragonite between 16 degrees and 96 degrees C. *Geochimica et Cosmochimica Acta* 33: 1-17.

Kitano Y, & Oomori T (1971) The coprecipitation of uranium with calcium carbonate. *Journal of the Oceanographic Society of Japan* 27: 34–42.

Kitano Y, Kanamori N, & Oomori T (1971) Measurements of distribution coefficients of strontium and barium between carbonate precipitate and solution - abnormally high values of distribution coefficients measured at early stages of carbonate formation. *Geochmical Journal* 4: 183-206.

Kitano Y, Okumura M, & Idogaki M 1980. Abnormal behaviors of copper(II) and zinc ions in parent solution at the early stage of calcite formation. *Geochemical Journal* 14: 167-175.

Klein RT, Lohmann KC, & Kennedy GL (1997) Elemental and isotopic proxies of paleotemperature and paleosalinity: Climate reconstruction of the marginal northeast Pacific ca 80 ka. *Geology* 25: 363-366.

Klein RT, Lohmann KC, & Thayer CW (1996a) Bivalve skeletons record sea-surface temperature and $\delta^{18}O$ via Mg/Ca and $^{18}O/^{16}O$ ratios. *Geology* 24: 415-418.

Klein RT, Lohmann KC, & Thayer CW (1996b) Sr/Ca and $^{13}C/^{12}C$ ratios in skeletal calcite of *Mytilus trossulus*: Covariation with metabolic rate, salinity, and carbon isotopic composition of seawater. *Geochimica et Cosmochimica Acta* 60: 4207-4221.

Kohout FA, & Kolipinski MC (1967) Biological zonation related to groundwater discharge along the shore of Biscayne Bay, Miami, Florida. In: Lauff GH (ed.) *Estuaries*. American Association for the Advancement of Science, Publication No. 83, Washington D.C., USA. Pp 488-499.

Koide M, Lee DS, Goldberg ED (1982) Metal and transuranic records in mussel shells, byssal threads and tissues. *Estuarine, Coastal and Shelf Science* 15: 679-695.

Krantz DE, Williams DF, & Jones DS (1987) Ecological and paleoenvironmental information using stable isotope profiles from living and fossil mollusks. *Palaeogeography Palaeoclimatology Palaeoecology* 58: 249-266.

Kucera M, Rosell-Melé A, Schneider R, Waelbroeck C, & Weinelt M (2005) Multiproxy approach for the reconstruction of the glacial ocean surface (MARGO). *Quaternary Science Reviews* 24: 813–819.

Kump LR & Arthur MA (1999) Interpreting carbon-isotope excursions: carbonates and organic matter. *Chemical Geology* 161: 181-198.

Kvenvolden KA, Blunt DJ, & Clifton HE (1979) Amino-acid racemization in Quaternary shell deposits at Willapa Bay, Washington. *Geochimica et Cosmochimica Acta* 43: 1505-1520.

Labonne M, & Hillaire-Marcel C (2000) Geochemical gradients within modern and fossil shells of *Concholepas concholepas* from Northern Chile: An insight into U-Th systematics and diagenetic/authigenic isotopic imprints in mollusk shells. *Geochimica et Cosmochimica Acta* 64: 1523-1534.

Landmeyer JE, Bradley PM, Bullen TD (2003) Stable lead isotopes reveal a natural source of high lead concentrations to gasoline-contaminated groundwater. *Environmental Geology* 45: 12-22.

Lares ML & Orians KJ (1997) Natural Cd and Pb variations in *Mytilus californianus* during the upwelling season. *Science of the Total Environment* 197: 177-195.

Lauenstein GG, Cantillo AY, O'Connor TP (2002) The status and trends of trace element and organic contaminants in oysters, *Crassostrea virginica*, in the waters of the Carolinas, USA. *Science of the Total Environment* 285: 79-87.

Lazareth CE, Vander Putten E, André L, & Dehairs F (2003) High-resolution trace element profiles in shells of the mangrove bivalve *Isognomon ephippium*: a record of environmental spatio-temporal variations? *Estuarine Coastal and Shelf Science* 57: 1103-1114.

Lazareth CE, Willenz P, Navez J, Keppens E, Dehairs F, & André L (2000) Sclerosponges as a new potential recorder of environmental changes: Lead in *Ceratoporella nicholsoni*. *Geology* 28: 515-518.

Lea D. W., Shen G. T., and Boyle E. A. (1989) Coralline barium records temporal variability in equatorial Pacific upwelling. *Nature* 340: 373–376.

Lea DW (1993) Constraints on the alkalinity and circulation of glacial circumpolar deep-water from benthic foraminiferal barium. *Global Biogeochemical Cycles* 7: 695-710.

Lea DW (2003) Elemental and Isotopic Proxies of Marine Temperatures. In: *The Oceans and Marine Geochemistry*, Elderfield H (ed.), Oxford: Elsevier-Pergamon, pp. 365-390.

Lea DW, & Boyle E (1989) Barium content of benthic foraminifera controlled by bottom-water composition. *Nature* 338: 751-753.

Lea DW, & Boyle E (1991) Barium in planktonic foraminifera. *Geochimica et Cosmochimica Acta* 55: 3321-3331.

Lea DW, & Boyle E (1993) Determination of carbonate-bound barium in foraminifera and corals by isotope dilution plasma-mass spectrometry. *Chemical Geology* 103: 73 - 84.

Lea DW, & Spero HJ (1992) Experimental determination of barium uptake in shells of the planktonic foraminifera *Orbulina universa* at 22°C. *Geochimica et Cosmochimica Acta* 56: 2673-2680.

Lea DW, & Spero HJ (1994) Assessing the reliability of paleochemical tracers: Barium uptake in the shells of planktonic foraminifera. *Paleoceanography* 9: 445-452.

Lea DW, Martin PA, Chan DA, & Spero HJ (1995) Calcium uptake and calcification rate in the planktonic foraminifer *Orbulina universa*. *Journal of Foraminiferal Research* 25: 14-23.

Lea DW, Mashiotta TA, & Spero HJ (1999) Controls on magnesium and strontium uptake in planktonic foraminifera determined by live culturing. *Geochimica et Cosmochimica Acta* 63: 2369-2379.

Lécuyer C, & O'Neil JR (1994) Stable-isotope compositions of fluid inclusions in biogenic carbonates. *Geochimica et Cosmochimica Acta* 58: 353-363.

Lécuyer C, Reynard B, & Martineau F (2004) Stable isotope fractionation between mollusc shells and marine waters from Martinique Island. *Chemical Geology* 213: 293-305.

Leermakers M, Gao Y, Gabelle C, Lojen S, Wartel M, & Baeyens W (in press) Determination of high resolution pore water profiles of trace metals in sediments of the Rupel River (Belgium) using DET (diffusive equilibrium in thin films) and DGT (diffusive gradients in thin films) techniques. *Water, Air and Soil Pollution*

Lehane C & Davenport J (2002) Ingestion of mesozooplankton by three species of bivalve; *Mytilus edulis*, *Cerastoderma edule* and *Aequipecten opercularis*. *Journal of the Marine Biological Association of the United Kingdom* 82: 615-619.

Lehane C & Davenport J (2004) Ingestion of bivalve larvae by *Mytilus edulis*: experimental and field demonstrations of larviphagy in farmed blue mussels. *Marine Biology* 145: 101-107.

Levinton JS, Ward JE, & Shumway SE (2002) Feeding responses of the bivalves *Crassostrea gigas* and *Mytilus trossulus* to chemical composition of fresh and aged kelp detritus. *Marine Biology* 141: 367-376.

Lewis DE, & Cerrato RM (1997) Growth uncoupling and the relationship between shell growth and metabolism in the soft shell clam *Mya arenaria*. *Marine Ecology Progress Series* 158: 177-189.

Linsley BK, Messier RG, Dunbar RB (1999) Assessing between-colony oxygen isotope variability in the coral *Porites lobata* at Clipperton Atoll. *Coral Reefs* 18: 13-27.

Linsley BK, Wellington GM, & Schrag DP (2000) Decadal Sea Surface Temperature Variability in the Subtropical South Pacific from 1726 to 1997 A.D. *Science* 290: 1145-1148.

Lobel PB, Longerich HP, Jackson SE, & Belkhode SP (1991) A major factor contributing to the high degree of unexplained variability of some elements concentrations in biological tissue - 27 elements in 5 organs of the mussel *Mytilus* as a model. *Archives of Environmental Contamination and Toxicology* 21: 118-125.

Longerich HP, Gunther D, Jackson SE (1996) Elemental fractionation in laser ablation inductively coupled plasma mass spectrometry. *Fresenius Journal of Analytical Chemistry* 355: 538-542.

Lorens RB (1978) A study of biological and physiological controls on the trace metal content of calcite and aragonite. *Ph.D. thesis*, University of Rhode Island.

Lorens RB (1981) Sr, Cd, Mn and Co distribution coefficients in calcite as a function of calcite precipitation rate. *Geochimica et Cosmochimica Acta* 45: 553-561.

Lorens RB, & Bender ML (1977) Physiological exclusion of magnesium from *Mytilus edulis* calcite. *Nature* 269: 793-794.

Lorens RB, & Bender ML (1980) The impact of solution chemistry on *Mytilus edulis* calcite and aragonite. *Geochimica et Cosmochimica Acta* 44: 1265-1278.

Lorrain A, Gillikin DP, Paulet Y-M, Chauvaud L, Navez J, Le Mercier A, & André L (submitted a) Strong kinetic effects on Sr/Ca ratios in the calcitic bivalve *Pecten maximus*. *Geology*

Lorrain A, Gillikin DP, Paulet Y-M, Paillard C, Navez J, André L, Dehairs F, Baeyens W, & the CALMARs group (2004b) Toward a mechanistic understanding of trace element proxy incorporation in bivalve shells, International Paleo-environments Symposium (*QRA2004*), Brussels, Belgium. (abstract)

Lorrain A, Paillard C, Paulet Y-M, Gillikin DP, Mellado T, Donval A, Navez J, & André L (submitted b) Biological and inorganic elemental characterization of hemolymph and extrapallial fluid in two bivalve species. *Journal of Experimental Marine Biology and Ecology*

Lorrain A, Paulet Y-M, Chauvaud L, Dunbar R, Mucciarone D, & Fontugne M (2004a) $\delta^{13}C$ variation in scallop shells: Increasing metabolic carbon contribution with body size? *Geochimica et Cosmochimica Acta* 68: 3509-3519.

Lorrain A, Paulet Y-M, Chauvaud L, Savoye N, Donval A, & Saout C (2002) Differential $\delta^{13}C$ and $\delta^{15}N$ signatures among scallop tissues: implications for ecology and physiology. *Journal of Experimental Marine Biology and Ecology* 275: 47-61.

Lorrain A, Paulet Y-M, Chauvaud L, Savoye N, Nezan E, & Guerin L (2000) Growth anomalies in *Pecten maximus* from coastal waters (Bay of Brest, France): relationship with diatom blooms. *Journal of the Marine Biological Association of the United Kingdom* 80: 667-673.

Lorrain A, Savoye N, Chauvaud L, Paulet Y-M, & Naulet N (2003) Decarbonation and preservation method for the analysis of organic C and N contents and stable isotope ratios of low-carbonated suspended particulate material. *Analytica Chimica Acta* 491: 125-133.

Lorrain A. (2002) Utilisation de la coquille Saint-Jacques comme traceur environnemental: approches biologique et biogéochimique. *PhD thesis*, Université de Bretagne occidentale, Brest, France.

Mann ME & Hughes MK (2002) Tree-ring chronologies and climate variability. *Science* 296: 848-848.

Mann ME, Bradley RS, & Hughes MK (1998) Global-scale temperature patterns and climate forcing over the past six centuries. *Nature* 392: 779-787

Mannino MA, Spiro BF, & Thomas KD (2003) Sampling shells for seasonality: oxygen isotope analysis on shell carbonates of the inter-tidal gastropod *Monodonta lineata* (da Costa) from populations across its modern range and from a Mesolithic site in southern Britain. *Journal of Archaeological Science* 30: 667-679.

Marchitto TA, Jones GA, Goodfriend GA, & Weidman CR (2000a) Precise temporal correlation of Holocene mollusk shells using sclerochronology. *Quaternary Research* 53: 236-246.

Marchitto TM, Curry WB, & Oppo DW (2000b) Zinc concentrations in benthic foraminifera reflect seawater chemistry. *Paleoceanography* 15: 299-306.

Marechal-Abram N, Debenay JP, Kitazato H, & Wada H 2004. Cadmium partition coefficients of cultured benthic foraminifera *Ammonia beccarii*. *Geochemical Journal* 38: 271-283.

Marin F, & Luquet G (2004) Molluscan shell proteins. *Comptes Rendus Palevol* 3: 469-492.

Maslin MA, Hall MA, Shackleton NJ, & Thomas E (1996) Calculating surface water pCO_2 from foraminiferal organic $\delta^{13}C$. *Geochimica et Cosmochimica Acta* 60: 5089-5100.

Maslin MA, Thomas E, Shackleton NJ, Hall MA, & Seidov D (1997) Glacial northeast Atlantic surface water pCO_2: Productivity and deep-water formation. *Marine Geology* 144: 177-190.

Mathew S, Peterson J, de Gaulejac B, Vicente N, Denis M, Bonaventura J, & Pearce LL (1996) Manganese and "pinnaglobin" in *Pinna nobilis*. *Comparative Biochemistry and Physiology Part B: Biochemistry and Molecular Biology* 113: 525-532.

McConnaughey TA (1989a) ^{13}C and ^{18}O isotope disequilibria in biological carbonates. 1. Patterns. *Geochimica et Cosmochimica Acta* 53: 151-162.

McConnaughey TA (1989b) ^{13}C and ^{18}O isotopic disequilibrium in biological carbonates: 2. In vitro simulation of kinetic isotope effects. *Geochimica et Cosmochimica Acta* 53: 163-171.

McConnaughey TA (2003) Sub-equilibrium oxygen-18 and carbon-13 levels in biological carbonates: carbonate and kinetic models. *Coral Reefs* 22: 316-327.

McConnaughey TA, Burdett J, Whelan JF, & Paull CK (1997) Carbon isotopes in biological carbonates: respiration and photosynthesis. *Geochimica et Cosmochimica Acta* 61: 611-622.

McCorkle DC, Emerson SR, & Quay PD (1985) Stable carbon isotopes in marine porewaters. *Earth and Planetary Science Letters* 74: 13-26.

McCrea JM (1950) On the isotopic chemistry of carbonates and a paleotemperature scale. *Journal of Chemical Physics* 18: 849–857.

McCulloch MT, Gagan MK, Mortimer GE, Chivas AR, & Isdale PJ (1994) A high resolution Sr/Ca and $\delta^{18}O$ coral record from the Great Barrier Reef, Australia, and the 1982-83 El Niño. *Geochimica et Cosmochimica Acta* 58: 2747 - 2754.

McCulloch MT, Tudhope AW, Esat TM, Mortimer GE, Chappell J, Pillans B, Chivas AR, & Omura A (1999) Coral record of equatorial sea-surface temperatures during the penultimate deglaciation at Huon Peninsula. *Science* 283: 202–204.

McManus J, Berelson WM, Hammond DE, & Klinkhammer GP (1999) Barium cycling in the North Pacific: Implications for the utility of Ba as a paleoproductivity and paleoalkalinity proxy. *Paleoceanography* 14: 53-61.

McManus J, Dymond J, Dunbar RB, & Collier RW (2002) Particulate barium fluxes in the Ross Sea. *Marine Geology* 184: 1-15.

Meece DE, & Benninger LK 1993. The coprecipitation of Pu and other radionuclides with $CaCO_3$. *Geochimica et Cosmochimica Acta* 57, 1447-1458.

Meibom A, Cuif JP, Hillion FO, Constantz BR, Juillet-Leclerc A, Dauphin Y, Watanabe T, Dunbar RB (2004) Distribution of magnesium in coral skeleton. *Geophysical Research Letters* 31, L23306, doi: 10.1029/2004GL021313.

Meibom A, Stage M, Wooden J, Constantz BR, Dunbar RB, Owen A, Grumet N, Bacon CR, & Chamberlain CP (2003) Monthly Strontium/Calcium oscillations in symbiotic coral aragonite: Biological effects limiting the precision of the paleotemperature proxy. *Geophysical Research Letters* 30, 1418, doi:10.1029/2002GL016864.

Meng L (2004) Can bivalves be used as archives of anthropogenic carbon input to the marine environment? *M.Sc. thesis*, Vrije Universiteit Brussel, Belgium, 49 pp.

Middelburg JJ, & Nieuwenhuize J (1998) Carbon and nitrogen stable isotopes in suspended matter and sediments from the Schelde Estuary. *Marine Chemistry* 60: 217-225.

Middelburg JJ, Barranguet C, Boschker HTS, Herman PMJ, Moens T, & Heip CHR (2000) The fate of intertidal microphytobenthos carbon: An in situ ^{13}C-labeling study. *Limnology and Oceanography* 45: 1224-1234.

Middleton WEK (1966) *A History of the Thermometer and Its Use in Meteorology*. Johns Hopkins University Press, Maryland USA. 268 pp.

Min GR, Edwards RL, Taylor FW, Recy J, Gallup CD, & Beck JW (1995) Annual cycles of U/Ca in coral skeletons and U/Ca thermometry. *Geochimica et Cosmochimica Acta* 59: 2025-2042.

Misogianes MJ, & Chasteen ND (1979) Chemical and spectral characterization of the extrapallial fluid of *Mytilus edulis*. *Analytical Biochemistry* 100: 324-334.

Mitsuguchi T, Matsumoto E, Abe O, Uchida T, & Isdale PJ (1996) Mg/Ca thermometry in coral-skeletons. *Science* 274: 961-963.

Miyajima T, Yamada Y, Hanba YT, Yoshii K, Koitabashi T, & Wada E (1995) Determining the stable-isotope ratio of total dissolved inorganic carbon in lake water by GC/C/IRMS. *Limnology and Oceanography* 40: 994-1000.

Miyamoto H, Miyashita T, Okushima M, Nakano S, Morita T, & Matsushiro A (1996) A carbonic anhydrase from the nacreous layer in oyster pearls. *Proceedings of the National Academy of Sciences of the United States of America* 93: 9657-9660.

Mook WG (1971) Paleotemperatures and chlorinities from stable carbon and oxygen isotopes in shell carbonate. *Palaeogeography Palaeoclimatology Palaeoecology* 9: 245-263.

Mook WG (2000) *Environmental Isotopes in the Hydrological Cycle: Principles and Applications*. IAEA, available at: http://www-naweb.iaea.org/napc/ih/volumes.asp

Mook WG, & Tan FC (1991) Stable carbon isotopes in rivers and estuaries. In: Degens ET, Kempe S, & Richey JE (eds.) *Biogeochemistry of Major World Rivers*, John Wiley and Sons Ltd., p. 245-264.

Mook WG, & Vogel JC (1968) Isotopic equilibrium between shells and their environment. *Science* 159: 874-875.

Moore WS, & Edmond JM (1984) Radium and barium in the Amazon River system. *Journal of Geophysical Research -Oceans* 89 (NC2), 2061-2065.

Morse JW, & Bender ML (1990) Partition coefficients in calcite: Examination of factors influencing the validity of experimental results and their application to natural systems. *Chemical Geology* 82: 265-277.

Morton B (1992) The evolution and success of the heteromyarian form in the Mytiloida. In: Gosling E (ed.), *The mussel Mytilus: Ecology, Physiology, Genetics and Culture. Developments in Aquaculture and Fisheries Science*. Vol. 25, Elsevier, pp. 21-52

Mount AS, Wheeler AP, Paradkar RP, & Snider D (2004) Hemocyte-mediated shell mineralization in the eastern oyster. *Science* 304: 297-300.

Mucci A (1987) Influence of temperature on the composition of magnesian calcite overgrowths precipitated from seawater. *Geochimica et Cosmochimica Acta* 51: 1977-1984.

Mucci A, & Morse JW (1983) The incorporation of Mg^{2+} and Sr^{2+} into calcite overgrowths - influences of growth-rate and solution composition. *Geochimica et Cosmochimica Acta* 47: 217-233.

Mucci A, & Morse JW (1990) Chemistry of low-temperature abiotic calcites: Experimental studies on coprecipitation, stability and fractionation. *Reviews in Aquatic Sciences* 3: 217-254.

Munksgaard NC, Antwertinger Y, & Parry DL (2004) Laser ablation ICP-MS analysis of Faviidae corals for environmental monitoring of a tropical estuary. *Environmental Chemistry* 1: 188-196.

Murozumi M, Chow TJ, & Patterson CC (1969) Chemical considerations of pollutant lead aerosols, terrestrial dusts and sea salts in Greenland and Antarctic snow strata. *Geochimica et Cosmochimica Acta* 33: 1247-1294.

Nägler T, Eisenhauer A, Muller A, Hemleben C, & Kramers J (2000) The δ^{44}Ca-temperature calibration on fossil and cultured *Globigerinoides sacculifer*: New tool for reconstruction of past sea surface temperatures. *Geochemistry, Geophysics, Geosystems* 1 (9), doi: 10.1029/2000GC000091.

Nair P S, & Robinson WE (1998) Calcium speciation and exchange between blood and extrapallial fluid of the quahog *Mercenaria mercenaria* (L.). *Biological Bulletin* 195: 43-51.

Nair P S, & Robinson WE (2000) Cadmium speciation and transport in the blood of the bivalve *Mytilus edulis*. *Marine Environmental Research* 50 : 99-102.

NCSCO (2004) North Carolina State Climate Office. http://www.nc-climate.ncsu.edu/climate/hurricanes.html (accessed May 2004).

Neftel A, Oeschger H, Schwander J, Stauffer B, & Zumbrunn R (1982) Ice core sample measurements give atmospheric CO_2 content during the past 40,000 years. *Nature* 295: 220-223.

Newell RIE (1989) Species profiles: life histories and environmental requirements of coastal fishes and invertebrates (North - Mid-Atlantic). Blue Mussel. *U.S. Fisheries & Wildlife Service, Biological Report* 82(11.102). *U.S. Army Corps of Engineers,* TR EL-82-4, pp. 25. Available at: http://www.nwrc.usgs.gov/wdb/pub/0169.pdf

Nicholson S, & Szefer P (2003) Accumulation of metals in the soft tissues, byssus and shell of the mytilid mussel *Perna viridis* (Bivalvia : Mytilidae) from polluted and uncontaminated locations in Hong Kong coastal waters. *Marine Pollution Bulletin* 46: 1039-1043.

Nier AO, & Gulbransen EA (1939) Variations in the relative abundance of the carbon isotopes. *Journal of the American Chemical Society* 61: 697.

NIST (1992) National Institute of Standards and Technology. *Report of Investigation – Reference materials 8543-8546 (NBS18, NBS19, LSVEC, NBS28).* Available at: https://srmors.nist.gov/certificates/view_cert2gif.cfm?certificate=8543

NIST (2003) National Institute of Standards and Technology. *Report of Investigation – Reference materials 8535, 8536, 8537 (VSMOW, GISP, SLAP).* Available at: https://srmors.nist.gov/certificates/view_cert2gif.cfm?certificate=8535

NOAA (2003) U.S. Climate at a Glance.
http://www.ncdc.noaa.gov/oa/climate/research/cag3/cag3.html.

Nürnberg D, Bijma J, & Hemleben C (1996) Assessing the reliability of magnesium in foraminiferal calcite as a proxy for water mass temperatures. *Geochimica et Cosmochimica Acta* 60: 803-814.

O'Donnell TH, Macko SA, Chou J, Davis-Hartten KL, & Wehmiller JF (2003) Analysis of $\delta^{13}C$, $\delta^{15}N$, and $\delta^{34}S$ in organic matter from the biominerals of modern and fossil *Mercenaria* spp. *Organic Geochemistry* 34: 165-183.

Oomori T, Kaneshima H, Maezato Y, & Kitano Y (1987) Distribution coefficient of Mg^{2+} ions between calcite and solution at 10-50°C. *Marine Chemistry* 20, 327 - 336.

Owen R, Kennedy H, Richardson C (2002) Experimental investigation into partitioning of stable isotopes between scallop (*Pecten maximus*) shell calcite and sea water. *Palaeogeography, Palaeoclimatology, Palaeoecology* 185: 163-174.

Paerl HW, Bales JD, Ausley LW, Buzzelli CP, Crowder LB, Eby LA, Fear JM, Go M, Peierls BL, Richardson TL, & Ramus JS (2001) Ecosystem impacts of three sequential hurricanes (Dennis, Floyd, and Irene) on the United States' largest lagoonal estuary, Pamlico Sound, NC. *Proceedings of the National Academy of Sciences of the United States of America* 98: 5655-5660.

Pagani M, Lemarchand D, Spivack A, & Gaillardet J (2005) A critical evaluation of the boron isotope-pH proxy: The accuracy of ancient ocean pH estimates. *Geochimica et Cosmochimica Acta* 69: 953–961.

Pak DK, Lea DW, & Kennett JP (2004) Seasonal and interannual variation in Santa Barbara Basin water temperatures observed in sediment trap foraminiferal Mg/Ca *Geochemistry Geophysics Geosystems* 5: Q12008 doi: 10.1029/2004GC000760.

Palacios R, Orensanz JM, & Armstrong DA (1994) Seasonal and lifelong variation of Sr/Ca ratio in shells of *Mya arenaria* from Grays Harbor (Washington) - an ancillary criterion in demographic studies. *Estuarine and Coastal Shelf Science* 39: 313-327.

Paneth P. and M. H. O'Leary. Carbon isotope effect on dehydration of bicarbonate ion catalyzed by carbonic-anhydrase. *Biochemistry* 24 (19):5143-5147, 1985.

Paquette J, & Reeder RJ (1995) Relationship between surface-structure, growth-mechanism, and trace-element incorporation in calcite. *Geochimica et Cosmochimica Acta* 59: 735-749.

Patterson WP, Smith GR, & Lohmann KC (1993) Continental paleothermometry and seasonality using the isotopic composition of aragonite otoliths of freshwater fishes. In Swart PK, Lohmann KC, Mckenzie J, & Savin S (eds.) *Climate Change in Continental Isotopic Records*, Geophysical Monographs Ser. 78: 191-202.

Paulson AJ, & Feely RA (1985) Dissolved trace-metals in the surface waters of Puget Sound. *Marine Pollution Bulletin* 16: 285-291.

Paytan A, & Kastner M (1996) Benthic Ba fluxes in the central Equatorial Pacific, implications for the oceanic Ba cycle. *Earth and Planetary Science Letters* 142: 439-450.

Pearce NJG, Perkins WT, Westgate JA, Gorton MP, Jackson SE, Neal CR, & Chenery SP (1997) A compilation of new and published major and trace element data for NIST SRM 610 and NIST SRM 612 glass reference materials. *Geostandards Newsletter* 21: 115-144.

Peterson CH (1986) Quantitative allometry of gamete production by *Mercenaria mercenaria* into old-age. *Marine Ecology-Progress Series* 29: 93-97.

Peterson CH (2002) Recruitment overfishing in a bivalve mollusc fishery: hard clams (*Mercenaria mercenaria*) in North Carolina. *Canadian Journal of Fisheries and Aquatic Sciences* 59: 96-104.

Peterson CH, & Fegley SR (1986) Seasonal allocation of resources to growth of shell, soma, and gonads in *Mercenaria mercenaria*. *Biological Bulletin* 171: 597-610.

Peterson CH, Duncan PB, Summerson HC, & Safrit GW (1983) A mark-recapture test of annual periodicity of internal growth band deposition in shells of hard clams, *Mercenaria mercenaria*, from a population along the Southeastern United States. *Fishery Bulletin* 81: 765-779.

Peterson CH, Duncan PB, Summerson HC, Beal BF (1985) Annual band deposition within shells of the hard clam, *Mercenaria mercenaria* - consistency across habitat near Cape Lookout, North Carolina. *Fisheries Bulletin* 83, 671-677.

Peterson CH, Summerson HC, & Fegley SR (1987) Ecological consequences of mechanical harvesting of clams. *Fishery Bulletin* 85: 281-298.

Petit JR, Jouzel J, Raynaud D, Barkov NI, Barnola JM, Basile I, Bender M, Chappellaz J, Davis M, Delaygue G, Delmotte M, Kotlyakov VM, Legrand M, Lipenkov VY, Lorius C, Pepin L, Ritz C, Saltzman E, & Stievenard M (1999) Climate and atmospheric history of the past 420,000 years from the Vostok ice core, Antarctica. *Nature* 399: 429-436.

Pingitore NE, & Eastman MP (1984) The experimental partitioning of Ba^{2+} into calcite. *Chemical Geology* 45: 113-120.

Pitts LC & Wallace GT (1994) Lead deposition in the shell of the bivalve, *Mya arenaria* - an indicator of dissolved lead in seawater. *Estuarine, Coastal and Shelf Science* 39: 93-104.

Pocker Y, & Tanaka N (1978) Inhibition of carbonic-anhydrase by anions in carbon dioxide-bicarbonate system. *Science* 199: 907-909.

Price GD, & Pearce NJG (1997) Biomonitoring of pollution by *Cerastoderma edule* from the British Isles: a laser ablation ICP-MS study. *Marine Pollution Bulletin* 34: 1025-1031.

Prosser SJ, Brookes ST, Linton A, & Preston T (1991) Rapid, automated-analysis of ^{13}C and ^{18}O of CO_2 in gas samples by continuous-flow, isotope ratio mass-spectrometry. *Biological Mass Spectrometry* 20: 724-730.

Purton L, & Brasier M (1997) Gastropod carbonate $\delta^{18}O$ and $\delta^{13}C$ record strong seasonal productivity and stratification shifts during the late Eocene in England. *Geology* 25: 871-874.

Purton LMA, Shields GA, Brasier MD, & Grime GW (1999) Metabolism controls Sr/Ca ratios in fossil aragonitic mollusks. *Geology* 27: 1083-1086.

Qiu JW, Tremblay R, & Bourget E (2002) Ontogenetic changes in hyposaline tolerance in the mussels *Mytilus edulis* and *M. trossulus*: implications for distribution. *Marine Ecology-Progress Series* 228: 143-152.

Quayle DB, & Bourne N (1972) The clam fisheries of British Columbia - butter clam. *Fisheries Research Board of Canada Bulletin* 179: 27-37.

Quitmyer IR, Jones DS, & Arnold WS (1997) The sclerochronology of hard clams, *Mercenaria* spp., from the south-eastern USA: A method of elucidating the zooarchaeological records of seasonal resource procurement and seasonality in prehistoric shell middens. *Journal of Archaeological Science* 24: 825-840.

Raith A, Perkins WT, Pearce NJG, Jeffries TE (1996) Environmental monitoring on shellfish using UV laser ablation ICP-MS. *Fresenius Journal of Analytical Chemistry* 355: 789-792.

Ramos AA, Inoue Y, & Ohde S (2004) Metal contents in Porites corals: Anthropogenic input of river run-off into a coral reef from an urbanized area, Okinawa. *Marine Pollution Bulletin* 48: 281-294.

Rau GH, Takahashi T, Des Marais DJ, Repeta KJ, & Martin JH (1992) The relationship between $\delta^{13}C$ of organic matter and $[CO_{2\,(aq)}]$ in ocean surface water: data from a JGOFS site in the northeast Atlantic Ocean and a model. *Geochimica et Cosmochimica Acta* 56: 1413-1419.

Reinhardt EG, Blenkinsop J, & Patterson RT (1999) Assessment of a Sr isotope vital effect ($^{87}Sr/^{86}Sr$) in marine taxa from Lee Stocking Island, Bahamas. *Geo-Marine Letters* 18: 241-246.

Ren L, Linsley BK, Wellington GM, Schrag DP, & Hoegh-Guldberg O (2003) Deconvolving the delta O-18 seawater component from subseasonal coral delta O-18 and Sr/Ca at Rarotonga in the southwestern subtropical Pacific for the period 1726 to 1997. *Geochimica et Cosmochimica Acta* 67: 1609-1621.

Reuer MK, Boyle E, & Cole JE (2003) A mid-twentieth century reduction in tropical upwelling inferred from coralline trace element proxies. *Earth and Planetary Science Letters* 210: 437-452.

Rhoads DC, & Lutz RA (1980) *Skeletal Growth of Aquatic Organisms: Biological Records of Environmental Change*. Plenum Press, New York, 750 p.

Richardson CA (2001) Molluscs as archives of environmental change. *Oceanography and Marine Biology: an Annual Review* 39: 103-164.

Richardson CA, Chenery SRN, & Cook JM (2001) Assessing the history of trace metal (Cu, Zn, Pb) contamination in the North Sea through laser ablation ICP-MS of horse mussel *Modiolus modiolus* shells. *Marine Ecology-Progress Series* 211: 157-167.

Richardson CA, Peharda M, Kennedy H, Kennedy P, Onofri V (2004) Age, growth rate and season of recruitment of *Pinna nobilis* (L) in the Croatian Adriatic determined from Mg:Ca and Sr:Ca shell profiles. *Journal of Experimental Marine Biology and Ecology* 299: 1-16.

Rimstidt JD, Balog A, & Webb J (1998) Distribution of trace elements between carbonate minerals and aqueous solutions. *Geochimica et Cosmochimica Acta* 62: 1851-1863.

Riu J, & Rius FX (1996) Assessing the accuracy of analytical methods using linear regression with errors in both axes. *Analytical Chemistry* 68: 1851-1857.

RiveraDuarte I, & Flegal AR (1997) Porewater gradients and diffusive benthic fluxes of Co, Ni, Cu, Zn, and Cd in San Francisco Bay. *Croatica Chemica Acta* 70: 389-417.

Roberts D, Rittschof D, Gerhart DJ, Schmidt AR, & Hill LG (1989) Vertical migration of the clam *Mercenaria mercenaria* (L) (Mollusca, Bivalvia) - environmental correlates and ecological significance. *Journal of Experimental Marine Biology and Ecology* 126: 271-280.

Roditi HA, Fisher NS, & Sanudo-Wilhelmy SA (2000) Uptake of dissolved organic carbon and trace elements by zebra mussels. *Nature* 407: 78-80.

Rollion-Bard C, Chaussidon M, & France-Lanord C (2003) pH control on oxygen isotopic composition of symbiotic corals. *Earth and Planetary Science Letters* 215: 275-288.

Romanek CS, Grossman EL, & Morse JW (1992) Carbon isotopic fractionation in synthetic aragonite and calcite - effects of temperature and precipitation rate. *Geochimica et Cosmochimica Acta* 56: 419-430.

Roopnarine PD, Fitzgerald P, Byars G, & Kilb K (1998) Coincident boron profiles of bivalves from the Gulf of California: Implications for the calculation of paleosalinities. *Palaios* 13: 395-400.

Ropes JW (1985) Modern methods to age oceanic bivalves. *Nautilus* 99: 53-57.

Rosenberg GD (1980) An ontogenic approach to the environmental significance of bivalve shell chemistry. In: Rhoads DC & Lutz RA (eds.) *Skeletal Growth of Aquatic Organisms: Biological Records of Environmental Change*, Plenum Press, New York. p. 133-168.

Rosenberg GD, & Hughes WW (1991) A metabolic model for the determination of shell composition in the bivalve mollusk, *Mytilus edulis*. *Lethaia* 24: 83-96.

Rosenheim BE, PK Swart, & SR Thorrold (in press) Minor and trace elements in sclerosponge *Ceratoporella nicholsoni*: Biogenic aragonite near the inorganic endmember? *Paleogeography, Paleoclimatology, Paleoecology*

Rosenheim BE, Swart PK, Thorrold SR, Eisenhauer A, & Willenz P (2005) Salinity change in the subtropical Atlantic: Secular increase and teleconnections to the North Atlantic Oscillation. *Geophysical Research Letters* 32, L02603, doi: 10.1029/2004GL021499.

Rosenheim BE, Swart PK, Thorrold SR, Willenz P, Berry L, & Latkoczy C (2004) High-resolution Sr/Ca records in sclerosponges calibrated to temperature in situ. *Geology* 32: 145-148.

Rowley RJ, & Mackinnon DI (1995) Use of the flourescent marker calcein in biomineralisation studies of brachiopods and other marine organisms. *Bulletin de l'Institut Oceanographique, Monaco* 14: 111-120.

Rueda JL & Smaal AC (2004) Variation of the physiological energetics of the bivalve *Spisula subtruncata* (da Costa, 1778) within an annual cycle. *Journal of Experimental Marine Biology and Ecology* 301: 141-157.

Russell AD, Honisch B, Spero HJ, & Lea DW (2004) Effects of seawater carbonate ion concentration and temperature on shell U, Mg, and Sr in cultured planktonic foraminifera. *Geochimica et Cosmochimica Acta* 68: 4347-4361.

Russo RE, Mao XL, Liu HC, Gonzalez J, Mao SS (2002) Laser ablation in analytical chemistry - a review. *Talanta* 57: 425-451.

Saavedra Y, Gonzalez A, Fernandez P, Blanco J (2004) The effect of size on trace metal levels in raft cultivated mussels (*Mytilus galloprovincialis*). *Science of the Total Environment* 318: 115-124.

Salata GG, Roelke LA, & Cifuentes LA (2000) A rapid and precise method for measuring stable carbon isotope ratios of dissolved inorganic carbon. *Marine Chemistry* 69: 153-161.

Sanyal A, Bijma J, Spero H, & Lea DW (2001) Empirical relationship between pH and the boron isotopic composition of *Globigerinoides sacculifer*: Implications for the boron isotope paleo-pH proxy. *Paleoceanography* 16: 515-519.

Savoye N, Aminot A, Treguer P, Fontugne M, Naulet N, & Kerouel R (2003) Dynamics of particulate organic matter $\delta^{15}N$ and $\delta^{13}C$ during spring phytoplankton blooms in a macrotidal ecosystem (Bay of Seine, France). *Marine Ecology-Progress Series* 255: 27-41.

Schmidt GA (1998) Oxygen-18 variations in a global ocean model. *Geophysical Research Letters* 25: 1201-1204.

Schmidt GA, Bigg GR, & Rohling EJ (1999) Global Seawater Oxygen-18 Database. http://www.giss.nasa.gov/data/o18data/

Schmidt MW, Spero HJ, & Lea DW (2004) Links between salinity variation in the Caribbean and North Atlantic thermohaline circulation. *Nature* 428:160-163.

Schöne BR, Castro ADF, Fiebig J, Houk SD, Oschmann W, & Kroncke I (2004) Sea surface water temperatures over the period 1884-1983 reconstructed from oxygen isotope ratios of a bivalve mollusk shell (*Arctica islandica*, southern North Sea). *Palaeogeography, Palaeoclimatology, Palaeoecology* 212: 215-232.

Schöne BR, Fiebig J, Pfeiffer M, & Oschmann W (2005) Climate oscillations and trends in the North Atlantic during the last 500 years recorded in shells of *Arctica islandica*. *Geophysical Research Abstracts* 7: 02943 (abstract).

Schöne BR, Fiebig J, Pfeiffer M, Gleß R, Hickson J, Johnson ALA, Dreyer W & Oschmann W (in press) Climate records from a bivalved Methuselah (*Arctica islandica*, Mollusca; Iceland). *Palaeogeography, Palaeoclimatology, Palaeoecology*

Schöne BR, Lega J, Flessa KW, Goodwin DH, & Dettman DL (2002) Reconstructing daily temperatures from growth rates of the intertidal bivalve mollusk *Chione cortezi* (northern Gulf of California, Mexico), *Palaeogeography, Palaeoclimatology, Palaeoecology* 184: 131-146.

Schöne BR, Oschmann W, Rossler J, Castro ADF, Houk SD, Kroncke I, Dreyer W, Janssen R, Rumohr H, & Dunca E (2003a) North Atlantic Oscillation dynamics recorded in shells of a long-lived bivalve mollusk. *Geology* 31: 1037-1040.

Schöne BR, Tanabe K, Dettman DL, & Sato S (2003b) Environmental controls on shell growth rates and $\delta^{18}O$ of the shallow-marine bivalve mollusk *Phacosoma japonicum* in Japan. *Marine Biology* 142: 473-485.

Schweingruber FH (1988) Tree *Rings: Basics and Applications of Dendrochronology* Kluwer Acad., Norwell, Mass. 276 pp.

Scott PJB (1990) Chronic pollution recorded in coral skeletons in Hong Kong. *Journal of Experimental Marine Biology and Ecology* 139: 51-64.

Shackleton NJ (1967) Oxygen isotope analyses and Pleistocene temperatures re-assessed. *Nature* 215, 15–17.

Shackleton NJ (1973) Oxygen isotope analysis as a means of determining season of occupation of prehistoric midden sites. *Archaeometry* 15: 133-141.

Sharma P, Gardner LR, Moore WS, & Bollinger MS (1987) Sedimentation and bioturbation in a salt marsh as revealed by ^{210}Pb, ^{137}Cs, and ^{7}Be studies. *Limnology and Oceanography* 32: 313-326.

Shaw TJ, Moore WS, Kloepfer J, & Sochaski MA (1998) The flux of barium to the coastal waters of the southeastern USA: The importance of submarine groundwater discharge. *Geochimica et Cosmochimica Acta* 62: 3047-3054.

Shemesh A, Macko SA, Charles CD, & Rau GH (1993) Isotopic evidence for reduced productivity in the glacial Southern-Ocean. *Science* 262: 407-410.

Shen CC, Lee T, Chen CY, Wang CH, Dai CF, & Li LA (1996) The calibration of D[Sr/Ca] versus sea surface temperature relationship for *Porites* corals. *Geochimica et Cosmochimica Acta* 60: 3849-3858.

Shen GT, & Boyle EA (1987) Lead in corals - reconstruction of historical industrial fluxes to the surface ocean. *Earth and Planetary Science Letters* 82: 289-304.

Shen GT, & Boyle EA (1988) Determination of lead, cadmium and other trace-metals in annually-banded corals. *Chemical Geology* 67: 47-62.

Shen GT, & Dunbar RB (1995) Environmental controls on uranium in reef corals. *Geochimica et Cosmochimica Acta* 59: 2009-2024.

Shen GT, Campbell TM, Dunbar RB, Wellington GM, Colgan MW, & Glynn PW (1991) Paleochemistry of manganese in corals from the Galapagos Islands. *Coral Reefs* 10: 91-100.

Shevenell AE, Kennett JP, & Lea DW (2004) Middle Miocene Southern Ocean cooling and Antarctic cryosphere expansion. *Science* 305: 1766-1770.

Shvedov O (1892) Trees as chroniclers of drought. *Meteorologicheskii Vestnik* 5: 163-178.

Sime NG, De La Rocha CL, & Galy A (2005) Negligible temperature dependence of calcium isotope fractionation in 12 species of planktonic foraminifera. *Earth and Planetary Science Letters* 232: 51-66.

Simenstad CA, & Wissmar RC (1985) $\delta^{13}C$ evidence of the origins and fates of organic carbon in estuarine and nearshore food webs. *Marine Ecology - Progress Series* 22: 141-152.

Sinclair DJ (in press) Non river-flood barium signals in the skeletons of corals from coastal Queensland, Australia. *Earth and Planetary Science Letters*

Sinclair DJ, & McCulloch MT (2004) Corals record low mobile barium concentrations in the Burdekin River during the 1974 flood: evidence for limited Ba supply to rivers? *Palaeogeography, Palaeoclimatology, Palaeoecology* 214: 155-174

Sinclair DJ, Kinsley LPJ, & McCulloch MT (1998) High resolution analysis of trace elements in corals by laser ablation ICP-MS. *Geochimica et Cosmochimica Acta* 62: 1889-1901.

Skinner LC, & Elderfield H (2005) Constraining ecological and biological bias in planktonic foraminiferal Mg/Ca and $\delta^{18}Occ$: A multispecies approach to proxy calibration testing. *Paleoceanography* 20, PA1015, doi:10.1029/2004PA001058.

Spangenberg JV, & Cherr GN (1996) Developmental effects of barium exposure in a marine bivalve (*Mytilus californianus*). *Environmental Toxicology and Chemistry* 15: 1769-1774.

Spero HJ, Bijma J, Lea DW, & Bemis BE (1997) Effect of seawater carbonate concentration on foraminiferal carbon and oxygen isotopes. *Nature* 390: 497-500.

Stecher HA, & Kogut MB (1999) Rapid barium removal in the Delaware estuary. *Geochimica et Cosmochimica Acta* 63: 1003-1012.

Stecher HA, Krantz DE, Lord CJ, Luther GW, & Bock KW (1996) Profiles of strontium and barium in *Mercenaria mercenaria* and *Spisula solidissima* shells. *Geochimica et Cosmochimica Acta* 60: 3445-3456.

Steenmans D (2004) Do marine bivalve shells record paleo-productivity? *M.Sc. thesis*. Vrije Universiteit Brussel, Belgium.

Steffani CN & Branch GM (2003) Growth rate, condition, and shell shape of *Mytilus galloprovincialis*: responses to wave exposure. *Marine Ecology-Progress Series* 246: 197-209.

Stoll HM, & Schrag DP (2000) Coccolith Sr/Ca as a new indicator of coccolithophorid calcification and growth rate. *Geochemistry Geophysics Geosystems* 1 doi: 10.1029/1999GC000015.

Stoll HM, Klaas CM, Probert I, Ruiz Encinar J, & Garcia Alonso JI (2002b) Calcification rate and temperature effects on Sr partitioning in coccoliths of multiple species of coccolithophorids in culture. *Global and Planetary Change* 34: 153-171.

Stoll HM, Rosenthal Y, & Falkowski P (2002a) Climate proxies from Sr/Ca of coccolith calcite: calibrations from continuous culture of *Emiliania huxleyi*. *Geochimica et Cosmochimica Acta* 66: 927-936.

Stott L (1992) Higher temperatures and lower pCO_2: A climate enigma at the end of the Paleocene Epoch. *Paleoceanography* 7: 395-404.

Stott L, Cannariato K, Thunell R, Haug GH, Koutavas A, & Lund S (2004) Decline of surface temperature and salinity in the western tropical Pacific Ocean in the Holocene epoch. *Nature* 431: 56-59.

Stott LD (2002) The influence of diet on the $\delta^{13}C$ of shell carbon in the pulmonate snail *Helix aspersa*. *Earth and Planetary Science Letters* 195: 249-259.

Strom A, Francis RC, Mantua NJ, Miles EL, & Peterson DL (2004) North Pacific climate recorded in growth rings of geoduck clams: A new tool for paleoenvironmental reconstruction. *Geophysical Research Letters* 31, L06206, doi: 10.1029/2004GL019440.

Sukhotin AA & Pörtner H-O (2001) Age-dependence of metabolism in mussels *Mytilus edulis* (L.) from the White Sea. *Journal of Experimental Marine Biology and Ecology* 257: 53-72.

Surge D, Lohmann KC, & Dettman DL (2001) Controls on isotopic chemistry of the American oyster, *Crassostrea virginica*: implications for growth patterns. *Palaeogeography, Palaeoclimatology, Palaeoecology* 172: 283-296.

Swaileh KM (1996) Seasonal variations in the concentrations of Cu, Cd, Pb and Zn in *Arctica islandica* L (Mollusca: Bivalvia) from Kiel Bay, western Baltic Sea. *Marine Pollution Bulletin* 32: 631-635.

Swan EF (1956) The meaning of strontium - calcium ratios, *Deep Sea Research* 4: 71.

Swart PK & Hubbard JAEB (1982) Uranium in coral skeletons. *Coral Reefs* 1: 13-19.

Swart PK (1983) Carbon and oxygen isotope fractionation in Scleractinian corals: A review. *Earth-Science Reviews* 19: 51-80.

Swart PK, & Grottoli A (2003) Proxy indicators of climate in coral skeletons: a perspective. *Coral Reefs* 22: 313-315.

Swart PK, Elderfield H, & Greaves MJ (2002b) A high-resolution calibration of Sr/Ca thermometry using the Caribbean coral *Montastraea annularis*. *Geochemistry Geophysics Geosystems* 3(11), 8402, doi: 10.1029/2002GC000306.

Swart PK, Healy G, Greer L, Lutz M, Saied A, Anderegg D, Dodge RE, & Rudnick D (1999) The use of proxy chemical records in coral skeletons to ascertain past environmental conditions in Florida Bay. *Estuaries* 22: 384-397.

Swart PK, Healy GF, Dodge RE, Kramer P, Hudson JH, Halley RB, & Robblee MB (1996a) The stable oxygen and carbon isotopic record from a coral growing in Florida Bay: A 160 year record of climatic and anthropogenic influence. *Palaeogeography Palaeoclimatology Palaeoecology* 123: 219-237.

Swart PK, Leder JJ, Szmant AM, & Dodge RE (1996b) The origin of variations in the isotopic record of scleractinian corals: I. Carbon. *Geochimica et Cosmochimica Acta* 60: 2871-2885.

Swart PK, Szmant A, Porter JW, Dodge RE, Tougas JI, & Southam JR (2005) The isotopic composition of respired carbon dioxide in scleractinian corals: Implications for cycling of organic carbon in corals. *Geochimica et Cosmochimica Acta* 69: 1495-1509.

Swart PK, Thorrold S, Rosenheim BE, Eisenhauer A, Harrison CGA, Grammer M, & Latkoczy C (2002a) Intra-annual variation in the stable oxygen and carbon and trace element composition of sclerosponges. *Paleoceanography* 17 (3) 1045, doi:10.1029/2000PA000622.

Swart PK, White KS, Enfield D, Dodge RE, & Milne P (1998) Stable oxygen isotopic composition of corals from the Gulf of Guinea as indicators of periods of extreme precipitation conditions in the sub-Sahara. *Journal of Geophysical Research-Oceans* 103 (C12): 27885-27891.

Szefer P, Frelek K, Szefer K, Lee Ch, Kim B-S, Warzocha J, Zdrojewska I, & Ciesielski T (2002) Distribution and relationships of trace metals in soft tissue, byssus and shells of *Mytilus edulis trossulus* from the southern Baltic. *Environmental Pollution* 120: 423-444.

Takesue RK, & van Geen A (2004) Mg/Ca, Sr/Ca, and stable isotopes in modern and Holocene *Protothaca staminea* shells from a northern California coastal upwelling region. *Geochimica et Cosmochimica Acta* 68: 3845-3861.

Takesue RK, Bacon CR, & Brown CL (2003) Estuarine salinity variations from bivalve shell B/Ca ratios measured in situ by ion microprobe (SHRIMP RG). *Geochimica et Cosmochimica Acta* 67: A473 (abstract).

Tanaka N, Monaghan MC, & Rye DM (1986) Contribution of metabolic carbon to mollusk and barnacle shell carbonate. *Nature* 320: 520-523.

Tarutani T, Clayton RN, & Mayeda T (1969) The effect of polymorphism and magnesium substitution on oxygen isotope fractionation between calcium carbonate and water. *Geochimica et Cosmochimica Acta* 33: 987-996.

Taylor JW (2004) The Little Ice Age and the Koniag tradition at Karluk, Alaska: geochemical and isotope analyses of *Saxidomus giganteus*. *Undergraduate Honors Thesis*, University of Washington, Seattle.

Taylor SR, & McLennan SM (1985) *The Continental Crust: Its Composition and Evolution.* Blackwell Sci., Malden, MA. 312 pp.

Tesoriero A J, & Pankow JF (1996) Solid solution partitioning of Sr^{2+}, Ba^{2+}, and Cd^{2+} to calcite. *Geochimica et Cosmochimica Acta* 60: 1053-1063.

Thamdrup B, Fossing H, & Jorgensen BB (1994) Manganese, iron, and sulfur cycling in a coastal marine sediment, Aarhus Bay, Denmark. *Geochimica et Cosmochimica Acta* 58: 5115-5129.

Thorrold SR, Campana SE, Jones CM, & Swart PK (1997) Factors determining $\delta^{13}C$ and $\delta^{18}O$ fractionation in aragonitic otoliths of marine fish. *Geochimica et Cosmochimica Acta* 61: 2909-2919.

Tieszen LL, Boutton TW, Tesdahl KG, Slade NA (1983) Fractionation and turn-over of stable carbon isotopes in animal tissues: implications for $\delta^{13}C$ analysis of diet. *Oecologia* 57: 32-37.

Toland H, Perkins B, Pearce N, Keenan F, Leng MJ (2000) A study of sclerochronology by laser ablation ICP-MS. *Journal of Analytical Atomic Spectrometry* 15: 1143-1148.

Torres ME, Barry JP, Hubbard DA, & Suess E (2001) Reconstructing the history of fluid flow at cold seep sites from Ba/Ca ratios in vesicomyid clam shells. *Limnology and Oceanography* 46:1701-1708.

Tripati A, Richardson CA, Scourse J, & Elderfield H (2004) The potential use of Sr/Ca ratios in the aragonitic shell of the long-lived clam *Arctica islandica* in the reconstruction of ocean temperatures. *Geophysical Research Abstracts* 6, 07395 (abstract).

Tudhope AW, Lea DW, Shimmield GB, Chilcott CP & Head S (1996) Monsoon climate and Arabian Sea coastal upwelling recorded in massive corals from southern Oman. *Palaios* 11: 347-361.

Ulens H (2003) The potentials of *Saxidomus giganteus* as a paleoclimate proxy. *M.Sc. thesis.* Gent University, Belgium.

UN (United Nations) (1997) *Kyoto Protocol to the United Nations Framework Convention on Climate Change*, Kyoto, 11 December 1997 (http://www.un.org).

Urey HC (1947) The thermodynamic properties of isotopic substances. *Journal of the Chemical Society* 562-581.

Urey HC, Epstein S, & McKinney CR (1951) Measurement of paleotemperatures and temperatures of the Upper Cretaceous of England, Denmark, and the southeastern United States. *Geological Society of America Bulletin* 62: 399-416.

Usdowski E, & Hoefs J (1993) Oxygen isotope exchange between carbonic acid, bicarbonate, and water: A re-examination of the data of McCrea (1950) and an expression for the overall partitioning of oxygen isotopes between the carbonate species and water. *Geochimica et Cosmochimica Acta* 57: 3815–3818.

Usdowski E, Michaelis J, Bottcher ME, & Hoefs J (1991) Factors for the oxygen isotope equilibrium fractionation between aqueous and gaseous CO2, carbonic acid, bicarbonate, carbonate, and water (19°C). *Zeitschrift fur Physikalische Chemie* 170: 237–249.

USEPA (1997) *The incidence and severity of sediment contamination in surface waters of the United States. EPA 823-R-97-006.* US Environmental Protection Agency, Washington, DC.

Van den Driessche K (2001) Potentials of stable water isotopes as a natural tracer in the Schelde basin. *PhD Thesis*, Vrije Universiteit Brussel, Belgium, 244 pp.

Vander Putten E (2000) High resolution distribution of trace elements (analysed by Laser Ablation Microprobe-ICP-MS) in the shell of modern *Mytilus edulis*: an archive of environmental variations? *Ph.D. thesis*, Vrije Universiteit Brussel, 350 pp.

Vander Putten E, Dehairs F, André L, Baeyens W (1999) Quantitative in situ microanalysis of minor and trace elements in biogenic calcite using infrared laser ablation - inductively coupled plasma mass spectrometry: a critical evaluation. *Analytica Chimica Acta* 378: 261-272.

Vander Putten E, Dehairs F, Keppens E, & Baeyens W (2000) High resolution distribution of trace elements in the calcite shell layer of modern *Mytilus edulis*: Environmental and biological controls. *Geochimica et Cosmochimica Acta* 64: 997-1011.

Vengosh A, Kolodny Y, Starinsky A, Chivas AR, & McCulloch MT (1991) Coprecipitation and isotopic fractionation of boron in modern biogenic carbonates. *Geochimica et Cosmochimica Acta* 55: 2901–2910.

Verheyden A, De Ridder F, Schmitz N, Beeckman H, & Koedam N (2005a) High-resolution time series of vessel density in Kenyan mangrove trees reveal link with climate. *New Phytologist* Aug. 2005 issue, doi: 10.1111/j.1469-8137.2005.01415.x

Verheyden A, Helle G, Schleser GH, Dehairs F, Beeckman H, & Koedam N (2004) Annual cyclicity in high-resolution stable carbon and oxygen isotope ratios in the wood of the mangrove tree *Rhizophora mucronata. Plant, Cell and Environment* 27: 1525–1536.

Verheyden A, Roggeman M, Bouillon S, Elskens M, Beeckman H, & Koedam N (2005b). Comparison between $\delta^{13}C$ of α-cellulose and bulk wood in the mangrove tree *Rhizophora mucronata*: implications for dendrochemistry. *Chemical Geology* 219: 275-282.

Verheyden S (2001) Speleothems as palaeoclimatic archives: A study of the stable isotopic and geochemical behaviour of the cave environment and its Late Quaternary records. *Ph.D. thesis*, Vrije Universiteit Brussel, 131 pp.

Verheyden S, Keppens E, Fairchild IJ, McDermott F, & Weis M (2000) Mg, Sr and Sr isotope geochemistry of a Belgian Holocene speleothem: Implications for palaeoclimatic reconstructions, *Chemical Geology* 169: 144–161.

Verma MP (2004) Salt effect on the CO_2-H_2O isotopic exchange equilibration: preliminary results. *Symposium on Quality Assurance for Analytical Methods in Isotope Hydrology*, IAEA, Vienna.

Vitale AM, Monserrat JM, Castilho P, & Rodriguez EM (1999) Inhibitory effects of cadmium on carbonic anhydrase activity and ionic regulation of the estuarine crab *Chasmagnathus granulata* (Decapoda, Grapsidae). *Comparative Biochemistry and Physiology C-Pharmacology Toxicology & Endocrinology* 122: 121-129.

Vonhof HB, Wesselingh FP, & Ganssen GM (1998) Reconstruction of the Miocene western Amazonian aquatic system using molluscan isotopic signatures. *Palaeogeography Palaeoclimatology Palaeoecology* 141: 85-93.

Vonhof HB, Wesselingh FP, Kaandorp RJG, Davies GR, van Hinte JE, Guerrero J, Rasanen M, Romero-Pittman L, & Ranzi A (2003) Paleogeography of Miocene Western Amazonia: Isotopic composition of molluscan shells constrains the influence of marine incursions. *Geological Society of America Bulletin* 115: 983-993.

Wada K, & Fujinuki T (1976) Biomineralization in bivalve molluscs with emphasis on the chemical composition of the extrapallial fluid, In Watabe N & Wilbur KM (EDS.) *The Mechanisms of Mineralization in the Invertebrates and Plants*, University of South Carolina Press, Columbia. pp. 175–190.

Walls RA, Ragland PC, & Crisp EL (1977) Experimental and natural early diagenetic mobility of Sr and Mg in biogenic carbonates. *Geochimica et Cosmochimica Acta* 41: 1731-1737.

Wang S, Hong H, & Wang X (in press) Bioenergetic responses in green lipped mussels (*Perna viridis*) as indicators of pollution stress in Xiamen coastal waters, China. *Marine Pollution Bulletin* doi:10.1016/j.marpolbul.2005.02.024.

Wara MW, Delaney ML, Bullen TD, & Ravelo AC (2003) Possible roles of pH, temperature, and partial dissolution in determining boron concentration and isotopic composition in planktonic foraminifera. *Paleoceanography* 18 (4): 1100, doi:10.1029/2003GC000525.

Ward JE, & Shumway SE (2004) Separating the grain from the chaff: particle selection in suspension- and deposit-feeding bivalves. *Journal of Experimental Marine Biology and Ecology* 300: 83-130.

Watabe N (1965) Studies on shell formation, XI crystal–matrix relationships in the inner layers of mollusk shells. *Journal of Ultrastructure Research* 12: 351–370.

Watanabe T, Meibom A, Cuif J-P, Yokoyama K, Nakamori T, & Oba T (2004) Isotopic and trace elemental distributions in daily growth lines of giant clam. In *ICP VIII, 8th International Conference on Paleoceanography: An Ocean View of Global Change*, Biarritz, France, p. 214 (abstract).

Watanabe T, Winter A, & Oba T (2001) Seasonal changes in sea surface temperature and salinity during the Little Ice Age in the Caribbean Sea deduced from Mg/Ca and $^{18}O/^{16}O$ ratios in corals. *Marine Geology* 173: 21-35.

Watmough SA, Hughes RJ, & Hutchinson TC (1999) Pb-206/Pb-207 ratios in tree rings as monitors of environmental change. *Environmental Science and Technology* 33: 670-673.

Weber JN & Woodhead PMJ (1970) Carbon and oxygen isotope fractionation in the skeletal carbonate of reef-building corals. *Chemical Geology* 6: 93-117.

Weber JN (1973) Incorporation of strontium into reef coral skeletal carbonate. *Geochimica et Cosmochimica Acta* 37: 2173-2190.

Wefer G, & Berger WH (1991) Isotope paleontology - growth and composition of extant calcareous species. *Marine Geology* 100: 207-248.

Weidman CR, Jones GA, & Lohmann KC (1994) The long-lived mollusk *Arctica-islandica* - a new paleoceanographic tool for the reconstruction of bottom temperatures for the continental shelves of the northern North-Atlantic Ocean. *Journal of Geophysical Research-Oceans* 99 (C9), 18305-18314.

Weiner S, & Dove PM (2003) An Overview of Biomineralization Processes and the Problem of the Vital Effect. In Dove PM, De Yoreo JJ, & Weiner S (eds.) *Biomineralization. Reviews in Mineralogy & Geochemistry* 54. pp. 1-29.

Wheeler AP (1992) Mechanisms of molluscan shell formation. In Bonucci E (ed.) *Calcification in Biological Systems*, CRC press, pp. 179-216.

Wilbur KM & Saleuddin ASM (1983) Shell formation. In: Saleuddin ASM & Wilbur KM (eds.) *The Mollusca*, Academic Press, Inc., p. 235-287.

Willenz P, & Hartman WD (1985) Calcification rate of *Ceratoporella nicholsoni* (Porifera: Sclerospngiae): an in situ study with calcein. *Proceedings of the Fifth International Coral Reef Congress, Tahiti* 5: 113-118.

Winograd IJ, Coplen TB, Landwehr JM, Riggs AC, Ludwig KR, Szabo BJ, Kolesar PT, & Revesz KM (1992) Continuous 500,000-year climate record from vein calcite in Devils Hole, Nevada. *Science* 258: 255-260.

Winslow SD, Prakash B, Domino MM, & Pepich BV (2001) Considerations necessary in gathering occurrence data for selected unstable compounds in the USEPA unregulated contaminant candidate list in USEPA method 526. *Environmental Science & Technology* 35: 1851-1858.

Witbaard R, Jansma E, & Sass-Klaassen U (2003) Copepods link quahog growth to climate. *Journal of Sea Research* 50: 77-83.

Wong WH, Levinton JS, Twining BS, Fisher NS, Kelaher BP, & Alt AK (2003) Assimilation of carbon from a rotifer by the mussels *Mytilus edulis* and *Perna viridis*: a potential food-web link. *Marine Ecology-Progress Series* 253: 175-182.

Yap CK, Ismail A, Tan SG, & Rahim IA (2003) Can the shell of the green-lipped mussel *Perna viridis* from the west coast of Peninsular Malaysia be a potential biomonitoring material for Cd, Pb and Zn? *Estuarine, Coastal and Shelf Science* 57: 623-630.

Yu X, & Inesi G (1995) Variable stoichiometric efficiency of Ca^{2+} and Sr^{2+} transport by the sarcoplasmic reticulum ATPase. *Journal of Biological Chemistry* 270: 4361-4367.

Zacherl DC, Paradis G, & Lea DW (2003) Barium and strontium uptake into larval protoconchs and statoliths of the marine neogastropod *Kelletia kelledi*. *Geochimica et Cosmochimica Acta* 67: 4091-4099.

Zachos JC, Stott LD, & Lohmann KC (1994) Evolution of early Cenozoic marine temperatures. *Paleoceanography* 9: 353–387.

Zeebe RE (1999) An explanation of the effect of seawater carbonate concentration on foraminiferal oxygen isotopes. *Geochimica et Cosmochimica Acta* 63: 2001–2007.

Zeebe RE, & Wolf-Gladrow D (2001) *CO_2 in Seawater: Equilibrium, Kinetics, Isotopes.* Elsevier Oceanography Series, 65, 346 p.

Zhang J, Quay PD, & Wilbur DO (1995) Carbon-isotope fractionation during gas-water exchange and dissolution of CO_2. *Geochimica et Cosmochimica Acta* 59: 107-114.

Zhong S, & Mucci A (1989) Calcite and aragonite precipitation from seawater solutions of various salinities: Precipitation rates and overgrowth compositions. *Chemical Geology* 78: 283-299.

Zhou GT & Zheng YF (2003) An experimental study of oxygen isotope fractionation between inorganically precipitated aragonite and water at low temperatures. *Geochimica et Cosmochimica Acta* 67: 387-399.

Zwolsman JJG, & van Eck GTM (1999) Geochemistry of major elements and trace metals in suspended matter of the Scheldt estuary, southwest Netherlands. *Marine Chemistry* 66: 91-111.